3RD AVENUE BRIDGE
Bridge Inspection and Condition Evaluation Report

Minneapolis, MN

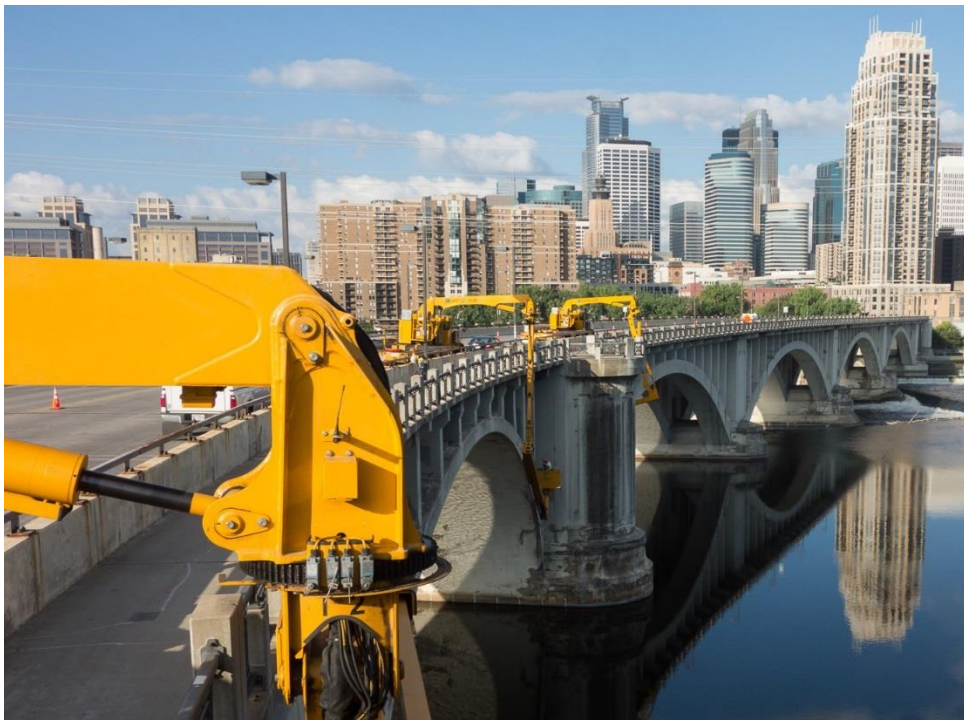

Final Report
October 25, 2017
WJE No. 2017.1436

Prepared for:
HNTB Corporation
5500 Wayzata Boulevard, #450
Golden Valley, MN 55416

Minnesota Department of Transportation
3485 Hadley Avenue North
Oakdale, MN 55128

Prepared by:
Wiss, Janney, Elstner Associates, Inc.
330 Pfingsten Road
Northbrook, Illinois 60062
847.272.7400 tel | 847.291.9599 fax

3RD AVENUE BRIDGE
Bridge Inspection and Condition Evaluation Report

Minneapolis, MN

John S. Lawler
Associate Principal

Mark R. Chauvin, PE (MN)
Associate Principal and Minneapolis Unit Manager

Jonah C. Kurth
Senior Associate

Arne P. Johnson, PE (MN)
Principal and Project Manager
Licensed Professional Engineer
State of Minnesota No. 51145

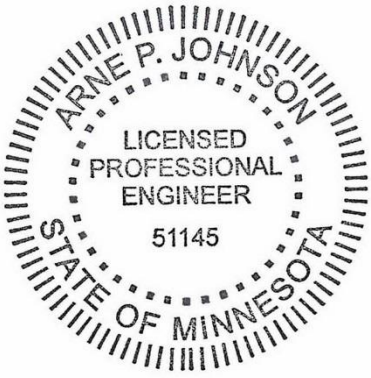

Final Report
October 25, 2017
WJE No. 2017.1436

Prepared for:
HNTB Corporation
5500 Wayzata Boulevard, #450
Golden Valley, MN 55416

Minnesota Department of Transportation
3485 Hadley Avenue North
Oakdale, MN 55128

Prepared by:

Wiss, Janney, Elstner Associates, Inc.
330 Pfingsten Road
Northbrook, Illinois 60062
847.272.7400 tel | 847.291.9599 fax

TABLE OF CONTENTS

Executive Summary i
Structural Distress Conditions x
1. Introduction 1
1.1. Background 1
1.2. Organization of Report 1
2. Bridge Description and Repair History 3
2.1. General Description and Nomenclature 3
2.1.1. Bridge Deck 7
2.1.2. Deck Framing in Arch Spans 8
2.1.3. Arch Ribs and Barrel Arches 9
2.1.4. Arch Piers 11
2.1.5. Approach Spans and Abutments 14
2.1.6. Suspended Catwalk 16
2.2. Bridge Geometry 16
2.3. Bridge Inspection and Repair History 17
2.4. Historical Significance 20
3. Bridge Inspection Work Plan 22
3.1. General Approach and Methodology 22
3.1.1. In-Depth Element Level Bridge Inspection 22
3.1.2. Follow-up Testing and Material Sampling 24
3.2. Background Regarding Relevant Deterioration Mechanisms 25
3.2.1. Corrosion of Steel Embedded in Concrete 25
3.2.1.1. Carbonation-Induced Corrosion 25
3.2.1.2. Chloride-Induced Corrosion 25
3.2.2. Freezing and Thawing Damage 28
3.2.3. Distress from Mechanical Action 28
3.3. Follow-up Testing Methods 28
3.3.1. Field Testing 29
3.3.1.1. Material Sampling 29
3.3.1.2. Delamination Survey 30
3.3.1.3. Corrosion Survey 30
3.3.1.4. Reinforcement Cover Survey 35
3.3.1.5. Field Carbonation Testing 36
3.3.1.6. Other Test Materials 37
3.3.2. Laboratory Analysis 39
3.3.2.1. Concrete Compressive Strength and Elastic Modulus 39
3.3.2.2. Chloride Testing 39
3.3.2.3. Petrographic Analysis 39
3.3.2.4. Steel Strength and Composition 40
4. In-Depth Element Level Inspection Results 41
4.1. Work Performed 41
4.2. Documentation of Inspection Conditions 41
4.2.1. Plannotate – Electronic Data Collection 43
4.2.2. Condition State Definitions 43
4.3. MnDOT / NBI Routine Inspection Data for SIMS Entry 46
4.4. General Observations by Element 47

4.4.1. Arch Spans 47
4.4.1.1. Deck Components 47
4.4.1.2. Superstructure 55
4.4.1.3. Substructure 66
4.4.2. South Approach Spans 71
4.4.2.1. Deck 71
4.4.2.2. Superstructure 72
4.4.2.3. Substructure 74
4.4.3. North Approach Spans 75
4.4.3.1. Deck 75
4.4.3.2. Superstructure 76
4.4.3.3. Substructure 76
4.4.4. Other Elements 78
4.4.4.1. Pedestrian Railing 78
4.4.4.2. Traffic Barrier 80
4.4.4.3. Other Items 82
4.4.5. Conditions That Could Affect Structural Analysis and Load Rating 83
4.5. Distress Quantity Ratios by Element Category 84
4.5.1. Definition of Distress Quantity Ratio 84
4.5.2. Summary of Distress Quantity Ratios by Element Category 84
5. Deck Joint Movement and Related Structural Distress 102
5.1. Background to the Issue 102
5.1.1. Chronological History of Bridge Deck Joints and Related Conditions 102
5.1.2. Observations During 2017 Bridge Inspection 108
5.2. Deck Joint Gap Measurements and Analysis 108
5.2.1. Gap Measurements 108
5.2.2. Deck Joint Movement Patterns 111
5.3. Summaries of Related Structural Distress Conditions 114
5.3.1. General 114
5.3.2. Piers 1 and 8 Structural Distress 115
5.3.3. Spandrel Column and Wall Movement-Related Distress 118
5.3.4. Cap Beam Mechanical Spalling 120
5.3.5. Cap Beam Shear or Torsional Cracking 122
5.3.6. Deck Fascia Compression Spalling 123
6. Follow-Up Testing and Material Sampling Results 124
6.1. Material Sampling and Common Material Characteristics 135
6.1.1. Material Sampling 135
6.1.2. Concrete 135
6.1.3. Steel Strength and Composition 141
6.2. Test Results By Element Type 144
6.2.1. Deck Topside (Roadway, Sidewalk, and Underside) - Arch Spans 144
6.2.2. Upper Spandrel Columns and Walls (1980 Construction) - 1980 Expansion Joint 154
6.2.3. Upper Spandrel Columns and Walls (1980 Construction) - Never Expansion Joint 164
6.2.4. Lower Spandrel Columns and Walls - Always Expansion Joint and 1980 Joint 167
6.2.5. Lower Spandrel Columns and Walls – Never Expansion Joint and 1918-1980 Joint 180
6.2.6. Arch Ribs 188
6.2.7. Barrel Arches 198
6.2.8. Arch Pier Walls 204

6.2.9. Arch Pier Bases 211
6.2.10. Deck Topside (Roadway, Sidewalk, & Underside) - Approach Spans 213
6.2.11. Weathering Steel Girders (South Approach) 222
6.2.12. South Abutment 222
6.2.13. South Bent Pier 226
6.2.14. Prestressed Girders (North Approach) 230
6.2.15. North Abutment 233
6.2.16. North Bent Pier 236
6.2.17. North Retaining Walls 239
6.2.18. Deck Rail Elements 244
7. Findings 247
7.1. Results That Could Impact As-Inspected Structural Model 247
7.2. Interpretation of Distress Quantity Ratios 247
7.2.1. MnDOT Guideline Thresholds for Corrective Actions 248
7.2.2. Federal Guidelines 249
7.2.3. Distress Quantity Summaries by Element Category 250
7.2.4. Comparison with Franklin Avenue Bridge 253
7.3. Deterioration Mechanisms and Anticipated Remaining Service Life by Element 258
7.3.1. Deck - Approach and Arch Spans 259
7.3.2. Upper Spandrel Columns and Walls (Including Cap Beams) 260
7.3.3. Lower Spandrel Columns and Walls 261
7.3.4. Arch Ribs and Barrel Arches 262
7.3.5. Arch Pier Walls 263
7.3.6. Arch Pier Bases 263
7.3.7. Approach Span Elements 263
7.3.8. North Retaining Walls 264
7.3.9. Deck Railing Elements 264
8. Summary and Considerations for Rehabiliation Alternatives 265
8.1. Deck 265
8.2. Upper Spandrel Columns/Walls and Cap Beams at Expansion Joints 265
8.3. Upper Spandrel Columns/Walls and Cap Beams Away From Expansion Joints 266
8.4. Lower Spandrel Columns and Walls at Current Expansion Joints 266
8.5. Lower Spandrel Columns and Walls Away From Current Expansion Joints 266
8.6. Arch Ribs and Barrel Arches 266
8.7. Arch Pier Walls and Bases 267
8.8. Approach Spans 268
8.9. Pedestrian Railings 268
8.10. Structural Distress Conditions 268

APPENDICES

Appendix 1 - Bridge Inspection Work Plan
Appendix 2 - Inspection Field Sheets
Appendix 3 - Draft MnDOT SIMS Element Level Bridge Inspection Report 2017
Appendix 4 - Inspection Results That Could Affect As-Inspected Structural Model (WJE Memorandum)
Appendix 5 - Condition State Quantities by Element
Appendix 6 - Follow-up Testing - Summary Drawings
Appendix 7 - Follow-up Testing - Locations and Summary Data
Appendix 8 - Follow-up Testing - Material Samples
Appendix 9 - Follow-up Results That Could Affect As-Inspected Structural Model (WJE Memorandum)
Appendix 10 - Petrographic Analysis Report
Appendix 11 - Pedestrian Railing Testing - Ultrasonic Thickness and X-Ray Florescence
Appendix 12 - Study Areas Plannotate Notes and Data
Appendix 13 - Deck Study Areas Plannotate Notes and Data
Appendix 14 - Graphical Summaries of Follow-up Testing Results
Appendix 15 - Collins Engineers Field Inspection Sheets

3RD AVENUE BRIDGE
Bridge Inspection and Condition Evaluation Report

Minneapolis, MN

EXECUTIVE SUMMARY

The Minnesota Department of Transportation (MnDOT) retained HNTB Corporation to conduct a multi-phase rehabilitation design project for Bridge 2440 under MnDOT Contract No. 1000045. Phase 1 is to complete a structural evaluation and load rating of the bridge concurrent with an in-depth element level bridge inspection. Wiss, Janney, Elstner Associates, Inc. (WJE) was retained as a subconsultant to HNTB to perform the bridge inspection, materials sampling and testing, and evaluation of the bridge condition.

WJE's work was performed in two parts: an **initial in-depth element level inspection** of all components of the bridge, and **follow-up testing and material sampling** in representative study areas. The in-depth element level inspection was performed primarily during the first three weeks in May 2017. The follow-up testing and material sampling commenced immediately thereafter and occupied another week and three additional weekends.

The in-depth element level inspection included a visual and sounding survey of all above-water components of the bridge. Condition state information was documented in accordance with MnDOT Bridge Inspection Field Manual (2016) for a Structural Element Condition Survey. The objectives of the in-depth inspection were to identify and document:

- The range and types of distress and deterioration conditions present in the various elements
- Signs and evidence of the root causes of the distress and deterioration conditions present
- Prudent locations for follow-up field testing and material sampling
- Locations and quantities of deterioration to facilitate the development of accurate repair drawings

The scope and methods of the inspection were included in the **Bridge Inspection Work Plan** that was developed and submitted for this project (Appendix 1). In general, a close-up visual inspection was performed of all exposed bridge surfaces. All locations that appeared suspect (where close-up inspection indicated conditions that may warrant a repair) were mechanically sounded. Representative non-suspect locations were also sounded to confirm visual indications.

All inspection notes were taken using WJE's Plannotate software (described in Section 4.2.1) and are available online for access. Links to the Plannotate website are provided in this report, where appropriate, and static copies of the complete field sheets using Plannotate are included in Appendix 2.

The follow-up testing and materials sampling work was initiated immediately after the in-depth inspection with the following objectives:

- Determine by testing and laboratory analysis the root causes of the distress and deterioration conditions present in the various elements
- Provide a basis for projecting future performance of the structural elements of the bridge
- Quantify the properties of the concrete and steel, as needed to conduct the structural, load rating and service life analyses
- Provide a basis for developing service life estimates, repair methods and repair details that will address the root causes of the deterioration, that will be long-lasting, and that will further define the extent of the repairs (such as how deep the concrete repairs will need to be)

The scope of the follow-up testing included:

- Field testing:
  - Material sampling (concrete core removal and steel sampling)
  - Delamination surveys
  - Corrosion surveys (half-cell corrosion potential, resistivity, and corrosion rate testing)
  - Reinforcement cover and location surveys
  - Field carbonation tests
  - Other test methods (ultrasonic thickness, strain relief, and X-ray florescence testing)
- Laboratory analysis:
  - Concrete compressive strength and elastic modulus testing
  - Concrete chloride testing
  - Concrete petrographic analysis
  - Steel strength and composition testing

In total, 137 locations were accessed close-up for follow-up testing, 73 areas received non-destructive testing, 81 core samples were extracted, and 10 steel samples were removed.

Given the scale, historic nature, and complexity of this bridge—and the design team's desire to provide a thorough documentation of the bridge's condition in response to the scope outlined by MnDOT—this report is long. For that reason, the report has been organized in a manner intended to be user-friendly both for those seeking overview information and for those seeking specific details about specific elements.

A road map to this report's presentation of the results of the bridge inspection and testing is as follows:

- **Chapters 1 and 2** provide background to the project and a description of the bridge structure. Chapter 2 concludes with a summary of pertinent information from past bridge inspection reports dating back to the 1960s, as well as an overview of past repairs to the bridge.
- **Chapter 3** explains the Bridge Inspection Work Plan that was developed and executed, and includes detailed background information on the common deterioration mechanisms for historic concrete and the individual testing methods that were utilized for this assessment.
- **Chapters 4 and 6** present the bridge inspection and follow-up testing procedures and results, respectively. They are organized according to bridge element category, as described below.
- Intervening **Chapter 5** describes issues that were discovered during the inspection related to deck joint movements that have resulted in structural distress in various bridge elements. Joint details from original construction, the 1980 rehabilitation, and the 2003 joint replacement are described, as well as joint measurements and how the patterns of joint movement correspond with the structural distress.
- **Chapter 7** presents the findings derived from the results of the inspection and testing. This includes discussion of the deterioration mechanisms affecting each element and a qualitative prediction of the anticipated remaining service life for each element.
- **Chapter 8** provides a summary and considerations for development of rehabilitation alternatives.
- Several **Appendices**, bound separately, contain the detailed inspection notes, test results and supporting documentation that will be useful for record purposes and for more detailed review.

Chapters 4 through 7 of the report are organized according to **Element Categories**, which WJE defined in view of the different element types and exposure conditions as well as all the different categories of concrete mixtures that were identified in the petrographic analysis, as follows:

Element Categories in Arch Spans

- Deck Topside (Roadway, Sidewalk) and Underside

- Upper Spandrel Columns and Walls (1980 Construction; including Cap Beams)
  - Always At Expansion Joint
  - Never At Expansion Joint
- Lower Spandrel Columns and Walls (1918 Construction)
  - Always At Expansion Joint
  - At Joint Since 1980
  - At Joint Between 1918-1980
  - Never At Expansion Joint
- Arch Ribs
- Barrel Arches
- Arch Pier Walls (defined as hollow sections above solid bases)
- Arch Pier Bases (defined as solid sections below tops of arches)
- Deck Rail Elements (Traffic Barrier and Pedestrian Railing)

Element Categories in Approach Spans
- Deck Topside (Roadway, Sidewalk) and Underside
- South Approach Weathering Steel Girders
- South Abutment
- South Bent Pier
- North Approach Prestressed Girders
- North Abutment
- North Bent Pier
- North Retaining Walls

By referring to the **Table of Contents** provided at the beginning of the report, the user can quickly find detailed inspection information (Chapter 4), test results (Chapter 6), and overall findings and anticipated remaining service life (Chapter 7) for each **Element Category**. Supporting appendix information is referenced within each chapter.

So, for example, if a reader is seeking **detailed information** regarding the bridge deck in the arch spans, referencing the Table of Contents would yield the following:
- Inspection observations: Section 4.4.1.1 (and Table 4.4 for distress quantity summaries)
- Field and laboratory testing results: Section 6.2.1 (including Figure 6.13 graphical summary)
- Deterioration mechanisms and anticipated remaining service life: Section 7.3.1
- Considerations for rehabilitation alternatives: Section 8.1

As a **high-level summary** of the results, the first table below summarizes the **distress typically observed** and the **distress quantity ratios**[1] for each element category. Since potential re-use of the spandrel columns and walls is critical to development of rehabilitation alternatives, the second table provides a breakdown of the distress quantity ratios by element sub-category for the spandrel columns, walls and cap beams.

[1] To allow interpretation of the structure's current condition, WJE utilized Plannotate to aggregate the very large amount of condition state data from the inspection into a single **distress quantity ratio** for each element (sometimes simply referred to as distress quantity or distress percentage). The distress quantity ratio was calculated by adding the mapped areas of all of the below-listed conditions for a given element and dividing by the total exposed surface area of that element.
- Delaminated and spalled areas: CS2 (delaminated), CS3 (moderate-depth spalls), and CS4 (deep spalls)
- Pre-existing patches and repairs: CS3 (deteriorated) and CS4 (failed or debonded patches)
- Freeze-thaw distress: CS3 (up to 2 inches of deterioration) and CS4 (more than 2 inches of deterioration)

Element Category	Sub-Category	Distress Typically Observed	Distress Quantity Ratio
Deck - Arch Spans (1980)	Topside	Dense network of usually narrow but occasionally wide transverse and longitudinal cracks; very occasional delaminations and spalls	< 1% to 2%
	Underside	Widespread spalls with corroded reinforcing at downstream fascia, below bridge centerline, along cap beams at deck joints, and around manholes in southbound lane	14%
Deck - Approach Spans (1980)	Topside, underside	Much less cracking than in arch spans and much less underside distress	1%
Cap Beams (1980)	See next table	Below deck joints: Widespread deep spalls along top corners, occasional distress at sides and bottom Away from deck joints: little distress	6 to 34% (see next table)
Upper Spandrel Columns and Walls (1980)	See next table	Below deck joints: Occasional delaminations and spalls; structural distress at bases Away from deck joints: little distress	1 to 7% (see next table)
Lower Spandrel Columns and Walls (1918)	See next table	Below deck joints: Very widespread delaminations and spalls with corroded reinforcing; paste erosion on most surfaces; occasional freeze-thaw damage; structural distress at bases Away from deck joints: Same distress types as below joints but generally less frequent	7 to 36% (see next table)
Arch Ribs and Barrel Arches (1918)	--	Frequent cracking and intermittent delaminations and spalling along arch rib corners; longitudinal cracking along Melan truss angles; deep freeze thaw damage at arch spring line regions and occasionally elsewhere	3 to 19%
Arch Piers (1918)	Walls	Isolated delaminations and spalls, more frequent at Piers 1, 6 and 8; occasional freeze-thaw damage	6%
	Bases	Very widespread, deep freeze-thaw damage and failed previous repairs; very deep freeze-thaw damage below drain outfalls	78%
North Retaining Walls (1918, 1980)	--	Occasional delaminations and spalls; deep freeze-thaw damage at joints and along top edge; rotation of 1980 cap atop 1918 wall especially at downstream side	8%

Element Category	Sub-Categories	No. of Elements	No. of Elements With Distress Quantity in Range			Average Distress Quantity for all Elements in Category*
			0-10%	10-20%*	>20%*	
Lower Spandrel Columns and Walls (1918)	Never Expansion Joint	33	25	6	2	7%
	Expansion Joint 1918-1980	16	8	7	1	10%
	Expansion Joint 1980-Present	20	10	3	7	17%
	Always Expansion Joint	17	0	5	12	36%
Upper Spandrel Columns and Walls (1980)	Never Expansion Joint	130	128	2	0	< 1%
	Always Expansion Joint	98	76	17	5	7%
Cap Beams (1980)	Never Expansion Joint	47	47	0	0	6%
	Always Expansion Joint	38	5	9	24	34%

** Compare to MnDOT Preservation Guide thresholds: Major preservation: 10-20%, Rehabilitation: >20% (see below)*

For much more detailed information on distress quantity ratios by element refer to Section 4.5.2 and color-coded Tables 4.4 through 4.22.

Guideline thresholds for corrective actions are provided in the MnDOT Bridge Preservation and Improvement Guidelines. The two main categories of actions are "Preservation" and "Improvement." Preservation can take the form of either maintenance or major preservation, whereas improvement includes bridge rehabilitation and bridge replacement (not considered for the 3rd Avenue Bridge given its historic nature):

- **Major preservation** activities include but are not limited to actions such as joint repair or replacement; deck overlays; partial deck replacement; concrete element patching repairs; or installation of cathodic protection.
- **Bridge rehabilitation** activities are more extensive types of work, such as full-scale replacement of components (deck, superstructure, substructure), bridge widening, or major structural repairs that increase capacity.

The guideline thresholds[2] applicable to the 3rd Avenue Bridge are generally as follows:

- Bridge decks: Major preservation: 2-10% Rehabilitation: 10-25%
- Superstructure elements: Major preservation: 10-20% Rehabilitation: >20%
- Substructure elements: Major preservation: 10-40% Rehabilitation: >40%

By comparison to the quantity data in the foregoing tables, it is apparent that the **guideline thresholds for major preservation and rehabilitation have been reached** for many of the 3rd Avenue Bridge elements. However, it is understood that the guideline thresholds are not necessarily applicable to a historic bridge of this nature and therefore must be viewed with caution. The guidelines are nonetheless a useful reference and were used by WJE to define "end of life"[3] in the predictions of anticipated remaining service life (see explanation below).

As a point of reference, the condition of the 3rd Avenue Bridge was also **compared to that of the Franklin Avenue Bridge**, a bridge of similar construction, vintage and exposure for which HNTB and WJE performed the inspection and rehabilitation design from 2007 to 2017. See Section 7.2.4 for additional details on this comparison.

- *Deck topside*: 3rd Avenue has less unsound area (up to 2 percent) than Franklin Avenue (up to 9 percent), but 3rd Avenue has more cracking in the overlay and deck than Franklin Avenue
- *Deck underside:* 3rd Avenue has much more underside distress (15 percent) than Franklin Avenue (3 percent), and some of the distress at 3rd Avenue will require full-depth deck repair
- *Arch ribs:* Similar conditions were observed at each bridge
- *Pier walls:* Similar conditions were observed at each bridge for piers not located below deck joints; much worse conditions were observed at Franklin Avenue for piers located below deck joints
- *Pier bases:* Much worse condition at 3rd Avenue
- *Replaced spandrel columns and cap beams:* Similar conditions were observed at each bridge
- *Original spandrel columns:* None remaining at Franklin Avenue

[2] MnDOT defines the guideline thresholds as unsound concrete and the sum of CS3 and CS4 conditions. The distress quantity ratios calculated by element in this report are formulated to be directly comparable to these thresholds (see Section 7.2.1).

[3] What constitutes the "end of life" of a member (onset of corrosion, collapse, etc.) must always be defined in a service life analysis. Using percent of damage to define end of life is one rational method, which is used herein.

The follow-up testing and material sample program provided valuable insight into the mechanisms that are causing deterioration of the various bridge elements. To review the detailed results, the reader is referred to the Table of Contents for Chapters 6 and 7 that references the test results by element category. Also, one-page graphical summaries of the test results for each element category are provided at the end of each section in Chapter 6, as well as altogether in Appendix 14. The graphical summaries are a useful tool for reviewing all the test data for each element in one place.

From the inspection and test data, WJE developed qualitative estimates of **anticipated remaining service life** for each element category. Anticipated remaining service life was defined as the time until the quantity of distress in a given element, without corrective action or intervention,[4] will reach or exceed the guideline thresholds for a "rehabilitation" action (see percentages listed above), as follows:

- **Short** - Rehabilitation action threshold already reached or likely to be reached within 5 years
- **Moderate** - Rehabilitation action threshold likely to be reached in 5 to 15 years
- **Long** - Rehabilitation action threshold likely not to be reached for more than 15 years

The table below summarizes the **primary deterioration mechanisms** identified for each element category, along with contributing secondary deterioration mechanisms. For repairs to be long-lasting, they will need to be designed to counteract or eliminate these particular mechanisms. The table also provides the **anticipated remaining service life**, as defined above, for each element category.

For brevity, the table does not include the approach span elements, pedestrian railings, or traffic barriers. These elements were found to be in generally good condition and to have a moderate to long anticipated remaining service life. Refer to the body of the report for additional details.

Element Category	Sub-Categories	Primary (and Secondary) Deterioration Mechanisms	Anticipated Remaining Service Life (Without Corrective Action or Intervention)[4]
Deck - Arch Spans	Topside	Chloride	Moderate
	Underside	Chloride	Short
Deck - Approach Spans	Topside	Chloride	Moderate to Long
	Underside	Chloride	Moderate to Long
Upper Spandrel Columns and Walls, Including Cap Beams	Always Expansion Joint	Chloride, Structural Movement	Short to Moderate
	Never Expansion Joint	Chloride, Structural Movement	Long
Lower Spandrel Columns and Walls	Always Expansion Joint and Expansion Joint 1980-Present	Chloride (Carbonation; Freeze-Thaw)	Short
	Never Expansion Joint and Expansion Joint 1918-1980	Carbonation (Chloride; Freeze-Thaw)	Moderate
Arch Ribs and Barrel Arches	--	Chloride (Carbonation; Freeze-Thaw)	Short to Moderate

[4] Service life estimates for bridge elements after they have been treated with various rehabilitation alternatives will be studied in the Rehabilitation Alternatives portion of this project to follow.

Element Category	Sub-Categories	Primary (and Secondary) Deterioration Mechanisms	Anticipated Remaining Service Life (Without Corrective Action or Intervention)[4]
Arch Piers	Walls	Chloride; Carbonation; Structural Movement (Freeze-Thaw)	Piers 2-7: Moderate to Long; Piers 1 and 8: Short to Moderate
	Bases	Freeze-thaw; Erosion	Short

Development of rehabilitation alternatives is the next task in the 3rd Avenue Bridge project, and will be a collaborative effort between MnDOT, the Project Historian and the HNTB design team. Presented below are summary comments for each bridge element category that should be considered in the development of rehabilitation alternatives, based on this inspection and condition evaluation effort. Refer to the body of the report for supporting information.

Deck. The deck topside currently has a relatively small amount of distress (2 percent or less), but the overlay exhibits a high density of cracking, and elevated chloride concentrations are present at the level of the reinforcing steel where cracking is present in the deck. Accordingly, deck topside distress will continue and likely accelerate in the coming years. The deck underside in the arch spans currently exhibits a relatively high percentage of distress (approximately 15 percent), and full-depth deck replacement will be needed in several areas (e.g., at southbound lane manholes, along nearly the full length of the downstream fascia, and along the deck centerline). Given these factors, anticipated remaining service life of the deck (i.e., time until rehabilitation thresholds are reached, without intervention) is judged to be short (less than 5 years) for the underside and moderate (5 to 15 years) for the topside. The deck underside is in better condition in the approach spans, but scheduling rehabilitation actions separately for the arch and approach spans seems inefficient.

Given the condition of the deck and its supporting elements (cap beams and spandrel columns/walls), the deck will need to be either completely or partially replaced (i.e., in sections along the joints) in the not-too-distant future. If partial or complete replacement are delayed, two general options could be implemented in the interim: 1) remove and replace the existing overlay to protect the substrate deck and to keep options open for possible partial deck replacement in a larger future rehabilitation project; or 2) seal the cracks and repair the topside distress as it develops in the deck, and plan for complete deck replacement as part of a larger future rehabilitation project. In either option, full-depth deck repairs in localized areas will need to be performed.

Upper Spandrel Columns/Walls and Cap Beams at Expansion Joints. The 1980 upper spandrel columns and walls, including the cap beams, located at deck joints exhibit a high distress quantity (7 and 34 percentage on average for columns and cap beams, respectively) due to high chloride content at the level of the reinforcing steel as well as extensive mechanical spalling at the top corners of the cap beams. Distress quantities for some elements are already near or above rehabilitation thresholds. Movement-related structural distress is evident in cap beams and columns that are full-height. The viability of these elements is also limited by the even worse condition of the 1918 lower spandrel columns and walls upon which some are supported.

Given these factors, anticipated remaining service life for the cap beams and many of the upper spandrel columns and walls located at expansion joints is judged to be short (less than 5 years). Replacement seems prudent as a component of any partial or complete deck replacement project.

Upper Spandrel Columns/Walls and Cap Beams Away From Expansion Joints. Away from deck expansion joints, the 1980 cap beams and upper spandrel columns and walls are in generally good condition, with relatively low distress quantities, low chlorides, and little carbonation. These elements have the potential for reuse in a rehabilitation project, as long as the 1918 lower spandrel columns and walls upon which some are supported can be retained and properly repaired.

Lower Spandrel Columns and Walls at Current Expansion Joints. Approximately 142 of the original 228 spandrel columns and walls were replaced full-height in the 1980 rehabilitation project. Of the 86 lower spandrel columns and walls that remain, 37 are located at current expansion joints. These elements are in poor condition and have a short anticipated remaining service life (less than 5 years) without intervention. The elements exhibit a very high distress quantity (28 and 40 percent on average for columns and walls, respectively), have very high chloride levels at the depth of the reinforcing steel, and have deep carbonation in some areas. Movement-related structural distress exists at the bottom of some of these elements. Paste erosion has rendered the surfaces of these elements generally rough, making application of a protective surface treatment difficult.

Retaining the lower spandrel columns for the long term will require substantial rehabilitation and protection measures that will be costly and likely alter the appearance of the elements. Replacement of these elements in any long-term rehabilitation scheme seems likely once all factors are considered.

Lower Spandrel Columns and Walls Away From Current Expansion Joints. Of the 86 lower spandrel columns and walls that remain, 49 are located away from current expansion joints (i.e., never at a joint or at a joint only from 1918-1980). These columns and walls are in better condition than those at current joints. The distress quantity is 8 percent on average but varies widely (up to over 50 percent) among the columns and walls in this category. Chloride contents at the depth of the reinforcing steel are below or near the corrosion threshold, but carbonation has penetrated to the reinforcing steel in some areas. In addition, paste erosion has rendered the surface of these elements generally rough.

Given these factors, anticipated remaining service life for these elements is judged to be moderate (5 to 15 years) without intervention. Retaining these elements in a rehabilitation scheme is possible if protection measures are implemented, though such measures will be challenging, costly, and could alter the historic appearance. Surface treatments, sealers, or cathodic protection may all be options, but effectiveness, service life extension, and costs require further study. Surface roughness will create challenges for initial application and potentially future performance of surface treatments.

Arch Ribs and Barrel Arches. Current distress quantities for the outer arch ribs and barrel arches are 18 and 13 percent on average, respectively, which are similar quantities to those observed at the Franklin Avenue Bridge before its rehabilitation. The middle rib at the 3rd Avenue Bridge is in somewhat better condition due to sheltering from the deck. Deterioration mechanisms include corrosion due to elevated chlorides and freeze thaw damage in zones of water saturation. Section loss due to corrosion of the embedded Melan truss reinforcing angles is limited to isolated locations where the corners have spalled and the angles have been exposed to chloride-laden run-off.

Long-term service life of the arch ribs and barrel arches is achievable if corrective actions are taken, such as well-designed localized concrete repairs and protection of the elements from water penetration (such as by application of an appropriate water-resistant coating). Since above-threshold chlorides are present at the depth of some Melan truss angles, targeted cathodic protection should be considered to enhance durability of these elements, particularly at the corners where exposure is worst. Drain outfalls should be redirected away from the arches. Longitudinal cracks, which are allowing chloride ingress, should be sealed against water penetration.

Arch Pier Walls and Bases. Distress quantities in the arch pier walls are low (3 to 4 percent on average at present), although testing showed chloride levels near the corrosion threshold in some areas and carbonation depths deeper than the cover depth in some areas. Approach-facing sides of Piers 1 and 8 have more distress due to past leakage from deck joints located above them. The pier walls have a long anticipated remaining service life, and service life could be enhanced by implementing protection measures to mitigate corrosion, such as applying a water-resistant coating.

The pier bases are suffering from widespread distress (typically well more than 40 percent at present) primarily due to deep freeze thaw damage and failed previous concrete repairs. The maximum depth of freeze thaw damage at the locations cored was 15 inches (i.e., surface erosion plus damage within remaining concrete); however, areas of even deeper surface erosion were visually observed and measured during the in-depth inspection. Considering the deepest surface erosion observed and the deepest freeze-thaw damage detected in the cores, a very conservative maximum damage depth of 25 inches could be considered for preliminary structural analysis. Freeze thaw damage will continue to penetrate into the pier base concrete as long as water saturation continues.

As a first priority, in any maintenance, preservation or rehabilitation scheme, the drain outfalls should be redirected away from the pier bases to forestall additional erosion and freeze thaw damage.

In any major rehabilitation project, the pier bases should be repaired. Such work will require considerations for the challenging access conditions that exist, including the turbulent river flow and underlying rock conditions. Given the widespread, deep deterioration that is present, a reinforced concrete jacket around the base of each pier seems to be the practical solution. At least a portion of the depth of the freeze thaw damaged concrete should be removed and a reinforced concrete layer applied around the full perimeter to restore the original profile lines of the piers. Pier jackets are not needed at the bases of Piers 1 and 2, which were repaired in this fashion in 2014.

To determine the available time window before pier jacketing is needed, a very conservative approach would be for HNTB to assess the structural performance of the piers discounting the outer 25 inches of concrete at the present time (around the full perimeter of the pier, when in actuality the deepest loss is concentrated under the drains) and considering an additional loss of material at a rate of approximately 1/2 to 1 inch per year in the future. The extent of damage and analysis could be refined, if needed.

Approach Spans. Condition of the 1980 abutments, bent piers, weathering steel girders spans, and precast girders spans is generally good at present. Anticipated remaining service life, assuming proper ongoing maintenance, is long.

The reinforced concrete caps constructed on top of the original 1918 north retaining walls are rotating outward, particularly at the downstream side. This condition should be repaired in any rehabilitation scheme. Geotechnical review by others determined that the 1918 concrete retaining walls below the 1980

caps are marginally stable but repairable. Rehabilitation of the 1918 wall sections should include surface repairs and removal of freeze-thaw damage along the tops of the walls.

Pedestrian Railings. The aluminum railing segments are in very good condition considering their age. Distress is limited primarily to impact damage and corrosion of anchor bolt hardware at the concrete posts. The concrete posts have a moderate anticipated remaining service life, although some have been undermined by deep deck spalling at the downstream fascia.

Structural Distress Conditions

In addition to the deterioration conditions described above, the inspection identified several conditions of significant structural distress caused by unintended volume change movement of the deck and superstructure when subjected to thermal changes. These conditions included the following:

- Pier 8 - Very wide diagonal shear cracking, sliding along horizontal construction joint, fractured and bent reinforcing steel across joint
- Pier 1 - Wide vertical and diagonal shear cracking
- Spandrel columns and walls, particularly below expansion joints - Structural distress at bases, including wide cracking, diagonal shear cracking, and delamination and spalling, sometimes severe
- Cap beams below expansion joints - Deep spalling along top corners and shear or torsional cracking
- South abutment - Missing and fractured anchor bolts at fixed bearings

The timing and nature of the repairs to address these structural distress conditions should be determined based on structural review of the individual conditions by HNTB in consultation with MnDOT. Some of the conditions appear relatively urgent, such as the very wide diagonal cracking in Pier 8, while others could be delayed until a major rehabilitation project is undertaken. Future structural distress can be avoided by rearticulating the bridge deck joints in a targeted program or as part of a major rehabilitation project.

1. INTRODUCTION

1.1. Background

The 3rd Avenue Bridge (Bridge 2440) is an open-spandrel, concrete arch bridge constructed between 1914 and 1918 in downtown Minneapolis, Minnesota. Open-spandrel concrete arch bridges, a common bridge design in the United States during the early 1900s, feature long spans and tall profiles that are well suited to the topography of ravines and wide river valleys. In the Minneapolis-St. Paul area, several of these bridges were constructed across both the Minnesota and Mississippi River valleys. Examples include the Anoka-Champlin Mississippi River Bridge, Franklin Avenue Bridge, Mendota Bridge, Ford Parkway Bridge, 10th Street Bridge and Lake Street Bridge.

The 1,888-foot long 3rd Avenue Bridge carries four lanes of traffic over the Mississippi River, located slightly upstream from the historic Stone Arch Bridge and St. Anthony Falls. In order to overcome difficult foundation conditions that were associated with the history of the St. Anthony Falls site, the 3rd Avenue Bridge was constructed with a reverse S-curve alignment. Much more information about the development of the site and history of the bridge is available in other documents and reports associated with this project, most notably the Historic Features Evaluation Report.

The 3rd Avenue Bridge is showing signs of its nearly 100 years of exposure to a harsh northern climate. Obvious deterioration is present on many of the original bridge elements, particularly the arch ribs, spandrel columns located below deck expansion joints, and piers near the waterline. The bridge deck, cap beams and upper portions of the spandrel columns were all replaced in 1980. While most of the reconstructed elements are in comparatively better condition, many also exhibit obvious signs of deterioration.

The Minnesota Department of Transportation (MnDOT) retained HNTB Corporation to conduct a multi-phase rehabilitation design project for Bridge 2440 under MnDOT Contract No. 1000045. Phase 1 is to complete a structural evaluation and load rating of the bridge concurrent with an in-depth element level bridge inspection. Wiss, Janney, Elstner Associates, Inc. (WJE) was retained as a subconsultant to HNTB to perform the bridge inspection, materials sampling and testing, and evaluation of the bridge condition. WJE deliverables to date include a Draft and Final Bridge Inspection Work Plan, several interim presentations and memoranda on inspection results, and this Bridge Inspection and Condition Evaluation Report.

1.2. Organization of Report

This report is organized into eight chapters. Tables and figures are embedded in the text or provided at the end of each chapter.

The report begins with an executive summary and this introductory chapter. Chapter 2 provides a description of the bridge structure and its repair history. Chapter 3 describes the inspection and testing work plan developed and executed for this project.

Chapters 4 and 6 present the bridge inspection and follow-up testing procedures and results, respectively. Intervening Chapter 5 describes unique issues that were discovered during the inspection related to deck expansion joint movements.

Findings of the inspection and condition evaluation are presented and discussed in Chapter 7, along with estimates of anticipated remaining service life for each element category.

Chapter 8 presents a brief summary and overall considerations for rehabilitation alternatives that follow from the inspection findings.

The body of the report is followed by several appendices, as follows:

Appendix 1 - Bridge Inspection Work Plan
Appendix 2 - Inspection Field Sheets
Appendix 3 - MnDOT SIMS Element Level Bridge Inspection Report 2017
Appendix 4 - Inspection Results That Could Affect As-Inspected Structural Model (WJE Memorandum)
Appendix 5 - Condition State Quantities by Element
Appendix 6 - Follow-up Testing - Summary Drawings
Appendix 7 - Follow-up Testing - Locations and Summary Data
Appendix 8 - Follow-up Testing - Material Samples
Appendix 9 - Follow-up Results That Could Affect As-Inspected Structural Model (WJE Memorandum)
Appendix 10 - Petrographic Analysis Report
Appendix 11 - Pedestrian Railing Testing - Ultrasonic Thickness and X-Ray Florescence
Appendix 12 - Study Areas Plannotate Notes and Data
Appendix 13 - Deck Study Areas Plannotate Notes and Data
Appendix 14 - Graphical Summaries of Follow-up Testing Results
Appendix 15 - Collins Engineers Field Inspection Sheets

2. BRIDGE DESCRIPTION AND REPAIR HISTORY

2.1. General Description and Nomenclature

Completed in 1918, the 3rd Avenue Bridge (Bridge 2440) is a seven-span, open-spandrel concrete arch bridge, flanked by north and south approaches of two spans each. The bridge, shown in Figure 2.1 through Figure 2.4, carries four lanes of traffic on 3rd Avenue over the Mississippi River. As shown in the location plan of Figure 2.5, the bridge is located just upstream (northwest) of the Interstate 35W Saint Anthony Falls Bridge and the historic Stone Arch Bridge, in the St. Anthony Falls Historic District of downtown Minneapolis.

The bridge has a total length of 1,888 feet and a reverse S-curve longitudinal profile, which was designed to accommodate the unique geological structure of the riverbed. Arch Spans 1 through 5 consist of three arch ribs that extend 211 feet from pier face to pier face. Arch Spans 6 and 7 consist of full-width barrel arches that span 134 feet between piers. The north and south approaches are composed of prestressed and steel girder spans, respectively, which extend from the last arch piers (Piers 1 or 8) to the abutments at the ends of the bridge.

Figure 2.1. Overview of the bridge from the downstream side, south bank.

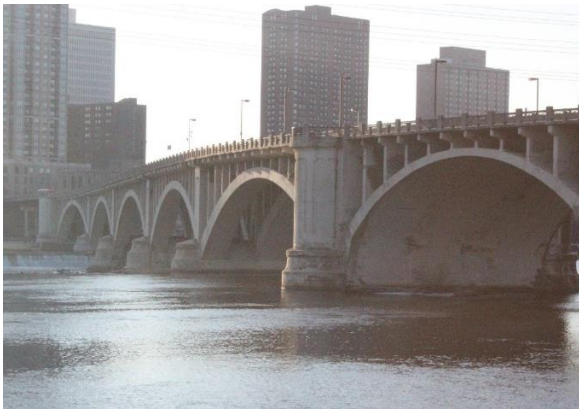

Figure 2.2. Overview of the bridge from the north bank (downstream side).

Figure 2.3. Overview of the bridge from the south bank (upstream side).

Figure 2.4. Isometric of bridge showing span and pier numbering (background from Google Earth).

Figure 2.5. Bridge location plan (background from Google Maps).

A general plan and elevation of the bridge are shown in Figure 2.6 and Figure 2.7, which along with Figure 2.4 indicate the numbering scheme and nomenclature employed in this report. Project north is indicated as away from downtown Minneapolis (toward the St. Anthony Main area). The abutments, piers and arch spans are numbered consecutively from project south to north. The arch piers are numbered 1 through 8, and the bent piers of the approach spans are numbered 1 and 2. The arch spans are numbered 1 through 7, the south approach spans 1 to 2, and the north approach spans 1 to 2. Within each arch span, the spandrel columns and cap beams are numbered and lettered consecutively from south to north. For example, the fourth spandrel column line from the south end of Span 5 is designated column line 5-D.

South Approach Spans 1 and 2 cross over a bicycle path and West River Parkway, a two lane roadway divided by Bent Pier 1 (Figure 2.8). North Approach Span 1 is located over the east embankment and North Approach Span 2 crosses over Main Street (Figure 2.9). Arch Spans 1 through 7 cross the river and spillway.

Piers 3 and 4 are within the spillway, also called the lower pool. Piers 1, 2, 5, 5, 6, 7 and 8 are within the upper pool (upstream of the spillway).

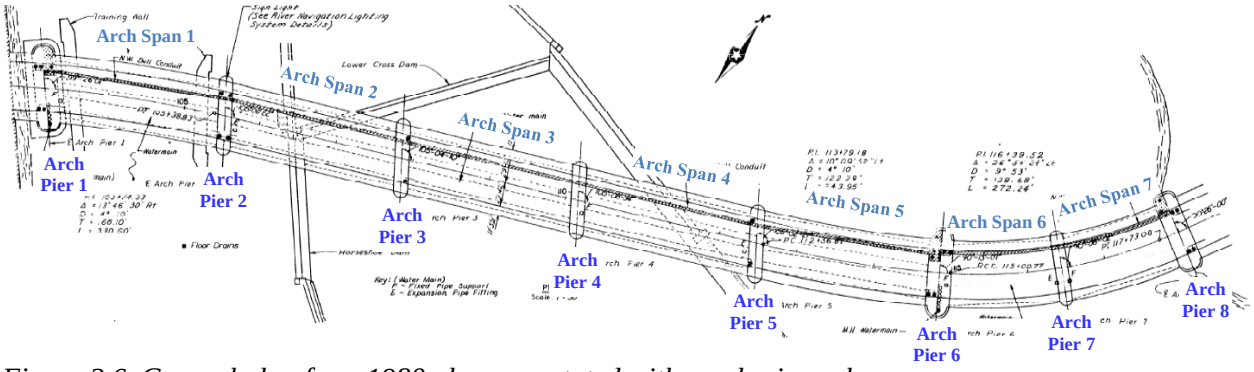

Figure 2.6. General plan from 1980 plans annotated with numbering scheme.

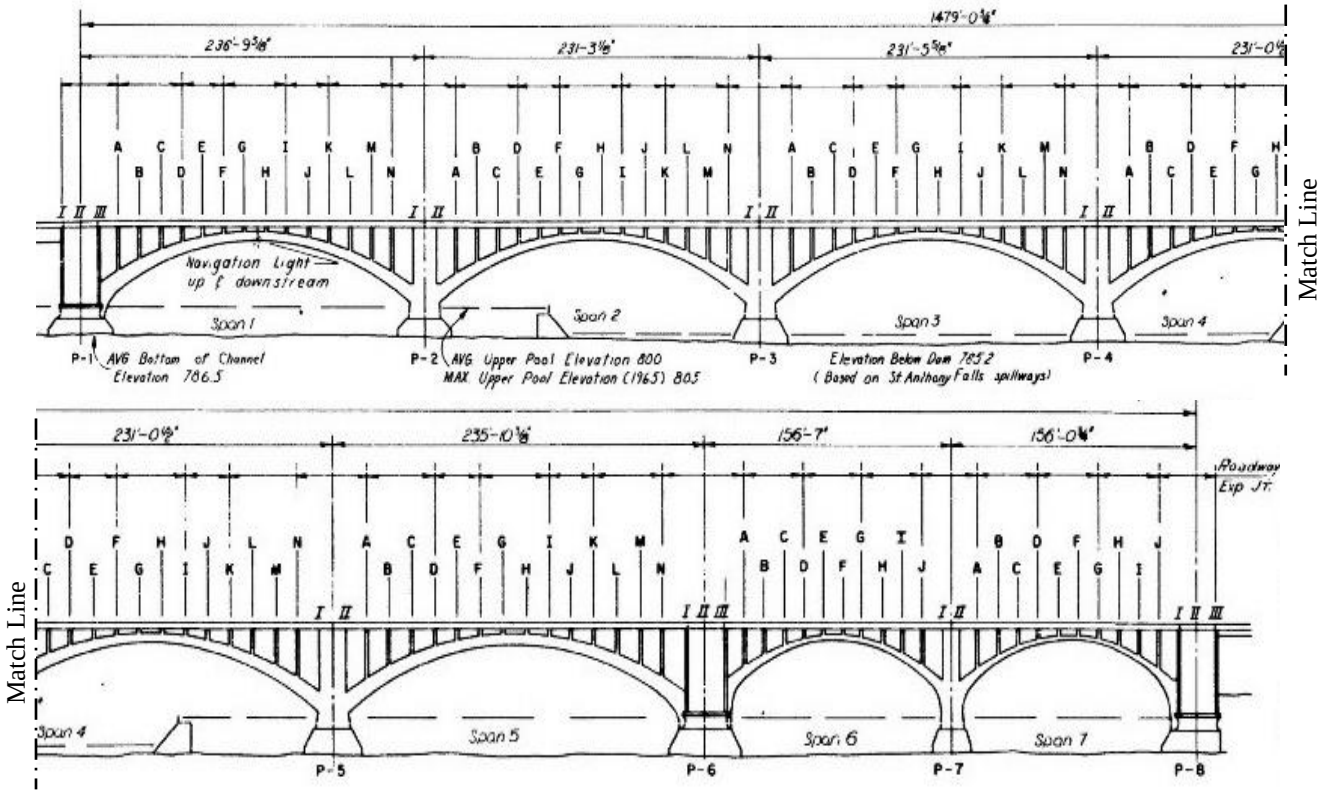

Figure 2.7. General elevation from 1980 plans (south half at top and north half at bottom) showing arch spans and historical numbering scheme, which was adopted for this inspection and report.

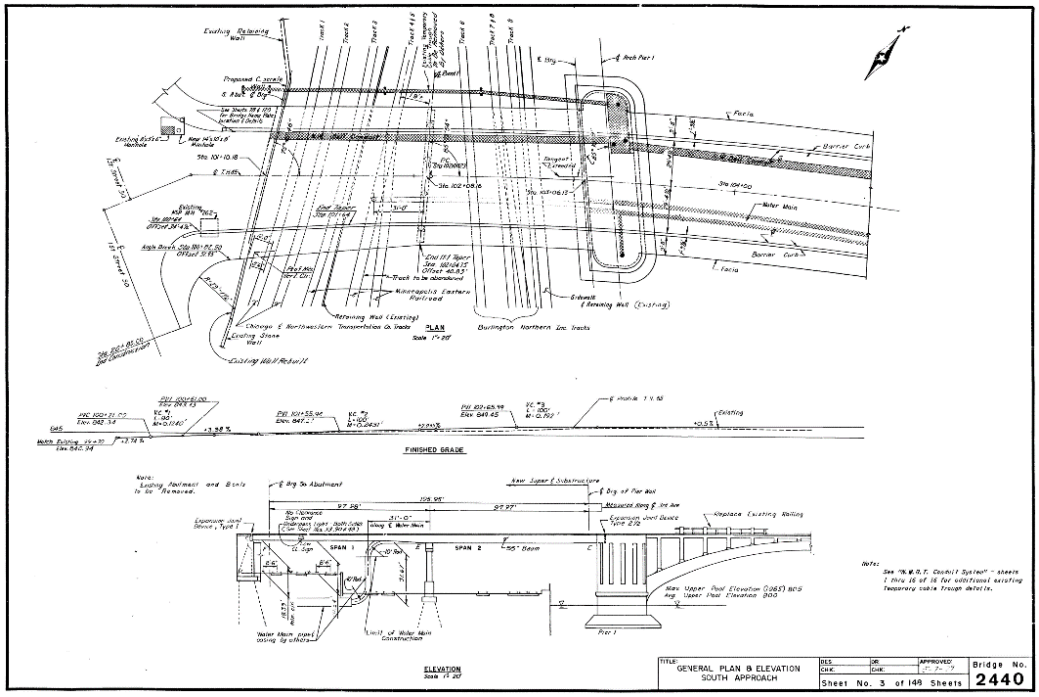

Figure 2.8. South approach plan and elevation (from 1980 plans).

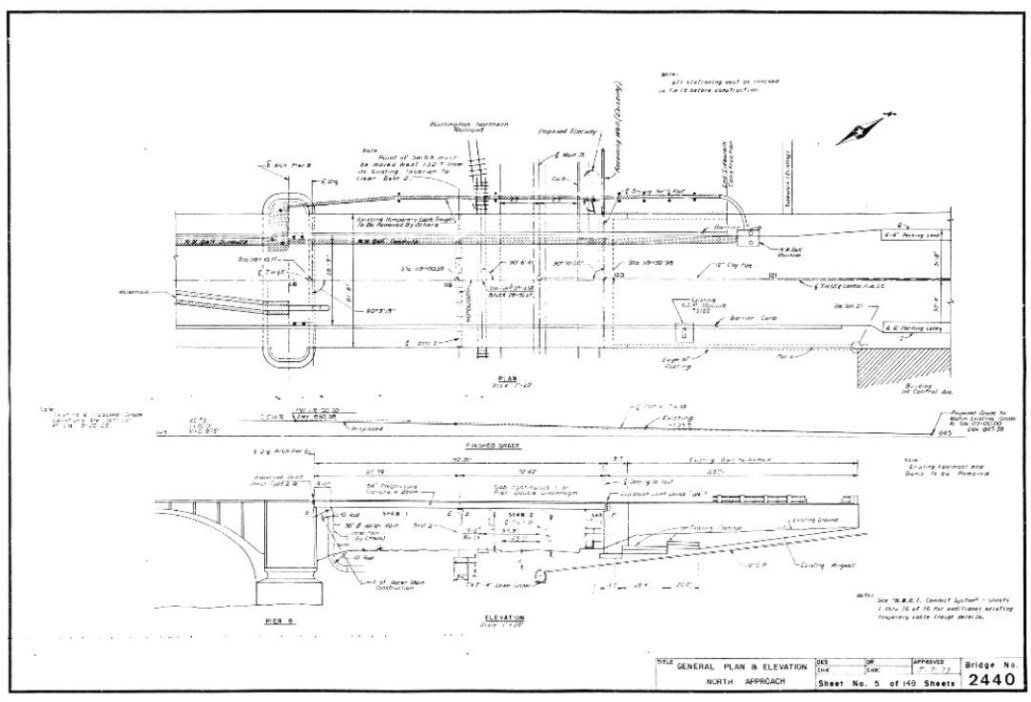

Figure 2.9. North approach plan and elevation (from 1980 plans).

2.1.1. Bridge Deck

The existing bridge deck carries four lanes of traffic and includes sidewalks along both the upstream and downstream edges, as shown in the cross section of Figure 2.10 and overall photograph of Figure 2.11. The deck has a typical overall width of 81 feet 8 inches, which is comprised of a 58 foot 9 inch wide roadway flanked on each side by 1 foot 9 1/2 inch wide traffic barriers, 8 foot 6-1/2 inch wide sidewalks, and 1 foot 1-1/2 inch wide railings, plus reveal. The bridge deck is locally wider above Piers 1, 6 and 8 where the sidewalk includes bridge overlook areas on both the upstream and downstream sides.

The original bridge deck (1918) was removed and replaced as part of a major rehabilitation of the bridge in 1980. The replacement deck in the roadway is 9 inches thick in the approach spans and 11 inches thick in the arch spans, including a 2 inch thick (minimum) low slump concrete overlay. The bridge deck is reinforced with two layers of ASTM A615 Grade 60 reinforcing bars. The top mat of bars is epoxy-coated, and the bottom mat is plain. The clear cover over the top mat of reinforcement in the base deck is 1 inch (3 inches including the 2 inch overlay); clear cover over the bottom reinforcement is 1 inch. The sidewalks are 11 inches thick in both the approach and arch spans, without any overlay.

In the 1980 rehabilitation project, the joints in the replacement bridge deck were configured as poured sealant joints. In 2003, portions of the joints were replaced with 2 inch wide strip seal expansion joints, and concrete repairs were performed to the deck adjacent to the joints. See Chapter 5 for further information regarding the bridge deck joints.

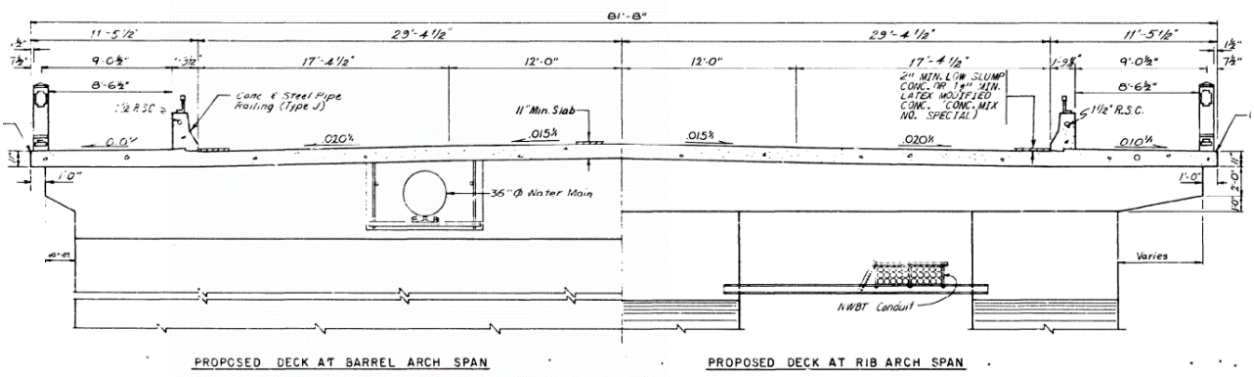

Figure 2.10. Typical bridge deck cross section in arch spans (from 1980 plans).

Figure 2.11. Overall photo of existing bridge deck.

2.1.2. Deck Framing in Arch Spans

The bridge deck in the arch spans is supported by concrete cap beams and spandrel columns or spandrel walls (Figure 2.12 and Figure 2.13). Arch Spans 1 through 5 each contain fourteen lines of spandrel columns; Arch Spans 6 and 7 contain 10 lines of spandrel walls. The cap beams and the upper portions of the spandrel columns and walls were replaced as part of the 1980 rehabilitation project, as shown in the cross section of Figure 2.14. The cap beams typically measure 3 feet high by 2 feet 4 inches wide and are spaced approximately 14 feet 6 inches apart. The cap beams in Arch Spans 1 through 5 are each supported by three spandrel columns, with each column centered over the arch ribs. The cap beams cantilever beyond the outer spandrel columns to support the sidewalks. The spandrel columns are typically 2 feet thick by 10 feet or 12 feet wide above the outside arch ribs, and 16 feet wide above the middle arch rib. The spandrel columns vary in height from approximately 3 feet 4 inches to 25 feet 7 inches, following the curvature of the arch ribs.

According to the original bridge plans, the vertical reinforcement in the spandrel columns was to consist of "3/4" bars staggered 24" o.c." Based on field testing performed by WJE, as described later in this report, the vertical bars in the original spandrel column sections are spaced at approximately 4 feet on center along each face. These field observations suggest the term "staggered" applied to the alignment of the reinforcing at the opposing column faces. The vertical reinforcing steel in the upper spandrel columns, reconstructed in 1980, consists of #8 bars spaced at 2 feet on center, as shown on the plans and documented during WJE field testing.

The cap beams in Arch Spans 6 and 7 are monolithic with spandrel walls beneath them. The spandrel walls, extend the full width of the barrel arches and are typically 1-1/2 to 2 feet thick, spaced at 11 feet 2 inches on center. The height of the spandrel walls varies from approximately 14 inches to 16 feet 3 inches, following the curvature of the barrel arches.

Figure 2.12. Typical spandrel column and cap beam, supported on arch rib.

Figure 2.13. Typical spandrel columns and cap beams, supported on arch rib.

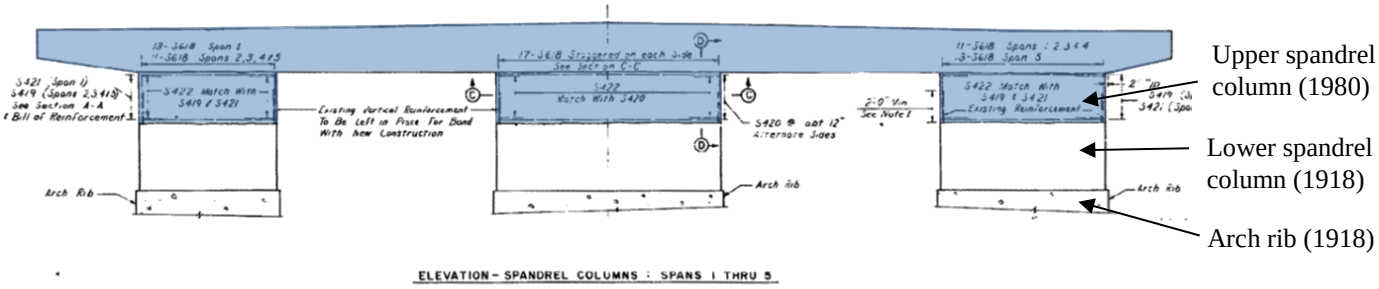

Figure 2.14. Typical bridge cross section from 1980 plans. Blue shading indicates cap beams and upper portions of spandrel columns that were replaced in 1980.

2.1.3. Arch Ribs and Barrel Arches

Reinforced concrete arch ribs or barrel arches span from pier to pier and support the spandrel columns or walls and cap beams beneath the bridge deck. Arch Spans 1 through 5 each contain three arch ribs spaced 16 feet apart (face to face), and Arch Spans 6 and 7 each contain full-width barrel arches. Typical views looking along the arch ribs and barrel arches are shown in Figure 2.15 through Figure 2.18.

In the arch spans, the upstream and downstream arch ribs are typically 10 feet wide, except for at the outside of the curved sections of the bridge where the arch ribs are 12 feet wide. The middle arch ribs are 16-feet wide. The arch ribs vary in thickness from 8 feet at the piers to 4 feet 6 inches at the crown and have a vertical rise of approximately 36 feet above the spring line. In Spans 6 and 7, the barrel arches have a constant width of 76 feet and range in thickness from 6 feet 1 inch at the piers to 2 feet 6 inch at the arch crowns. The vertical rise of the barrel arches is approximately 38 feet above the spring line.

Pipes servicing drains in the bridge deck were originally configured to penetrate and pass through the arch ribs; however, this condition was modified as a component of a prior repair project. Abandoned holes associated with the original drain pipes were observed by WJE at certain arch ribs during the field inspection work (see Figure 2.16).

Figure 2.15. Overall view of arch ribs supporting spandrel columns and cap beams.

Figure 2.16. Example of hole (arrow) through arch rib for previous drain pipe penetration.

Figure 2.17. Typical view looking along the arch ribs from beneath Arch Span 5.

Figure 2.18. Typical view of barrel arches in Arch Spans 6 and 7.

The arch ribs are reinforced with Melan type steel truss reinforcement[5] composed of back-to-back double angle chords that are rivet-connected together, with bar lattice webbing and angle or bar lateral braces. According to the original plans and available historic images of the bridge construction, the steel trusses were field erected between the bases of the piers and then concrete was cast around them. The steel trusses embedded in the arch ribs now serve as permanent reinforcing steel for the arch ribs. Sections from the original plans are reproduced in Figure 2.19 and Figure 2.20.

In Arch Spans 1 through 5, the double angle chords are typically 4x4x1/2 inch members. The chords are laced with 2-1/2x3/8 inch diagonal bars and braced vertically and horizontally at regular intervals with 3x3x5/16 inch angles. Each of the 16 foot wide arch ribs contains six lines of double angle chords, while the 12 feet wide and 10 feet wide arch ribs contain five and four lines, respectively. Riveted splice plate connections occur intermittently along the length of the chords.

[5] For background regarding Melan truss reinforcement, see the Historic Features Report for this project, along with "The Franklin Avenue Bridge, Part 1: History, Investigation and Rehabilitation" by Arne Johnson, John Lawler, Dan Enser, Travis Konda and Paul Backer, Concrete International, June 2017.

The barrel arches in Arch Spans 6 and 7 encase 3x3x5/16 inch double angle chords spaced at 34 inches on center across the entire width of the arches. The chords are laced with 2-1/2x1/4 inch diagonal bars and cross-braced intermittently with 3x3x3/8 inch angles.

According to the original plans, the concrete clear cover over the tips of the vertical legs of the chord angles was to be 3 inches, and the distance from the vertical legs of the corner angles to the side faces of the arch ribs was to vary from 9 to 11 inches. It would be expected that the actual clear cover would vary because the chord angles are straight-line segments, while the finished top and bottom surfaces of the arches are a curved profile.

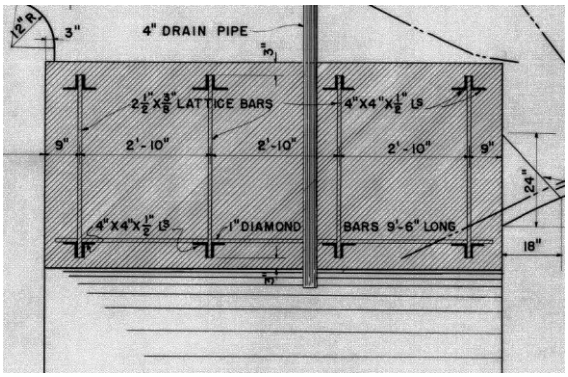

Figure 2.19. Typical cross section through outer arch rib (from 1918 plans).

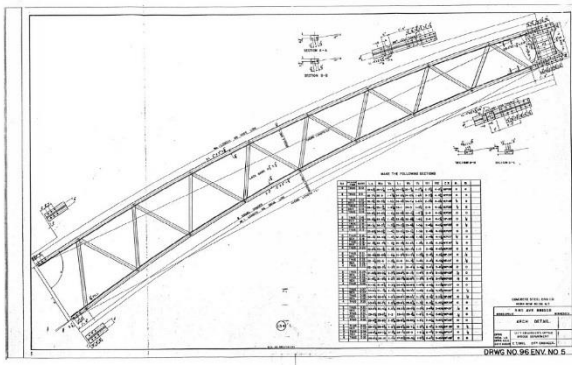

Figure 2.20. Typical elevation of Melan truss reinforcement in arch rib (from 1918 plans)

2.1.4. Arch Piers

The arch ribs and barrel arches frame into eight massive reinforced concrete piers (arch piers). Arch Piers 1 through 7 are located in the Mississippi River, while Arch Pier 8 is positioned partially in the river and partially on the north bank. All of the piers are supported on spread footings that bear on a layer of limestone below the riverbed. Dimensions and details of the arch piers were not completely defined in the bridge plans available from the MnDOT Central File at the time of the WJE field inspection. Bridge plans later obtained from the City of Minneapolis are more complete, yet discrepancies still exist between dimensions specified in those plans and those measured by WJE in the field at spot locations. WJE is aware that HNTB has retained others to perform a survey of the bridge, including the arch piers, using Light Detection and Ranging (LIDAR) sensing methods. It is expected that the collected LIDAR data will allow actual dimensions of the piers to be more accurately defined.

Piers 1 and 6 (as shown in Figure 2.21 through Figure 2.24) include rounded overlooks at the bridge deck level. These piers are larger than the other piers at arch spans, with outside plan dimensions of approximately 130 feet (transverse to span) by 30 feet. Pier 1 has a square nosing at the upstream face and a round nosing at the downstream face. A reinforced concrete jacket was constructed around the base of Pier 1 as a component of a 2014 foundation repair project. Pier 6 has a round pier nosing on the upstream and downstream sides. The lower portions of the piers (termed "pier bases" in this report, defined as the solid sections of piers below tops of arches) are solid concrete to just above the arch spring lines and are highlighted by protruding horizontal concrete bands at their top. Above the bands, the pier construction consists of perimeter reinforced concrete pier walls with one interior wall oriented transverse to the span. The interior pier walls, and the transverse-oriented perimeter pier walls, each contain two arched openings

located between the three arch ribs (Figure 2.22). The pier walls are approximately 2 feet thick and the arched openings are approximately 19 feet tall by 12 feet wide.

Figure 2.21. Overall view of Arch Pier 1 from upstream side.

Figure 2.22. Arched openings in the walls of Arch Pier 1.

Figure 2.23. Overall view of Arch Pier 6 from downstream side.

Figure 2.24. Interior of Pier 6.

Piers 2 through 5 have outside plan dimensions of approximately 105 feet (transverse to span) by 37 feet. The piers have a round pier nosing at the upstream and downstream elevations. The pier bases are solid to just above the arch rib junctions. A reinforced concrete jacket was constructed around the base of Pier 2 as a component of a 2014 foundation repair project. Above the top of the pier base, each pier consists of three columns that extend to the bridge deck. The center pier column is approximately 16 feet 6 inch by 16 feet in plan, while the outer pier columns are 16 feet by 11 feet 6 inch or 12 feet 6 inch to accommodate the widths of the arch ribs. Each pier column resembles a box and is constructed of four perimeter reinforced concrete walls (thus, the pier columns are also termed pier walls in this report). The north and south walls, oriented transverse to the arch spans, are approximately 2 feet thick while the upstream and downstream walls are approximately 1 foot 6 inch thick. Arched openings measuring approximately 10 feet high by 6 feet wide are present at the base of each outer pier column on the interior facing surface. The center pier

column has two arched openings, one at its upstream and downstream faces. Figure 2.25 and Figure 2.26 illustrate this pier type.

Figure 2.25. Typical view of piers with three pier columns (Piers 2, 3 and 4 shown).

Figure 2.26. Typical pier column (Pier 2 shown).

Piers 7 and 8 (Figure 2.27 and Figure 2.28) have outside plan dimensions of approximately 101 feet by 24 feet and 104 feet by 30 feet, respectively. Similar to Piers 2 through 5, Piers 7 and 8 have a round pier nosing at both the upstream and downstream elevations. The pier bases consist of solid concrete up to the top of the intersection between the adjacent barrel arches and the pier. Above the barrel arch junctions, both piers resemble a box with perimeter reinforced concrete walls. Pier 7 is approximately 11 feet wide on the downstream side and tapers to approximately 9 feet wide on the upstream side. The pier walls are approximately 2 feet 6 inch thick at the upstream and downstream elevations and 2 feet thick at the north and south elevations. The north and south elevations contain two arched openings that are approximately 10 feet high by 6 feet wide. Pier 8 is approximately 26 feet wide and contains one transverse interior wall. The upstream, downstream and interior pier walls each contain two arched openings. The pier walls are approximately 2 feet thick and the arched openings are approximately 21 feet tall and 12 feet wide. Similar to Piers 1 and 6, Pier 8 includes a rounded overlook at the deck level.

Figure 2.27. Arch Pier 7, downstream side.

Figure 2.28. Arch Pier 8, upstream side

2.1.5. Approach Spans and Abutments

The original construction of the 3rd Avenue Bridge included four approach spans of different construction at both the north and south ends of the bridge. The 1980 rehabilitation project included the replacement of the original approach spans, reducing both the north and south approaches to two spans each.

The south approach (Figure 2.29) is composed of weathering steel girders that span parallel to the roadway from the south abutment to Bent Pier 1, and from Bent Pier 1 to Arch Pier 1. The girders are welded I-shapes that vary in depth from 36 to 56 inches and have a web thickness of 3/8 inches, and are laterally braced by transverse channel sections or cross frames connected to the beams with gusset plates. The girder ends are supported on fixed bearings at the south abutment, and elastomeric expansion bearings at Bent Pier 1 and Arch Pier 1. The south abutment consists of a cast-in-place, reinforced concrete stem wall and integral wing walls supported by spread footings. Bent Pier 1 consists of a pier cap supported by four circular concrete columns atop a reinforced concrete wall. The pier cap measures approximately 5 feet high by 3 feet 4 inch wide, the pier columns measure approximately 3 feet diameter and are spaced approximately 22 feet apart, and the pier wall measures approximately 71 feet 8 inch wide by 3 feet 4 inch thick and 9 feet 6 inch high.

The north approach (Figure 2.30) is composed of prestressed concrete girders that span parallel to the roadway from the north abutment to Bent Pier 2, and from Bent Pier 2 to Arch Pier 8. The girders have an I-shaped cross section that is 54 inches deep, 1 foot 8 inches wide at the top, 8 inches wide at mid-height, and 2 feet 2 inches wide at the bottom. The girders are spaced 8 feet 3 inches on center and are laterally braced with 46 inch deep transverse concrete beams. The north abutment consists of a reinforced concrete stem wall and integral wing walls that are supported by spread footings. The wing walls abut original (1918) retaining walls that extend farther to the north (see below). Bent Pier 2 consists of a concrete wall that is 79 feet 2 inches wide and approximately 27 feet 6 inches in height above grade. The wall is 2 feet thick at its base, 3 feet 4 inches thick at its top, and contains four arched openings that are 23 feet high and 12 feet 3-1/2 inches wide. The ends of the precast girders are supported on fixed bearings at the north abutment and on elastomeric expansion bearings at Arch Pier 8 and Bent Pier 2.

Figure 2.29. South approach framing, looking toward Bent Pier 1 and south abutment.

Figure 2.30. North approach framing, looking toward Bent Pier 2 and north abutment.

A vertical circulation stair tower is present at the northwest corner of the north approach and allows pedestrians to travel from the upstream sidewalk of the bridge deck to the city sidewalk located along Main Street directly below. An original spiral stairway existed at the same location but was replaced as part of

the 1980 rehabilitation project. A typical view of the current stair tower is shown in Figure 2.31. The stair tower consists of a cast-in-place concrete spiral with four straight stair sections and three round landings that encircle a central pier. The stair sections consist of concrete filled steel stair pans.

Massive concrete retaining walls constructed in 1918 extend northward from the 1980 wing walls at both the upstream and downstream sides of the north abutment. The upstream wall has relatively discrete portions exposed above grade (Figure 2.32) alongside an adjacent apartment building. The downstream wall is largely exposed above grade (Figure 2.33) but access is limited by the presence of adjacent commercial buildings. In 1980, the original walls were capped with a new reinforced concrete wall (cap). The new caps were doweled into the tops of the original walls and built integrally with the new sidewalks, as shown in Figure 2.34.

Figure 2.31. Spiral stairway at northwest corner of north approach.

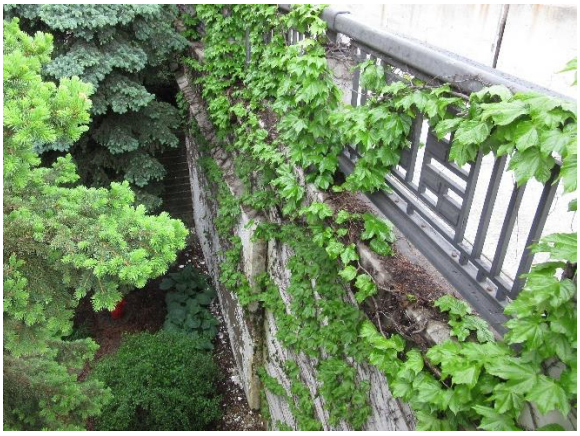

Figure 2.32. View along north retaining wall, upstream side of bridge.

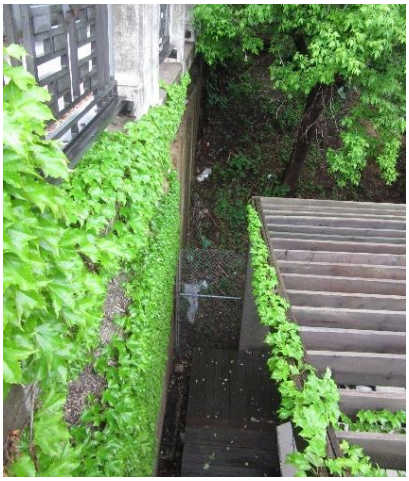

Figure 2.33. View along north retaining wall, downstream side.

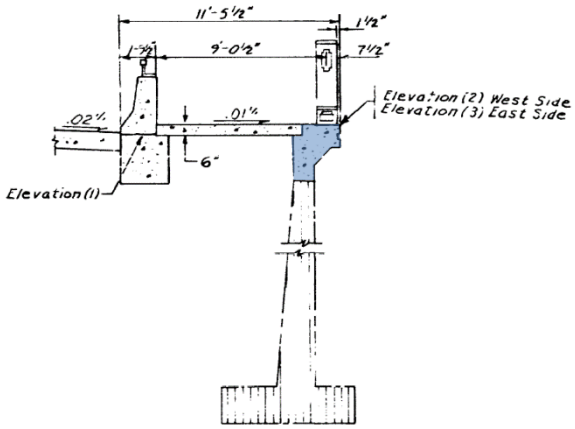

Figure 2.34. Section through north retaining wall showing 1980 concrete cap (shaded blue).

2.1.6. Suspended Catwalk

A water main with adjacent catwalk is suspended below the bridge deck continuously between Arch Piers 1 and 8. The catwalk, shown in Figure 2.35 and Figure 2.36, was constructed with the water main as part of the 1980 rehabilitation. The catwalk is positioned approximately 6 feet below the bridge deck and just downstream of the middle arch rib. The catwalk consists of approximately 2 foot wide walkway surfaces that straddle the 36 inch diameter water main. The walkway surfaces consist of steel grating that rests on 4x3x3/8 inch steel edge angles. The edge angles span between back-to-back 8x8x9/16 inch steel angles oriented transverse to the catwalk that are connected to the spandrel columns with bolted brackets. A guardrail system exists at the upstream and downstream sides of the catwalk and is constructed of 1-1/2 inch diameter piping at typical elevations of 1 foot 9 inch and 3 feet 6 inch above the steel grating. The guardrail is secured to 1 inch diameter steel hanger rods that are connected to the cap beams via bolted brackets.

Figure 2.35. View of catwalk and water main suspended from cap beam.

Figure 2.36. Catwalk and water main spanning parallel to arch ribs.

2.2. Bridge Geometry

The 3rd Avenue Bridge carries four lanes of traffic, two northbound and two southbound, on a 58 feet 9 inch wide roadway. In 2004, the bridge was classified as urban/minor arterial and had an Average Daily Traffic (ADT) of 15,500. The maximum elevation of the roadway surface is located near the middle of Span 4, with a constant slope down to the north or south from that point. The lowest elevation of the roadway surface is located at the south abutment and is approximately 9 feet lower than the peak. Between the banks of the Mississippi River, the bridge exhibits a reverse S-curve alignment.

At its north end (Figure 2.37), the bridge is accessed from Central Avenue Southeast (MN-65), with a signaled intersection located just beyond the north approach at 2nd Street Southeast. At its south end (Figure 2.38), the bridge is accessed from 3rd Avenue South, with a signaled intersection just beyond the south approach at 1st Street South.

The bridge crosses the Mississippi River near downtown Minneapolis to the south and St. Anthony Main to the north. West River Parkway is located below the south approach and is a two-lane roadway that carries local traffic, with both sidewalks and bicycle paths located adjacent to the roadway (Figure 2.39). Main

Street is located below the north approach and is a two-lane city street that serves restaurants, businesses, and residential areas, also flanked by bicycle and walking paths (Figure 2.40).

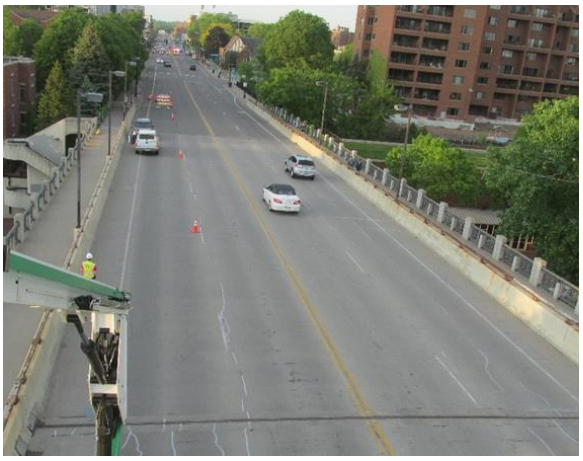

Figure 2.37. Overview of north approach from bridge.

Figure 2.38. Overview of south approach to bridge.

Figure 2.39. View looking east along West River Parking below south approach.

Figure 2.40. View looking east along Main Street below north approach.

2.3. Bridge Inspection and Repair History

The 3rd Avenue Bridge has undergone several significant rehabilitation projects since its original construction. The information below is intended to be an overview of these past projects as described in various reports and repair plans associated with the work, as well as in the Historic Features Evaluation Report associated with this project.

In 1938-1939, rehabilitation work was performed to address deterioration of the bridge that had occurred in the 20 years following its original construction. This work included repairs to spandrel columns and cap beams. The project also included the construction of new sidewalks, and the space below the sidewalks was designated for utilities. Raised curbs with a steel pipe traffic barrier were constructed between the roadway and sidewalks. The original concrete balustrade railings along the edges of the bridge deck were replaced with new Art Deco style pedestrian railings consisting of concrete posts and aluminum panels. Finally, the

original concrete light standards were repaired, reinstalled, and augmented with horizontal arms out over the roadway.

In 1953, repairs were made on a failed concrete pier cap at the south approach. In 1954, the streetcar tracks were buried under an asphalt wearing course on the bridge deck. Between 1958 and 1965, the decorative concrete light poles were replaced with metal poles at the same locations. In 1964, the deteriorating approach spans to the bridge were reinforced with supplementary steel beams. Also in the 1950's and 1960's, application of de-icing salts to the roadway would have begun, based on historical bridge maintenance practice.

In 1968, an in-depth inspection of the bridge was performed including limited material testing.[6] The inspection report concluded: "The present condition of many beams of the approaches and areas of the deck at the deck expansion joints and downspouts of the deck at the deck drains suggests that failures, localized and/or progressive, could possibly occur unless the present rate of deterioration is checked." Recommendations were presented for replacement of the approach spans, replacement of the bridge deck, replacement of the upper portions of the spandrel columns and walls, and localized repairs to the piers, arch ribs, barrel arches, and lower portions of spandrel columns and walls. The 1968 inspection report contained the following specific information:

- The bridge deck was originally covered with soil and sand fill and surfaced with street car tracks, granite blocks and creosoted wood blocks; at some point well before 1968, the original wearing surfaces were removed and an asphalt wearing surface was installed.
- "Water seeping through the deck, the expansion joints and over the outer edge of the sidewalks, has caused considerable deterioration to the upper portion of many spandrel columns and walls. Approximately one-third of the columns have areas of mineral deposits and spalls on the cap beams and the upper three feet of the columns. The lower portion of the columns have some areas of light spalling…."
- "It is estimated that, on the average, the top 5 feet of the spandrel columns and walls at deck expansion joints and the top 1 foot of all other spandrel columns and walls and pier walls contain unsound concrete and need replacement." Note that an article published during the 1980 rehabilitation project that followed this report suggests that approximately 50 percent of the spandrel columns and walls required replacement due to the extent of deterioration that was present.[7]
- Longitudinal cracking was noted in the barrel arches and was attributed to thermal effects (without explanation). Recommendations were made to fill the cracks with epoxy or epoxy mortar.
- Surface spalling was noted at the bases of the arch piers from the water line to the top of the arch ribs.
- Vertical cracks were noted in the north and south walls of Piers 1 and 7, but no structural cracks were noted in the upstream or downstream faces of Piers 1 or 8.
- No structural cracks were noted in the spandrel columns or walls.
- The report recommended use of "neoprene seal expansion joints" in lieu of "mastic filled joints" in the new bridge deck, as well as application of a surface treatment to all repaired original bridge elements in order to "seal out water and corrosive chemicals."

[6] "Bridge Inspection, Third Avenue Bridge Over the Mississippi River, Minneapolis, Engineering Report, November 1968," prepared by Howard, Needles, Tammen & Bergendoff Consulting Engineers.
[7] Construction Bulletin, 1981, "Contractor Operates Double Shifts to Complete Third Avenue Bridge Renovation a Year Early."

In 1979-1980, a major rehabilitation project was conducted. The entire bridge deck, all cap beams and the top portions of the spandrel columns and walls were removed and replaced. The profile of the bridge was raised approximately 5 feet by extending the spandrel columns and walls. Localized concrete repairs were performed to the arch ribs and arch piers and the remaining portions of the original spandrel columns and walls. The work also included the installation of new traffic barriers and new light standards. The Art Deco pedestrian railings from 1938-1939 were removed, cleaned, and reinstalled. The four approach spans at either end of the bridge were replaced with two spans each. At the north approach, the original cast-in-place concrete structure was replaced with prestressed concrete girders and a central concrete bent, and a new spiral stairway was constructed. At the south approach, the original steel spans were replaced with welded plate girders and a central concrete bent. The abutments and wing walls at both ends of the bridge were replaced, and the original retaining walls beyond the north approach were repaired and extended upward. Utilities were relocated below the bridge deck. Finally, bridge elements were coated with a cementitious surface treatment.

Through the 1980s and 1990s, routine bridge inspections were performed, and the associated reports indicated the following relevant items:

- Cracking in Pier 1 was first reported in 1985 and was described as "horizontal and vertical cracks" in the pier. (It is not clear whether this is the diagonal shear cracking that is currently present on the upstream face or solely the cracking on the north and south faces).
- Cracking in Pier 8 was first reported in 1992 and was described as wide diagonal and vertical cracking. The report indicated that cracks in the downstream face were as wide as 3/4 inch, but cracks in the upstream face were narrower.
- Structural cracking in spandrel columns was first reported in 1994/1995 and described as: "Span 1: H-1 spandrel: concrete is sheared in east arch. C/L arch spandrel has start of shear crack. Span 7: solid arch and spandrel. Concrete in spandrel D, E, F and G is cracked at cold joint in portion of spandrel east of utility opening."
- Damaged anchor bolts at the south abutment bearings were first reported in 1991 and were described as bolts that were bent southward and/or sheared off. The ends of the steel girders were reported to be contacting the top of Arch Pier 1.
- Longitudinal cracks in arch ribs were first reported in 1994. (WJE suspects that some longitudinal cracking in the arch ribs was present before but not noted, as longitudinal cracking in the barrel arches was prominently noted in the 1968 report.)
- Rotation of the north retaining wall was first reported in 1992 as "northeast retaining wall (along north abutment approach) is tipping outward 2-1/2 inches (lower portion of the wall is original 1917 construction) and should be monitored (offset along sidewalk and railing above). The northwest retaining wall is also tipped out slightly (1/2 inch gap offset at coping)."
- Spalling of cap beams below deck expansion joints was mentioned in 1983 and 1987; however, it is not clear whether this condition existed at the top corners of cap beams or at the sides and bottoms of the beams. The 1983 reports states, "A good share of the spandrel caps that support the deck where contraction/expansion joints are located are spalling or have spalled. Nothing serious yet."

In 2000, MnDOT performed an in-depth bridge inspection, and the associated report indicated the following relevant items:

- Structural cracking in spandrel columns and walls:
  - "Severe diagonal…shear cracks have developed in column stubs near center of arch spans (some have cracked through and shifted up to 1/4")…these may require reconstruction."

  - "Some spandrel walls have horizontal cracking and spalling along the base construction joints - some have shifted slightly (1/4")."
- Structural cracking in cap beams:
  - "Some caps (mainly near the center of each arch span) have severe shear cracking above the exterior arch connections (first observed in 1991)."
- Spalling of cap beams below deck expansion joints:
  - "The spandrel caps located below poured deck joints have rust stains, leaching, and horizontal cracking/delamination. In some locations, there is severe spalling (up to 12" deep) along the top edge of the cap (along the bottom of the slab)…these should be patched or reconstructed."
- Poured sealant deck joints:
  - "The arch span slab has numerous transverse poured joints…. The joints are Type Q (with rubber waterstop cast into deck below hot pour seal). Despite numerous repair attempts by the bridge crew, the poured joints in the arch spans are leaking (seal material has failed). There is extensive spalling and patching along these joints, and severe slab deterioration below. This joint design simply does not accommodate the thermal expansion and contraction of a bridge this length. These joints should be reconstructed (perhaps replaced with strip seals) to prevent further slab and superstructure deterioration."

In 2003, in view of the problems that had manifested, a repair project focusing on the deck expansion joints was undertaken. The poured sealant joints installed during the 1980 rehabilitation project were repaired or replaced with strip seal expansion joints. The strip seal joints were installed across nearly the full width of the bridge deck adjacent to piers, including the roadway and sidewalks (but not between railing posts), but were limited to the roadway section of the deck at all other joints (see Chapter 5 for further details). Localized concrete repairs were also performed to address areas of deterioration on cap beams, spandrel columns, spandrel walls, and arch ribs. At the south approach, additional repairs were made to the pavement, median, and curb and gutter.

Since the 2003 repair project, routine bridge inspection reports have generally referred back to previous inspection reports for the conditions described above. Worsening of conditions at the piers and bridge deck have been noted. For example, spalling of the downstream fascia of the deck, with exposed rebar, was reported to be present over 75 percent of the bridge length in the 2014 report. Underwater inspection reports have also been prepared and have identified underwater deterioration and scour problems at some piers. In 2014, a rehabilitation project was performed to address identified issues at Arch Piers 1, 2 and 5. The work included repairs to scour problems at the footings, as well as repair of advanced concrete deterioration below the arch rib junctions. On the upstream face of the base of Arch Pier 1, a 15 feet tall by 15 feet wide by 1 foot 6 inch thick delamination that had partially fallen into the river was removed and the face of the pier repaired. The entire perimeter of the base of Arch Piers 1 and 2 was encased in a reinforced concrete jacket that was placed using self-consolidating concrete. At Arch Piers 1 and 5, voids in the footings and scour holes below the footings were repaired by removing unsound material down to the limestone bearing surface and filling with reinforced concrete.

2.4. Historical Significance

Information regarding the historical significance of the 3rd Avenue Bridge can be found in the Historic Features Evaluation Report prepared by Hess Roise Historical Consultants, Olson & Nesvold Engineers, P.S.C., and HNTB. In short, the 3rd Avenue Bridge was deemed a contributing property to the Saint Anthony Falls Historic District that was listed in the National Register of Historic Places in 1971. The bridge possesses character defining features that include, but are not limited to, the Melan-system

reinforced-concrete arches, the reverse S-curve alignment, the incised linear detailing on the piers and the protruding bands at their base, the Art Deco aluminum railings, and the cantilevered sidewalks and observation platforms. The great bridges exemplified by the 3rd Avenue Bridge were designed in response to the transportation obstacle of the Mississippi River and its high bluffs, the arrival of the automobile, and the convergence of new highways with greater volumes of traffic and concentrated loadings on the older bridges of these urban centers.

3. BRIDGE INSPECTION WORK PLAN

3.1. General Approach and Methodology

As required by the contract, WJE developed a Draft and Final Bridge Inspection Work Plan based on review of project documents and an initial site visit to the bridge. The work plan documents were submitted and reviewed by MnDOT and other involved parties before the inspection began. Draft work plans were submitted on April 11 and April 15, 2017. Upon receiving and incorporating all comments, the Final Inspection Work Plan was submitted on April 26, 2017. The complete plan is reproduced in Appendix 1 and is summarized below.

The overall objectives of the inspection and ensuing evaluations were to gather sufficient data to determine the deterioration mechanisms at the 3rd Avenue Bridge, develop repair methods and rehabilitation alternatives targeted to address those mechanisms, and prepare cost estimates for the rehabilitation alternatives. Phase 1 is the bridge inspection and condition evaluation, reported herein.

The work was performed in two distinct parts: an initial in-depth element level inspection of all components of the bridge, followed by testing and material sampling in representative study areas. The in-depth element level inspection was performed primarily during the first approximately three weeks of the work. The follow-up testing and material sampling commenced immediately thereafter and occupied another week and three additional weekends.

3.1.1. In-Depth Element Level Bridge Inspection

The inspection began with an in-depth element level inspection of all above-water components of the bridge in accordance with MnDOT Bridge Inspection Field Manual (2016) for a Structural Element Condition Survey. The objectives of the in-depth inspection were to identify and document:

- The range and types of distress and deterioration conditions present in the various elements
- Signs and evidence of the root causes of the distress and deterioration conditions present
- Prudent locations for follow-up field testing and material sampling
- Locations and quantities of deterioration so that accurate repair quantity estimates and repair drawings can be developed

The methods and other details of the inspection are included in the full inspection plan that is appended. In general, a close-up visual inspection was performed of all exposed bridge surfaces, and surfaces not accessible using the planned access methods were noted on the field sheets. All locations that appeared suspect (where close-up inspection indicated conditions that may warrant a repair) were mechanically sounded. Representative non-suspect locations were also sounded to confirm visual indications.

Most of the work was performed on weekdays during the weeks of May 1, May 8, and May 15. Traffic control, which was provided by Warning Lites under contract to HNTB, consisted of closing either the upstream or downstream outside lane to allow 9 to 10 hours of inspection time per field day. Inspection of the center two lanes of deck occurred under a separate lane closure during one of the follow-up weekends.

For access, WJE rented one under-bridge inspection unit (snooper) and utilized another unit provided by MnDOT. Three teams of two WJE personnel performed the inspection: one team worked in each snooper, and the other team (“ground team”) worked on areas accessible by foot. The ground team utilized aerial lifts and extension ladders as needed to get close-up to out-of-reach elements.

The inspection took more time than planned due to worse-than-anticipated conditions. For example, actual inspection time for one side of an arch span (arch ribs, spandrel columns and cap beams) was approximately 1-1/2 days for one snooper team compared to the 1 day that was programmed based on prior experience with similar historic bridge structures in Minneapolis. To avoid increased expenses for snooper rental, WJE completed the field work that required snoopers in the allotted three weeks by shifting more work to the ground team. The ground team worked off catwalks, aerial lifts, ladders, and ground (deck, approach spans, retaining walls); inspected the top surface of the barrel arches in Spans 6 and 7 on foot; inspected the arch ribs and cap beams accessible from the catwalk; and inspected all the pier interiors. The ground team worked the first three weeks and then came back on the fourth week and various days during the ensuing weeks and weekends to complete the inspections.

The following elements were included in the inspection:

1. North and south approach spans
    a. Deck: reinforced concrete deck, wearing surface, expansion joints
    b. Deck railings: historic railings; cursory inspection of barrier walls
    c. Superstructure: girders, stringers, cross-bracing, diaphragms
    d. Bearings
    e. Substructure: Columns, pier walls, bent caps, abutments, wing walls, back walls
    f. Retaining walls beyond north abutment
    g. North approach span vertical circulation structure
2. Main arch spans
    a. Deck: reinforced concrete deck, wearing surface, expansion joints
    b. Deck railings: historic railings; cursory inspection of barrier walls
    c. Superstructure: spandrel columns, spandrel walls, cap beams, arch ribs, barrel arches
    d. Substructure: arch piers to the waterline*

* Inspection of the pier concrete within arm's reach of the waterline, as well as the below-water portions of piers, was performed by Collins Engineers under a separate contract with MnDOT. Refer to WJE memorandum dated April 5, 2017 (included in Appendix 1 for reference) for coordination of Collins' scope and methods of inspection with the broader bridge inspection led by WJE. Collins' field inspection sheets are included as Appendix 15.

The following items were excluded from the inspection:

1. Catwalk: framing, walkway, access ladders
2. Drains and drain pipes, except that WJE noted general functionality including broken pipes, leakage, and contribution to local deterioration
3. Manholes and covers
4. Water main
5. Utilities (conduit, piping, supports, etc.), except that WJE noted obviously failed supports especially if related to concrete distress
6. Light poles, signs, and other appurtenances, except that WJE noted where lighting mounted on traffic barrier exhibited obvious impact damage or was missing
7. Stone walls next to abutment wing walls
8. On-grade sidewalks along north retaining walls

3.1.2. Follow-up Testing and Material Sampling

Immediately after the in-depth inspection, WJE commenced non-destructive field testing and material sampling, followed by laboratory analysis of samples, and synthesis of collected data. The objectives of the testing and materials evaluation work were as follows:

- Determine by testing and laboratory analysis the root causes of the distress and deterioration conditions present in the various elements
- Provide a basis for projecting future performance of the structural elements of the bridge
- Quantify the properties of the concrete and steel needed to conduct the structural, load rating and service life analyses
- Provide a basis for developing repair methods and details that will address the root causes of the deterioration and provide long-term performance, and that will further define the extent of the repairs (such as how deep the concrete repairs will need to be)

The deterioration mechanisms considered and the test methods employed are described in the remainder of this chapter. The results are presented in Chapter 6. In total, 137 locations were accessed close-up for follow-up testing, 73 areas received non-destructive testing, 81 core samples were extracted, and 10 steel samples were removed.

Follow-up testing and material sampling work was performed on weekdays during the week of May 22 and on the weekends of July 8-9, July 15-16, and August 5-6. Note that the weekend dates and associated traffic control were revised from the Final Bridge Inspection Work Plan due to conflicts identified by the City of Minneapolis subsequent to issuance of the work plan.

Traffic control, which was provided by Warning Lites under contract to HNTB, and access methods that were utilized including the following:

- Week of May 22:
  - Closure of the upstream or downstream outer lane to allow 9 to 10 hours of inspection time per day
  - Two snoopers with a 2-person WJE team in each
- Weekend of July 8-9:
  - Closure of center two lanes on July 8 to allow 12 hours of inspection and testing on the deck
  - No snoopers required
- Weekend of July 15-16:
  - Closure of two northbound and two southbound lanes on July 15 and 16, respectively, to allow 12 to 14 hours of inspection per day
  - Three snoopers with three 2-person teams plus an extra 2-person team working on the deck and catwalks
- Weekend of August 5-6:
  - Closure of outer northbound and southbound lanes to allow for 12 to 14 hours of inspection per day
  - Three snoopers with three 2-person teams plus an extra 2-person team working on the bridge deck and from the catwalks

For further details, refer to the full Bridge Inspection Work Plan that is included in Appendix 1.

3.2. Background Regarding Relevant Deterioration Mechanisms

The following sections provide background regarding the deterioration mechanisms that are most relevant to historic concrete in general, and to the 3rd Avenue Bridge in particular. These include the following:

- Corrosion of steel embedded in concrete
  - Carbonation-induced corrosion
  - Chloride-induced corrosion
- Freezing and thawing damage to concrete
- Distress from mechanical action

3.2.1. Corrosion of Steel Embedded in Concrete

Corrosion of reinforcement in concrete, initiated by carbonation and chloride ion contamination, is a common cause of structure degradation. Corrosion of reinforcing steel in new concrete typically does not occur because cement hydration products are highly alkaline (pH of 12.5 to 13.5) by nature, and this quickly produces a stable, thin oxide film (or passive film) on the surface of reinforcing bars embedded in concrete. This passive film impedes corrosion. There are two primary mechanisms that can develop as the structure ages, resulting in the destruction of the passive film (depassivation) and causing corrosion of reinforcing steel: carbonation and chloride ion contamination.

When these two processes, singularly or in combination, are coupled with moisture and oxygen, corrosion of the reinforcing bars in the concrete will proceed. Where the depassivation occurs first, the steel becomes anodic or corrodes and supports the reaction that, in the presence of water, produces red rust (hydrated ferric oxide) and other corrosion products. Adjacent areas of the steel become cathodic (non-corroding), where oxygen and water react. Both anodic and cathodic reactions, in combination with an electronic current path (the steel) and an ionic current path (the concrete) are needed to complete the corrosion cell. Once the corrosion cell develops, the corrosion products (rust) that result occupy a much larger volume than the steel from which they were formed. This increased volume leads to expansive pressures inside the concrete that result in cracking, delamination, and ultimately spalling of the cover concrete.

The rate at which corrosion proceeds is controlled by many factors, such as dissolved oxygen availability, moisture content, resistivity of concrete, and temperature. Because concrete acts as an impediment to flow of water, chloride ions, carbonation and oxygen, the depth of cover over the bars, cracks, and permeability of concrete influence the rate that corrosion will occur. It is a rule of thumb that corrosion rates of steel in concrete typically double for a temperature increase of 18°F (Tuutti, 1982)[8], though it has been suggested that the rate may increase by as much as a factor of five for that magnitude of temperature increase (Broomfield, 2007) [9]. The ratio of the anodic area to cathodic area can also control the corrosion rate; the condition where small anodes are surrounded by large cathodes produces the most rapid corrosion.

3.2.1.1. Carbonation-Induced Corrosion

Carbonation of concrete occurs when carbon dioxide present in the air diffuses through pores in the concrete and reacts with moisture and cement hydration products within the concrete. The main reaction is calcium hydroxide within the cement paste reacting with carbon dioxide to form calcium carbonate. Carbonation of portland cement paste has two distinct effects, one chemical and one physical. The chemical effect is to lower the pH of the pore solution from approximately 13 to about 9 or less. The protective passive film on

[8] Tuutti, K. 1982. *Corrosion of Steel in Concrete.* Stockholm, Sweden: Swedish Cement and Concrete Research Institute.
[9] Broomfield, John P. 2007. *Corrosion of Steel in Concrete.* New York: Taylor and Francis.

the bar starts to break down at a pH of 10 to 11, permitting active corrosion to develop (Broomfield, 2007). The physical effects of carbonation are irreversible shrinkage and a moderate increase in density of the carbonated layer. Carbonation also can free chloride ions that were chemically bound in the aluminate phases of the cement paste, further aggravating corrosion of embedded steel.

Once depassivation has occurred and sufficient oxygen is available, the corrosion rate in concrete is strongly influenced by the resistivity of the concrete (Alonso, Andrade, & Gonzalez, 1988)[10]. This is because the concrete forms the ionic current path, and a more resistive concrete will slow current. The resistivity of concrete is strongly influenced by moisture in the concrete; this can be quantified in relation to the relative humidity within the concrete (Enevoldsen, Hansson, & Hope, 1994)[11]. A number of studies of the relationship between corrosion rate and relative humidity have been reported in the literature, and it was found that this relationship is different depending on whether the corrosion is prompted by carbonation or chloride contamination (Broomfield, 2007). Generally, corrosion rates increase significantly as relative humidity within the concrete increases beyond 75 percent. The corrosion rates reach a peak at 95 to 97 percent relative humidity, above which the additional moisture in the concrete impedes the ingress of the oxygen necessary to support the cathodic reaction.

3.2.1.2. Chloride-Induced Corrosion

In the absence of carbonation, chloride ions must accumulate to a critical concentration for corrosion to initiate on reinforcing steel that is embedded in sound concrete. The onset of corrosion is governed by the time required for chloride in the environment to penetrate through the concrete cover over the steel and build up at the bar depth to levels above the chloride threshold value. Chloride ions can also be present in the concrete from initial construction in the form of admixtures used to accelerate strength gain or in contaminated aggregate, such as sea sand.

When chloride ions accumulate to a sufficient concentration—known as the chloride corrosion threshold—the naturally occurring passive oxide film protecting the steel from corrosion breaks down. The chloride corrosion threshold is dependent on a number of conditions within the concrete, including cement content and chemistry, moisture conditions, steel chemistry and surface conditions, and proximity and condition of other embedded steel elements. The chloride corrosion threshold for initiation of corrosion of embedded mild, uncoated steel is considered to be approximately 0.20 percent total (acid-soluble) chloride by weight of cement in non-carbonated concrete (Broomfield, 2007). This is the lowest chloride corrosion threshold at which corrosion may be expected to initiate if all other conditions conducive to corrosion are present. The likelihood, severity, and rate of corrosion increase as chloride concentrations increase above this threshold level.

It is important to recognize that corrosion of the reinforcing is not certain at chloride concentrations at and above the corrosion threshold, since multiple environmental factors affect the influence of chloride concentration on corrosion. Further, since testing of existing structures is performed on samples of concrete not cement, a conversion is needed based on the content of cement in the concrete mix and the unit weight of the sampled concrete. For typical normal weight concrete, a value of 0.030 to 0.035 percent by weight of concrete is often cited as the chloride threshold within the construction industry, as this provides a

[10] Alonso, C., Andrade, C., & Gonzalez, J. A. 1988. "Relation between resistivity and corrosion rate of reinforcements in carbonated mortar made with several cement types." *Cement and Concrete Research, 18*(5), 687-698.

[11] Enevoldsen, J. N., C. M. Hansson, and B. B. Hope. 1994. "The Influence of Internal Relative Humidity on the Rate of Corrosion of Steel Embedded in Concrete and Mortar." *Cement and Concrete Research* 24 (7): 1373-1382.

conservative limit to prevent corrosion. At the same time, published literature contains widely varying statements about the chloride corrosion threshold, indicating that there is not a consensus within the industry and practice.

Based on available research and the authors' experience, the risk of corrosion due to elevated chloride concentrations are interpreted in this report as follows:

Table 3.1. Summary of Interpretation Thresholds for Chloride Concentrations

Risk of chloride-induced corrosion	Uncoated (Black Bar) Reinforcement		Epoxy-Coated Reinforcement	
	Chloride concentration by weight of cement (% chloride by weight of cement)[1]	Chloride concentration in normal weight (140 pcf) concrete[2] (% chloride by weight of concrete)	Chloride concentration by weight of cement (% chloride by weight of cement)[3]	Chloride concentration in normal weight (140 pcf) concrete[2] (% chloride by weight of concrete)
Very Low	<0.2	<0.03	<0.3	< 0.05
Low	0.2-0.4	0.03-0.06	0.3-0.7	0.05- 0.11
Moderate	0.4-1.0	0.06-0.15	0.7-1.9	0.11-0.29
High	>1.0	>0.15	> 1.9	>0.29

[1] *From* (Broomfield, 2007)
[2] *Concentrations by weight of concrete assume cement content of 564 lbs/cu yd (i.e., a 6 bag mix)*
[3] *Based on previous work performed by WJE: "Statistical distributions for chloride threshold of carbon steel and epoxy coated reinforcing bars for probability service life modeling," John Lawler, et al.*

The above threshold values refer to bare uncoated steel reinforcing bars and epoxy-coated reinforcing bars in concrete, separately. The chloride content required to initiate corrosion on epoxy coated reinforcing bars is higher.

In addition to the factors relative to chloride threshold outlined above, chloride ions can also be chemically or physically bound to the cement paste as they ingress into the material. This chloride is typically referred to as bound chloride; in contrast, chloride remaining dissolved in the pore solution is referred to as free chloride. Because the chloride binding is reversible, depending on both chloride concentration and pore solution pH, total chloride content (bound plus free chloride) is used as the basis for interpretation of corrosion thresholds.

Chloride contamination and carbonation exhibit a synergistic effect, promoting corrosion when both occur in concrete beyond what would be expected by one mechanism alone. If the concrete is carbonated, with a pH less than approximately 10, the presence of even low levels of chloride will encourage corrosion of mild steel. In addition, chloride is hygroscopic and tends to keep moisture within the concrete. Furthermore, the presence of chloride lowers the resistivity of concrete, supporting more rapid corrosion rates (Enevoldsen, Hansson, & Hope, 1994).

3.2.2. Freezing and Thawing Damage

Freezing and thawing deterioration occurs in non-air-entrained concrete when the concrete becomes saturated with water and the moisture trapped within the concrete pore structure is subjected to freezing. Concrete distress occurs because water increases in volume as it freezes, generating high capillary water pressure within the concrete. When internal concrete pressure exceeds the concrete's tensile strength, the concrete may crack. Cracking of the concrete permits additional ingress of moisture, and subsequent freezing and thawing events often lead to progressively deeper deterioration, which typically manifests itself as parallel planes of narrow cracks. This mechanism eventually results in erosion (disintegration and loss) of the concrete surface as pieces of loose concrete become dislodged. More rapid deterioration is typical at areas of greater moisture exposure, including below drain outlets and at the corners and waterline regions of concrete elements situated in bodies of water.

Modern concrete, that is concrete produced after about the 1940s, relies on air entrainment to avoid freezing and thawing deterioration. Entrained air is a network of fine, closely spaced air bubbles that are intentionally created in fresh concrete through the use of chemical admixtures. These bubbles remain in the concrete after it hardens and provide spaces where water can move when nearby moisture within the concrete freezes. This relieves the pressures created by freezing and thawing exposure and prevents damage to the concrete.

3.2.3. Distress from Mechanical Action

Distress from mechanical action occurs when external forces cause physical damage or distress to an element. Mechanical action distress is also called structural distress, especially when the distress has an effect on the structural performance of an element. Examples include structural cracking or spalling of a concrete element due to external loads or forced displacements applied to the element. Distress from mechanical action is in contrast to deterioration that develops in an element over time due to internal stresses from material degradation, such as from corrosion of reinforcing steel or freezing and thawing damage.

3.3. Follow-up Testing Methods

As outlined in WJE's work plan, a range of follow-up field and laboratory tests were employed to assess the condition of the bridge materials. The locations for follow-up testing were selected to sample the range of conditions observed among the element categories, as defined at the beginning of Chapter 6.

The scope of the follow-up testing effort included:

- Field Testing
  - Material sampling (concrete core removal and steel sampling)
  - Delamination surveys
  - Corrosion surveys (half-cell corrosion potential, resistivity, and corrosion rate testing)
  - Reinforcement cover surveys
  - Field carbonation tests
  - Other test methods (ultrasonic thickness, strain relief, and X-ray florescence testing).
- Laboratory analysis
  - Compressive strength testing, elastic modulus testing
  - Chloride testing
  - Petrographic analysis
  - Steel strength and composition testing

The methodologies for each of the follow-up test methods are described below. The results of these studies are presented in Chapter 6 of this report. The locations of testing are identified in Appendices 2, 6 and 7.

3.3.1. Field Testing

3.3.1.1. Material Sampling

The material samples collected for laboratory testing included concrete cores, reinforcing bars, and truss steel samples. The condition of these samples were documented in the field after removal from the structure and upon receipt by WJE's laboratory in Northbrook, Illinois. The samples collected are summarized in Appendix 8.

3.3.1.1.1. Concrete Core Removal

Concrete core samples were extracted with a diamond impregnated, water-cooled core drill. After removal, the core holes were photographed and then patched with a rapid-setting, cementitious repair material. The condition of each core was documented with photographs and notes, including location on the structure and condition of the sample. Select samples from the arch rib corners were removed by field sawcutting. Concrete samples were selected for either compressive strength testing, modulus of elasticity testing, chloride concentration profile evaluation, evaluation by petrographic analysis, or some combination of these tests.

Figure 3.1. Example of concrete core removal.

Figure 3.2. Example of concrete core removed from core hole.

3.3.1.1.2. Reinforcing Bar and Truss Sample Removal

Reinforcing bars were extracted from concrete core samples and at locations where cover concrete had spalled exposing the embedded reinforcing steel. Sections of the Melan truss angles were extracted from the arch ribs at locations where the concrete had deteriorated or concrete removal was performed in support of some other aspect of the testing program. Steel samples were tested for tensile strength and chemical composition.

Figure 3.3. Sample removed from delaminated and spalling arch rib corner by cutting edge of angle.

Figure 3.4. Melan truss steel sample removed by coring.

3.3.1.2. Delamination Survey

In each study area, the concrete was hammer-sounded and visually assessed to confirm the results of the element level inspection, and to identify areas for material sampling and follow-up testing. These assessment methods were the same as those described in Section 3.1.1 and in general accordance with ASTM D4580, *Standard Practice for Measuring Delaminations in Concrete.*

3.3.1.3. Corrosion Survey

Corrosion surveys were performed to assess the extent of corrosion of the embedded reinforcing steel using half-cell potential testing, concrete resistivity measurements, and corrosion rate testing, where applicable. These test methods are described below. As described in Section 6.2, corrosion testing (corrosion rate and resistivity) was not successful in some study areas due to highly-resistive carbonated concrete, large cover to reinforcing steel, or equipment issues.

3.3.1.3.1. Corrosion Potential (Half-Cell Potential Testing)

Half-cell potential (HCP) testing provides an indication of corrosion risk for reinforcing steel in concrete. Highly negative potential (voltage) readings indicate a high probability that active corrosion is occurring. HCP measurements do not locate spalls, delaminations, or other damage sites; however, these conditions are often associated with corrosion, and thus usually coincide with more negative potential readings. Anodic (corroding) regions that have not yet caused delaminations or spalls can be identified by this technique, and thus HCPs can be used as an indicator of regions likely to become damaged by corrosion in the near future.

WJE performed HCP testing in general accordance with ASTM C876 *Standard Test Method for Corrosion Potentials of Uncoated Reinforcing Steel in Concrete* over selected areas of the structure. The HCP surveys were performed by establishing an electrical connection (ground) to the reinforcement and placing a reference electrode on the surface of the concrete. Before commencing HCP measurements, electrical continuity testing was performed in each portion of the structure to verify the electrical continuity between two distant electrical connections to the reinforcing steel. Potentials were measured using either a rolling wheel with a data logger and integrated voltmeter (Canin+ by Proceq) or with a standard half-cell electrode and volt meter. Potential measurements were performed in a grid pattern or over areas of interest (e.g., over reinforcing bars). All HCP measurements are presented in terms of mV versus copper-copper sulfate

electrode and have been corrected for temperature to equivalent value at 72 ºF, in accordance with ASTM C876.

Half-cell potentials can be influenced by a number of parameters, including temperature, concrete resistivity, measurement circuit resistivity, and electrochemical conditions at the steel reinforcement. Concrete resistivity is affected by moisture, chloride content, and surface carbonation, Electrochemical conditions at the steel are affected by the cement pore chemistry, oxygen availability, and chloride concentration. Saturated concrete causes very negative potentials because the oxygen availability is limited, and thus affects the passive film on the bar. Carbonated concrete has a higher resistivity than uncarbonated concrete and can result in positive potentials, but if the carbonated layer is deep enough it may also destabilize the passive film on the bar and allow corrosion.

Typical ranges for half-cell potentials in a number of conditions are provided in Table 3.2 along with an associated risk of corrosion. Separately, guidelines for interpretation of the half-cell data per ASTM C876 are shown in Table 3.3. Interpretation of HCPs using the guidelines in ASTM C876 is generally applicable for chloride-induced corrosion in uncarbonated, atmospherically-exposed elements, and may be applicable to epoxy-coated bars if they have a number of damage locations and good electrical connectivity. However, these guidelines are not applicable where moisture conditions are highly variable and carbonation has developed, as is the case in many of the elements of this bridge. In such conditions, interpretation of corrosion risk by examination of potential gradients is preferred over assessment of risk by absolute potential values. Areas of more negative potential surrounded by areas of more positive potential suggest the areas of more negative potential are anodic and likely undergoing corrosion, while those of more positive potential are cathodic and not generating corrosion product. Other things being equal, higher corrosion currents will flow between points of high and low potential that are closer to each other. As a guideline for this examination, potential differences of 150 mV over a 3 foot distance indicate active corrosion.

Table 3.2. Typical Half-Cell Potential Ranges (RILEM TC-154)

Concrete condition	Typical Range of Half-cell potentials, mV vs CSE, with [risk of corrosion activity]		
	Chloride-contaminated	Carbonated	Chloride free
Humid, non-saturated	-600 to -400 [high]	-400 to +100 [moderate]	-200 to +100 [low]
Saturated, oxygen-starved	-1000 to -900 [low]	no data	-1000 to -900 [low]
Dry	no data	0 to +200 [low]	0 to +200 [low]

Table 3.3. Half-Cell Potential Corrosion Risk (ASTM C876)

Uncarbonated or Chloride-Driven Corrosion (based on uncoated rebar in non-saturated conditions)	
HCP vs. CSE	Corrosion Activity
> -200 mV	low - 10% probability of corrosion
-200 to -350 mV	moderate - increasing probability of corrosion
< -350 mV	high - 90% probability of corrosion

Figure 3.5. HCP survey with CSE electrode and volt meter (barrel arch underside).

Figure 3.6. HCP survey with rolling CSE electrode (deck topside).

3.3.1.3.2. Concrete Resistivity

Concrete surface resistivity was measured with a four-pin Wenner-type probe (Respiod by Proceq) or measured simultaneously with corrosion rate with the iCOR equipment (see Section 3.3.1.3.3). Prior to taking readings, reinforcing steel in the vicinity was located with GPR, and surficial paints or coatings were removed to reduce their effect on measurement of the concrete resistivity. Readings made with the Wenner-type probe were taken avoiding reinforcing bars, or if unavoidable, perpendicular to a single bar such that the bar did not influence the current path between probe points. With the iCOR equipment, concrete resistivity (i.e., solution resistivity), along with polarization resistance, is determined as part of the corrosion rate measurement, and testing was conducted over single reinforcing bars.

Concrete resistivity is correlated with the rate of corrosion in concrete structures. As resistivity increases, the rate of corrosion decreases at locations where corrosion is occurring. The categories described in Table 3.4 were used to correlate the resistivity measurement to the rate of corrosion.

Table 3.4. Interpretation of Resistivity Measurements

Resistivity (kΩ-cm)	Corrosion Rate
> 100	Negligible. Cannot distinguish between active and passive steel.
50 to 100	Low. Corrosion rates likely to be low.
10 to 50	Moderate. Moderate to high corrosion rates possible in active areas.
< 10	High. Resistivity is not the controlling factor in corrosion rates.

Sources: (Broomfield, Corrosion of Steel in Concrete, 2007)*; iCOR operating manual; Resipod operating manual.*

Figure 3.7. Resistivity survey with Resipod (arch rib underside).

3.3.1.3.3. Corrosion Rate

Instantaneous corrosion rate testing was performed to identify locations and rate of active corrosion of reinforcement. The corrosion rate was measured at selected locations where the half-cell potentials indicated corrosion might be occurring. The same electrical connection made to the reinforcement for the HCP surveys was used during this testing. Corrosion is a dynamic process and the results presented are instantaneous measurements of the rate of corrosion; consequently, changes in the site conditions, particularly temperature and moisture content, will influence the rate of corrosion. Note that the calculation of the corrosion rate is sensitive to many factors, including assumptions made about the surface area and the corrosion activity of the steel polarized during the test. Therefore, some variability in corrosion rate measurements should be expected (Broomfield, 2007).

The corrosion rate was measured using one of two non-destructive techniques: linear polarization technique (LPR), using the LPR Handheld Meter manufactured by BAC Corrosion Control; or the Connection-less Electrical Pulse Response Analysis (CEPRA) technique, using the iCOR by Giatec.

In linear polarization measurements, an external electric current is introduced between the instrument and the reinforcing steel. The shift in the corrosion potential from the equilibrium potential is measured; the ratio of this potential change to the applied current is defined as the polarization resistance. The corrosion current is inversely proportional to the polarization resistance. The corrosion rate, calculated as a current density, is expressed as the ratio of this corrosion current to the estimated surface area of the reinforcing steel participating in the test. This is then converted to a rate of steel thickness loss per year.

Using the CEPRA technique, the instrument measures the electrical response of a reinforcing bar to constant AC current. The frequency of the current is swept low to high, and the system response is analyzed. Because the response to the current sweep of a corroding rebar is different from that of a non-corroding rebar, the rate of corrosion can be assessed. This is illustrated schematically in Figure 3.8 and Figure 3.9 below. Concrete resistivity is also measured during this process.

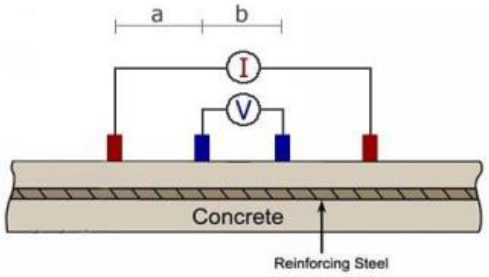

Figure 3.8. Configuration of four probes on the surface of concrete in CEPRA corrosion rate testing (from iCOR manual).

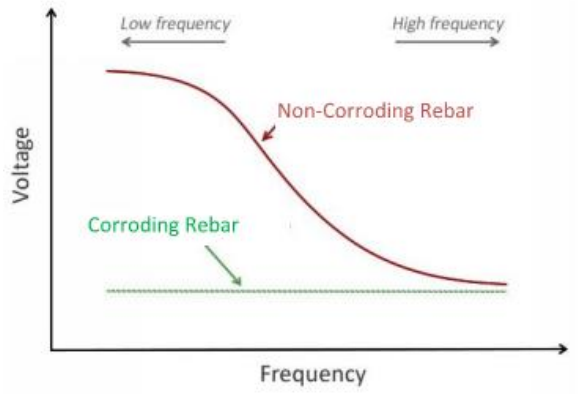

Figure 3.9. Schematic illustration of voltage-frequency response of a corroding and non-corroding rebar, as evaluated by CEPRA corrosion rate testing (from iCOR manual).

Qualitative interpretations of ranges of corrosion rate measurements are summarized in Table 3.5. Note, these values were developed for uncoated reinforcing bars. Epoxy coating on the bars can limit the area that is available to participate in the measurement, but based on WJE's previous experience with corrosion rate testing of epoxy-coated bars, these interpretations of corrosion rate are still reasonable. No adjustment for coating was made in the reporting of results for bridge elements containing epoxy-coated steel (i.e., steel area was entered and calculated in the instrument as if the bar was uncoated).

Table 3.5. Interpretation of Corrosion Rate Measurements

Corrosion Rate		Classification
iCOR (µA/cm²)	**BAC Meter (µm/yr)**	
< 1.0	< 10	Passive / Low
1 to 3	10 to 30	Moderate
3 to 10	30 to 100	High
> 10	> 100	Severe

Figure 3.10. Corrosion rate survey (north abutment).

Figure 3.11. Corrosion rate survey (deck topside).

3.3.1.4. Reinforcement Cover Survey

To determine locations and concrete cover of reinforcing steel, two nondestructive evaluation (NDE) techniques were used: electro-magnetic cover meter and ground penetrating radar (GPR). In addition to the non-destructive testing, limited destructive measures (e.g., drilling and coring) were used for correlation and calibration of the NDE testing results.

Electro-magnetic cover meters utilize a hand-held probe and control unit to identify the location and depth of reinforcement. The probe typically consists of two wire coils; one coil generates a magnetic field, and the second coil monitors changes in the magnetic field caused by the presence of conducting materials. One limitation is that dimension of the reinforcing steel (i.e., bar size) is required for accurate cover depth measurements.

GPR involves the use of a high-frequency radar antenna, which transmits electromagnetic radar pulses along a discrete longitudinal scan at the surface of a structural element. Electromagnetic signals reflected from material interfaces having different dielectric properties (i.e., reinforcing steel embedded in concrete) are collected by the antennae and displayed graphically for direct interpretation in the field. Guidelines for GPR considered during this work included ACI 228.2R-98 *Nondestructive Test Methods for Evaluation of Concrete in Structures* and ASTM D6432 - 11 *Standard Guide for Using the Surface Ground Penetrating Radar Method for Subsurface Investigation*. GPR testing was completed using a handheld GPR 'StructureScan Mini' unit manufactured by GSSI, operating at a central frequency of 2600 MHz.

The approximate depth and spacing of the reinforcing steel were determined using these methods. The results of the testing were verified and calibrated by drilling holes to and directly measuring the cover depth at representative locations in each study area; these drill holes were also used for half-cell ground locations (see Section 3.3.1.3). These methods were also used in combination with visual assessment and sounding to select locations for core sampling. The "representative minimum cover depth" results reported for each study area (see Section 6) are based on interpretation of the various cover measurements.

Figure 3.12. GPR survey on arch rib face

Figure 3.13. GPR survey on deck topside

3.3.1.5. Field Carbonation Testing

Carbonation of concrete was measured in the field by applying a pH indicator (phenolphthalein) to freshly exposed concrete surfaces. The pH indicator was applied to most core samples immediately after extraction. Also, in some study areas, incremental drilling was performed (at approximately 1/16 inch increments) and the pH indicator was applied to the drill holes after each increment. The pH indicator changes from colorless to bright purple above a pH of about 8.5, which is approximately the pH threshold level associated with depassivation of the steel due to carbonation. The depth at which the color change was observed is assumed to be representative of the depth of the carbonation front. These values were recorded for the elements surveyed. Carbonation testing was also repeated on fresh, fractured surfaces on concrete core samples at WJE's laboratory. The "representative carbonation" results reported for each study area (see Section 6) are based on interpretation of all carbonation measurements including lab and field.

Figure 3.14. Example of field carbonation measurement.

Figure 3.15. Example of incremental drilling to determine depth of carbonation.

3.3.1.6. Other Test Methods

3.3.1.6.1. Ultrasonic Thickness Measurements

Ultrasonic thickness testing (UT) was performed on aluminum railing components and on top and bottom chord angles of Melan truss reinforcement as outlined in WJE's memorandum reproduced in Appendix 11. UT testing is conducted using a high-frequency ultrasonic transducer which generates stress waves in metals and measures the travel time of this wave through the cross section. Based on assumed density and wave propagation properties of the material, the measured travel time is converted into the distance traveled, which in turn is used to determine the thickness of the inspected element.

Figure 3.16. Ultrasonic thickness measurement on aluminum railing.

Figure 3.17. Ultrasonic thickness measurement on Melan truss angle in delaminated and spalling corner of arch rib.

3.3.1.6.2. Strain Relief Testing

Strain relief testing was performed as outlined in WJE's memorandum reproduced in Appendix 9. A mock-up of this testing was first performed at WJE's laboratory on a short section of L3.5x3.5x1/4 steel angle with no induced stresses, and the test was repeated in the field on an embedded section of the Melan truss angle identified for testing by HNTB. The test involved removing concrete to expose the outside faces of the truss angle, installing a strain gage on the top surface of the horizontal leg of the angle, and cutting out a 2 inch diameter disc of the angle leg around the strain gage using a magnetic drill press. The strain in the disc before and after cutting was recorded with a C2A-06-062WW-350 stacked Rosette strain gage and a Micro-Measurements P3 strain indicator.

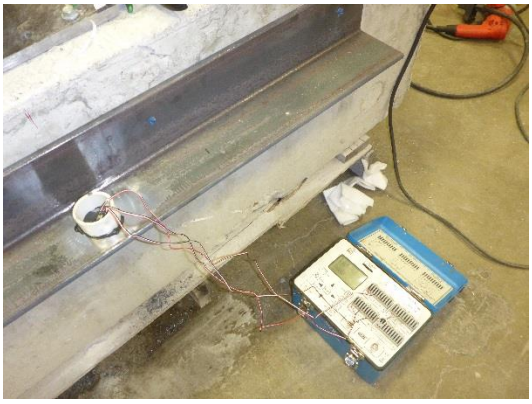

Figure 3.18. Strain measurement on lab mock-up before coring out disc.

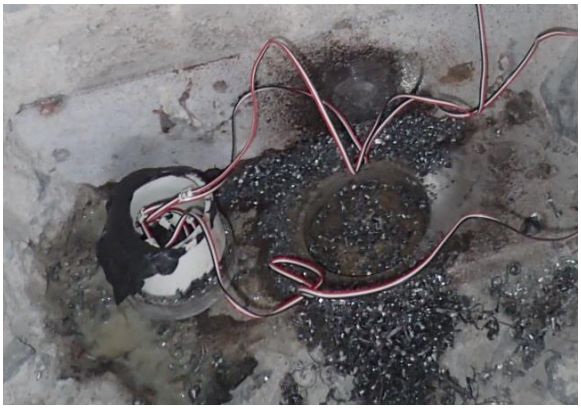

Figure 3.19. Strain measurement in field after coring out disc.

3.3.1.6.3. X-ray Florescence Testing

X-ray florescence (XRF) testing was performed on the aluminum railing components as outlined in WJE's memorandum reproduced in Appendix 11.RF is a technique allowing non-destructive elemental analysis of materials. The surface to be analyzed is irradiated with x-rays, resulting in the production of fluorescent x-rays, the energies of which are characteristic of the elements present. The instrument provides a table with the concentrations of the detected elements. The concentrations reported and internal calibration curves are used to identify different material types, including metal alloy identification. Portions of the metal to be analyzed were exposed and analyzed with the Innov-X-Systems Olympus Omega-6000 handheld XRF using Xpress Alloy mode, which is suitable for alloy identification.

Figure 3.20. XRF testing on bottom rail of aluminum railing.

Figure 3.21. Disassembly of railing connection for XRF testing of various components.

3.3.2. Laboratory Analysis

Materials testing was performed at WJE's laboratory facility in Northbrook, Illinois as described below.

3.3.2.1. Concrete Compressive Strength and Elastic Modulus

The compressive strength and modulus of elasticity of the concrete were evaluated as described in WJE's memorandum to HNTB reproduced in Appendix 9. Concrete core samples were prepared and tested in general accordance to ASTM C42 *Standard Test Method for Obtaining and Testing Drilled Cores and Sawed Beams of Concrete*. For select core samples, elastic modulus was measured according to ASTM C469 *Standard Test Method for Static Modulus of Elasticity and Poisson's Ratio of Concrete in Compression*.

3.3.2.2. Chloride Testing

Chloride content testing was performed on selected core samples to determine whether chloride contamination from deicing salts has accumulated to sufficient levels to promote corrosion. Selected core samples were cut into slices at pre-determined depths, and the slices were pulverized to facilitate acid-soluble chloride content analysis in general conformance with ASTM C1152 *Test Method for Acid-Soluble Chloride in Mortar and Concrete*. The acid-soluble chloride content represents both water-soluble and chemically-bound chloride within the cement paste and any chloride that may be present in the aggregate. Chloride concentrations listed in this report are given in terms of percent by weight of concrete.

Typically, four to eight 1/8 to 1/4 inch thick slices were cut from the tested core samples, at depths ranging from 1/4 to 6 inches from the exterior surface. When evaluating cracked cores, sawcuts were made 1 inch on either side of the crack (for a total width of 2 inches), and the portions of concrete away from the crack were discarded; then, 1/4 inch thick slices were cut from the remaining sample at five depths generally spaced between the surface and the reinforcing bars. On core samples subject to two-sided exposure (e.g., through-thickness deck cores and a core through the web of a prestressed girder), slices were collected working inward from both exposed surfaces. Chloride concentrations were also measured at a sufficient depth such that diffusion of surface chlorides was unlikely, so that any measured chloride concentration could be assumed to be an initial chloride concentration or "background" chloride concentration. Based on the obtained chloride profiles (see Section 6.0), which taper to near zero chloride levels with depth from the surface, no background (e.g., admixed chloride as an accelerator) or bound chloride (e.g., in the aggregate) is present in the tested samples.

3.3.2.3. Petrographic Analysis

Petrographic analysis of selected core samples were conducted as described in WJE's memorandum reproduced in Appendix 10 - Petrographic Analysis. The samples of concrete selected for petrographic analysis were examined visually and microscopically in accordance with the applicable procedures of ASTM C 856 *Standard Practice for Petrographic Examination of Hardened Concrete*. A petrographic examination consists of a series of observations that are interpreted to draw conclusions about the composition, quality, and cause(s) of any deterioration present.

The core samples were first visually assessed to categorize the different concrete mixtures present throughout the structure. Then, based on these results, in-depth petrographic examinations were performed on representative samples from each mixture type.

For the in-depth petrographic examinations, each core was generally cut in half parallel to the core axis using a continuous-rim, water-cooled diamond saw blade. One of the resulting plane surfaces was lapped

(ground smooth and polished) using progressively finer grinding abrasives or diamond-impregnated plates. A thin section (a 15- to 20-micrometer thick slice taken from the concrete specimen) was also prepared for Core 10, Core 12, and Core 37. The lapped surfaces and the thin sections were examined microscopically using methods outlined in ASTM C856. Powder immersion mounts of the paste from selected cores were also prepared and examined to determine the composition of cementitious materials and secondary deposits.

Depth of carbonation was also tested by breaking the cores and applying phenolphthalein solution and/or universal pH solution onto freshly exposed concrete surfaces. This testing was performed on nearly all samples received, including core samples scheduled for compressive strength, chloride ion analysis, and petrography.

Finally, selected cores taken in areas of visually apparent freeze-thaw distress were sectioned, and a cut surface was examined to determine the affected depth of freeze-thaw distress.

3.3.2.4. Steel Strength and Composition

Tensile strength testing and chemical composition determination were conducted as described in WJE's memorandum to HNTB reproduced in Appendix 9. Samples were selected by WJE, and the specimens were tested by Engineering Systems, Inc. (ESI) of Aurora, IL. Tensile properties were evaluated on specimens machined from the as-received steel specimens in accordance with ASTM A370, *Standard Test Methods and Definitions for Mechanical Testing of Steel Properties*. Chemical composition was evaluated by optical emission spectroscopy (OES) in accordance with ASTM E415, *Standard Test Method for Analysis of Carbon and Low-Alloy Steel by Spark Atomic Emission Spectrometry*.

4. IN-DEPTH ELEMENT LEVEL INSPECTION RESULTS

This chapter summarizes the results of the in-depth element level inspections, including the findings of both up-close visual and sounding examinations, performed as described in Chapter 3. The condition-state information collected by the field inspection was the as-found condition, and not necessarily the quantity or area that would need repair or replacement in a bridge rehabilitation program.

All inspection information was documented on WJE's Plannotate software (described in more detail in Section 4.2) and is available online for access. Various links in this report and its appendices are made to the Plannotate website. Because the site is access-controlled for data integrity, external usernames have been created for MnDOT and HNTB's use. Contact the authors of this report for access information and training.

https://plannotate2.wje.com/prod

4.1. Work Performed

The in-depth inspection work was performed by WJE on weekdays primarily during the weeks of May 1, May 8, and May 15. Traffic control was provided by Warning Lites, under contract to HNTB, and consisted of closing either the upstream or downstream outer lane to allow 9 to 10 hours of inspection time per day. Inspection of the center two lanes of deck occurred under a separate lane closure during a follow-up weekend. Some elements accessible without snoopers were inspected by two-person WJE teams on subsequent weeks, including arch span superstructure and abutment elements accessible from grade or from the catwalks.

The following elements were included in the inspection:

1. North and south approach spans
   a. Deck: reinforced concrete deck, wearing surface, expansion joints
   b. Deck railings: historic pedestrian railings; cursory inspection of barrier walls
   c. Superstructure: girders, stringers, cross-bracing, diaphragms
   d. Bearings
   e. Substructure: Columns, pier walls, bent caps, abutments, wing walls, back walls
   f. Retaining walls beyond north abutment
   g. North approach span vertical circulation structure
2. Main arch spans
   a. Deck: reinforced concrete deck, wearing surface, expansion joints
   b. Deck railings: historic pedestrian railings; cursory inspection of barrier walls
   c. Superstructure: spandrel columns, spandrel walls, cap beams, arch ribs, barrel arches
   d. Substructure: arch piers to the waterline[12]

4.2. Documentation of Inspection Conditions

Inspection observations, notes, and locations of photographs were documented electronically using tablet computers prepopulated with the necessary elevation or plan view field sheets. The field sheets were

[12] Inspection of the pier concrete within arm's reach of the waterline, as well as the below-water portions of piers, was performed by Collins Engineers under a separate contract with MnDOT. Refer to WJE memorandum dated April 5, 2017 (included in Appendix 1) for coordination of Collins' scope and methods of inspection with the broader bridge inspection led by WJE. Collins' field inspection sheets are included as Appendix 15.

developed by WJE based on review of historical drawing information provided by HNTB and MnDOT, as well as from field observations and photographs where historical drawings were not available or complete.

WJE's inspection field sheets for the various bridge elements are listed in Table 4.1. In the right-hand column of the table, links are provided to the completed field sheets in Plannotate. Clicking on the links in the table will open WJE's Plannotate software and display all of the field inspection notes for that particular element. Login credentials will be required as described above. Within Plannotate, the user can view all inspection notes that were recorded, including condition states, special notes, and photographs of the various conditions present. Static PDFs of all of the completed field sheets, along with a legend for the annotation symbols that were utilized for this project, are attached to this report as Appendix 2.

Table 4.1. List of Field Sheets and Links to Completed Inspection Notes

Sheet Name	Number of Pages	Elements	Link to Plannotate Sheet with All Inspection Notes
Approach Spans			
Bents and Abutments	5	▪ South Approach Abutment ▪ South Approach Wing Walls ▪ South Approach Retaining Walls ▪ South Approach Bent B1 ▪ North Approach Abutment ▪ North Approach Wing Walls ▪ North Approach Retaining Walls ▪ North Approach Bent B2	Link
Deck Underside - Approaches	2	▪ South Approach Deck and Superstructure ▪ North Approach Deck and Superstructure	Link
Arch Spans			
Deck Underside - Arch Spans	9	▪ Arch Span 1-7 Deck Underside (one page per span; pages 1 & 9 show approach spans for reference only)	Link
Arch Pier 1	2	▪ Arch Pier 1 interior and exterior	Link
Arch Pier 2	2	▪ Arch Pier 2 interior and exterior	Link
Arch Pier 3	2	▪ Arch Pier 3 interior and exterior	Link
Arch Pier 4	2	▪ Arch Pier 4 interior and exterior	Link
Arch Pier 5	2	▪ Arch Pier 5 interior and exterior	Link
Arch Pier 6	2	▪ Arch Pier 6 interior and exterior	Link
Arch Pier 7	2	▪ Arch Pier 7 interior and exterior	Link
Arch Pier 8	2	▪ Arch Pier 8 interior and exterior	Link
Arch Piers_FloorPlans	2	▪ Plan views of tops of bases for Arch Piers 1 through 8	Link
S1_Arch Ribs	3	▪ Span 1 Arch Ribs - downstream, middle, and upstream ▪ Span 1 Spandrel Columns - upstream and downstream elevations	Link
S2_Arch Ribs	3	▪ Span 2 Arch Ribs - downstream, middle, and upstream ▪ Span 2 Spandrel Columns - upstream and downstream elevations	Link
S3_Arch Ribs	3	▪ Span 3 Arch Ribs - downstream, middle, and upstream ▪ Span 3 Spandrel Columns - upstream and downstream elevations	Link

Sheet Name	Number of Pages	Elements	Link to Plannotate Sheet with All Inspection Notes
S4_Arch Ribs	3	▪ Span 4 Arch Ribs - downstream, middle, and upstream ▪ Span 4 Spandrel Columns - upstream and downstream elevations	Link
S5_Arch Ribs	3	▪ Span 5 Arch Ribs - downstream, middle, and upstream ▪ Span 5 Spandrel Columns - upstream and downstream elevations	Link
S6_Arch Ribs	3	▪ Span 6 Arch Ribs - downstream, middle, and upstream ▪ Span 6 Spandrel Columns - upstream and downstream elevations	Link
S7_Arch Ribs	3	▪ Span 7 Arch Ribs - downstream, middle, and upstream ▪ Span 7 Spandrel Columns - upstream and downstream elevations	Link
S1_Spandrel Columns	2	▪ Span 1 Spandrel Columns - north and south elevations	Link
S2_Spandrel Columns	2	▪ Span 2 Spandrel Columns - north and south elevations	Link
S3_Spandrel Columns	2	▪ Span 3 Spandrel Columns - north and south elevations	Link
S4_Spandrel Columns	2	▪ Span 4 Spandrel Columns - north and south elevations	Link
S5_Spandrel Columns	2	▪ Span 5 Spandrel Columns - north and south elevations	Link
S6_Spandrel Columns	2	▪ Span 6 Spandrel Columns - north and south elevations	Link
S7_Spandrel Columns	2	▪ Span 7 Spandrel Columns - north and south elevations	Link

4.2.1. Plannotate – Electronic Data Collection

Plannotate® is WJE's in-house electronic field-note platform. Deployed on iPads for use in the field, it allows multiple users to make annotations to PDFs in real-time and tag photographs to specific locations. Data from Plannotate is uploaded to a remote cloud server and stored in a database so that engineers in the field and in the office are updated on status in real-time. This system also allows project work to stop and resume exactly where the last inspector left-off, which provides flexibility in performing assessments when access may be limited to irregular time periods or operational demands. Because WJE developed the software in-house, the Plannotate system is customizable by WJE software experts to fit the needs of any particular structure or defined assessment plan. On large scale multi-week projects such as this, Plannotate allows for improved efficiency, organization and consistency in the data collection.

4.2.2. Condition State Definitions

For this in-depth inspection, Plannotate was customized to record conditions and observations in line with the condition states defined in the 2016 MNDOT Bridge Inspection Field Manual. This included customized definitions of cracking, delaminations and spalls, efflorescence, moisture/rust staining, patches, and scale, wear or abrasion. WJE added other types of concrete distress that were not listed in the Bridge Inspection Field Manual, namely freeze-thaw and coating conditions states.

The condition state definition associated with each pre-defined condition state is summarized in Table 4.2 below, and the legend showing their representation on the field sheets is reproduced in Figure 4.1. Note that the colors darken as the severity of the condition worsens. Representative photographs of the non-standard "Coating" and "Freeze-Thaw" conditions states created by WJE for this project are provided in Figure 4.2 through Figure 4.9.

Table 4.2. Customized Plannotate Condition States for In-depth Inspection

Condition State	Units	Definition for Purpose of Inspection			
		CS1	CS2	CS3	CS4
		Good	Fair	Poor	Severe
Coating	SF	Sound	Fair, some distress	Moderate, lots of flaking	Severe, failure
Crack*	LF	<0.012" or sealed	0.012 to 0.050"	> 0.050"	Structural impact
Delamination, spall, or exposed rebar*	SF	N/A	Delamination, or spall < 1" deep	Spall 1-4" deep or exposed bars	Spall >4" deep or severe rebar section loss
Efflorescence*	SF	N/A	Light leaching, little build-up	Heavy leaching with build-up	N/A
Freeze-thaw	SF	Map cracking only	Fair, surface scaling, no exposed bars	Poor, up to 2", no exposed bars	Severe, 2" or more, exposed bars
Moisture staining / rust staining*	SF	N/A	Moisture or minor rust stains (chairs)	Moderate moisture of severe rust stains	N/A
Patch*	SF	N/A	Sound patch	Deteriorated patch	Failed patch**
Scale, wear or abrasion*	SF	<1/4" deep	1/4" to 1/2" deep	1/2" to 1-1/2" deep	> 1-1/2" deep

** Aligned with definition in MnDOT Bridge Inspection Field Manual*
*** To provide distinction from deteriorated patches, any patch which had failed (spalled or delaminated) was rated as CS4. However, none met the MnDOT CS4 definition, which is a patch that requires immediate or high-priority repair.*

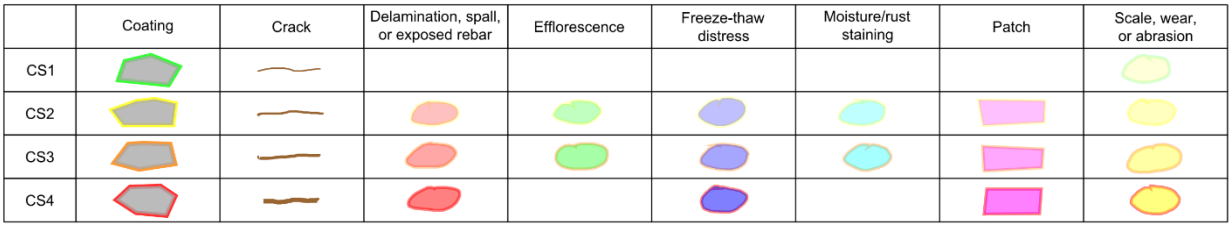

Figure 4.1. Customized legend for condition states shown on field sheets.

Coating Condition States

Figure 4.2. ***Coating Condition State 1.*** *Sound, no distress.*

Figure 4.3. ***Coating Condition State 2.*** *Fair, some distress, including cracking and evidence of moisture movement behind coating.*

Figure 4.4. ***Coating Condition State 3.*** *Flaking and small areas of debonding.*

Figure 4.5. ***Coating Condition State 4.*** *Debonding of large areas of coating.*

Freeze-Thaw Condition States

Figure 4.6. ***Freeze-Thaw Condition State 1.*** *Map cracking and moisture staining only.*

Figure 4.7. ***Freeze-Thaw Condition State 2.*** *Surface scaling without substantial material loss.*

Figure 4.8. ***Freeze-Thaw Condition State 3.*** *Up to 2 inches (by depth) of concrete deterioration.*

Figure 4.9. ***Freeze-Thaw Condition State 4.*** *Concrete disintegration and erosion extending greater than 2 inches in depth from original section, or exposed bars.*

4.3. MnDOT / NBI Routine Inspection Data for SIMS Entry

In addition to this report, WJE provided the results of the bridge inspection in the form of a routine MnDOT element level bridge inspection. This data, including quantities and associated condition states, was transmitted to HNTB and MnDOT in a draft document on September 6, 2017, which is reproduced in Appendix 3 for reference. During preparation of the data, WJE interacted with Ms. Jennifer Wells of MnDOT to confirm how certain elements and quantities should be identified in order to follow MnDOT's element level inspection procedures.

For ease of use, the data was provided in the same format as the 2016 inspection report performed by MnDOT for Bridge 2440, with all changes and updates to the information highlighted in yellow. Changes

included confirmation or revision to the total quantities for the elements, breakdown of quantities by condition state definition (CS1 through CS4) for each element, and updated notes regarding special conditions observed for each element. It is anticipated that MnDOT will review and enter the data into SIMS as the 2017 routine inspection for the bridge. As part of this data, WJE recommended a reduction in the NBI rating for the bridge superstructure (from 6 to 4) and bridge deck (from 6 to 5) in keeping with the inspection findings as described in the remainder of this report (also see Section 7.2.2).

It should be noted that the manner in which the elements are identified and the quantities are calculated in the element level inspection procedure are different than will be needed in order to develop repair quantities for a bridge rehabilitation project. For example, in the element level inspection, the arch ribs and spandrel columns are considered together using a quantity of linear foot (not square foot) along the length of the arch rib. This is clearly much different than will be needed to estimate and specify concrete repairs, which usually are based on a square footage of surface area and are likely to require unique considerations and details that account for the type and geometry of the element, the nature and rationale for repair, and the cause and severity of the distress.

4.4. General Observations by Element

This section summarizes typical and most atypical conditions observed during the inspection. Complete and more detailed information is contained in WJE's Plannotate notes that are accessible online as described above.

4.4.1. Arch Spans

4.4.1.1. Deck Components

4.4.1.1.1. Deck Underside

Condition of the deck underside in the five arch rib and two arch barrel spans was similar. Overall, concrete distress was more prevalent and advanced on the downstream side of the deck.

Typical Conditions

- Severe concrete distress was present in a band approximately 1 to 2 feet wide on the downstream deck edge (fascia). This was typical on all arch spans, with spalls, exposed bars, delaminations, cracks, and efflorescence present (Figure 4.10). The exposed reinforcing bars were heavily corroded and had significant section loss, with multiple locations of loose and/or missing rebar. At some locations, the spalls coincided with the concrete posts for the pedestrian railings above. Similar distress was present on the upstream slab edge, but was comparatively less advanced and sparser (Figure 4.11).
- Spalls were present at the bottom corner of the expansion joints on the downstream deck edge (Figure 4.12). On the upstream edge, spalls and concrete distress were not as widespread and were more varied. Deteriorated concrete repair material was observed along the edge regions of at least 50 percent of the expansion joints (Figure 4.13).
- Longitudinally-oriented 1 to 3 foot wide strips of concrete distress were located at the center line and quarter-point between the center and deck edge (Figure 4.14). Corrosion staining was typically visible along the surface of the delaminated concrete, and intermittent spalls and exposed bars were present. However, where the bottom bars were exposed, section loss was typically minor (less than 10 percent).
- Along expansion joints, either previous concrete repairs or concrete distress was present in a strip approximately 1 to 2 foot wide on the north and south sides of cap beams (Figure 4.15). These repairs

were partial depth shotcrete, based on surface appearance and exposure at a few spalled areas. The repairs were often delaminated and cracked, and occasionally spalled. Where concrete repairs had not been performed, an approximately 1 to 2 foot wide delamination was typically present alongside the cap beam.

- In areas away from the expansion joints, intermittent longitudinal cracks with light efflorescence, light rust staining, and occasional delaminations were present (Figure 4.16).

Atypical Conditions

- Large spalls with exposed and severely corroded bottom reinforcing bars were present at the deck underside around the manholes in the outer southbound lane above Piers 1, 6, and 8 (Figure 4.17). Section loss to the reinforcing steel was severe and measured up to 50 percent at Pier 8. This condition is further described in a WJE memorandum to HNTB reproduced in Appendix 4.

Figure 4.10. Downstream deck edge condition.

Figure 4.11. Upstream deck edge condition.

Figure 4.12. Downstream deck edge spall at expansion joint.

Figure 4.13. Upstream deck edge repair at expansion joint.

Figure 4.14. Slab underside delamination at centerline of deck.

Figure 4.15. Slab underside concrete repair at expansion joints.

Figure 4.16. Slab underside cracks and delaminations throughout deck.

Figure 4.17. Slab underside spalls and rebar section loss at manholes in southbound lane.

4.4.1.1.2. Deck Topside - Wearing Surface

Typical Conditions

- Numerous, densely-spaced longitudinal and transverse cracks were present throughout the wearing surface, often spaced 1 to 2 feet on center and ranging from 0.005 to 0.020 inches wide. Very occasional cracks were greater than 0.050 inches wide, including a longitudinal crack typically located a few feet downstream from the roadway centerline. Crack density was greater over cap beams (Figure 4.18).
- Wider longitudinal cracks visible on the wearing surface, and aligned with longitudinal cracks visible on the deck underside, were present in some regions and indicated full-thickness cracking conditions. In most spans, this generally included a crack near the centerline and two to three other cracks between the centerline and the edge of the deck on both the northbound and southbound sides. This is illustrated for a typical arch span in the representative views of the topside and underside shown in Figure 4.19.
- The riding surface was in generally good condition, with little to no scale, wear, or abrasion of the overlay surface.

- Delaminations and shallow spalls were occasionally present. Spalls were most common along the construction joint in the overlay at the roadway centerline, along the wide longitudinal crack just downstream from the centerline, and at the interface between the concrete slab and nosing material at expansion joints.
- Concrete repairs had been performed around expansion joints and at occasional areas away from joints. Most of the concrete repairs on the wearing surface were sound.
- Crack density in each span was calculated based on field measurements and digital mapping of the cracks that allowed quantity calculations. A color-graduated plot of the crack density by span is shown in Figure 4.20. Overall, crack density was highest in the arch spans, averaging 0.33 to 0.53 feet of crack / sq. ft. of deck. Cracking in the approach spans was much less, at 0.19 ft / sq. ft. for the south approach and 0.07 ft / sq. ft. for the north approach. Crack density in the sidewalks was also much less, averaging 0.09 ft / sq. ft.

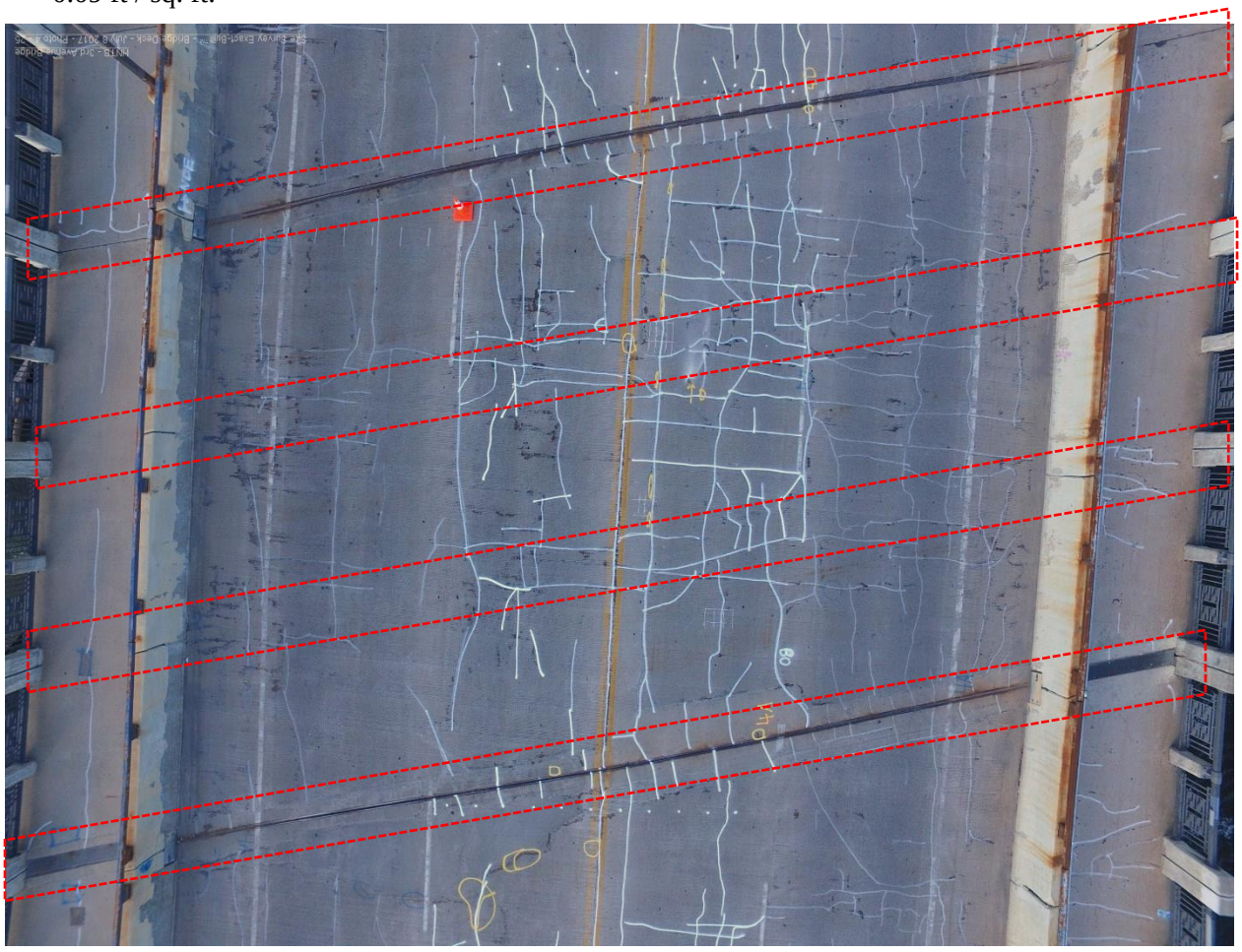

Figure 4.18. Sample aerial drone image of deck span 4A to 4D. Deck cracks were field-marked with non-permanent white spray chalk. Delaminations were circled in yellow. Locations of cap beams below indicated by dotted red lines.

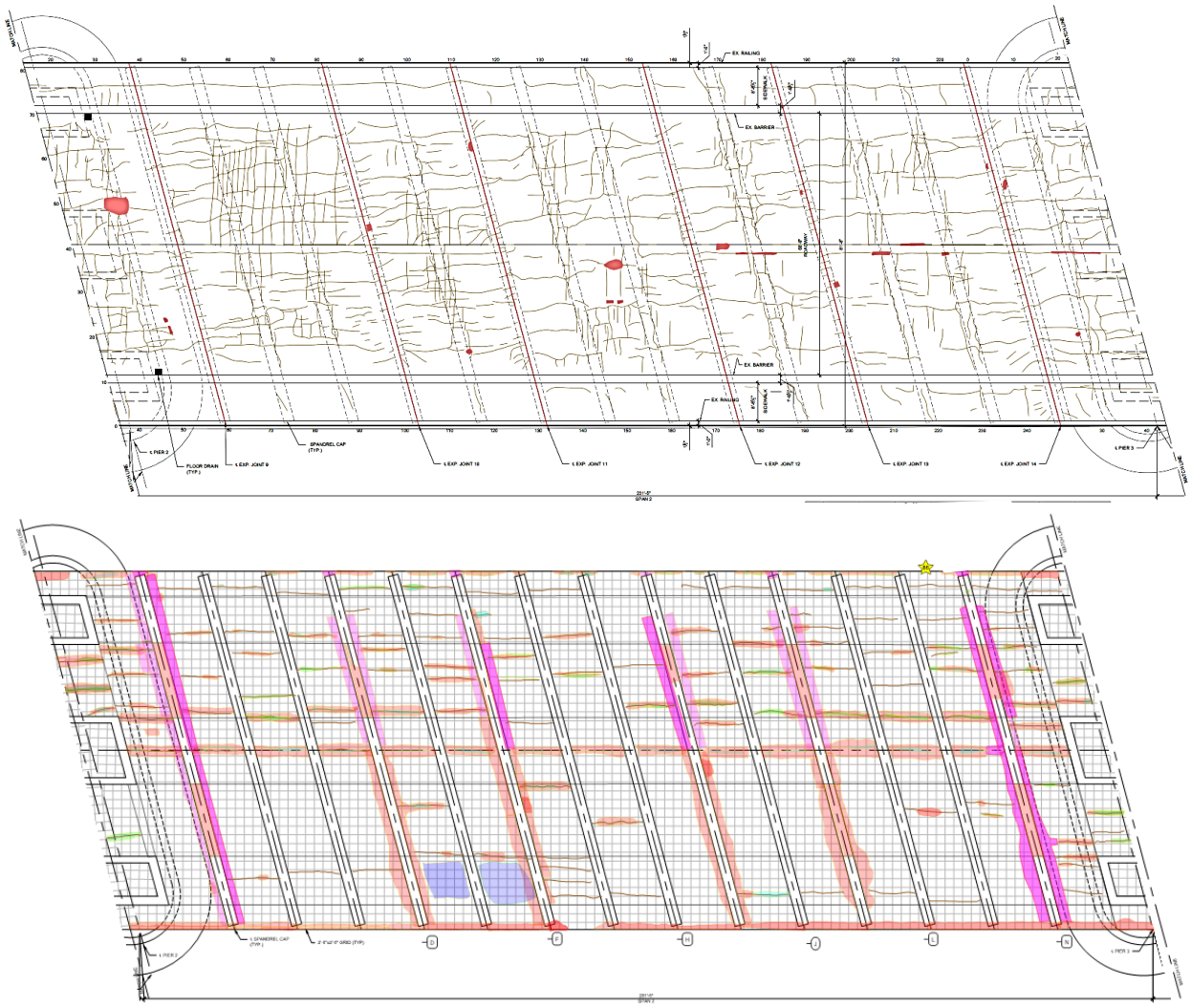

Figure 4.19. Concrete distress for representative arch span (Arch Span 2) deck topside (top figure) and deck underside (bottom figure). See legend in Figure 4.1. See Appendix 2 for field inspection sheets for all spans and all elements.

	South Approach Spans						Arch Span 1						Arch Span 2						Arch Span 3					
Bridge Span	00-40	40-80	80-120	120-16-	160-200	200-1A	1A-1D	1D-1F	1F-1I	1I-1K	1K-1N	1N-2A	2A-2D	2D-2F	2F-2I	2I-2K	2K-2N	2N-3A	3A-3D	3D-3F	3F-3I	3I-3K	3K-3N	3N-4A
SB Sidewalk	0.05	0.00	0.00	0.00	0.00	0.00	0.12	0.11	0.13	0.08	0.13	0.13	0.10	0.11	0.12	0.13	0.15	0.08	0.12	0.08	0.07	0.05	0.07	0.11
SB Right lane	0.02	0.14	0.22	0.21	0.11	0.59	0.54	0.46	0.48	0.34	0.51	0.40	0.50	0.26	0.29	0.27	0.31	0.25	0.25	0.19	0.29	0.22	0.19	0.23
SB Center Lane	0.16	0.11	0.16	0.15	0.09	0.27	0.34	0.34	0.40	0.42	0.38	0.45	0.60	0.62	0.34	0.37	0.26	0.42	0.31	0.37	0.44	0.32	0.34	0.36
NB Center Lane	0.08	0.19	0.33	0.26	0.17	0.48	0.51	0.37	0.39	0.58	0.62	0.42	0.47	0.57	0.35	0.34	0.35	0.38	0.34	0.49	0.49	0.33	0.58	0.46
NB Right Lane	0.03	0.06	0.17	0.12	0.11	0.39	0.49	0.40	0.31	0.56	0.43	0.33	0.35	0.35	0.33	0.30	0.24	0.33	0.26	0.31	0.30	0.23	0.35	0.34
NB Sidewalk	0.00	0.05	0.24	0.13	0.00	0.09	0.05	0.05	0.08	0.07	0.04	0.05	0.03	0.03	0.06	0.10	0.17	0.17	0.13	0.29	0.13	0.13	0.13	0.32

	Arch Span 4						Arch Span 5						Arch Span 6				Arch Span 7				North Approach Spans				
Bridge Span	4A-4D	4D-4F	4F-4I	4I-4K	4K-4N	4N-5A	5A-5D	5D-5F	5F-5I	5I-5K	5K-5N	5N-6A	6A-6D	6D-6G	6G-6J	6J-7A	7A-7D	7D-7G	7G-7J	7J-N_APP	00-40	40-80	80-120	120-60	160-200
SB Sidewalk	0.08	0.10	0.05	0.04	0.01	0.03	0.07	0.11	0.08	0.07	0.05	0.42	0.11	0.13	0.11	0.08	0.12	0.13	0.12	0.20	0.00	0.00	0.00	0.00	0.00
SB Right lane	0.23	0.26	0.24	0.24	0.20	0.30	0.23	0.23	0.35	0.23	0.34	0.56	0.35	0.42	0.35	0.30	0.48	0.36	0.30	0.43	0.01	0.00	0.00	0.00	0.02
SB Center Lane	0.48	0.52	0.36	0.50	0.56	0.47	0.47	0.47	0.70	0.64	0.50	1.02	0.71	0.74	0.46	0.52	0.62	0.59	0.50	0.50	0.15	0.09	0.10	0.06	0.15
NB Center Lane	0.66	0.41	0.78	0.63	0.68	0.93	0.61	0.69	0.47	0.54	0.53	0.84	0.57	0.78	0.60	0.67	0.60	0.63	0.49	0.53	0.05	0.13	0.18	0.09	0.06
NB Right Lane	0.47	0.42	0.48	0.50	0.52	0.44	0.53	0.50	0.42	0.42	0.46	0.61	0.49	0.57	0.53	0.45	0.29	0.44	0.22	0.33	0.04	0.06	0.11	0.03	0.04
NB Sidewalk	0.22	0.26	0.20	0.16	0.05	0.09	0.05	0.11	0.08	0.07	0.03	0.34	0.11	0.15	0.11	0.12	0.09	0.14	0.09	0.12	0.00	0.00	0.00	0.00	0.00

Figure 4.20. Crack density by span for the deck topside. Green colors indicate values closer to zero and red indicates values closer to 1 ft crack / sq ft of deck.

4.4.1.1.3. Deck Topside - Sidewalk

Typical Conditions

- Transverse cracks, typically 0.005 to 0.02 inches wide, were typically present over cap beams. The overall crack density on the sidewalk was much lower than on the wearing surface (see Figure 4.20 and Figure 4.21).
- A longitudinal crack was present in the sidewalk at the centerline between the upstream edge of the deck and the upstream concrete barrier over 50 percent of the length of the arch spans (Figure 4.22).
- Cracks originated at the corners of penetrations in the sidewalk such as catwalk access hatches and utility vault access manholes. Most cracks were 0.005 to 0.020 inches wide, though occasional cracks were wider than 0.050 inches. (Figure 4.23).
- Closely-spaced cracks parallel and adjacent to joints, similar in appearance to slab-on-grade D-cracking, were present at poured sealant joints (Figure 4.24). Small spalls and delaminations were occasionally associated with this cracking.
- Other delaminations and shallow spalls were occasionally present (Figure 4.25). Intermittent spalls less than one square foot in area appeared to be caused by aggregate popouts (Figure 4.26).

Figure 4.21. Sidewalk cracks over cap beam.

Figure 4.22. Longitudinal crack along upstream sidewalk.

Figure 4.23. Cracks originating from catwalk access hatch.

Figure 4.24. Distress similar to D-cracking at poured sealant joints.

Figure 4.25. Large sidewalk delamination.

Figure 4.26. Small aggregate pop-out.

4.4.1.1.4. Expansion Joints

Typical Conditions

- Above Columns A and N adjacent to piers, the strip seal expansion joints continued from the roadway into the sidewalk and were covered by metal cover plates. At expansion joints at other columns (D, F, I, and K), strip seal joints were present in the roadway but poured sealant joints were present in the sidewalks.
- Previous concrete repairs were present adjacent to poured sealant joints, likely associated with the 2003 deck expansion joint rehabilitation project. Concrete repairs along strip seal expansion joints over Columns A and N were typical and spanned the entire width of the sidewalk (Figure 4.27, Figure 4.28).
- Strip seal glands were filled with debris (Figure 4.29). Where the debris was removed for inspection, the glands appeared in good condition.
- Transverse cracks and small spalls were present in the strip seal nosing material. Most cracks were less than 0.010 inches wide.
- Surface corrosion was present on the exposed strip seal steel nosing. The corrosion did not appear to affect the function of the joints.
- D-cracking, delaminations, and shallow spalls were present in concrete adjacent to poured sealant joints (see Figure 4.24 in sidewalk conditions).
- Sections of poured sealant were missing. These sections of missing sealant typically did not exceed 3 feet in length (Figure 4.30). In some locations, the poured sealant joints were tightly closed in the sidewalks.
- Joint width measurements were performed at different times over the course of the field work. See Chapter 5 for data and related findings.
- Evidence of past leakage was evident at most of the expansion joints, in the form of efflorescence, moisture, or rust stains on the concrete elements below them. However, the current water tightness of the joint system seemed relatively good. Over the course of the inspection, rain events were occasionally observed. At those times, active leaks were observed through only a few joints. WJE estimates the leaking regions of expansion joint represented approximately 10 percent or less of the sealed joint area.

Figure 4.27. Concrete repair and delamination at poured seal.

Figure 4.28. Repair material at steel cover plates over strip seal joints.

Figure 4.29. Strip seal gland filled with debris. Cracks and spalls are present in the nosing material.

Figure 4.30. Missing section of poured sealant.

4.4.1.2. Superstructure

4.4.1.2.1. Cap Beams

Typical Conditions

- Along expansion joints, heavy moisture staining, efflorescence, and widespread delaminations were present on the north and south faces. These conditions were typically more severe between spandrel columns than directly over them (Figure 4.31). Away from expansion joints, cap beams were in much better condition and exhibited very infrequent deterioration.
- Beneath expansion joints, spalls and delaminations were often present on the undersides of the cap beams between spandrel columns. Wide cracks and rust stains were often present along the delaminated concrete on the vertical and underside faces. Where concrete was spalled, longitudinal rebar and stirrups were typically exposed, with section loss usually less than 10 percent (Figure 4.32).

Atypical Conditions

- A large spall with fractured stirrups was identified on the underside of Cap Beam 5N between the middle and upstream spandrel columns (Figure 4.33).
- Shear or torsional cracks were present on several cap beams in Spans 1 and 7 (e.g., in Span 1 at columns E, G, and H; and Span 7 at Columns E and F). The cracks were often wider than 0.050 inches and spalls were sometimes present along them (Figure 4.34).
- Deep spalls at the top corners of the cap beams, with exposed vertical dowels, were often present at the deck underside interface. This condition was present at Column A of all arch spans, Column N of Spans 1 through 5, Column K of Span 4, and Column J of Span 6. Exposed dowels were often severely corroded and in some cases bent or fractured at the deck/cap beam interface (Figure 4.35 and Figure 4.36). There was no evidence of foam surround at most of the exposed vertical dowels. Refer to Chapter 5 for additional details.

Figure 4.31. Cap beam conditions under expansion joints.

Figure 4.32. Cap beam underside delamination.

Figure 4.33. Cap beam stirrups corroded through.

Figure 4.34. Cap beam shear or torsional crack.

Figure 4.35. Deep cap beam spall with exposed vertical dowels into deck.

Figure 4.36. Deep spalling along top corner of cap beam.

4.4.1.2.2. Spandrel Columns and Walls

Typical Conditions - Spans 1 through 5 (Columns)

- The tops of all of the spandrel columns were rebuilt as part of the 1980 rehabilitation. The drawings showed, at minimum, the top two feet of each column were replaced. However, the drawings did not indicate the overall height of replacement on each column, which was found to vary at each location. In addition, some areas had partial-depth repairs, evidenced by repair material present only on one face of the column. The columns were all coated with a special surface finish after rehabilitation, somewhat obscuring the interface between the 1980 and 1918 concrete. WJE inspectors made a distinction between the three generations of concrete based on surface texture: the 1918 concrete had a distinct form board finish; the 1980 partial-depth repairs were rough in texture but did not have form-board finish and were often map-cracked; and the 1980 full-depth repairs were smooth-surfaced and did not have form-board finish (Figure 4.37).
- Cracks, delaminations, and spalls were widespread in the lower (1918) portions of the columns, particularly in those located below expansion joints. This distress often covered more than 50 percent of the surface area. The most common location of the distress was at vertical reinforcing bars at the center and corners of the columns (Figure 4.38). Some cracks exceeded 0.050 inches in width, also typically at the corners. Steel section loss was typically less than 10 percent.
- Surface deterioration of the original 1918 concrete was typical. At many locations where the coating had failed, the cement paste was eroded, exposing aggregate and near-surface voids. This condition was most common on columns located beneath expansion joints.
- The upper (1980) columns located at expansion joints often exhibited cracks, delaminations, and spalls. Usually this was limited, but on 5 columns this exceeded 20 percent of the surface area. On columns not at expansion joints, concrete distress due to corrosion was rare and was only identified in isolated areas.
- The partial-depth concrete repair material was often map cracked (Figure 4.39). The repairs themselves were sometimes debonded from the substrate concrete, as identified by hammer sounding. This repair material was often located at the corners of the columns where the 1980 rehabilitation work had left portions of the original 1918 concrete to remain below the new full-depth concrete. At a few locations of deterioration, steel wire mesh reinforcement was observed within the repair material. The thickness of the repair material was highly variable, ranging from as little as 1/4 inch up to 6 inches, with variation often identified within the same repair area (Figure 4.40).

Typical Conditions - Spans 6 and 7 (Walls)

- Cracks originated at corners of catwalk and utility duct openings. The cracks were typically greater than 0.020 inches wide, with some crack widths exceeding 0.050 inches (Figure 4.41 and Figure 4.42).
- Cracks and occasional delaminations were present along vertical and horizontal reinforcing bars. Full-height cracks between 0.010 and 0.020 inches in width were common at locations of vertical reinforcement. Delaminations, where present, were more common at walls located beneath expansion joints (Figure 4.43).
- Map cracks were present in concrete repair material, although the repair areas were typically sound (Figure 4.44).
- Surficial deterioration of the original concrete finish was common on walls A and J of both spans (Figure 4.45). The cement paste was generally worn, exposing aggregate and creating surface voids.

Atypical Conditions

- Wide cracks were present at spandrel column and wall bases, primarily in Spans 1 and 7. On Span 1 columns, the cracks were typically wider on the north face. On Span 7 walls, the cracks were typically wider on the south face. On some columns, the cracks were accompanied by delaminations, spalls, and diagonal cracking on the upstream and downstream faces, most notably at Columns G and H in Span 1 (Figure 4.46); and Columns E and F in Span 7. Refer to Chapter 5 for additional details.
- Cracks and delaminations were often present at or near catwalk and utility duct support connections on Spans 1 through 5 (Figure 4.47).

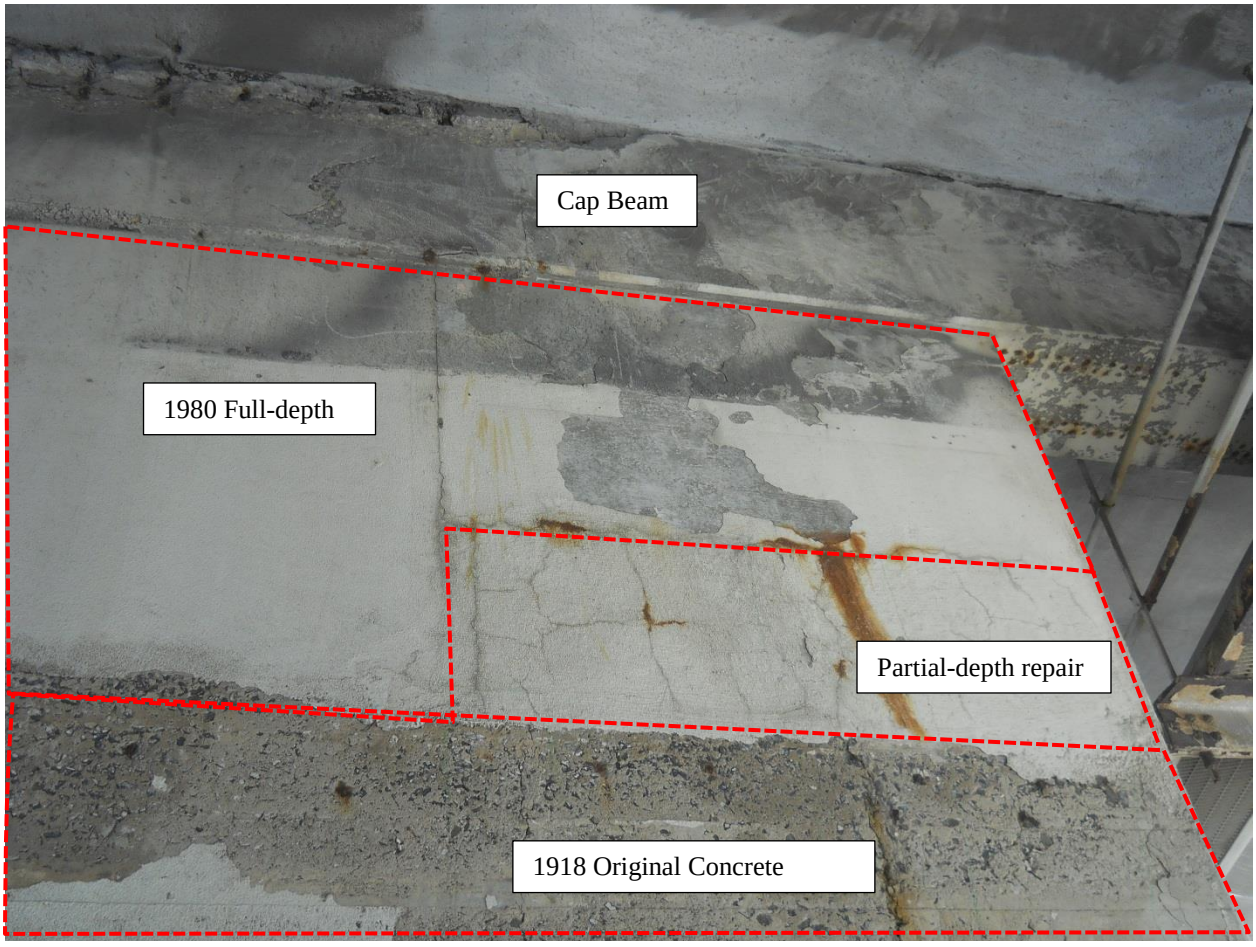

Figure 4.37. View of spandrel column with three types of concrete material illustrated (1980 full-depth concrete, partial-depth repair material, and original 1918 concrete). Note the difference in appearance among the three.

Figure 4.38. Spandrel column spalls at vertical rebar.

Figure 4.39. Spandrel column map cracking in repair material.

Figure 4.40. Spandrel column vertical cracking, coating failure and eroded concrete surface.

Figure 4.41. Spandrel column cracks at corners of catwalk opening.

Figure 4.42. Cracks emanating from corners of utility duct opening.

Figure 4.43. Delaminations along vertical and horizontal bars in original concrete.

Figure 4.44. Map-cracked repair material.

Figure 4.45. Surface erosion of cement paste.

Figure 4.46. Spandrel column shear crack.

Figure 4.47. Spandrel column corner delamination near utility duct support.

4.4.1.2.3. Arch Ribs

Typical Conditions

- Cracks, delaminations, and previous concrete repairs were present on arch rib corners. Many of the concrete repairs had deteriorated. Overall, these conditions were more widespread on the upstream and downstream arch ribs than the middle arch rib (Figure 4.48 and Figure 4.49).
- Freeze-thaw deterioration was present near the springline on the upstream and downstream arch ribs (Figure 4.50). Some freeze-thaw deterioration was present on the middle rib, but was less severe and more discrete. Deterioration was advanced below drain outfalls (Figure 4.51).
- Intermittent freeze-thaw deterioration was typically present on the topside corners of the arch ribs around column bases. At some locations, deterioration was also present on the underside corner below. The surface erosion typically extended less than 2 inches deep (Figure 4.52).
- Longitudinal cracks were present on the topside and underside faces of the arch ribs and were aligned with embedded Melan truss reinforcement. Cracks were typically present on the topside of the arch ribs along the entire length of the span, but crack on the underside were generally intermittent. The cracks were typically less than 0.020 inches wide but were sometimes considerably wider (Figure 4.53 and Figure 4.54).

Atypical Conditions

- Transverse cracks on the topside and vertical faces of arch ribs were present on some arches near the springline at the piers. The cracks were short (1/4 to 1/2 the depth of the face) and approximately 0.010 inches wide. The cracks were often continuous across two faces of the ribs (e.g., topside crack continues down the upstream face) (Figure 4.55 and Figure 4.56).
- Melan truss steel was exposed in isolated locations due to spalls, poor concrete consolidation, or freeze-thaw deterioration. Section loss of the exposed truss steel angle leg was usually estimated to be in the range of 10 to 20 percent and was more severe on arch ribs near drain outlets (Figure 4.57). See Chapter 6 for ultrasonic thickness measurements performed at representative severe locations.

Figure 4.48. Arch rib corner delamination

Figure 4.49. Arch rib deteriorated concrete repair.

Figure 4.50. Arch rib freeze-thaw deterioration at spring line.

Figure 4.51. Arch rib freeze-thaw deterioration under drain outlet.

Figure 4.52. Arch rib freeze-thaw deterioration at spandrel column base.

Figure 4.53. Arch rib topside cracks aligned with Melan truss angles.

Figure 4.54. Arch rib underside cracks aligned with Melan truss angles.

Figure 4.55. Arch rib transverse crack on upstream face.

Figure 4.56. Arch rib transverse crack on topside.

Figure 4.57. Arch rib exposed Melan truss angle at location of poor concrete consolidation.

4.4.1.2.4. Barrel Arches

Typical Conditions

- Longitudinal cracks and intermittent delaminations aligned with embedded Melan truss reinforcement were present on the topside and underside surfaces. Most cracks were 0.010 to 0.020 inches wide, although some were considerably wider (Figure 4.58 and Figure 4.59).
- Large, contiguous areas of deteriorated concrete repair material were often present on the upstream and downstream faces (Figure 4.60).
- Freeze-thaw deterioration was typically present near the arch spring lines. Some deterioration was greater than 2 inches deep (Figure 4.61).

Atypical Conditions

- Melan truss reinforcement was exposed at isolated locations due to spalls or freeze-thaw deterioration. Section loss on the exposed steel angle legs was usually estimated to be in the range of 10 to 20 percent (Figure 4.62). See Chapter 6 for ultrasonic thickness measurements to determine section loss.

Figure 4.58. Barrel arch topside cracks aligned with Melan truss angles.

Figure 4.59. Barrel arch underside cracks aligned with Melan truss angles.

Figure 4.60. Barrel arch deteriorated concrete repair.

Figure 4.61. Barrel arch freeze-thaw deterioration at arch spring line.

Figure 4.62. Exposed Melan truss angle at barrel arch.

4.4.1.3. Substructure

4.4.1.3.1. Arch Pier Walls

Typical Conditions

- At Piers 2 through 7, the exterior concrete surfaces were generally sound and only exhibited occasional and localized delaminations and signs of reinforcement corrosion (Figure 4.63 and Figure 4.64).
- At Piers 1 and 8, delaminations, spalls, and cracking were more widespread on the exterior surfaces (Figure 4.65). On each of these piers, deterioration was most severe on the approach span-side (south and north faces, respectively).
- At Piers 1, 6, and 8, the interior wall surfaces below the manhole openings and utility vault platforms exhibited widespread concrete distress and deterioration. The pattern of deterioration indicated it was related to water infiltration at the manhole opening above (Figure 4.66). The access platform in each of these piers was severely deteriorated. Refer to a separate WJE memo regarding these conditions included in Appendix 4.

Atypical Conditions

- Wide diagonal and vertical cracking, and sliding/faulting across construction joints and cracks, was present in the walls of Piers 1 and 8 (Figure 4.67). These conditions appeared to be related to overall structural movement. Refer to Chapter 5 and the WJE memorandum in Appendix 4 for further description of these conditions.
- Wide vertical cracks were present above arched openings in Piers 1, 7, and 8 (Figure 4.68).

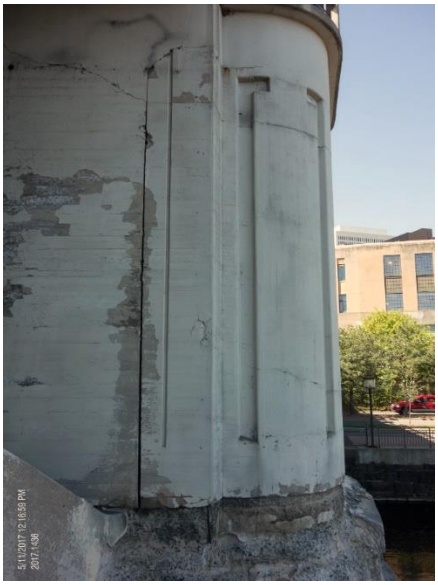

Figure 4.63. View of north face of Pier 1. Most of the wall face was sound with only isolated cracks and spalls.

Figure 4.64. Typical appearance of pier wall in good condition. Note original form board texture.

Figure 4.65. Deteriorated concrete on the north face of Pier 8 (outlined in spray chalk).

Figure 4.66. Deteriorated concrete below access platform on the inside of Pier 1.

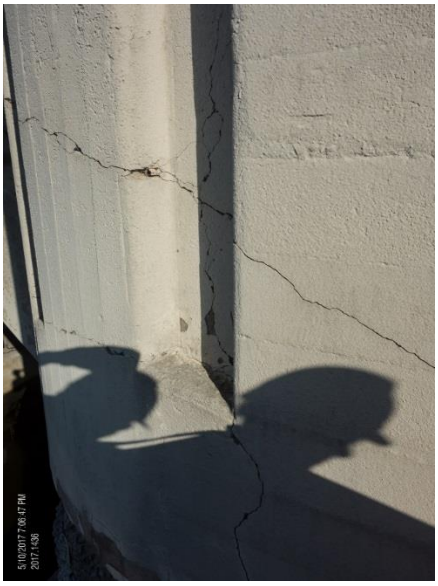

Figure 4.67. Wide diagonal crack at Pier 1, upstream face.

Figure 4.68. Wide crack over arched door opening in Pier 1.

4.4.1.3.2. Arch Pier Bases

Typical Conditions

- Freeze thaw distress was widespread and often deep in the pier bases (Figure 4.69 and Figure 4.70). Every pier exhibited at least some area of severe freeze thaw distress, with the depth of concrete material loss extending multiple inches into the element. Freeze thaw distress was most severe below the drain outfalls (Figure 4.71 and Figure 4.72). The depth of surface erosion (concrete section loss as measured from nearby, intact surfaces) was measured at a number of locations, as summarized in Table 4.1. In many areas of severe freeze thaw distress, the erosion was 6 inches or greater. Several areas had more than 12 inches of erosion, with a maximum of 17 inches identified among the locations measured.
- Most of the semi-circular projections at Piers 2, 3, 4, 5, and 7 had been repaired in the past with a partial-depth concrete material (Figure 4.73, Figure 4.74). The material was very hard and difficult to fracture with a hammer, but was often not well bonded to the substrate below. This material was also cracked and had spalled in many areas.
- Inspection of the pier footings at and below the waterline by Collins Engineers found similar conditions to those identified in WJE's inspection of the pier bases. Just above the waterline, the piers exhibited various degrees of unsound concrete, including freeze thaw distress, paste erosion, delaminations, and deteriorated repairs, similar in extent to what was identified by WJE. Below the waterline, Collins typically reported scaling of the pier surfaces with penetration from 1 to 3 inches deep. The south side of Arch Pier 7 contained a few isolated larger, deeper spalls (the largest of which was 20 feet wide by 10 inches tall by 16 inches deep). The recently-installed jackets on Piers 1 and 2 were in sound condition with only minor cracks.

Atypical Conditions

- Concrete jackets, at least 12 inches thick, had been installed at the bases of Piers 1 and 2. Some shrinkage cracks were observed on the jackets, but otherwise the jackets were sound and had no signs of deterioration (Figure 4.75 and Figure 4.76).

Table 4.3. Depth of Freeze-thaw Erosion Measured at Pier Bases

Pier	Location	Approximate maximum depth of erosion (inches)
1	Northeast corner, upstream of ribs	12
1	North face, below drain, between upstream and middle ribs	6
2	South face, below drain, between upstream and middle ribs	6
2	Southwest corner, upstream of ribs	12
2	North face, below drain, between upstream and middle ribs	17
2	North face, below drain, between downstream and middle ribs	6
3	North face, below drain, between downstream and middle ribs	12
6	South face, below doorway, between downstream and middle ribs	16

Pier	Location	Approximate maximum depth of erosion (inches)
6	Upstream of ribs	6
8	Northwest corner near barrel arch	8

Figure 4.69. Freeze thaw distress at the base of Pier 2.

Figure 4.70. Freeze thaw distress at the base of Pier 8.

Figure 4.71. Drain outfall at Pier 2 and concrete deterioration below.

Figure 4.72. Drain outfall at Pier 6 and concrete deterioration below.

Figure 4.73. Deteriorated repair material at the base of Pier 2.

Figure 4.74. Deteriorated repair material at the base of Pier 3.

Figure 4.75. Concrete jacket at the base of Pier 1.

Figure 4.76. Concrete jacket at the base of Pier 2.

4.4.2. South Approach Spans

4.4.2.1. Deck

- Transverse cracks were present on the wearing surface. Some of these cracks also lined up with cracking on the deck underside. Efflorescence was present on the deck underside along the upstream and downstream sidewalks at discrete cracking conditions. Most cracks were 0.005 to 0.020 inches wide (Figure 4.77).
- Intermittent transverse spalls and exposed reinforcement were present on the deck underside near the south bent. The spalls were typically 1 to 2 feet wide and spanned the length between the steel beams. Section loss of exposed rebar was less than 10 percent (Figure 4.78).
- The topside of the sidewalk was generally sound, with only isolated spalls (Figure 4.79). Narrow, transverse cracks were present and spaced about 5 to 10 feet on center.
- Two adjacent plow fingers were missing in the northbound traffic lane on the strip seal joint at the south abutment (Figure 4.80). Like in the arch spans, the strip seal glands were filled with debris.

Figure 4.77. South approach transverse cracks on slab underside along sidewalk.

Figure 4.78. South approach slab underside spalls near south bent.

Figure 4.79. Overall view of sidewalk on approach.

Figure 4.80. South approach strip seal joint with missing plow fingers.

4.4.2.2. Superstructure

- Fractured, bent or missing anchor bolts (smooth pins) were identified at the fixed bearings at the south abutment (Figure 4.81). One bearing had all bolts missing; one had fractured bolts; and eight had loose or missing pins and corrosion on steel plates.
- All of the anchors that were present were bent or rotated toward the south (Figure 4.82).
- Varying degrees of surface corrosion were present on steel components on both fixed and elastomeric bearings at the south abutment and Pier 1, respectively.
- Some of the bearing pads at Pier 1 had displaced, resulting in some overhanging the concrete support (Figure 4.83).
- At the time of the inspection (May 2017), some of the steel girders had near-restricted movement, with less than 1/2 inch remaining between the girder end and the south wall of Arch Pier 1 (Figure 4.84).
- Tape adhesion tests were performed on select areas of the weathering steel girders. In areas rated CS1, the patina was tightly adhered and flakes were less than 1/16 inch in diameter. In areas rated CS2 and CS3, some patina was removed by the tape. In areas rated CS4, large (greater than 1/2 inch in diameter) areas of flaking rust could be removed. Approximately 84 percent of the girder surface area was rated CS1, 14 percent was rated CS2, 2 percent was rated CS3, and 1 percent was rated CS4 (Figure 4.85 and Figure 4.86).

Figure 4.81. South abutment fixed bearing fractured anchor bolt.

Figure 4.82. South abutment fixed bearing bent or rotated anchor bolt.

Figure 4.83. Pier 1 expansion bearing pad deformed and displaced off edge of concrete support.

Figure 4.84. Pier 1 expansion bearing near-restricted movement between steel girder and pier wall.

Figure 4.85. South approach, tape adhesion test of weathering steel patina in good condition (CS1 rating).

Figure 4.86. South approach, tape adhesion test of weathering steel patina in poor condition and flaking (CS4 rating).

4.4.2.3. Substructure

- A few, isolated spalls with exposed reinforcement were present on the south abutment. The exposed rebar appeared to have shallow concrete cover (Figure 4.87).
- Moisture and rust stains were visible on the south abutment and the south bent pier cap (Figure 4.88).

Figure 4.87. South abutment spalls.

Figure 4.88. South bent pier cap rust stains.

4.4.3. North Approach Spans

4.4.3.1. Deck

- The wearing surface on the roadway was in good condition, with almost no distress. Very few longitudinal and transverse cracks were identified.
- A few, isolated spalls were present on the slab underside near the north abutment (Figure 4.89).
- Cracks with efflorescence were present on the slab underside at the north bent, between the slab edge and the fascia precast concrete girder (Figure 4.90).
- A torn strip seal gland was identified at the Pier 8/North Approach joint (Figure 4.91).

Figure 4.89. North approach slab underside spall near the north abutment.

Figure 4.90. North approach slab underside diagonal cracking and efflorescence at the north bent.

Figure 4.91. North approach strip seal gland tear.

4.4.3.2. Superstructure

- Some surface corrosion was observed on three of the fixed bearing plates (Figure 4.92).
- Cracks and delaminations with rust stains were present on precast concrete girder I at Pier 8 and girder B at the north abutment (Figure 4.93).
- All of the anchor bolts (smooth pins) in the fixed bearings at the north abutment were leaning to the north. No loose or fractured bolts were identified.

Figure 4.92. North abutment fixed bearing surface rust.

Figure 4.93. Precast beam concrete distress at north abutment.

4.4.3.3. Substructure

- A new reinforced concrete cap was constructed on top of the original north retaining walls in 1980. The northern portion of the downstream cap was rotated outward along most of its length, resulting in settlement of the adjacent sidewalk and leaning of the pedestrian railing. A gap between the sidewalk and the cap was approximately 4 inches wide and had been previously filled with asphalt (Figure 4.94 and Figure 4.95). Freeze-thaw deterioration was evident on the original concrete wall immediately below the cap (Figure 4.97). Measurements of the rotation of the downstream cap were taken with a smart level and digital angle. The measurements alongside each aluminum railing panel from the end of the railing to the north abutment are plotted in Figure 4.96. As seen in the plot, maximum rotation was approximately 8 degrees from plumb. Refer to separate reports by HNTB and Dan Brown and Associates (DBA) regarding this condition.
- Localized delaminations were present on the north abutment near the downstream edge (Figure 4.98). Other portions of the abutment wall were generally sound.

Figure 4.94. North approach, downstream railing leaning outward and gap at sidewalk due to retaining wall cap rotation.

Figure 4.95. North approach, downstream side, cap on top of original retaining wall rotated outward (left in photo).

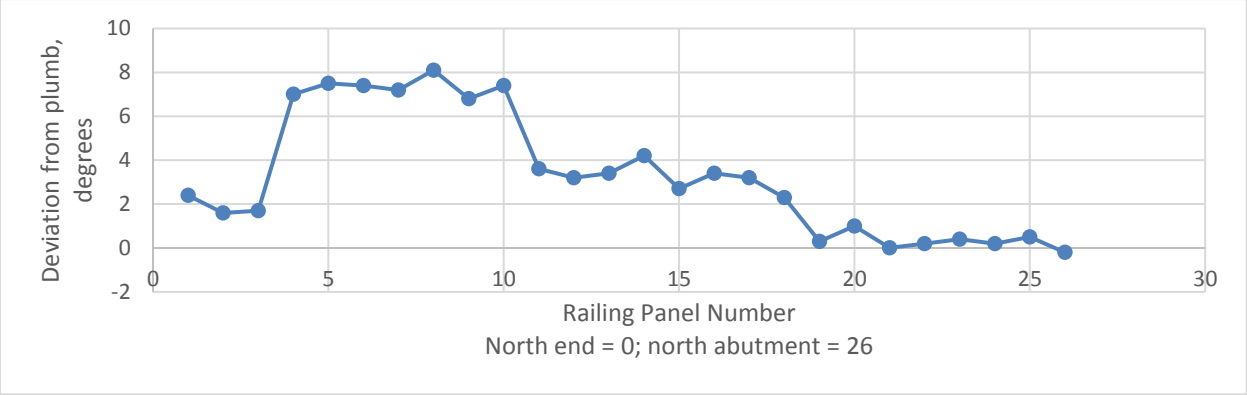

Figure 4.96. Plot of wall plumbness measurement at cap atop north retaining wall. Positive numbers indicate rotation outward (eastward).

Figure 4.97. View looking south along downstream retaining wall. Note freeze-thaw damage at top of original concrete.

Figure 4.98. North abutment delaminations.

4.4.4. Other Elements

4.4.4.1. Pedestrian Railing

Typical Conditions

- The metal aluminum railing segments were in generally sound condition, with a well-adhered oxide layer. Little evidence of deleterious oxidation, such as white powder or pitting, was observed.
- The fasteners for the railing to the concrete posts exhibited surface corrosion and pitting. Some fasteners appeared to be mild steel and some appeared to be galvanized, but very little if any of zinc coating remained. (Refer to X-ray florescence test results in Chapter 6 and Appendix 11.)
- Bird droppings, graffiti, or paint were present on a number of railing panels (Figure 4.99).
- Concrete posts were generally sound and in good condition with only narrow cracks present.

Atypical Conditions

- Deep spalls in the deck fascia below the concrete post bases were often present at expansion joints on the downstream side (Figure 4.100). At some locations, this spalling had resulted in undermining the post base support by a few inches.
- Distress noted in the aluminum railings included: missing fasteners between railing and post (Figure 4.101); missing railing elements (Figure 4.102); metal distortion (Figure 4.103); cracks in railings or connector plates (Figure 4.104 and Figure 4.105); top or bottom rails out of position; and unsound metal repairs (Figure 4.106).

Figure 4.99. View of typical pedestrian railing panel.

Figure 4.100. Deep spall in deck fascia below railing post.

Figure 4.101. Aluminum railing connection missing fastener.

Figure 4.102. Aluminum railing missing member.

Figure 4.103. Bottom railing distorted, likely from impact.

Figure 4.104. Aluminum railing crack.

Figure 4.105. Pedestrian railing crack at post connection.

Figure 4.106. Pedestrian railing unsound metal repairs.

4.4.4.2. Traffic Barrier

Typical Conditions

- The traffic barrier (roadway railing) consists of a concrete J-rail with line pipe (metal railing on top). Cracks, delaminations, and spalls were present on the concrete J-rail at expansion joints (Figure 4.107).
- The special surface finish on the J-rail was typically debonded, flaking, and failed over wide areas. Coating failure was more widespread on the downstream face of the upstream barrier (Figure 4.108).
- The coating on the metal railings at the top of the barrier was in generally poor condition. Large areas of the metal surface was exposed and corroding (Figure 4.109). Pack rust was present at the slip joint connections (Figure 4.110).

Atypical Conditions

- Missing fasteners for the railing to concrete connection were identified at one location on the south approach (Figure 4.111).
- Multiple adjacent railings were out of alignment on the downstream barrier on the north approach (Figure 4.112).

Figure 4.107. Spall in traffic barrier J-rail at expansion joint.

Figure 4.108. Traffic barrier failed coating.

Figure 4.109. Traffic barrier metal railing surface corrosion.

Figure 4.110. Traffic barrier metal railing pack rust at slip joint.

Figure 4.111. Traffic barrier metal railing missing fasteners.

Figure 4.112. Traffic barrier metal railing out of alignment.

4.4.4.3. Other Items

- **Deck drainage:** Deck drains and drain pipes were in generally fair condition. Limited evidence of leaks or breakage in the drain pipes themselves was observed. However, water from the drains discharges onto the base of the piers and the spring line of the arch ribs and has caused distress to the concrete as noted elsewhere.
- **Access platforms:** The access platforms at Piers 1, 6, and 8 were in generally poor condition, as further described in the WJE memorandum in Appendix 4. Deteriorated items included a crushed web at the south support of the downstream beam in Pier 1; severe corrosion of support beams, connections, and metal deck; and spalls and freeze-thaw deterioration on the pier walls at platform support connections. The platform in Pier 6 was in better condition than the platforms in Piers 1 and 8.
- **North vertical circulation stairway:** The north stairway was in generally fair condition. Concrete distress identified included rust stains and cracks on the upper landing/walkway to bridge (Figure 4.113); narrow radial cracks at the curved landings (Figure 4.114); and light rust stains at the stair tread edges (Figure 4.115).

Figure 4.113. North vertical circulation staircase rust stains and cracks at walkway to bridge.

Figure 4.114. North vertical circulation staircase cracks at landing.

Figure 4.115. North vertical circulation staircase rust stains at stair treads.

4.4.5. Conditions That Could Affect Structural Analysis and Load Rating

A number of items were identified by WJE during the in-depth inspection that could affect the structural behavior of the bridge, or that could indicate unintended structural movement of the structure. Descriptions of these items were provided to HNTB during the course of the inspection so that they could consider them in the structural analysis and load rating (see WJE memorandum in Appendix 4). These conditions included:

- Structural distress in Piers 1 and 8, as evidenced by wide diagonal cracks and sliding/faulting at construction joints and cracks.
- Structural distress at the bases of spandrel columns and spandrel walls, particularly in Arch Spans 1 and 7.
- Shear or torsional cracking in cap beams in Arch Spans 1 and 7.
- Spalling of cap beams below deck joints. Exposed, bent and severely corroded vertical dowels were observed in some of the deeper spalls.
- Flexural cracking on the topside of arch ribs at spring lines.
- Loss of cross-sectional area of arch ribs due to concrete deterioration, particularly at the spring lines near the interface with the piers.
- Section loss due to corrosion of reinforcing bars:
  - Arch piers
  - Spandrel columns
  - Cap beams
  - Deck underside, particularly around the manholes at Piers 1, 6, and 8.
- Exposure and section loss to Melan truss reinforcing angles at deep spalls in arch ribs.

4.5. Distress Quantity Ratios by Element Category

4.5.1. Definition of Distress Quantity Ratio

The condition state data can be conceptually split into two types of deterioration. The first type of condition states are primary measures of concrete deterioration and distress and include delaminations, spalls, freeze-thaw deterioration, and patched areas. Distress represented by these types of condition states are usually repaired in a major preservation or rehabilitation program. The second type of condition states can be considered leading indicators of future distress. These indicators include moisture staining, rust staining, and efflorescence. These types of distress are typically not repaired but should be considered in determining the extent or need for preventive maintenance. Cracking can fall into either category; for this analysis cracking is considered to be a leading indicator.

In order to allow interpretation of the structure's current condition, the very large amount of condition state data from the in-depth inspection was aggregated into a single "distress quantity ratio" for each bridge element. The distress quantity ratio was calculated by adding the mapped areas of all of the below-listed conditions for a given element and dividing by the total exposed surface area of that element.

- Delaminated and spalled areas: CS2 (delaminated), CS3 (moderate-depth spalls), and CS4 (deep spalls)
- Pre-existing patches and repairs: CS3 (deteriorated) and CS4 (failed or debonded patches)
- Freeze-thaw distress: CS3 (moderate, with up to 2 inches of deterioration) and CS4 (severe, more than 2 inches of deterioration).

As such, the distress quantity ratio for any given element is essentially the percentage of damaged surface area on that element, from 0 and 100 percent. The distress quantity ratio can also be viewed as a relative rating between elements, where 0 is the best and 100 is the worst condition.

The leading indicators of distress (cracking, moisture staining, etc.) were not included in the distress quantity ratios. This is because the presence of these types of distress alone does not presently require a concrete surface repair. However, their incidence may still be considered when assessing element durability and the need for future repairs or other preventative measures.

For the follow-up testing work performed by WJE, the distress quantity ratios were also defined locally within a given study area for relative comparisons between study areas within an element category. These quantities are presented with the follow-up testing results in Chapter 6.

4.5.2. Summary of Distress Quantity Ratios by Element Category

WJE utilized the Plannotate inspection notes together with a MATLAB algorithm to calculate the distress quantity ratios for each element category in the bridge. The color graduated tables following this section summarize the distress quantity ratios by element. Findings are briefly summarized below and will be used in Chapter 7 for further interpretation. (Note that the "distress quantity ratio" as defined above is sometimes simply referred to as "distress quantity" or "distress" as a percentage in this report.)

- **Deck Elements (Table 4.4)**
  - The deck topside on both the arch and approach spans exhibited low amounts of distress, with 2 percent or less in each span distressed. This value differs slightly from the value tabulated for "unsound deck percentage" in the element level inspection report because in that report leaking and wide cracks were considered as contributing to the unsound area.

- The deck underside was consistently deteriorated on the arch spans, with 13 to 16 percent of the area distressed. In the approach spans, a much smaller quantity was distressed, at 2 percent or less of the area in any span.

- **Cap Beams (Table 4.5, Table 4.6, and Table 4.7)**
  - Cap beams adjacent to expansion joints exhibited widespread distress. Out of 38 cap beams below joints, 24 had distress quantity that exceeded 20 percent of the element's surface area. The cap beams in Span 6 were an outlier from these results, with no cap beam exceeding distress over 10 percent of the area.
  - Cap beams away from expansion joints were in good condition, with most cap beams exhibiting less than 1 percent distress. Outliers to this value were in the cap beams at the crown of the arches in Spans 1 and 7, which exhibited delaminations, torsional cracking and other distress that was primarily caused by structural movements instead of corrosion.

- **Spandrel Columns and Walls (Table 4.8, Table 4.9, Table 4.10, Table 4.11,**

- Table 4.12**, Table 4.13, Table 4.14, and Table 4.15)**
  - Lower Spandrel Columns and Walls (1918 concrete) (Table 4.8 and Table 4.10)
    - The distress quantity depended strongly on the presence of expansion joints. Lower columns which have always had an expansion joint present exhibited the highest distress quantity ratios, with an average of 55 percent of area on the downstream columns and 26 percent of area on the middle columns. Spandrel columns with expansion joints for a more limited amount of time (either 1918-1980 or 1980-present) had somewhat less distress
    - Generally, the downstream columns were more distressed than the upstream or middle columns. Note that many of the upstream columns had been completely replaced during the 1980 rehabilitation.
    - Spandrel columns that have never been located below an expansion joint were in the best condition and generally had less than 10 percent of the area distressed. Two outliers to this general finding were the downstream 'B' column in Spans 2 and 5, both of which had distress quantity more than 30 percent of the surface area.
    - Spandrel walls showed a similar correlation to the presence of expansion joints. Walls with an expansion joint always present above had a distress quantity averaging 40 percent. Walls without an expansion joint had a distress quantity averaging 8 percent.
  - Upper Spandrel Columns and Walls (1980 concrete) (Table 4.9, Table 4.11,
  - Table 4.12 and Table 4.13
    - At expansion joints, the upper spandrel columns exhibited an average of 3 to 12 percent of distressed area, and ranged from none to 54 percent.
    - Distress on a span-by-span basis showed similar behavior among Spans 1-5. Elements in Span 6 exhibited slightly less distress than Span 7.
    - Downstream columns in Spans 1-5 exhibited more distress than the middle or upstream columns.
    - Columns and walls without expansion joints had very little distress, with most elements having distress quantity less than 1 percent of the surface area. One exception to this was the spandrel columns and wall at Spans 1 and 7, respectively, where overall structural movement had caused cracking and delaminations of the non-expansion joints elements at the top of the arches.

- Tables Table 4.14 and Table 4.15 provide distress quantities for the full height of all columns (lower columns and upper columns combined). As such, the tables lay out like a plan view of the bridge, showing all columns and walls from end to end of the structure.

- **Arch Ribs (Table 4.16)**
  - The downstream and upstream arch ribs were similar in condition, averaging approximately 20 percent distress over all spans. The ribs in Span 5 were in the best condition, averaging closer to 10 percent.
  - In Spans 2 through 5, the middle arch ribs had distress quantity less than 5 percent. In Span 1, distress quantities were greater and averaged 10 percent.
  - In Spans 6 and 7, the two barrel arches were similar in condition, averaging 12 and 16 percent for distress quantity, respectively.

- **Arch Pier Walls (Table 4.17)**
  - Piers 2 through 5 and Pier 7 were in the best condition overall. Distress quantities on both the interior and exterior surfaces averaged less than 5 percent.
  - Piers 1, 6, and 8 were more distressed than the other piers, both at the exterior and interior faces. Distress ranged from 7 to 17 percent. Distress on these pier walls was generally due to two reasons. First, manhole openings in the top of each pier had allowed leakage on the interior walls and caused distress. Second, expansion joints on the approach span side of Piers 1 and 8 had apparently leaked in the past and caused distress on the exterior wall faces.

- **Arch Pier Bases (Table 4.17)**
  - The bases of Piers 1, 2, 3, 4, and 6 exhibited moderate to severe freeze thaw distress, spalled concrete, or failed patches on the majority of the surface area. This resulted in distress quantities that were all greater, and in some cases much greater than 40 percent. Piers 5 and 7 were in comparably better condition, with only 21 to 27 percent of the area distressed.

- **Approach Span Superstructure (Table 4.18)**
  - On the north approach spans, the prestressed girders were generally in very good condition and only exhibited discrete distress at the ends of two beams. Total distress quantity was less than 6 linear feet.
  - On the south approach spans, the weathering steel girders were overall in fair to good condition. The weathering steel patina was in poor condition (CS3) on 44 linear feet of the beams, primarily near leaks at the expansion joint between Span S2 and Pier 1.

- **Approach Span Substructure (Table 4.19)**
  - The abutments (including integral wing walls) and columns were in very good condition, with only isolated areas of concrete distress. Less than 100 square feet of distress quantity was identified overall on the abutments.
  - The downstream retaining wall on the north approach was severely distressed, with the top of the wall rotated outward. Separately, the lower portion of the wall also exhibited delaminations and spalls, totaling 8 percent of the surface area.

- **Pedestrian Railings (Table 4.20, Table 4.21)**
  - Out of more than 600 aluminum panels, only 20 exhibited distress that would be considered poor or severe (CS3 and CS4). Most of this distress was due to cracks and distortion (such as caused by impact) or misalignment and connection distress caused by structure movements.

- Most of the concrete posts were in good condition. Spalls or major cracking were only identified on 6 out of the more than 600 posts.

- **Traffic Barrier (Table 4.22, Table 4.23)**
  - The metals rails exhibited widespread coating failure and surface corrosion. However, only 6 out of the 150 railing segments exhibited corrosion or connection distress that was poor to severe.
  - Approximately 1 percent of the surface area was distressed on the concrete J-rail.

Table 4.4. Distress Quantity Ratios for Deck Elements

Element Category	Span	Distress Quantity (sf)	Surface Area (sf)	Distress Quantity Ratio
Deck Topside - Arches				
Roadway	1	107	14562	1%
	2	285	13591	2%
	3	143	13595	1%
	4	136	13616	1%
	5	211	13867	2%
	6	105	9091	1%
	7	53	9921	1%
	Total	**1041**	**88243**	**1%**
Sidewalks	1	2	5226	0%
	2	59	4427	1%
	3	20	4419	0%
	4	8	4471	0%
	5	25	4679	1%
	6	18	3231	1%
	7	1	3615	0%
	Total	**131**	**30068**	**0%**
Deck Underside - Arches				
Underside	1	2435	19337	13%
	2	2988	18886	16%
	3	2707	18903	14%
	4	2655	18868	14%
	5	2836	19262	15%
	6	1780	12788	14%
	7	2078	12745	16%
	Total	**17480**	**120791**	**15%**
Deck Topside - Approaches				
Roadway	N1	0	5303	0%
	N2	0	5430	0%
	S1	15	5756	0%
	S2	0	5765	0%
	Total	**15**	**22254**	**0%**
Sidewalks	N1	0	1760	0%
	N2	0	1786	0%
	S1	2	2406	0%
	S2	1	1936	0%
	Total	**3**	**7888**	**0%**
Deck Underside - Approaches				
Underside	N1	2	7382	0%
	N2	8	7548	0%
	S1	169	10323	2%
	S2	56	8001	1%
	Total	**236**	**33253**	**1%**

Table 4.5. Distress Quantity Ratios for Cap Beams with Expansion Joints

Span	No.	Distress Quantity (sf)	Surface Area (sf)	Ratio
1	A	272	560	49%
	D	351	560	63%
	F	94	560	17%
	I	149	560	27%
	K	197	560	35%
	N	323	560	58%
2	A	439	560	78%
	D	308	560	55%
	F	143	560	26%
	I	197	560	35%
	K	283	560	51%
	N	377	560	67%
3	A	367	560	66%
	D	242	560	43%
	F	36	560	6%
	I	112	560	20%
	K	215	560	38%
	N	310	560	55%
4	A	321	560	57%
	D	82	560	15%
	F	57	560	10%
	I	84	560	15%
	K	117	560	21%
	N	310	560	55%
5	A	346	560	62%
	D	189	560	34%
	F	70	560	12%
	I	98	560	18%
	K	246	560	44%
	N	332	560	59%
6	A	16	550	3%
	D	13	550	2%
	G	5	550	1%
	J	48	550	9%
7	A	93	550	17%
	D	153	550	28%
	G	68	550	12%
	J	130	550	24%
Total		**7195**	**21200**	**34%**

Table 4.6. Distress Quantity Ratios for Cap Beams without Expansion Joints

Span	No.	Distress Quantity (sf)	Surface Area (sf)	Ratio
1	B	0	560	0%
	C	0	560	0%
	E	2	560	0%
	G	21	560	4%
	H	28	560	5%
	J	0	560	0%
	M	0	560	0%
2	B	0	560	0%
	C	0	560	0%
	E	0	560	0%
	G	0	560	0%
	H	0	560	0%
	J	0	560	0%
	M	1	560	0%
3	B	0	560	0%
	C	5	560	1%
	E	0	560	0%
	G	0	560	0%
	H	0	560	0%
	J	0	560	0%
	M	0	560	0%
4	B	0	560	0%
	C	0	560	0%
	E	0	560	0%
	G	0	560	0%
	H	0	560	0%
	J	0	560	0%
	M	0	560	0%
5	B	0	560	0%
	C	5	560	1%
	E	0	560	0%
	G	0	560	0%
	H	0	560	0%
	J	0	560	0%
	M	0	560	0%
6	B	0	550	0%
	C	0	550	0%
	E	0	550	0%
	F	2	550	0%
	H	0	550	0%
	I	0	550	0%
7	B	0	550	0%
	C	0	550	0%
	E	41	550	7%
	F	33	550	6%
	H	2	550	0%
	I	0	550	0%
Total		**140**	**26200**	**1%**

Table 4.7. Distress Quantity Ratios for Cap Beams by Span

Element Category	Span	Distress Quantity (sf)	Surface Area (sf)	Distress Quantity Ratio
Expansion Joint	1	1386	3360	41%
	2	1747	3360	52%
	3	1282	3360	38%
	4	971	3360	29%
	5	1282	3360	38%
	6	83	2200	4%
	7	444	2200	20%
	Total	**7195**	**21200**	**34%**
No Expansion Joint	1	51	3920	1%
	2	2	3920	0%
	3	5	3920	0%
	4	0	3920	0%
	5	5	3920	0%
	6	2	3300	0%
	7	76	3300	2%
	Total	**140**	**26200**	**1%**

Table 4.8. Distress Quantity Ratios for Lower Spandrel Columns (1918 Concrete), Spans 1-5

Expansion Joint Status	Span	No.	Downstream Columns			Middle Columns			Upstream Columns		
			Distress Quantity (sf)	Surface Area (sf)	Distress Quantity Ratio	Distress Quantity (sf)	Surface Area (sf)	Distress Quantity Ratio	Distress Quantity (sf)	Surface Area (sf)	Distress Quantity Ratio
Always Expansion Joint	1	A	--	--	--	108	788	14%	--	--	--
		N	303	475	64%	155	793	20%	--	--	--
	2	A	150	489	31%	328	814	40%	--	--	--
		N	--	--	--	224	671	33%	--	--	--
	3	A	425	491	87%	183	784	23%	--	--	--
		N	165	434	38%	120	726	16%	--	--	--
	4	A	--	--	--	223	776	29%	--	--	--
		N	--	--	--	145	765	19%	--	--	--
	5	A	--	--	--	132	731	18%	--	--	--
		N	--	--	--	258	802	32%	--	--	--
	Sub-Total		**1042**	**1888**	**55%**	**1875**	**7649**	**24%**	**--**	**--**	**--**
Expansion Joint 1918-1980 Only	1	C	--	--	--	42	328	13%	--	--	--
		L	34	243	14%	65	421	15%	--	--	--
	2	C	--	--	--	40	369	11%	--	--	--
		L	21	196	10%	11	281	4%	--	--	--
	3	C	--	--	--	0	330	0%	--	--	--
		L	--	--	--	22	314	7%	--	--	--
	4	C	--	--	--	26	360	7%	--	--	--
		L	0	227	0%	10	330	3%	3	186	2%
	5	C	--	--	--	62	323	19%	2	45	5%
		L	63	179	35%	37	320	12%	--	--	--
	Sub-Total		**118**	**845**	**15%**	**314**	**3375**	**9%**	**5**	**231**	**3%**
Expansion Joint 1980-Present Only	1	D	--	--	--	0	290	0%	46	119	38%
		K	32	169	19%	28	304	9%	--	--	--
	2	D	53	165	32%	19	264	7%	35	165	21%
		K	51	102	50%	23	162	14%	7	102	7%
	3	D	--	--	--	11	250	4%	--	--	--
		K	--	--	--	0	138	0%	--	--	--
	4	D	--	--	--	7	209	3%	--	--	--
		K	92	102	91%	4	129	3%	39	81	49%
	5	D	13	72	18%	10	115	8%	--	--	--
		K	42	70	60%	9	112	8%	--	--	--
	Sub-Total		**282**	**679**	**45%**	**110**	**1973**	**6%**	**127**	**467**	**29%**
Never Expansion Joint	1	B	16	273	6%	7	536	1%	15	427	3%
		M	51	384	13%	0	616	0%	40	463	9%
	2	B	122	341	36%	54	545	10%	24	341	7%
		M	15	296	5%	36	473	8%	0	296	0%
	3	B	16	346	5%	12	553	2%	--	--	--
		M	0	269	0%	19	462	4%	16	145	11%
	4	B	5	337	1%	4	539	1%	4	337	1%
		M	5	317	2%	7	506	1%	55	317	17%
	5	B	178	314	57%	3	503	1%	--	--	--
		M	34	316	11%	3	506	1%	3	380	1%
	Sub-Total		**442**	**3194**	**14%**	**146**	**5238**	**3%**	**157**	**2706**	**6%**
Span 1-5 Total			**1884**	**6607**	**28%**	**2446**	**18235**	**11%**	**289**	**3404**	**12%**

** "--" indicates no 1918 concrete remaining at that column location (i.e., full height of column replaced in 1980)*

Table 4.9. Distress Quantity Ratios for Upper Spandrel Columns (1980 Concrete), Spans 1-5

Span	Span	No.	Downstream			Middle			Upstream		
			Distress Quantity (sf)	Surface Area (sf)	Distress Quantity Ratio	Distress Quantity (sf)	Surface Area (sf)	Distress Quantity Ratio	Distress Quantity (sf)	Surface Area (sf)	Distress Quantity Ratio
Expansion Joint	1	A	35	533	7%	0	66	0%	13	641	2%
		D	15	202	7%	3	33	10%	0	123	0%
		F	0	99	0%	0	159	0%	8	119	7%
		I	11	113	10%	0	181	0%	8	136	6%
		K	33	62	54%	3	66	4%	23	278	8%
		N	10	82	12%	0	99	0%	50	670	7%
	2	A	3	83	3%	0	99	0%	57	572	10%
		D	0	62	0%	0	99	0%	6	62	10%
		F	6	53	11%	0	85	0%	0	53	0%
		I	2	69	3%	0	110	0%	2	69	3%
		K	18	62	29%	4	99	4%	0	62	0%
		N	95	503	19%	0	132	0%	29	503	6%
	3	A	11	62	17%	8	99	8%	58	553	11%
		D	42	198	21%	0	66	0%	0	198	0%
		F	0	83	0%	0	132	0%	0	83	0%
		I	3	83	4%	0	132	0%	0	83	1%
		K	2	189	1%	7	165	4%	10	189	5%
		N	50	103	49%	21	132	16%	10	537	2%
	4	A	66	568	12%	15	132	12%	46	568	8%
		D	3	213	2%	0	132	0%	0	213	0%
		F	2	98	2%	0	157	0%	0	98	0%
		I	0	98	0%	0	157	0%	7	98	7%
		K	1	103	1%	0	198	0%	0	124	0%
		N	55	541	10%	7	99	7%	17	541	3%
	5	A	50	538	9%	2	131	2%	41	647	6%
		D	29	123	23%	0	197	0%	0	234	0%
		F	15	82	18%	0	131	0%	0	99	0%
		I	0	82	0%	0	131	0%	0	99	0%
		K	17	123	14%	0	197	0%	3	232	1%
		N	78	542	14%	2	66	3%	33	651	5%
	Total		**653**	**5751**	**12%**	**73**	**3681**	**2%**	**424**	**8535**	**4%**

Table 4.9 (cont'd). Distress Quantity Ratios for Upper Spandrel Columns (1980 Concrete), Spans 1-5

Expansion Joint Status	Span	No.	Downstream			Middle			Upstream		
			Distress Quantity (sf)	Surface Area (sf)	Distress Quantity Ratio	Distress Quantity (sf)	Surface Area (sf)	Distress Quantity Ratio	Distress Quantity (sf)	Surface Area (sf)	Distress Quantity Ratio
Never Expansion Joint	1	B	0	123	0%	0	99	0%	0	49	0%
		C	11	287	4%	0	131	0%	2	345	1%
		E	0	140	0%	0	224	0%	0	169	0%
		G	5	82	6%	11	131	8%	1	99	1%
		H	14	89	16%	3	142	2%	11	107	10%
		J	3	149	2%	0	238	0%	0	179	0%
		L	0	82	0%	0	99	0%	0	391	0%
		M	0	62	0%	0	99	0%	0	74	0%
	2	B	0	83	0%	0	132	0%	0	83	0%
		C	0	313	0%	0	132	0%	0	313	0%
		E	1	165	1%	0	264	0%	2	165	1%
		G	0	34	0%	0	55	0%	0	34	0%
		H	0	38	0%	0	61	0%	0	38	0%
		J	0	103	0%	2	165	1%	0	103	0%
		L	0	62	0%	0	132	0%	0	258	0%
		M	0	83	0%	0	132	0%	0	83	0%
	3	B	0	62	0%	0	99	0%	0	408	0%
		C	0	289	0%	0	132	0%	0	289	0%
		E	0	127	0%	0	204	0%	0	127	0%
		G	0	62	0%	0	99	0%	0	62	0%
		H	0	62	0%	0	99	0%	0	62	0%
		J	4	126	3%	0	201	0%	0	126	0%
		L	3	279	1%	0	132	0%	0	279	0%
		M	0	124	0%	0	165	0%	0	248	0%
	4	B	0	83	0%	1	132	1%	0	83	0%
		C	1	308	0%	0	132	0%	0	308	0%
		E	0	146	0%	0	234	0%	0	146	0%
		G	0	79	0%	0	127	0%	0	79	0%
		H	0	79	0%	0	127	0%	0	79	0%
		J	0	143	0%	0	228	0%	0	143	0%
		L	0	62	0%	0	132	0%	0	103	0%
		M	0	83	0%	0	132	0%	0	83	0%
	5	B	1	82	1%	0	131	0%	2	477	0%
		C	0	284	0%	0	131	0%	0	296	0%
		E	0	133	0%	0	213	0%	0	160	0%
		G	0	65	0%	0	104	0%	0	78	0%
		H	0	65	0%	0	104	0%	0	78	0%
		J	1	132	0%	0	211	0%	1	158	1%
		L	0	103	0%	0	131	0%	1	339	0%
		M	0	82	0%	0	131	0%	1	99	1%
	Total		**43**	**4953**	**1%**	**17**	**5766**	**0%**	**20**	**6800**	**0%**

Table 4.10. Distress Quantity Ratios for Lower Spandrel Walls (1918 Concrete), Spans 6-7

Expansion Joint Status	Span	No.	Distress Quantity (sf)	Surface Area (sf)	Distress Quantity Ratio
Always Expansion Joint	6	A	635	963	66%
		D	--		
		G	--		
		J	883	1732	51%
	7	A	--		
		D	25	153	17%
		G	--		
		J	552	2140	26%
	Sub-Total		**2095**	**4987**	**40%**
Never Expansion Joint	6	B	74	993	7%
		C	31	306	10%
		E	--		
		F	--		
		H	--		
		I	60	459	13%
	7	B	--		
		C	--		
		E	--		
		F	--		
		H	52	611	9%
		I	24	1376	2%
	Sub-Total		**241**	**3745**	**8%**
Span 6-7 Total			**2336**	**8732**	**22%**

Table 4.11. Distress Quantity Ratios for Upper Spandrel Walls (1980 Concrete), Spans 6-7

Expansion Joint Status	Span	No.	Distress Quantity (sf)	Surface Area (sf)	Distress Quantity Ratio
Always Expansion Joint	6	A	154	1788	9%
		D	1	459	0%
		G	5	306	2%
		J	54	866	6%
	7	A	172	2751	6%
		D	46	459	10%
		G	40	306	13%
		J	38	459	8%
	Sub-total		**510**	**7392**	**7%**
Never Expansion Joint	6	B	3	993	0%
		C	0	764	0%
		E	1	306	0%
		F	0	153	0%
		H	0	611	0%
		I	1	917	0%
	7	B	1	1987	0%
		C	7	1070	1%
		E	20	306	6%
		F	2	153	1%
	Sub-total		**34**	**7259**	**1%**
Spans 6-7 Total			**544**	**14651**	**4%**

Table 4.12. Distress Quantity Ratios for Upper Spandrel Columns (1980 Concrete), Spans 1-5, Total by Span

Expansion Joint Status	Span	Downstream			Middle			Upstream		
		Distress Quantity (sf)	Surface Area (sf)	Distress Quantity Ratio	Distress Quantity (sf)	Surface Area (sf)	Distress Quantity Ratio	Distress Quantity (sf)	Surface Area (sf)	Distress Quantity Ratio
Always Expansion Joint	1	104	1090	15%	6	602	2%	102	1967	5%
	2	124	832	11%	4	624	1%	95	1321	5%
	3	109	718	15%	36	726	5%	79	1642	3%
	4	127	1622	4%	23	875	3%	71	1642	3%
	5	189	1490	13%	5	854	1%	78	1963	2%
	Sub-total	653	5751	12%	**73**	**3681**	**2%**	424	8535	4%
Never Expansion Joint	1	33	1013	3%	14	1163	1%	14	1412	1%
	2	1	881	0%	2	1073	0%	2	1078	0%
	3	6	1131	0%	0	1130	0%	0	1601	0%
	4	1	983	0%	1	1243	0%	0	1024	0%
	5	2	945	0%	0	1157	0%	5	1685	0%
	Sub-total	43	4953	1%	17	5766	0%	20	6800	0%
Total		**696**	**10704**	**6%**	**90**	**9447**	**1%**	**444**	**15336**	**2%**

Table 4.13. Distress Quantity Ratios for Upper Spandrel Walls (1980 Concrete), Spans 6-7, Total by Span

Expansion Joint Status	Span	Distress Quantity (sf)	Surface Area (sf)	Distress Quantity Ratios
Always Expansion Joint	6	214	3418	4%
	7	296	3974	9%
	Sub-total	**510**	**7392**	**7%**
Never Expansion Joint	6	5	3744	0%
	7	29	3515	2%
	Sub-total	**34**	**7259**	**1%**
Total		**544**	**14651**	**4%**

Table 4.14. Distress Quantity Ratios for Total Height of Spandrel Column (Both 1918 and 1980 Concrete) Spans 1-5

Span	No.	Downstream			Middle			Upstream		
		Distress Quantity (sf)	Surface Area (sf)	Ratio	Distress Quantity (sf)	Surface Area (sf)	Ratio	Distress Quantity (sf)	Surface Area (sf)	Ratio
1	A*	35	533	7%	108	854	13%	13	641	2%†
	B	16	396	3%	7	635	1%	15	477	2%
	C	11	287	4%†	42	460	6%	2	345	1%†
	D*	15	202	7%†	3	323	5%	46	243	19%
	E	0	140	0%	0	224	0%	0	169	0%
	F	0	99	0%	0	159	0%	8	119	7%
	G	5	82	6%	11	131	8%	1	99	1%
	H	14	89	16%	3	142	2%	11	107	10%
	I	11	113	10%	0	181	0%	8	136	6%
	J	3	149	2%	0	238	0%	0	179	0%
	K*	65	231	37%	31	369	7%	23	278	8%†
	L	34	325	7%	65	520	8%	0	391	0%†
	M	51	446	7%	0	714	0%	40	537	4%
	N*	313	557	38%	155	892	10%	50	670	7%
2	A*	153	572	17%	328	913	20%	57	572	10%†
	B	122	424	18%	54	677	5%	24	424	4%†
	C	0	313	0%†	40	501	5%	0	313	0%†
	D*	53	227	16%	19	363	4%	41	227	16%
	E	1	165	1%	0	264	0%	2	165	1%
	F	6	53	11%	0	85	0%	0	53	0%
	G	0	34	0%	0	55	0%	0	34	0%
	H	0	38	0%	0	61	0%	0	38	0%
	I	2	69	3%	0	110	0%	2	69	3%
	J	0	103	0%	2	165	1%	0	103	0%
	K*	69	164	40%	27	261	9%	7	164	3%
	L	21	258	5%	11	413	2%	0	258	0%†
	M	15	379	3%	36	605	4%	0	379	0%
	N*	95	503	19%†	224	803	17%	29	503	6%†
3	A*	436	553	52%	191	883	16%	58	553	11%†
	B	16	408	2%	12	652	1%	0	408	0%†
	C	0	289	0%†	0	462	0%	0	289	0%†
	D*	42	198	21%†	11	316	2%	0	198	0%†
	E	0	127	0%	0	204	0%	0	127	0%
	F	0	83	0%	0	132	0%	0	83	0%
	G	0	62	0%	0	99	0%	0	62	0%
	H	0	62	0%	0	99	0%	0	62	0%
	I	3	83	4%	0	132	0%	0	83	1%
	J	4	126	3%	0	201	0%	0	126	0%
	K*	2	189	1%†	7	303	2%	10	189	5%†
	L	3	279	1%†	22	446	4%	0	279	0%†
	M	0	393	0%	19	627	2%	16	393	5%
	N*	215	537	43%	141	858	16%	10	537	2%†
4	A*	66	568	12%†	238	908	20%	46	568	8%†
	B	5	420	1%	5	671	1%	4	420	1%
	C	1	308	0%†	26	492	4%	0	308	0%†
	D*	3	213	2%†	7	341	2%	0	213	0%†
	E	0	146	0%	0	234	0%	0	146	0%
	F	2	98	2%	0	157	0%	0	98	0%
	G	0	79	0%	0	127	0%	0	79	0%
	H	0	79	0%	0	127	0%	0	79	0%
	I	0	98	0%	0	157	0%	7	98	7%
	J	0	143	0%	0	228	0%	0	143	0%
	K*	93	205	46%	4	327	2%	39	205	24%
	L	0	289	0%	10	462	2%	3	289	1%
	M	5	399	1%	7	638	1%	55	399	9%
	N*	55	541	10%†	152	864	13%	17	541	3%†

Table 4.14. Distress Quantity Ratios for Total Height of Spandrel Column (Both 1918 and 1980 Concrete) Spans 1-5 (continued)

Span	No.	Downstream			Middle			Upstream		
		Distress Quantity (sf)	Surface Area (sf)	Ratio	Distress Quantity (sf)	Surface Area (sf)	Ratio	Distress Quantity (sf)	Surface Area (sf)	Ratio
5	A*	50	538	9%†	135	862	10%	41	647	6%†
	B	179	396	29%	3	635	0%	2	477	0%†
	C	0	284	0%†	62	454	10%	2	341	2%
	D*	42	195	21%	10	312	4%	0	234	0%†
	E	0	133	0%	0	213	0%	0	160	0%
	F	15	82	18%	0	131	0%	0	99	0%
	G	0	65	0%	0	104	0%	0	78	0%
	H	0	65	0%	0	104	0%	0	78	0%
	I	0	82	0%	0	131	0%	0	99	0%
	J	1	132	0%	0	211	0%	1	158	1%
	K*	59	193	37%	9	309	4%	3	232	1%†
	L	63	282	18%	37	451	6%	1	339	0%†
	M	34	398	5%	3	638	0%	4	479	1%
	N*	78	542	14%†	260	867	18%	33	651	5%†
Grand Total		**2580**	**17311**	**11%**	**2536**	**27682**	**5%**	**733**	**18740**	**4%**

** Indicates current expansion joint location*

† Indicates 1980 concrete full-height of column (i.e., no 1918 lower column remaining)

Table 4.15. Distress Quantity Ratios for Spandrel Walls (all concrete) Spans 6-7

Span	No.	Distress Quantity (sf)	Surface Area (sf)	Distress Quantity Ratio
6	A*	789	2751	37%
	B	77	1987	4%
	C	31	1070	5%
	D*	1	459	0%†
	E	1	306	0%†
	F	0	153	0%†
	G*	5	306	2%†
	H	0	611	0%†
	I	61	1376	7%
	J*	937	2598	29%
7	A*	172	2751	6%†
	B	1	1987	0%†
	C	7	1070	1%†
	D*	72	611	13%
	E	20	306	6%†
	F	2	153	1%†
	G*	40	306	13%†
	H	52	611	9%
	I	24	1376	2%
	J*	590	2598	17%
Grand Total		**2880**	**23384**	**10%**

** Indicates current expansion joint location*

† Indicates 1980 concrete full-height of column (i.e, no 1918 lower column remaining)

Table 4.16. Distress Quantity Ratios for Arch Ribs

Arch Type	Span	Downstream (Spans 1-5) / Full-width (Spans 6-7)			Middle (Spans 1-5)			Upstream (Spans 1-5)		
		Distress Quantity (sf)	Surface Area (sf)	Distress Quantity Ratio	Distress Quantity (sf)	Surface Area (sf)	Distress Quantity Ratio	Distress Quantity (sf)	Surface Area (sf)	Distress Quantity Ratio
Arch Ribs (Spans 1-5)	1	1681	6900	24%	908	9450	10%	1839	**7750**	24%
	2	1308	6900	19%	353	9450	4%	1139	**6900**	17%
	3	1375	6900	20%	188	9450	2%	1552	**6900**	23%
	4	819	6900	12%	21	9450	0%	1575	**6900**	23%
	5	644	6900	9%	75	9400	1%	829	**7700**	11%
	Total	**5827**	**34500**	**17%**	**1545**	**47200**	**3%**	**6933**	**36150**	**19%**
Barrel Arches (Spans 6-7)	6	3544	21650	16%						
	7	2678	21600	12%						
	Total	**6222**	**43250**	**14%**						

Table 4.17. Distress Quantity Ratios for Arch Pier Walls and Bases

Arch Pier No.	Exterior Wall Surfaces (sf)			Interior Wall Surfaces (sf)			Bases* (sf)		
	Distress Quantity (sf)	Surface Area (sf)	Distress Quantity Ratio	Distress Quantity (sf)	Surface Area (sf)	Distress Quantity Ratio	Distress Quantity (sf)	Surface Area (sf)	Distress Quantity Ratio†
1	1027	7880	13%	2148	12882	17%	2282	2142	107%
2	124	7674	2%	137	5144	3%	820	1224	67%
3	317	7587	4%	66	5057	1%	1750	1258	139%
4	149	7587	2%	62	3491	2%	1270	1258	101%
5	25	7674	0%	40	5144	1%	341	1258	27%
6	754	8364	9%	1098	15072	7%	629	1531	41%
7	184	5322	3%	62	4526	1%	108	527	21%
8	1000	6876	15%	1163	12128	10%	479	658	73%
Total	**3579**	**58963**	**4%**	**4774**	**63443**	**3%**	**7679**	**9856**	**72%**

** Includes area of arch piers inspected by WJE. Arch pier bases below the arch spring line were inspected by Collins Engineers. Although quantities from Collins' inspection are not included in this tabulation, their overall findings were generally similar in extent of distress.*

† Distress quantity for pier bases includes a significant amount of overlap between noted areas of delamination/spalling, freeze-thaw damage, and failed patches; as such, percentages are higher than actual and exceed 100% in some cases.

Table 4.18. Distress Quantity Ratios for Approach Span Superstructure

Element Category	Span	Distress Quantity (lf)	Total Quantity (lf)	Distress Quantity Ratio
Prestressed Girders	N1	2	914	0.2%
	N2	4	914	0.4%
	Total	**6**	**1828**	**0.3%**
Weathering Steel Girders	S1	0	971	0.0%
	S2	44	885	5.0%
	Total	**44**	**1856**	**2.4%**

Table 4.19. Distress Quantity Ratios for Approach Span Substructure

Element Category	Span	Distress Quantity (sf)	Surface Area (sf)	Distress Quantity Ratio
Abutments	N1	57	2921	2%
	S1	30	3281	1%
	Total	**86**	**6202**	**1%**
Columns	B1	0	774	0%
	B2	0	2350	0%
	Total	**0**	**3124**	**0%**
Retaining Walls	N1	236	3019	8%
	S1	0	154	0%
	Total	**236**	**3173**	**4%**

Table 4.20. Condition State Summary for Pedestrian Railings – Aluminum Panels

Condition State	Count of Railing Panels						
	Overall	Repairs	Corrosion	Cracking	Connection	Distortion	Misalignment
CS1	530	0	0	0	0	0	0
CS2	57	0	3	32	0	15	0
CS3	16	4	0	5	2	3	6
CS4	4	0	0	0	2	2	1
Total	607	4	3	37	4	20	7

Table 4.21. Condition State Summary for Pedestrian Railings – Concrete Posts

Condition State	Count of Posts
CS1	485
CS2	115
CS3	6
CS4	0
Total	606

Table 4.22. Condition State Summary for Traffic Barrier – Metal Rails

Condition State	Count of Railing Panels						
	Overall	Repairs	Corrosion	Cracking	Connection	Distortion	Misalignment
CS1	0	0	0	0	0	0	0
CS2	144	0	147	0	0	0	4
CS3	4	0	1	0	1	0	2
CS4	2	0	1	0	1	0	0
Total	150	0	149	0	2	0	6

Table 4.23. Distress Quantity Ratios Traffic Barrier – Concrete J-Rails

Span	Distress Quantity (sf)	Surface Area (sf)	Distress Quantity Ratio
South Approach	1	1464	0.1%
1	21	1506	1.4%
2	44	1386	3.2%
3	8	1386	0.6%
4	3	1386	0.2%
5	26	1428	1.8%
6	16	888	1.8%
7	21	966	2.1%
North Approach	9	1842	0.5%
Total	**149**	**12252**	**1.2%**

5. DECK JOINT MOVEMENT AND RELATED STRUCTURAL DISTRESS

5.1. Background to the Issue

5.1.1. Chronological History of Bridge Deck Joints and Related Conditions

Joints in the decks of open-spandrel arch bridges are provided to accommodate longitudinal movement relative to the arches, which rise or fall to accommodate temperature and shrinkage strain. The original deck completed in 1918 contained 6 joints in each arch rib span and 4 joints in each barrel arch span for a total number of 38 joints in the arch spans. The layout of the joints, taken from the 1918 plans, is shown in Figure 5.1. The figure also shows the locations of the current deck joints installed in 1980. In the arch rib spans, the total number of joints per span was not changed in 1980, but the locations of the joints was changed; the joint at the third spandrel column from each pier was relocated to the fourth spandrel column from each pier. The number and location of the joints in the barrel arch spans has not changed since original construction.

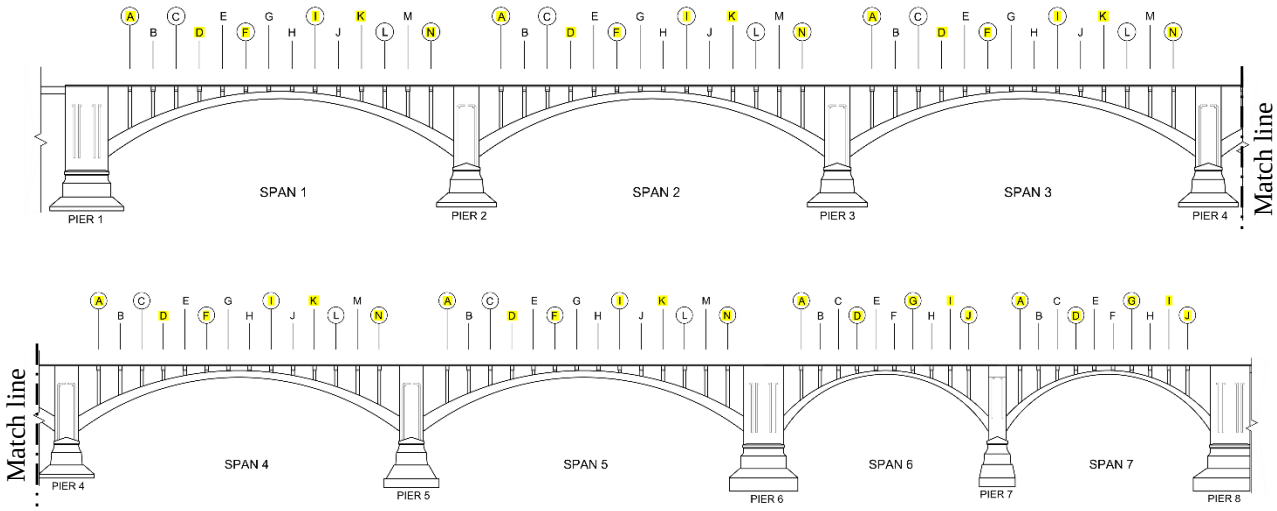

Figure 5.1. Elevation of bridge showing 1918 and 1980 deck joint locations. Column lines at original 1918 joints are circled; column lines at 1980 joints are highlighted in yellow.

The original drawings contained limited information about the deck joint details. One detail through the street car portion at the middle of the bridge deck (Figure 5.2) shows a deck joint with a call-out for "1/2" elastic filler." One detail of the railings (Figure 5.3) shows a 1/2 inch wide expansion joint between adjacent railing posts. From this information, we infer that the joints in the 1918 deck were either 1/2 inch wide gaps that were formed into the deck and filled with an elastomeric sealing material, or 1/2 inch wide gaps that were formed using an elastomeric filler board. "EXP. FILL" on the railing joint detail in Figure 5.3 indicates that these joints were intended to accommodate expansion.

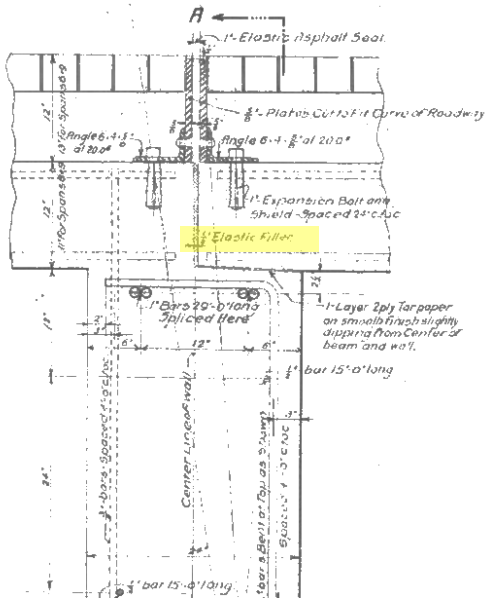

Figure 5.2. Detail from 1916 blue line plans with deck joint callout (highlighted).

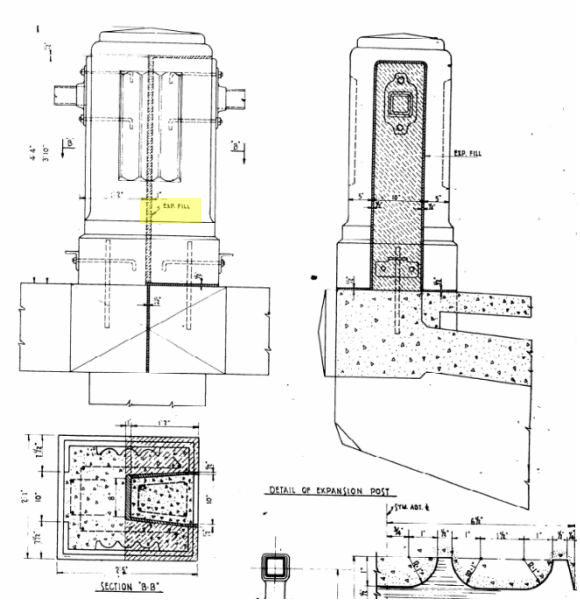

Figure 5.3. Detail from 1916 blue line plans with expansion joint shown in railing post (highlighted).

In 1968, a comprehensive inspection of the bridge[13] noted extensive leakage through the deck and deck joints, and, as a result, extensive surface deterioration to the deck and concrete elements below. However, the report did not note any structural distress that would indicate abnormal movement of the bridge associated with the behavior of the original deck joints. For example, the 1968 report noted vertical cracking in the north and south walls of Pier 1 but did not mention diagonal cracking in Piers 1 or 8, and the report did not mention any structural cracking in the spandrel columns or walls. Refer to Section 2.3 for further details from the 1968 inspection report.

In 1980, the deck, cap beams, and tops of the spandrel columns were replaced. The new deck (arch spans and approach spans) was designed with 43 poured sealant joints. The 1980 deck contained 6 joints in each arch rib span and 4 joints in each barrel arch span, the same joint quantities as existed in the original deck. The layout of the joints (as noted above) is the same as the original layout in the barrel arch spans but different in the arch rib spans.

Details for the 1980 deck joints can be seen in Figure 5.4 and Figure 5.5. As shown, the adjacent deck sections were cast against each other, and the top of the cap beams and mating deck surfaces were painted with asphalt to reduce bond and friction. The deck was secured to the cap beams with vertical dowels spaced at 12 inch centers along both sides of the joints. The dowels were wrapped in polystyrene foam to allow deck movement around the dowels. For water-tightness, a waterstop was cast between adjacent deck sections. The surface of the deck was sawcut and filled with sealant.

[13] "Bridge Inspection, Third Avenue Bridge Over the Mississippi River, Minneapolis, Engineering Report, November 1968," prepared by Howard, Needles, Tammen & Bergendogg Consulting Engineers.

Assuming an approximate joint spacing of 40 feet and a typical value for concrete shrinkage of 500 microstrain, the 1980 joints would have opened on the order of 1/4 inch as the deck concrete cured. Thus, the deck joint detail could only accommodate thermal expansion to the extent shrinkage opened the joint.

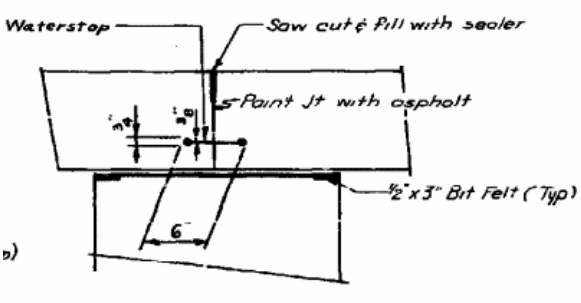

Figure 5.4. Typical joint detail from 1980 plans.

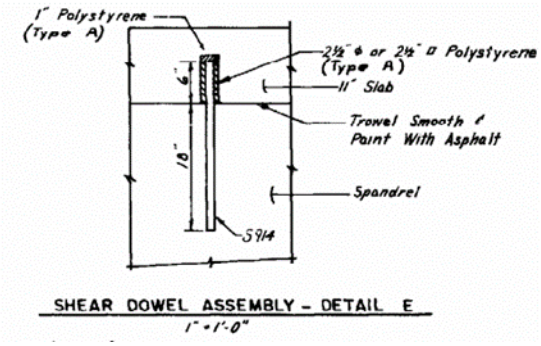

Figure 5.5. Detail of vertical dowels with foam surrounds, from 1980 plans.

In the 1980s and 1990s, bridge inspections noted structural distress developing in the bridge related to movement issues. This included the following (refer to Section 2.3 for further details):

- wide diagonal shear cracking in Pier 8 (first noted in 1992);
- shear cracking in spandrel columns, particularly severe in the short columns near the arch crowns in Spans 1 and 7 (first noted in 1994/1995); and
- shear cracking and spalling of cap beams (spalls at top corners of cap beams below joints first noted in 2000, shear cracking in cap beams first noted in 1991, and general spalls in cap beams first noted in 1986).

The 2000 bridge inspection report stated: "Despite numerous repair attempts by the bridge crew, the poured [sealant] joints in the arch spans are leaking (seal material has failed). There is extensive spalling and patching along these joints and severe slab deterioration below. This joint design simply does not accommodate the thermal expansion and contraction of a bridge this length. These joints should be reconstructed (perhaps replaced with strip seals), to prevent further slab and superstructure deterioration."

In 2003, the deck joints were reconstructed to their present-day configuration. The joints are located and numbered for reference in plan in Figure 5.6. In summary, 42 of the 43 poured sealant joints from the 1980 construction were locally demolished and reconstructed using strip seal expansion joint assemblies (2 inch design opening). A typical section through the 2003 deck joint is shown in Figure 5.7. The poured sealant joint at Joint 42 over Bent Pier 2 in the north approach was cleaned and resealed.

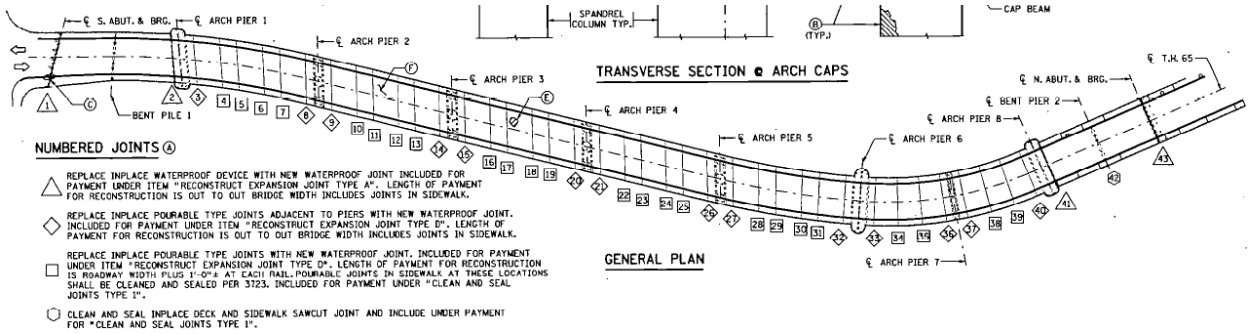

Figure 5.6. General plan of bridge deck showing 2003 deck joint locations and numbers (excerpted from 2003 joint replacement drawings).

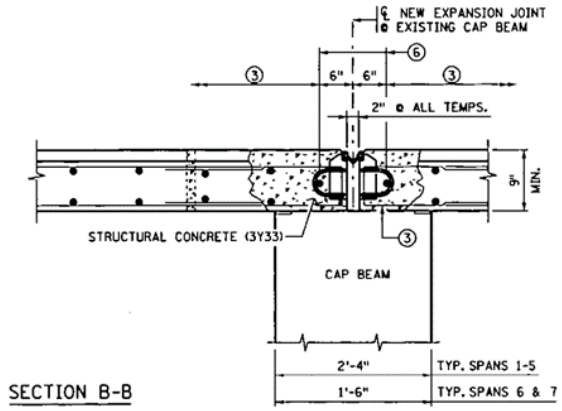

Figure 5.7. Typical joint repair detail from 2003 plans.

At the joints adjacent to the arch piers, the strip seal joint was extended throughout the roadway as well as the sidewalks (see Figure 5.8 and Figure 5.9). Steel cover plates were installed over the strip seal joints in the sidewalks. The strip seal joints were terminated at the inside face of the railing posts, thus leaving an approximately 1 foot wide poured sealant joint between the railing posts (see Figure 5.12). At the other joints within the arch spans, the strip seal joints were installed in the roadway only, and the original poured sealant joints in the sidewalks were cleaned and resealed (see Figure 5.10 and Figure 5.11).

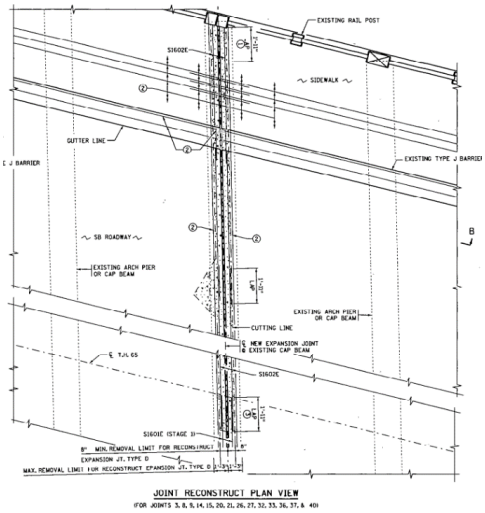

Figure 5.8. Half-deck plan showing strip seal joint in roadway and sidewalk for joints located adjacent to arch piers.

Figure 5.9. Photograph at pier showing strip seals and extending through roadway and sidewalk.

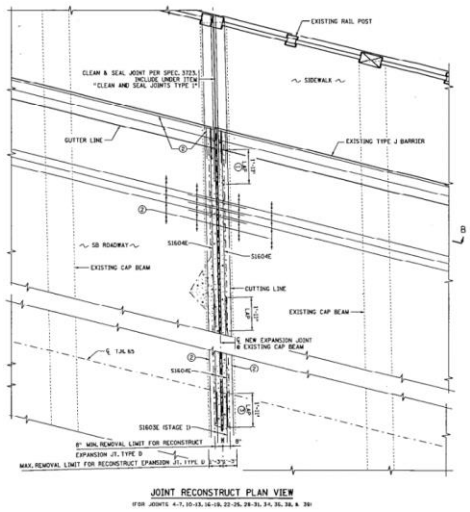

Figure 5.10. Half-deck plan showing strip seal in roadway only for joints located away from arch piers.

Figure 5.11. Photograph within arch span showing seals in roadway and poured sealant joints in sidewalk.

Figure 5.12. Termination of strip seal at inside face of railing post, with original poured sealant joint visible between posts.

Full-depth cast-in-place concrete repairs to the deck were executed along either side of the new strip seal joints installed in 2003. Partial-depth shotcrete repairs were also executed at spalls that were present on the deck underside and cap beams below the joints. Although the full-depth deck repairs exposed the vertical dowels between the cap beams and deck, the vertical dowels were not depicted on the 2003 plans. Construction photographs provided by MnDOT show that the vertical dowels were exposed in the repair areas (Figure 5.13). Some of the construction photographs show that foam surrounds were installed around dowels before casting the repair concrete (Figure 5.14).

Figure 5.13. Construction photograph from 2003 joint replacement project (provided by MnDOT). Note vertical dowels exposed in repair area.

Figure 5.14. Construction photograph from 2003 joint replacement project (provided by MnDOT). Note foam surrounds installed over vertical dowels.

Since 2003, bridge inspections have continued to note the movement-related distress conditions identified in the previous inspection reports, and some worsening of the conditions has been noted. In 2006, the Historic Bridge Management Plan for Bridge 2440 included the following recommendation: "The shearing

of spandrel column tops and the continual repair of expansion joints indicate that the bridge is moving in unanticipated directions. The movement patterns are likely complicated by the reverse curve alignment and the translation of the south approach spans north. Develop and implement a plan to monitor and collect the geometry of the bridge's superstructure and substructure as it moves with changes in temperature for a period of at least two years." The report also recommended that an in-depth inspection and concrete material testing program be conducted, and that recommendations be developed for future rehabilitation efforts.

5.1.2. Observations During 2017 Bridge Inspection

During the 2017 element-level bridge inspection, WJE noted many locations where distress conditions appeared to be related to movement restraint at the deck joints. These included wide diagonal cracking in Piers 1 and 8, shear cracking in spandrel columns, shear cracking and spalling of cap beams, and compression spalling of deck fascia. Deep spalls at the top corners of the cap beams exposed numerous vertical dowels between the cap beams and deck. Remnants of polystyrene foam were observed around a few dowels, but in most cases there was no evidence of foam surround, and the 2003 repair concrete was tight around the dowels. Dowels tight against the concrete essentially preclude joint movement. As noted above, construction photographs provided by MnDOT show that foam surrounds were provided in at least some locations.

During a progress meeting with HNTB and MnDOT while the present inspection was underway, WJE brought these conditions to MnDOT's attention and provided a presentation with example photographs. At that time, it was agreed that WJE would measure the gaps at all the deck joints and then repeat those measurements near the end of the inspection. The intent was to capture the greatest temperature change, and greatest joint gap change, during the available time window. The collected data would be reviewed in order to gain further understanding about the behavior of the deck joints.

5.2. Deck Joint Gap Measurements and Analysis

5.2.1. Gap Measurements

As part of the element-level inspection, WJE measured the width of the gaps at the strip seal expansion joints using a tape measure on May 5, 2017 at the downstream shoulder strip and on May 15, 2017 at the upstream shoulder stripe (Figure 5.15). Once expansion joint movement was identified as a key issue regarding the bridge behavior, WJE repeated the measurements along the downstream shoulder stripe using digital calipers across drilled alignment marks on May 26, 2017 (Figure 5.16). The measurements were repeated on August 6, 2017 during the last weekend of bridge inspection work.

Figure 5.15. Original gap measurements using tape measure at shoulder stripe.

Figure 5.16. Gap measurements using digital calipers between drilled alignment marks.

The temperatures associated with the measurements were taken as the daily average temperatures as well as the averaged daily temperatures from the 7 days prior to each of the surveys, as reported by the nearest airport weather station. These temperatures are summarized in Table 5.1.

Table 5.1. Temperatures at Times of Joint Gap Measurements

Location	Date	Daily Average Temperature, °F	Weekly Average Temperature, °F
Downstream shoulder			
Tape, initial	May 5, 2017	58	48
Tape, repeat	August 6, 2017	68	69
Calipers, initial	May 26, 2017	69	54
Calipers, repeat	August 6, 2017	68	69
Upstream shoulder			
Tape, initial	May 15, 2017	64	61
Tape, repeat	August 6, 2017	68	69

As shown, the differences in temperatures between the initial and repeat measurements with the calipers at the downstream shoulder were from 1 to 15°F, depending on whether daily or weekly average temperatures were assumed. At the upstream side, the temperature differences were even less.

During the course of WJE's field measurements, MnDOT provided HNTB and WJE with measurements of the joint gap widths that had been surveyed by MnDOT in the past. The data provided were for temperatures of -10°F, 50°F, and 90°F. WJE's measurements as well as the MnDOT survey data are shown in Table 5.2.

Table 5.2. Summary of Joint Gap Measurement Data

Downstream								Upstream				
Joint #	MnDOT Survey at -10F (in.)	MnDOT Survey at 50F (in.)	MnDOT Survey at 90F (in.)	WJE tape 5/5/2017 58F / 48F (in.)	WJE tape 8/6/2017 68F / 69F (in.)	WJE calipers 5/26/2017 69F / 54F (in.)	WJE calipers 8/6/2017 68F / 69F (in.)	MnDOT Survey at -10F (in.)	MnDOT Survey at 50F (in.)	MnDOT Survey at 90F (in.)	WJE tape 5/15/2017 64F / 61F (in.)	WJE tape 8/6/2017 68F / 69F (in.)
1	4.843	2.913	2.835	2.25	2.125	2.1545	2.134	3.819	3.346	3.228	2.5	2.500
2	4.213	3.110	2.795	2.5	2.313	2.3115	2.339	4.764	3.307	3.189	2.625	2.563
3	3.031	2.598	2.677	1.875	1.875	1.8515	1.875	3.071	2.520	2.480	1.75	1.750
4	2.677	2.677	2.638	2	2.000	1.9610	1.980	2.717	2.677	2.677	2	1.938
5	2.756	2.756	2.598	2	2.000	2.0090	2.021	2.480	2.402	2.441	2	2.000
6	3.071	2.756	2.677	2	2.000	1.9790	2.002	2.638	2.559	2.559	2	1.938
7	3.740	2.677	2.638	2.125	1.938	1.9175	1.938	2.835	2.835	2.795	2	2.000
8	2.795	2.441	2.165	1.625	1.500	1.4735	1.515	2.717	2.323	2.244	1.5	1.500
9	2.717	2.283	2.126	1.5	1.500	1.5335	1.510	2.992	2.362	2.244	1.75	1.625
10	2.717	2.717	2.677	2	2.000	2.0000	2.015	2.677	2.677	2.638	2	2.000
11	2.795	2.795	2.795	2	2.000	1.9725	1.995	2.835	2.835	2.835	2	2.000
12	2.874	2.874	2.835	2	2.000	1.9480	1.975	2.559	2.520	2.520	2	2.000
13	2.953	2.953	2.874	2	2.000	1.9585	1.970	2.717	2.638	2.638	2	2.000
14	2.874	2.402	2.205	1.625	1.500	1.5270	1.518	2.677	2.126	2.047	1.5	1.500
15	2.874	2.480	2.362	NA	1.500	1.5440	1.541	3.031	2.520	2.323	2	1.750
16	2.835	2.835	2.795	2	2.000	1.9715	1.973	2.756	2.717	2.677	2	2.000
17	3.031	3.031	2.953	2.125	2.063	2.0740	2.077	2.992	2.913	2.874	2.125	2.000
18	2.874	2.874	2.874	2	2.000	2.0470	2.067	2.795	2.795	2.795	2	1.938
19	2.874	2.874	2.795	2	2.000	2.0480	2.064	3.110	3.110	3.071	2.125	2.000
20	3.031	2.559	2.362	1.625	1.563	1.5965	1.601	2.913	2.402	2.362	1.625	NA
21	2.835	2.323	2.205	1.625	1.563	1.5875	1.618	3.307	2.677	2.598	1.625	1.625
22	2.835	2.835	3.071	2	2.000	1.9455	1.963	2.677	2.638	2.638	2	2.000
23	2.677	2.677	2.756	1.875	1.875	1.9225	1.943	2.992	2.913	2.874	2	1.938
24	2.756	2.756	2.717	2	2.000	1.9845	2.014	2.756	2.677	2.756	2.125	2.063
25	2.677	2.638	2.638	1.875	1.875	1.9085	1.905	2.874	2.874	2.835	2	2.000
26	2.874	2.283	2.126	1.625	1.563	1.9475	1.590	2.953	2.402	2.283	1.5	1.500
27	2.835	2.441	2.362	1.625	1.563	1.5965	1.585	3.110	2.520	2.402	1.75	1.750
28	2.756	2.756	2.717	2	2.000	2.0075	2.025	2.717	2.717	2.638	2	2.000
29	2.677	2.677	2.638	2	2.000	1.9850	2.001	2.756	2.677	2.717	2	2.000
30	2.717	2.677	2.638	2	2.000	1.9585	1.975	3.110	3.031	3.031	2	2.000
31	2.598	2.598	2.559	2	2.000	2.0670	2.074	2.874	2.717	2.756	2	2.000
32	2.874	2.362	2.165	1.625	1.625	1.6505	1.638	3.110	2.559	2.402	1.5	1.563
33	2.756	2.362	2.244	1.5	1..5	1.5190	1.497	2.756	2.244	2.165	1.5	1.813
34	2.795	2.795	2.677	1.875	1.938	1.9100	1.943	2.953	2.756	2.874	2	2.125
35	2.717	2.717	2.638	1.875	1.875	1.8715	1.883	3.071	3.071	3.071	2	2.000
36	2.559	2.559	2.520	1.75	1.813	1.7995	1.804	2.835	2.598	2.559	2	1.938
37	2.874	2.402	2.244	1.375	1.375	1.4210	1.401	3.110	2.598	2.441	1.5	1.500
38	2.874	2.874	2.874	1.875	1.875	1.9480	1.946	2.874	2.795	2.756	2	2.063
39	2.638	2.638	2.638	1.75	1.813	1.8720	1.875	2.598	2.598	2.598	2	2.063
40	2.835	2.835	2.717	1.75	1.750	1.7710	1.763	3.228	2.953	2.913	1.75	1.813
41	4.764	3.780	3.425	3	2.875	2.8965	2.886	4.921	3.780	3.583	2.75	2.750
43	3.150	3.150	3.031	2.5	2.500	2.5220	2.510	3.740	3.425	3.386	2.5	2.625

**Note: Differences between MnDOT survey data and WJE gap measurements suggest that the surveyors used a different gage length than WJE. See Figures 5.15 and 5.16 for WJE method. The MnDOT data and WJE data both seem internally consistent.*

5.2.2. Deck Joint Movement Patterns

Due to the relatively small change in temperature between WJE's initial and final measurements, the measurements supplied by MnDOT, which were recorded at more extreme temperature differences, were judged to be more useful and were analyzed further. The same general patterns of joint movement were observed in WJE's survey measurements, though to a lesser degree due to the smaller temperature changes.

Table 5.3 utilizes colored conditional formatting to illustrate the degree of movement occurring at each of the 43 deck joints during temperature changes of -10 to 50°F, 50 to 90°F, and -10 to 90°F. Values in the table have been normalized to movement per 10°F so that they can be compared. Measurements at the downstream side are shown; the upstream data shows similar trends.

Color coding in Table 5.3 (and in Figure 5.17) is as follows:

- Red text (lines): Essentially no movement occurring (movement < 0.015" for 10°F change, which is less than 0.5 times expected[14])
- Light green shading (lines): Roughly expected level of movement occurring (0.015" < movement < 0.1" for 10°F change, which is 0.5 to 3 times expected)
- Heavy green shading (lines): Much greater than expected movement occurring (movement > 0.1" for 10°F change, which is more than 3 times expected).

Figure 5.17 shows plan views of the bridge deck with the joints color-coded using the same coloring scheme listed above, in order to illustrate graphically which joints are moving. The top, middle and bottom of the figure shows joint movement patterns for temperature changes of -10 to 90°F , -10 to 50°F, and 50 to 90°F, respectively.

[14] For this review, the "expected level" of joint movement was taken to be an averaged, approximate value that was calculated by dividing the total length of the bridge by the number of joints and multiplying by a typical coefficient of thermal expansion for a 10°F temperature change.

Table 5.3. Evaluation of Joint Gap Measurement Data (Downstream Side)

Joint #	Gap at -10°F (in.)	Gap at 50°F (in.)	Gap at 90°F (in.)	Normalized Movement (in. per 10F)		
				-10 to 50°F	50 to 90°F	-10 to 90°F
1	4.843	2.913	2.835	0.322	0.020	0.201
2	4.213	3.110	2.795	0.184	0.079	0.142
3	3.031	2.598	2.677	0.072	-0.020	0.035
4	2.677	2.677	2.638	0.000	0.010	0.004
5	2.756	2.756	2.598	0.000	0.039	0.016
6	3.071	2.756	2.677	0.052	0.020	0.039
7	3.740	2.677	2.638	0.177	0.010	0.110
8	2.795	2.441	2.165	0.059	0.069	0.063
9	2.717	2.283	2.126	0.072	0.039	0.059
10	2.717	2.717	2.677	0.000	0.010	0.004
11	2.795	2.795	2.795	0.000	0.000	0.000
12	2.874	2.874	2.835	0.000	0.010	0.004
13	2.953	2.953	2.874	0.000	0.020	0.008
14	2.874	2.402	2.205	0.079	0.049	0.067
15	2.874	2.480	2.362	0.066	0.030	0.051
16	2.835	2.835	2.795	0.000	0.010	0.004
17	3.031	3.031	2.953	0.000	0.020	0.008
18	2.874	2.874	2.874	0.000	0.000	0.000
19	2.874	2.874	2.795	0.000	0.020	0.008
20	3.031	2.559	2.362	0.079	0.049	0.067
21	2.835	2.323	2.205	0.085	0.030	0.063
22	2.835	2.835	3.071	0.000	-0.059	-0.024
23	2.677	2.677	2.756	0.000	-0.020	-0.008
24	2.756	2.756	2.717	0.000	0.010	0.004
25	2.677	2.638	2.638	0.007	0.000	0.004
26	2.874	2.283	2.126	0.098	0.039	0.075
27	2.835	2.441	2.362	0.066	0.020	0.047
28	2.756	2.756	2.717	0.000	0.010	0.004
29	2.677	2.677	2.638	0.000	0.010	0.004
30	2.717	2.677	2.638	0.007	0.010	0.008
31	2.598	2.598	2.559	0.000	0.010	0.004
32	2.874	2.362	2.165	0.085	0.049	0.071
33	2.756	2.362	2.244	0.066	0.030	0.051
34	2.795	2.795	2.677	0.000	0.030	0.012
35	2.717	2.717	2.638	0.000	0.020	0.008
36	2.559	2.559	2.520	0.000	0.010	0.004
37	2.874	2.402	2.244	0.079	0.039	0.063
38	2.874	2.874	2.874	0.000	0.000	0.000
39	2.638	2.638	2.638	0.000	0.000	0.000
40	2.835	2.835	2.717	0.000	0.030	0.012
41	4.764	3.780	3.425	0.164	0.089	0.134
43	3.150	3.150	3.031	0.000	0.030	0.012

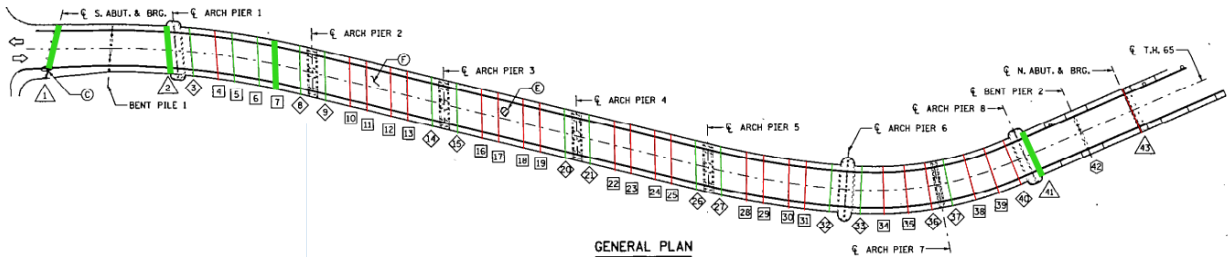

Joint Movement -10 to 90°F

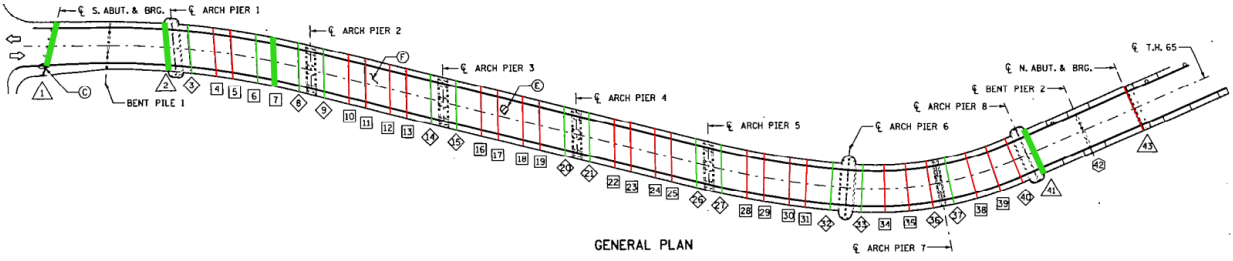

Joint Movement -10 to 50°F

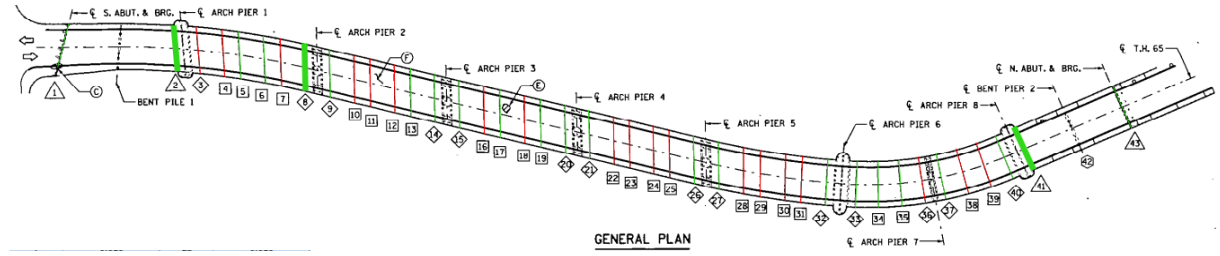

Joint Movement 50 to 90° F

Figure 5.17. Deck joint movement patterns based on Table 5.3 and legend below.

Legend:

- *Red lines: Essentially no movement occurring (movement < 0.015" for 10°F change, which is less than 0.5 times expected)*
- *Light green lines: Roughly expected level of movement occurring (0.015" < movement < 0.1" for 10°F change, which is 0.5 to 3 times expected)*
- *Heavy green lines: Much greater than expected movement occurring (movement > 0.1" for 10°F change, which is more than 3 times expected).*

Review of Table 5.3 and Figure 5.17 yields the observations listed below. Note that the measurements indicate changes in the joint gap widths, not absolute joint or deck position, so interpretation of the data is limited and must be made with care.

- In Spans 2 through 5, the joints adjacent to the piers that were reconstructed using strip seal joints across the full width of the bridge deck (except for between the railing posts), are moving. However, the intervening joints where the strip seal joints are only present in the roadway, are essentially locked. This is particularly true in the low temperature range; when temperatures become hotter, a few of the intervening joints begin to move a small amount.

- In Span 1, Joints 3, 6, 7 and 8 are moving in the low temperature range, with a large amount of movement occurring at Joint 7. However, in the high temperature range, Joints 3, 4 and 7 become essentially locked. Since locked Joints 3 and 4 are adjacent to Pier 1, the pier is likely getting pushed southward during periods of hot temperatures.

- In Spans 6 and 7, most of the joints are essentially locked, including the joints on the south sides of Piers 7 and 8. During the high temperature range, some of these joints begin to move a small amount. With so many of the joints in these spans essentially locked, and the joint on the south sides of the piers also locked, the piers are likely getting pushed northward in hot weather. (See discussion about resulting cracking in Pier 8 below; Pier 7 is very narrow and may be rocking to accommodate the northward push.)

The above indications can be confirmed and expanded, if necessary, by review of the LIDAR data that we understand will be collected during summer and winter temperature periods at the bridge. Since the LIDAR data will show absolute position of the structure at given points in time (rather than just change in deck joint gap widths), it will enable more definitive conclusions regarding structural movements.

5.3. Summaries of Related Structural Distress Conditions

5.3.1. General

The patterns of joint movement indicated by the joint gap measurements, together with the structural distress identified in the WJE and prior MnDOT bridge inspections, provide information regarding the current behavior of the bridge in response to thermal changes. The following general findings seem apparent based on WJE's inspection and joint gap measurements. Performance of the bridge under thermal loading is being studied in detail by HNTB as part of their structural analysis and modelling and will be reported by them separately.

Bridge inspection reports from the 1980s indicate that movement-related structural distress began to develop in the bridge soon after the 1980 rehabilitation. The 1980 poured sealant joints (essentially contraction joints only in the concrete deck) apparently did not provide enough separation at the joints for the necessary bridge deck expansion to occur.

The 2003 joint replacement project did not improve, and in some respects seems to have worsened the thermal behavior of the bridge. Movement of the 2003 strip seal joints is impeded, at least in some locations, by 2003 repair concrete that was cast tight around the vertical dowels. This condition was observed by WJE in almost all locations where spalling was present and dowels were exposed. Movement is also impeded by the direct contact (bond or friction) between the repair concrete and the top surface of the cap beams. Where the foam surround is absent, very little to no joint movement (i.e., opening or closing) can occur unless the

dowels deform or fracture, or the concrete around the dowels spalls. Even where foam surround is present, bond or friction between the repair concrete and cap beam may be sufficient to initiate spalling.

Furthermore, adjacent to the piers, the strip seal joints extend through the roadway and sidewalk but do not extend between the railing posts. Closing of the joints is limited by the narrow poured sealant joints that exist at the outer edges of the deck, between the railing posts. At the intervening joints within the arch spans, closing of the joints is limited by the narrow poured sealant joints that exist in the sidewalks and between the railing posts.

Because restrictions to free expansion and contraction exist at various deck joints, the bridge structure must utilize alternative methods to resolve or accommodate the significant thermal changes that occur throughout the year. The structural distress conditions observed by WJE in the various bridge elements appear consistent with these restrained thermal movements:

- Since the central arch piers are very rigid longitudinally, and since the joints adjacent to the piers are nearly full-width of the bridge, the deck joints adjacent to the piers have broken free by spalling the cap beams around the vertical dowels and spalling the deck fascia. With these joints operating, the intervening joints in the span that are also restrained generally do not need to move, until temperatures become high.

- In Spans 1, 6 and 7 where several joints within the spans are locked, excessive longitudinal translation of the deck resulting from the locked expansion joints has distressed many of the spandrel columns and walls.

- Since the end piers (Piers 1 and 8) are not balanced with arch spans on both sides, the outward (i.e., away from the river) pushing on the piers due to the locked joints must be resisted solely by the piers themselves. This has resulted in significant shear cracking in the pier walls, sliding along horizontal construction joints in the piers, and possibly some degree of rocking of the piers. Rocking of the narrow Pier 7 seems likely.

Further detail regarding the various structural distress conditions that have developed as a result of the unintended behavior of the deck joints is provided in the sections that follow. Further interpretation of the structural distress will be possible from the forthcoming LIDAR survey results, which will show absolute position of the structure during different temperature states.

5.3.2. Piers 1 and 8 Structural Distress

Unbalanced shear forces in the longitudinal direction on the top of Pier 1 (southward) and top of Pier 8 (northward) have caused distress in the pier walls. The magnitude of the distress is more severe at Pier 8, likely because more joints are locked in Spans 6 and 7 than in Span 1 (see Figure 5.17), or Pier 1 may be rocking to some degree.

Pier 8 exhibits wide (1-1/4 inch wide, maximum) diagonal shear cracking on its downstream face, as well as northward sliding (also 1-1/4 inches, maximum) along a horizontal construction joint near the top of the pier, indicative of lateral force on the top of the pier toward the north. Vertical reinforcing bars that cross the construction joint are bent or fractured. Similar though less severe cracking and faulting is present on the pier's upstream face (cracks as wide as 1/4 inch). The distress was first noted in the bridge inspection reports from the 1980s, but the current width of the cracks and degree of sliding/faulting is more than noted

at that time, indicating that the distress is worsening. Worsening is likely due to cracks filling with dirt and debris when they open such that the cracks do not close completely upon reversal of the thermal movement.

- Photographs of select conditions are shown in Figure 5.18 through Figure 5.23.
- Locations of all wide cracks (cracks wider than 0.050 inches) are indicated in Figures 3 and 4 of Appendix 4.
- Complete Plannotate notes and additional photographs can be accessed using the links provided in Chapter 4 and in Appendix 4.

Figure 5.18. Pier 8, downstream face.

Figure 5.19. Pier 8, close-up of top of downstream face showing wide diagonal cracking.

Figure 5.20. Pier 8, downstream face, sliding along horizontal joint near top.

Figure 5.21. Pier 8, downstream face, fractured bar across horizontal joint near top.

Figure 5.22. Pier 8, upstream face.

Figure 5.23. Pier 8, upstream face, close-up of shear cracking extending from deck.

Pier 1 exhibits vertical and diagonal cracking (up to 1/8-inch wide) on its upstream face in a pattern indicative of lateral force on the top of the pier toward the south. Horizontal cracking of pilasters at the pier interior may be a result of flexural behavior of the pier. Net southward movement of the top of the pier is consistent with near-contact of the pier stem wall against the bearings and the ends of the south approach steel girders, as noted in the inspection. Contact during high temperature periods may have caused net southward movement of the south approach spans and the bending and shearing of the bolts in the fixed bearings at the south abutment. The contact of Pier 1 with the steel girders and bearings, as well as the damaged bolts at the south abutment, were first noted in the bridge inspection reports from the 1980s.

- Photographs of select conditions are shown in Figure 5.24 and Figure 5.25.
- Locations of all wide cracks (cracks wider than 0.050 inches) are indicated in Figures 1 and 2 of Appendix 4.
- Complete Plannotate notes and photographs can be accessed using the links provided in Chapter 4 and Appendix 4.

Figure 5.24. Pier 1, upstream face, shear cracking.

Figure 5.25. Pier 1, upstream face, close-up of shear cracking.

Piers 2 through 6 do not exhibit cracking indicative of unbalanced lateral forces on the piers from deck joint movement issues. It seems that the deck and arches within Spans 2 through 5 are moving relatively

independently and that Piers 2 through 6 are acting as relatively rigid stationary points. Pier 7, which is considerably narrower than the other piers, may be accommodating the northward translation of the deck due to the locked joints in Span 6 by rocking or flexural behavior.

5.3.3. Spandrel Column and Wall Movement-Related Distress

Cracks less than 0.050 inches wide were often observed along the construction joint at the base of the spandrel columns. However, at some locations, wider cracks indicative of shear distress and/or possible flexural hinging at the base of the columns were observed.

Table 1 in Appendix 4 lists all locations at which cracks wider than 0.050 inches, and other structural distress, were noted in the inspection. The right-hand column in the table contains hyperlinks to each condition annotation in Plannotate, which includes photographs and notes for each location.

The severity of the distress observed at each column was categorized as follows:

- Distress Category 1:
  Wide cracks (CS3 or CS4, i.e., wider than 0.050 inches) at base, cracks primarily horizontal
  Example in Figure 5.26
  Total number of locations: 44
- Distress Category 2:
  Wide cracks (CS3 or CS4, i.e., wider than 0.050 inches) at base, inclined cracks at upstream or downstream faces
  Example in Figure 5.27
  Total number of locations: 4
- Distress Category 3:
  Wide cracks (CS3 or CS4, i.e., wider than 0.050 inches) at base, inclined cracks at upstream or downstream faces, spalling or delaminations along cracks
  Examples in Figure 5.28 and Figure 5.29
  Total number of locations: 12

Figure 5.26. Spandrel column structural distress, distress category 1.

Figure 5.27. Spandrel column structural distress, distress category 2.

Figure 5.28. Spandrel column structural distress, distress category 3.

Figure 5.29. Spandrel wall structural distress, distress category 3.

The locations of the spandrel column and wall distress conditions are illustrated graphically in Figure 5.30 below, which shows the columns with different distress categories overlain on the joint movement diagram. As shown, more column and wall distress occurs in Spans 1, 6 and 7 where net longitudinal movement of the deck toward the ends piers is suggested by the joint gap measurements. In these regions, the columns are subjected to an increased amount of longitudinal translation at their tops, which, due to the rigidity of the columns, creates a longitudinal shear force on the tops of the columns.

Fixed and stationary at their bases, the spandrel columns have, in certain cases, cracked and rotated about their bases, and in other cases sheared. Cracking and rotation was typically observed at the base of longer spandrel columns, while shearing was typically observed at shorter columns near the center of arch ribs.

Significant evidence of movement toward Pier 1 was observed in the Span 1 columns. Cracks were typically observed to be wider at the north face of the columns, and inclined cracks (where present) were angled downward toward Pier 1. Similarly, evidence of movement toward Pier 8 was observed in the Span 6 and 7 spandrel walls. Much less, if any, evidence of movement of spandrel columns and walls was observed in Spans 2 through 5.

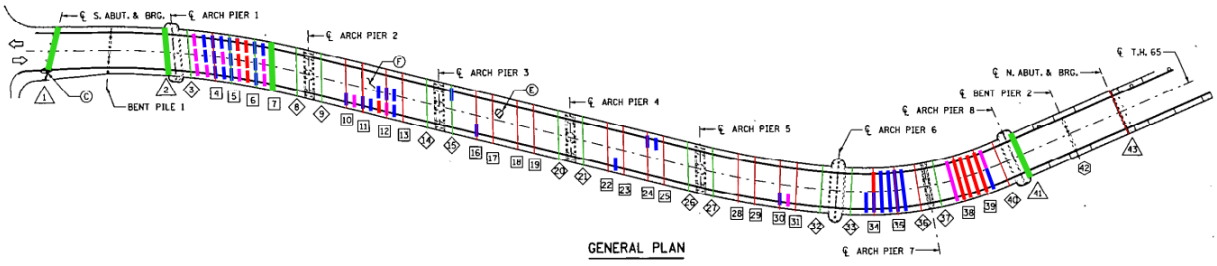

Figure 5.30. Plan view indicating locations of spandrel column distress overlaid on joint movement diagram (blue indicates distress category 1, purple indicates distress category 2, and red indicates distress category 3).

5.3.4. Cap Beam Mechanical Spalling

Deep spalls at the top corners of the cap beams that are located below bridge deck expansion joints were observed at the locations listed in Table 3 in Appendix 4. Vertical reinforcing bar dowels were typically exposed within these spalls, the dowels were typically heavily corroded, and polystyrene foam surround was typically not present around the dowels (i.e., the 2003 repair concrete was tight against the dowels). Remnants of foam surround were observed at a few locations. In some locations, the dowels were bent or fractured.

Figure 5.31 through Figure 5.36 show typical examples of the cap beam spalling conditions observed. Table 3 in Appendix 4 references additional photographs for each condition. As can be seen in the photographs, corrosion on the vertical dowels is typically severe at the deck-to-cap beam interface, but corrosion on the exposed reinforcing steel in the cap beam is only modest, not enough to have alone caused the degree of spalling that exists.

Figure 5.31. Spalling along top corner of cap beam.

Figure 5.32. Close-up of cap beam spalling, showing exposed vertical dowels.

Figure 5.33. Cap beam spall that was developing at the time of the inspection.

Figure 5.34. Close-up of vertical dowels, showing repair concrete tight against dowels.

Figure 5.35. Close-up of vertical dowel, showing corrosion of dowel and direct contact between repair concrete and top of cap beam.

Figure 5.36. Close-up of vertical dowel, showing repair concrete tight against dowel.

The locations of the cap beam spalls are illustrated graphically in Figure 5.37, which overlays the spall locations with the joint movement diagram. As shown, the deep spalls in the cap beams coincide with the locations where the deck joints are moving, typically at the joints adjacent to the piers.

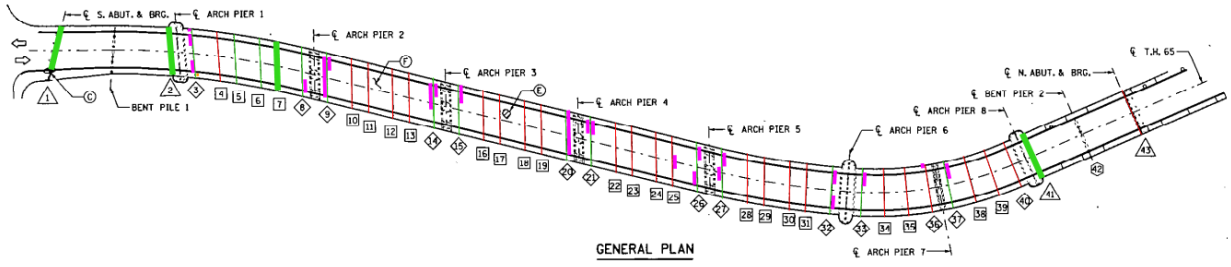

Figure 5.37. Plan view indicating locations of cap beam spalling, overlaid on joint movement diagram (purple indicates spall location).

The nature and location of the spalls suggest that the spalls were primarily mechanically-induced. Due to the restrained thermal movement, the vertical dowels have exerted outward force on the side face cover of the cap beams and eventually spalled the cover over the dowels. With the concrete cover spalled and some dowels fractured or bent, the strip seal joints at these locations are now relatively free to open and close to accommodate thermal changes. Frictional resistance between the top of the cap beams and the underside of the deck could have also contributed to the spalling.

Based on WJE's review of the previous bridge inspection reports and repair plans, some of the spalls noted in the 2017 inspection were present before the 2003 joint replacement program, but some were not. Of the 14 locations[15] at which spalls were noted in the 2000 bridge inspection report, it was apparent that three had been repaired in the 2003 repair program, but the repair material had since delaminated. At the other 11 locations, spalls were still present, and additional spalling appeared to have developed. It is unknown

[15] A location is defined as one face of a cap beam (i.e., Cap A north and Cap A south are considered two locations).

whether those 11 locations were repaired in 2003 and had spalled again, or whether they were not repaired in 2003. In addition, WJE noted similar spalls on other cap beams that were not noted in 2000. These spalls apparently developed after the 2003 repair program. Failure of the 2003 spall repairs and development of additional spalls since 2003 indicate that the mechanical damage is an ongoing problem that was perhaps worsened by the 2003 repair program.

5.3.5. Cap Beam Shear or Torsional Cracking

Diagonal cracking in cap beams, indicative of shear or torsional behavior, was observed at the locations shown in Table 2 of Appendix 4. The conditions occurred in Spans 1 and 7 where the most spandrel column and spandrel wall distress were also noted. In Span 7, the diagonal cracking was accompanied by delamination and spalling of the cap beam face. Examples of these conditions are shown in Figure 5.38 through Figure 5.41.

The nature and location of the cracking suggests that it was caused by differential thermal movement of the bridge deck along the length of the cap beams, which induced out-of-plane shear or torsional forces on the cap beams. Differential thermal movement could result from the edges of the deck being relatively free to move during temperature changes and direct sunlight exposure, whereas the interior of the deck is restrained by the arch ribs that are very stiff in the longitudinal direction, particularly near the arch crown where the columns are short. This effect is exaggerated in regions of the deck where the joints are locked.

Figure 5.38. Shear or torsional cracking in cap beam in Span 1, downstream side.

Figure 5.39. Shear or torsional cracking in cap beam in Span 1, downstream side.

Figure 5.40. Shear or torsional cracking in cap beam in Span 1, upstream side.

Figure 5.41. Shear or torsional cracking in cap beam in Span 7, downstream side.

5.3.6. Deck Fascia Compression Spalling

Spalling of previous shotcrete patches in the deck fascia adjacent to expansion joints was often evident. The spalls are more common and severe at the deck joints adjacent to piers, where the most joint movement is occurring and where the 1 foot width of deck between the railing posts is the narrow poured sealant joint rather than a strip seal expansion joint. It appears that thermal strains in the deck caused compression to develop in the edge of the deck between the railing posts, resulting in compression spalling of the deck concrete and shotcrete patches. Corrosion of the reinforcing steel at these locations is also contributing to the spalling. Examples of these conditions are shown in Figure 5.42 and Figure 5.43.

Figure 5.42. Spalling of deck fascia at deck joint.

Figure 5.43. Spalling of deck fascia at deck joint.

6. FOLLOW-UP TESTING AND MATERIAL SAMPLING RESULTS

The results of the follow-up testing and material sampling are summarized in this section of the report. Section 6.1 provides the overall results and describes findings that are common to multiple element categories within the bridge. Section 6.2 provides the specific results from testing of each of the individual element categories.

The goal of the follow-up testing was to characterize the distress observed during the in-depth element level inspections based on the material and exposure characteristics, and then to identify the deterioration mechanisms present in each element category. The results of the follow-up testing form the basis for the qualitative interpretations of durability potential (anticipated remaining service life) for each element category as presented in Section 7.

In total, 137 locations were accessed close-up for follow-up testing, 73 areas received non-destructive testing, 81 core samples were extracted, and 10 steel samples were removed. The locations of the testing are summarized in Figure 6.1 through Figure 6.9. Annotated on the elevation views are the locations of the deck joints from both the 1918 and 1980 construction. The figures illustrate the spatial distribution of the testing locations across the bridge and how the testing was focused on the different categories of structural elements.

The testing program was organized according to element category, where the category may include all such element types in the bridge or a subset of those elements differentiated by exposure or construction. The element categories defined for follow-up testing and material sampling are listed below.

Arch Spans

- Deck Topside (Roadway, Sidewalk) and Underside (see Sections 6.2.1, Figure 6.13)
- Upper Spandrel Columns and Walls (1980 Construction) - Always Below Expansion Joint (see Section 6.2.2, Figure 6.15, Figure 6.16, and Figure 6.17)
- Upper Spandrel Columns and Walls (1980 Construction) - Never Below Expansion Joint (see Section 6.2.3)
- Lower Spandrel Columns and Walls (1918 Construction) - Always Below Expansion Joint or Joint Since 1980 (see Section 6.2.4, Figure 6.15, Figure 6.16, Figure 6.21 and Figure 6.17)
- Lower Spandrel Column and Walls (1918 Construction) - Never Below Expansion Joint or Joint Between 1918-1980 (see Section 6.2.5, Figure 6.25 and Figure 6.26)
- Arch Ribs (see Section 6.2.6, Figure 6.28 and Figure 6.29)
- Barrel Arches (see Section 6.2.7, Figure 6.31)
- Arch Pier Walls (see Section 6.2.8, Figure 6.33Figure 6.)
- Arch Pier Bases[16] (see Section 6.2.9)

Approach Spans

- Deck Topside (Roadway, Sidewalk) and Underside (see Section 6.2.10, Figure 6.37 and Figure 6.38)
- South Approach Weathering Steel Girders (see Section 6.2.11)
- South Abutment (see Section 6.2.12)
- South Bent Pier (see Section 6.2.13)
- North Approach Prestressed Girder (see Section 6.2.14)
- North Abutment (see Section 6.2.15)

[16] As explained in Section 2.1.4, “arch pier bases” are defined in this report as the solid sections of pier below the tops of the arches.

- North Bent Pier (see Section 6.2.16)
- North Approach Retaining Wall (see Section 6.2.17)

Other Elements

- Deck Rail Elements (Traffic Barrier and Pedestrian Railing) (see Section 6.2.18)

After each element category listed above is the report section number where the detailed test results for that category can be found.

Also provided after the element categories listed above are figure references, which are one-page graphical summaries of the test results for that particular element category. These graphical summaries are a useful tool for reviewing all the test data for each element in one place. The graphical summaries are provided at the end of each section in Chapter 6.2 as well as altogether in Appendix 14.

Supporting information regarding the follow-up testing and material sampling program can be found in the following appendices of this report:

Appendix 6. Follow-up Testing - Summary Drawings
Appendix 7. Follow-up Testing - Locations and Summary Data
Appendix 8. Follow-up Testing - Material Samples
Appendix 9. Follow-up Testing Results That Could Affect As-Inspected Structural Model
Appendix 10. Petrographic Analysis Report
Appendix 11. Railing Testing - Ultrasonic Thickness and X-Ray Florescence
Appendix 12. Study Areas Plannotate Notes and Data
Appendix 13. Deck Study Areas Plannotate Notes and Data
Appendix 14. Graphical Summaries of Follow-up Testing Results

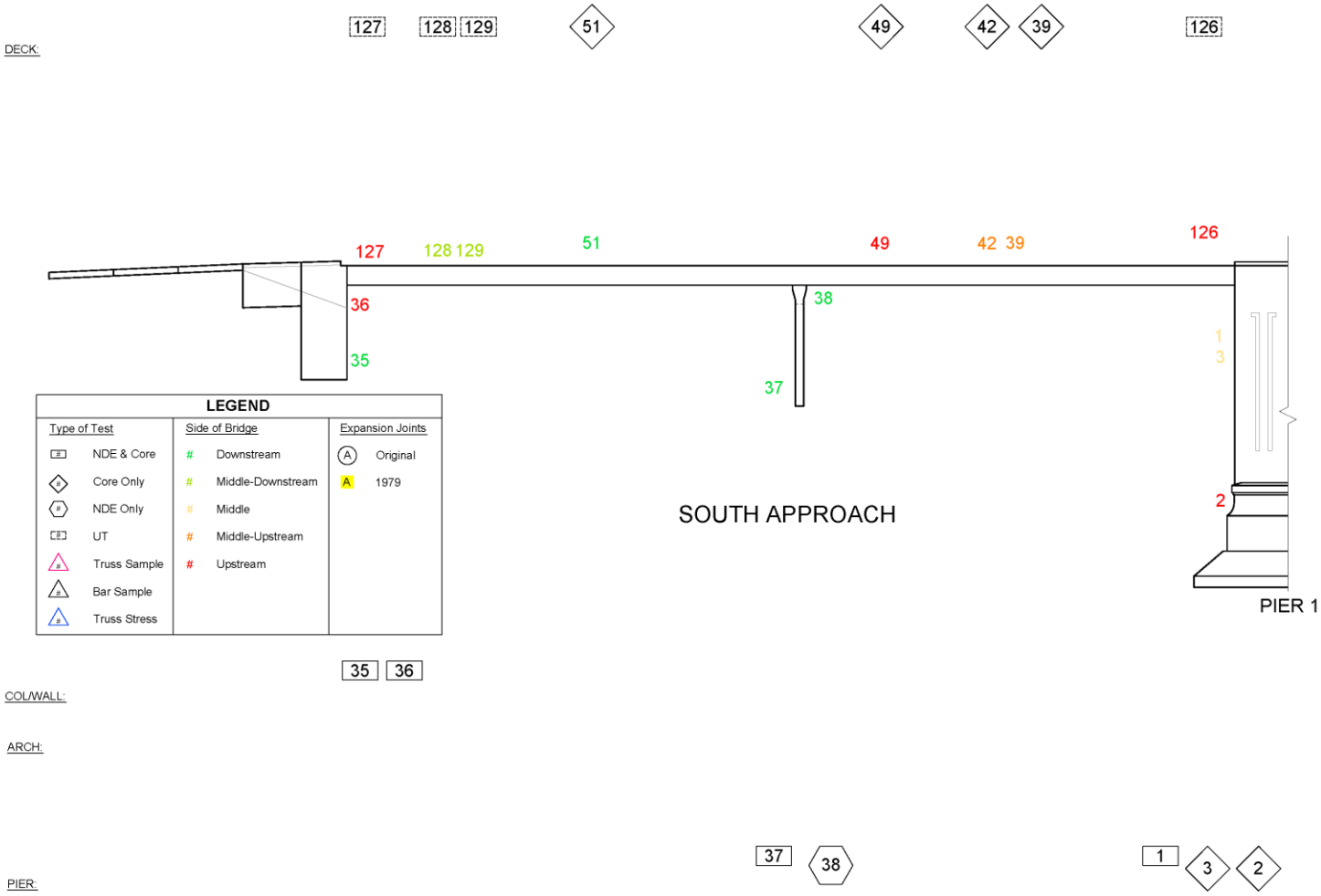

Figure 6.1. Follow-up Testing Location Summary - South Approach.

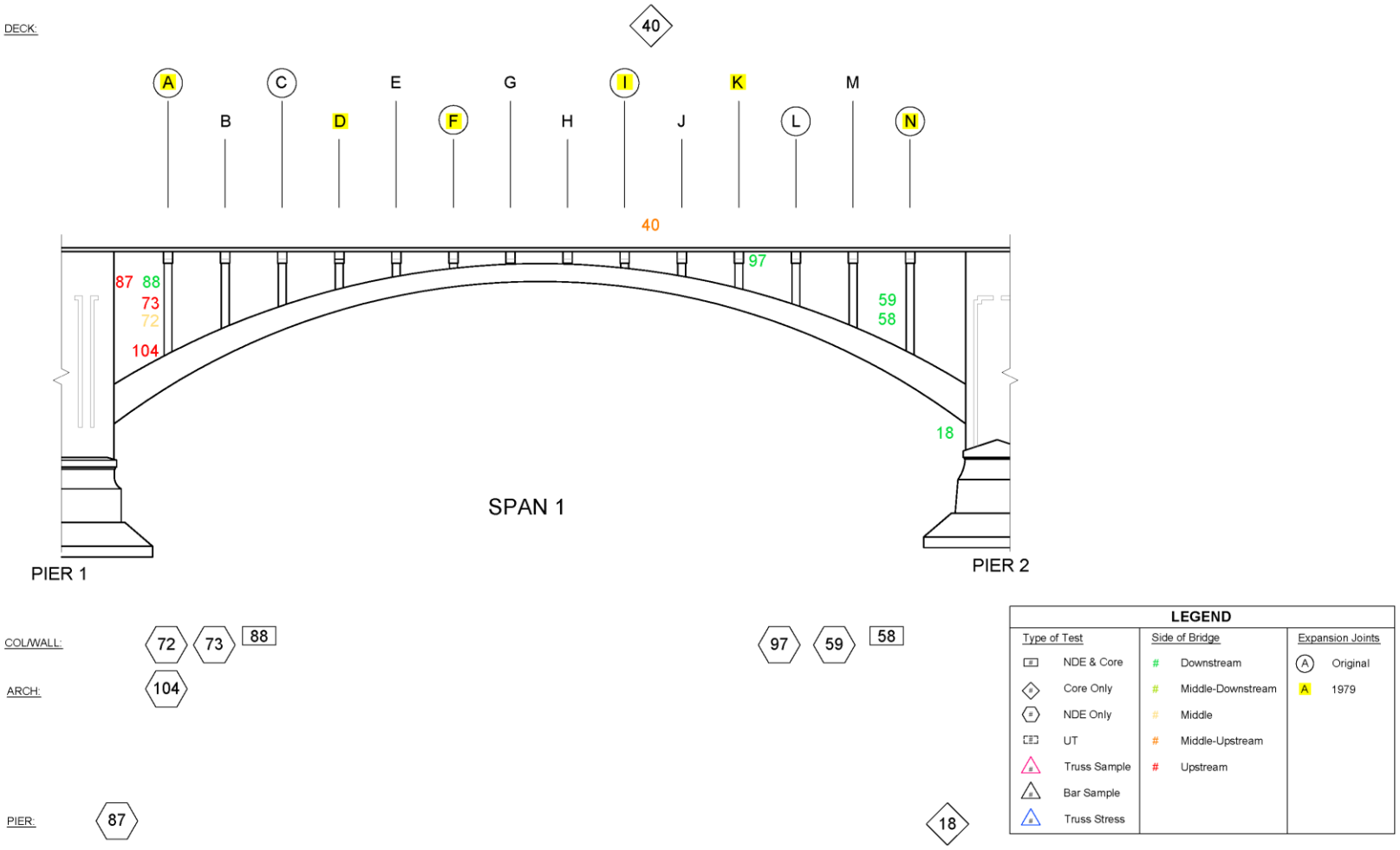

Figure 6.2. Follow-up Testing Location Summary - Arch Span 1.

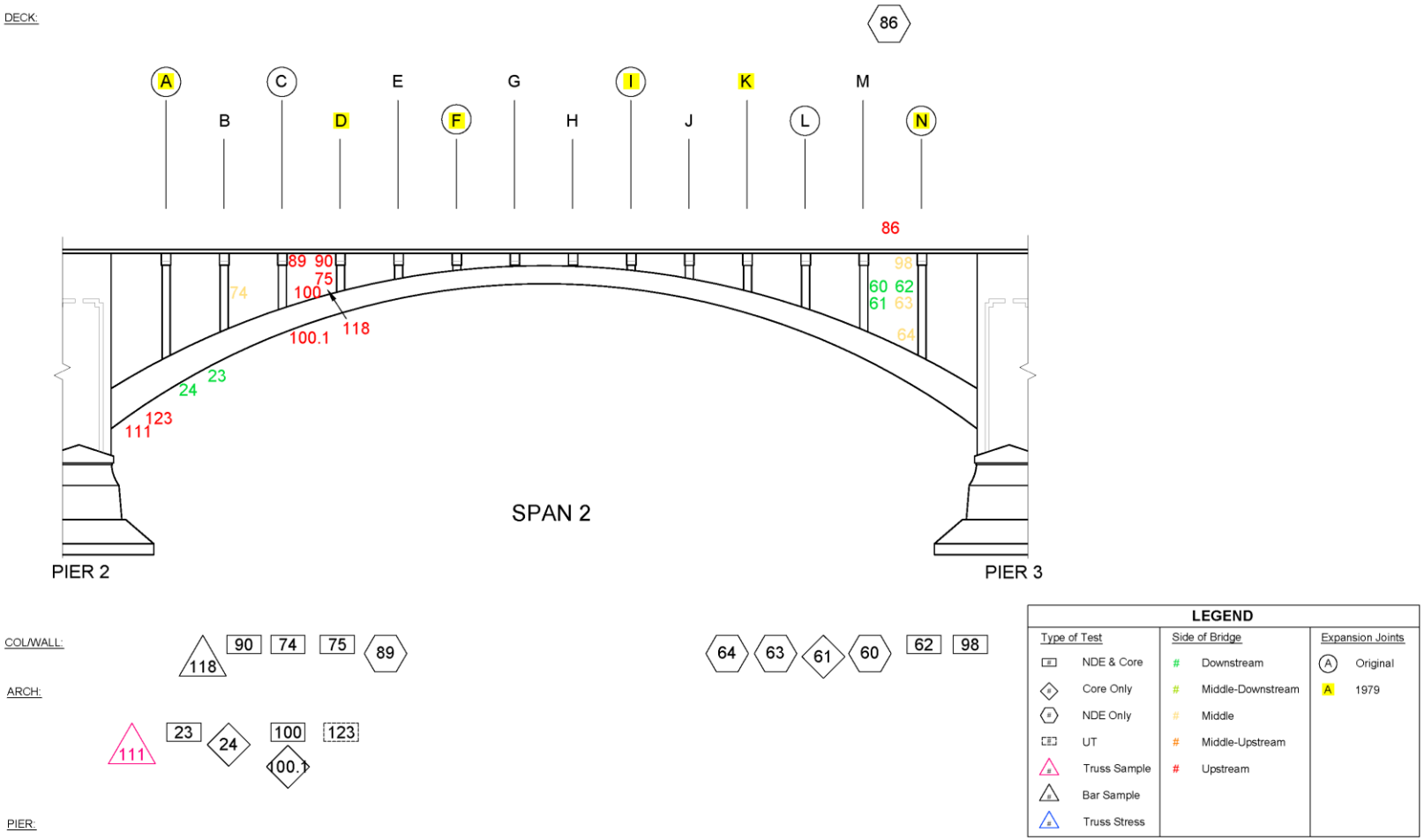

Figure 6.3. Follow-up Testing Location Summary - Arch Span 2.

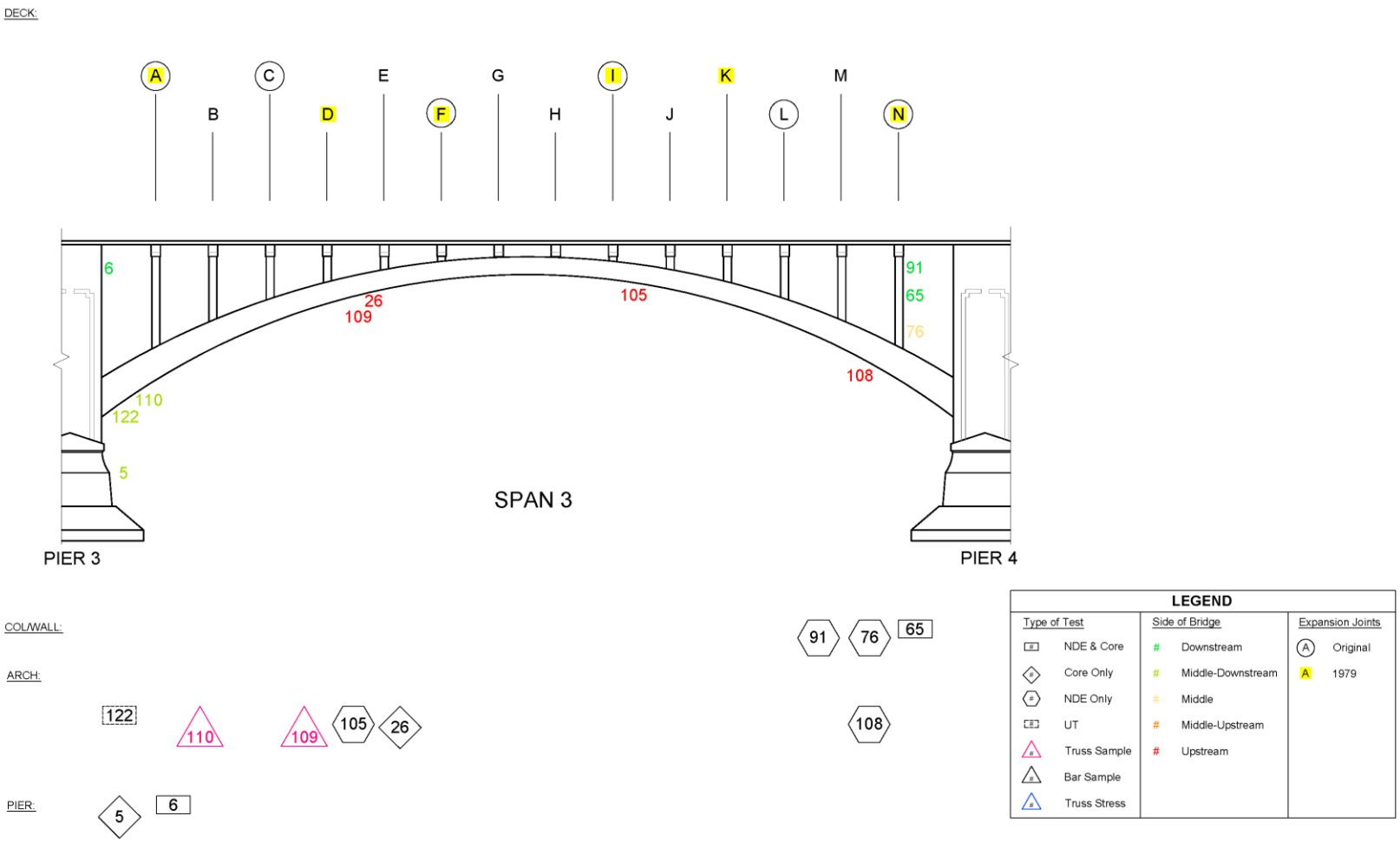

Figure 6.4. Follow-up Testing Location Summary - Arch Span 3.

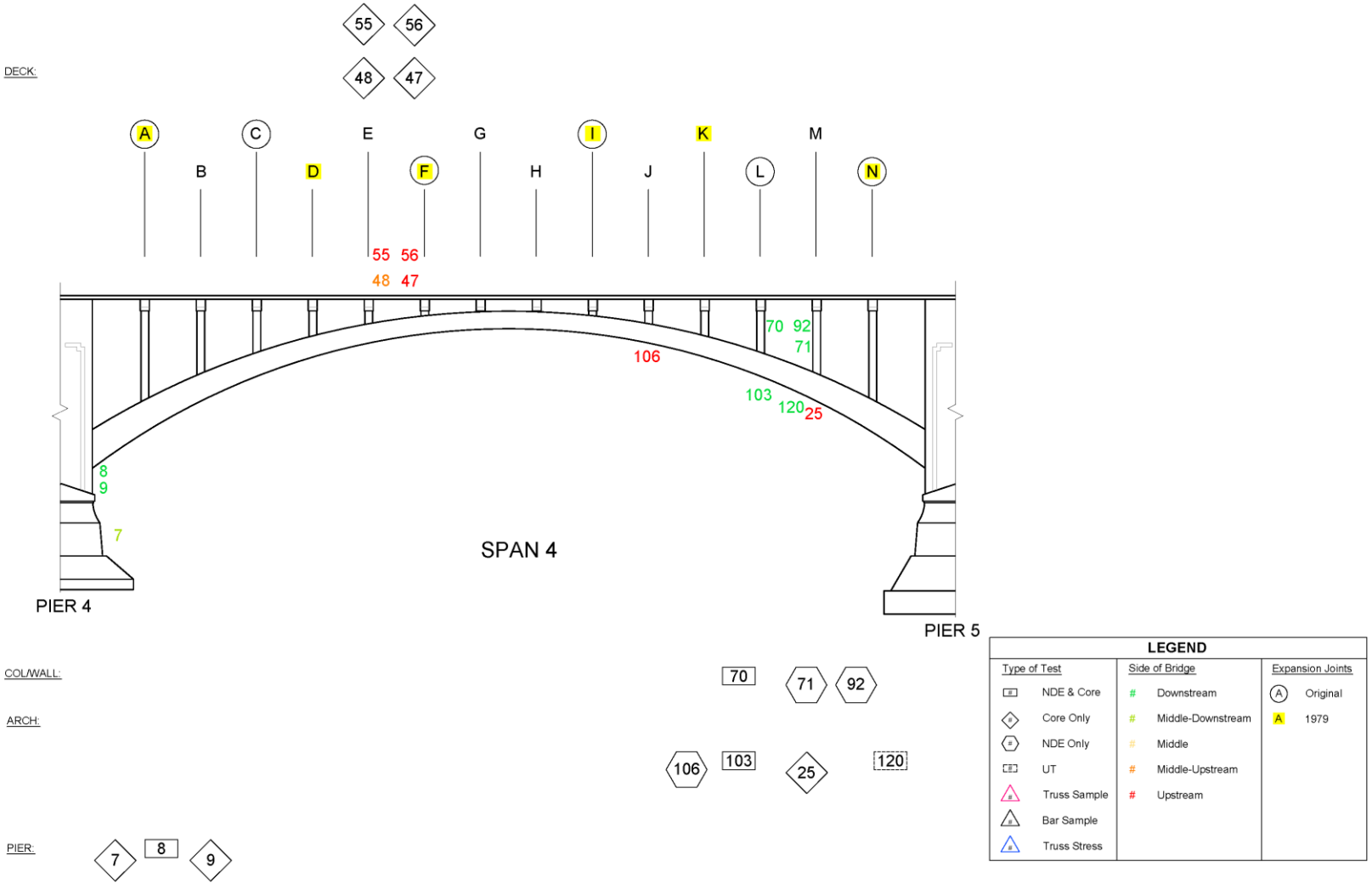

Figure 6.5. Follow-up Testing Location Summary - Arch Span 4.

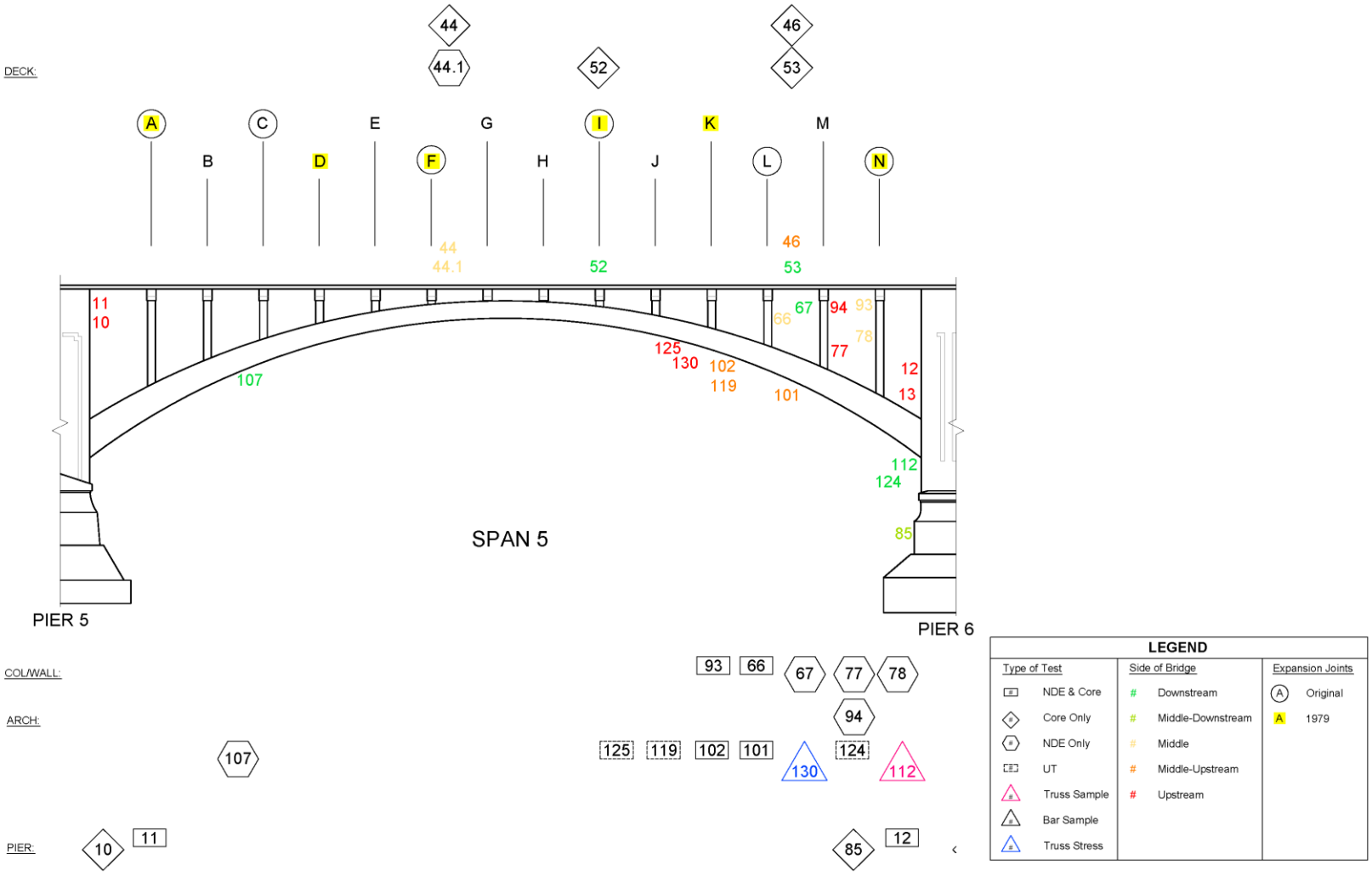

Figure 6.6. Follow-up Testing Location Summary - Arch Span 5.

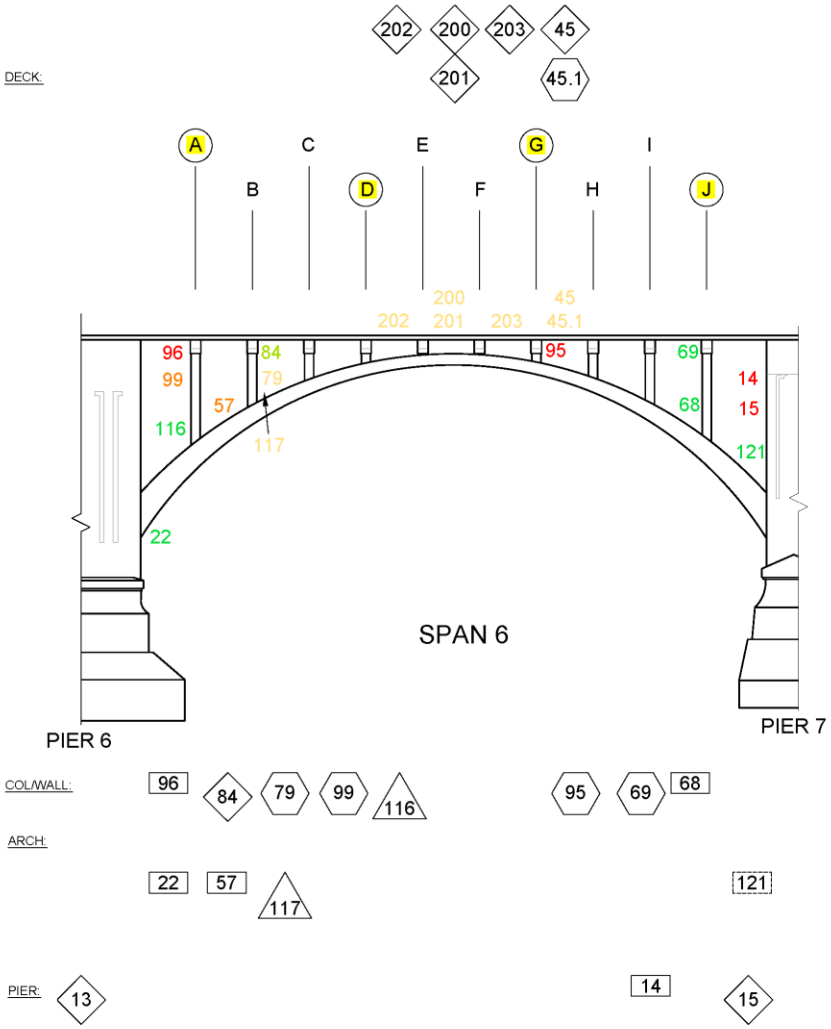

LEGEND		
Type of Test	Side of Bridge	Expansion Joints
NDE & Core	# Downstream	(A) Original
Core Only	# Middle-Downstream	A 1979
NDE Only	# Middle	
UT	# Middle-Upstream	
Truss Sample	# Upstream	
Bar Sample		
Truss Stress		

Figure 6.7. Follow-up Testing Location Summary - Arch Span 6.

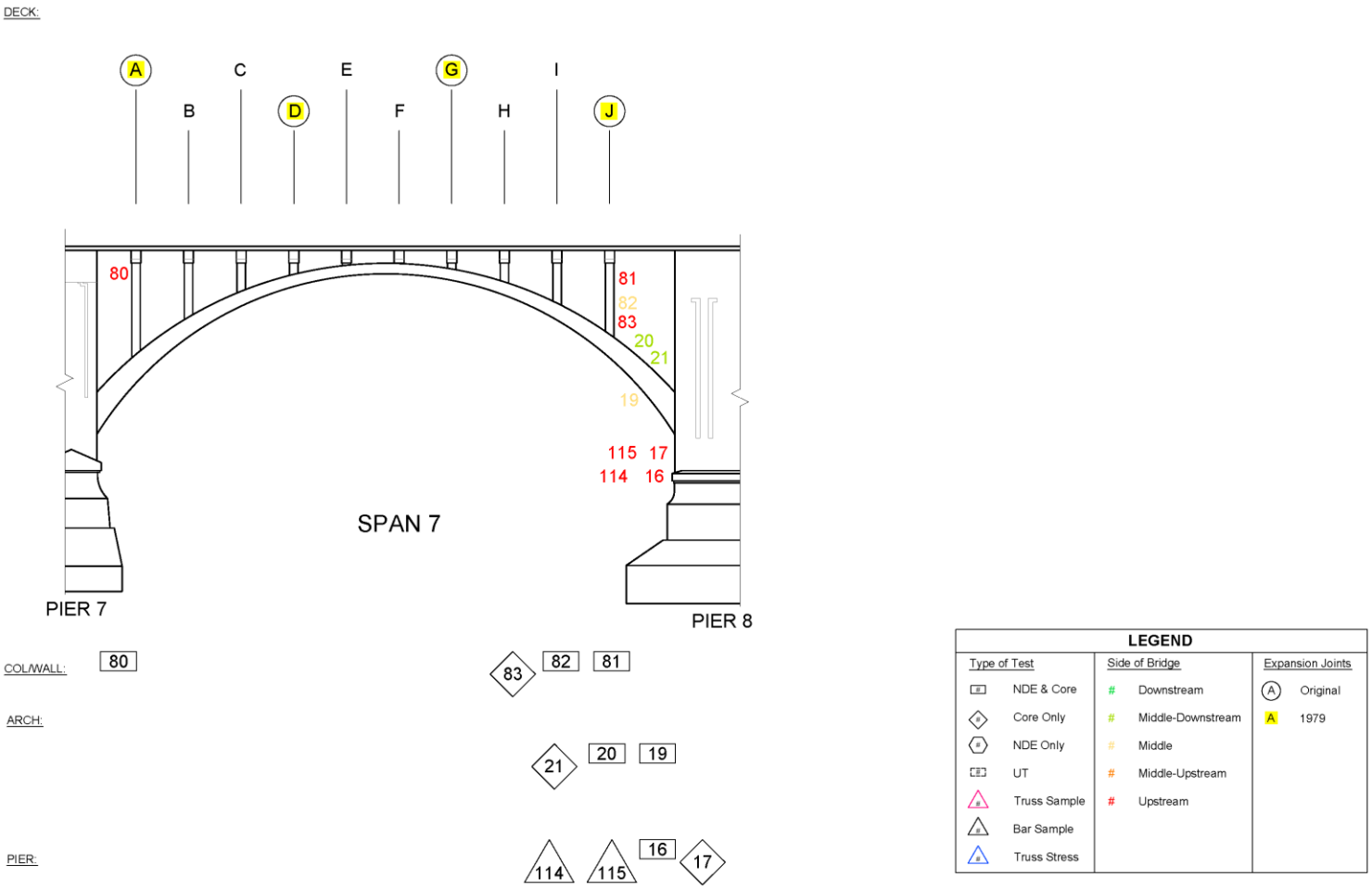

Figure 6.8. Follow-up Testing Location Summary - Arch Span 7.

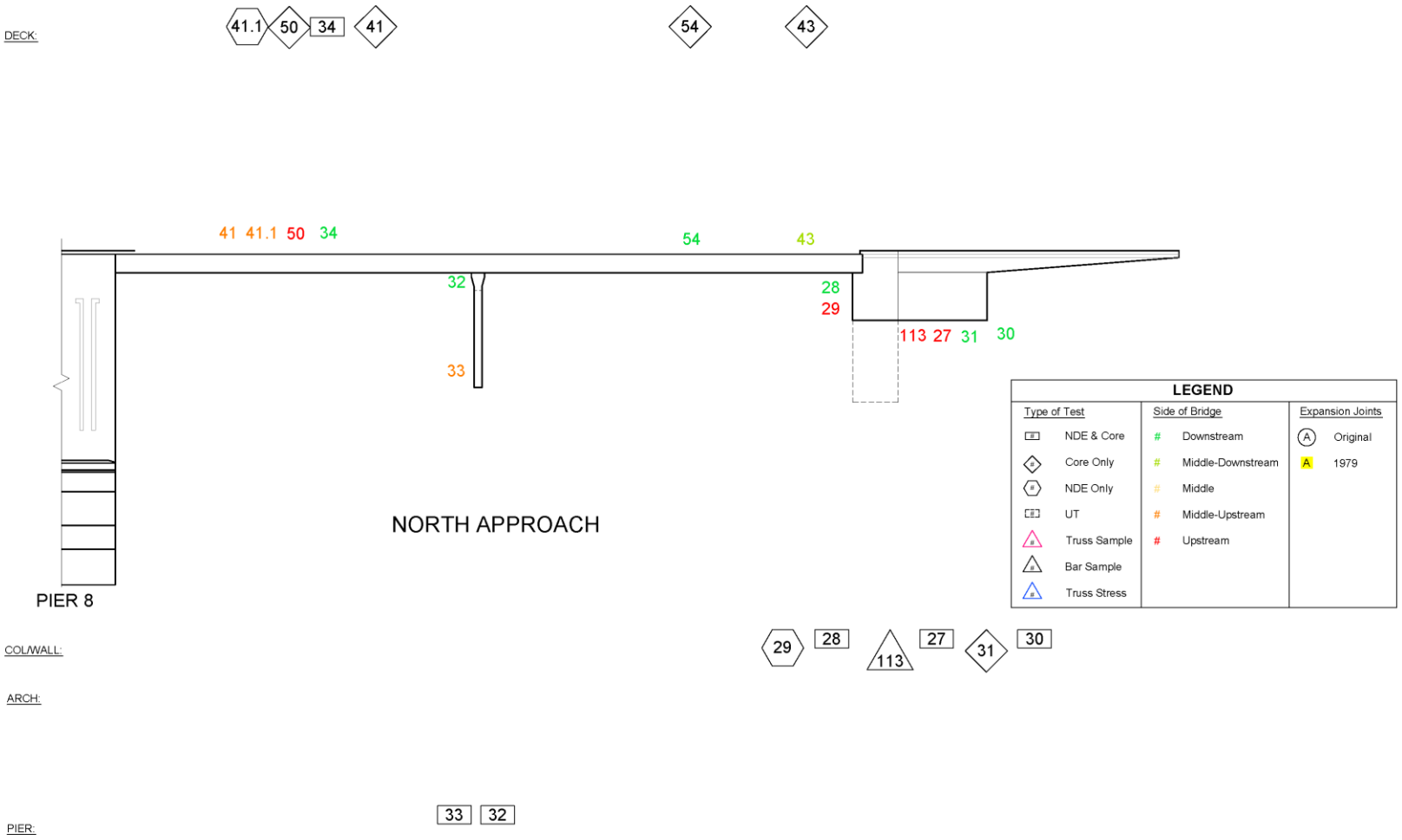

Figure 6.9. Follow-up Testing Location Summary - North Approach

6.1. Material Sampling and Common Material Characteristics

6.1.1. Material Sampling

Concrete cores and steel samples removed from various locations throughout the bridge structure were examined and documented in the field and upon receipt at WJE's laboratory in Northbrook, Illinois. The conditions of the samples including detailed core logs are summarized in Appendix 8 - Material Samples.

6.1.2. Concrete

6.1.2.1. Concrete Mixtures Identified

Laboratory tests performed on the concrete samples included chloride ion analysis, compressive strength and modulus of elasticity testing, and detailed petrographic examination. Based on differences in mixture composition in the concrete samples, including the paste characteristics and the top size and composition of coarse aggregate, and the available construction records, several different concrete mixtures were identified. (These definitions were developed with consideration of the findings of the petrographic analyses, described further below.) These mixtures are identified as follows:

- Mixture 1A - 1918: 2 inch Basalt
  - Original concrete (1918), 2 inch crushed basalt coarse aggregate; non-air-entrained portland cement paste; estimated water-cement ratio (w/c): varying from moderately high to high (0.57 to 0.63)
- Mixture 1B - 1918: 1 to 2 inch Basalt
  - Original concrete (1918), 1 to 2 inch crushed basalt coarse aggregate; non-air-entrained portland cement paste; estimated w/c: varying from moderately high to high (0.54 to 0.60)
- Mixture 2 - Pre-1980s: 3/4-inch Gravel
  - Pre-1980s repair concrete, 3/4 inch siliceous and calcareous gravel; apparent non-air-entrained portland cement paste; estimated w/c: varying from moderate to high (0.47 to 0.63)
- Mixture 3 - Deck 3/4 inch Gravel
  - Deck substrate (1980), 3/4 inch siliceous and calcareous gravel; adequately air-entrained portland cement paste; estimated w/c: 0.38 to 0.43
- Mixture 4 - 3/8 inch Crushed Granite
  - Deck overlay and deck rail elements (1980), crushed granite, 3/8 or 1/4 inch top size; marginally air-entrained portland cement paste; estimated w/c: 0.36 to 0.41
- Mixture 5 - 1/2 inch Gravel
  - Prestressed girder (1980), 1/2 inch siliceous gravel; likely air-entrained portland cement paste; estimated w/c: 0.39 to 0.44
- Mixture 6 - 3/4 inch Gravel
  - 1980 superstructure, 3/4 inch siliceous and calcareous gravel; finely air-entrained portland cement paste; estimated w/c: 0.36 to 0.41
- Repair Mortars
  - Light gray to medium grey repair mortar (shotcrete), vertical surfaces and deck underside; likely air entrained

All core samples were evaluated visually and the mixture each core represents was identified. A summary of the locations of cores extracted, the corresponding concrete mixtures, and the element categories represented by each mixture are provided in Table 6.1. The laboratory test program reported herein was designed such that properties of each of these concrete mixtures could be well characterized.

Table 6.1. Concrete Mixtures Identified in Structure Based on Extracted Core Samples

Mixture Designation	Description	Core Samples	Element Category
1A	1918: 2-in. Basalt	2, 5, 7, 85	Arch Pier Bases
		1, 3, 6, 8, 9, 10, 11, 14, 15, 16, 17, 18	Arch Pier Walls
1B	1918: 1- to 2-in. Basalt	19, 21, 22, 57	Barrel Arches
		24, 25, 26, 100, 100.1, 101, 102, 103	Arch Ribs
		27, 30, 31	North Approach Retaining Wall
		58, 61, 65, 66, 68, 75, 79, 81, 82, 83, 84	Lower Spandrel Columns and Walls
2	Pre-1980s: 3/4-in. Gravel	12, 13	Arch Pier Walls (Pier No. 6 only; likely repair material)
3	1980: Deck 3/4-in. Gravel	47, 52, 53	Deck Sidewalk - Arch Spans
		49, 50, 51, 54	Deck Sidewalk - Approach Spans
		44, 45, 46, 48, 200, 201, 202, 203	Deck Roadway - Arch Spans
		39, 41, 42, 43	Deck Roadway - Approach Spans
4	1980: 3/8-in. Crushed Granite	44, 45, 46, 48, 200, 201, 202, 203	Deck Roadway - Arch Spans
		39, 41, 42, 43	Deck Roadway - Approach Spans
		55	Traffic Barrier
		56	Pedestrian Railing Posts
5	1980: 1/2-in. Gravel	34	North Approach Prestressed Girder
6	1980: 3/4-in. Gravel	28	North Abutment
		32, 33	North Bent Pier
		35, 36	South Abutment
		37	South Bent Pier
		62, 80, 88, 90, 93, 96, 98	Upper Spandrel Columns and Walls
7	Repair Mortars	1	Arch Pier Walls
		7	Arch Pier Bases
		20	Barrel Arches
		23	Arch Rib
		65, 81	Lower Spandrel Columns
		45	Deck Roadway - Arch Spans (Underside)

6.1.2.2. Compressive Strength and Modulus

Compressive strength and modulus testing of concrete core samples was performed as described in Appendix 9. The results of this testing is reproduced in Table 6.2. The table is sorted by element type, and the corresponding concrete mixture is identified.

Table 6.2. Compressive Strength and Elastic Modulus for 3rd Avenue Bridge Cores

Core ID	Element Type	Average Capped Length, L inches	Average Diameter, D inches	L/D	Compressive Strength, psi	Modulus of Elasticity, ksi	Mixture Identification (see Table 6.1)
3	Arch Pier Wall	11.25	5.65	1.99	1,690[1]	--	1A
9	Arch Pier Wall	11.24	5.65	1.99	2,510[1]	--	1A
11	Arch Pier Wall	11.32	5.65	2.00	3,690	--	1A
13	Arch Pier Wall	11.37	5.66	2.01	5,770[2]	--	2
15	Arch Pier Wall	8.76	5.65	1.55	4,380	--	1A
17	Arch Pier Wall	7.36	5.66	1.30	4,980	--	1A
18	Arch Pier Wall	9.84	5.65	1.74	2,330[1]	--	1A
Average - Arch Pier Wall					*3,260*	--	--
21	Barrel Arch (Span 7)	6.21	5.65	1.10	7,910[3]	5,750	1B
24	Arch Rib (Span 2)	11.16	5.65	1.98	6,730	5,550	1B
25	Arch Rib (Span 4)	11.28	5.65	2.00	5,910	4,700	1B
26	Arch Rib (Span 3)	6.57	5.66	1.16	6,250[3]	--	1B
Average - Arch Rib and Barrel Arch					*6,300*	*5,330*	--
31	North Retaining Wall	11.28	5.65	2.00	5,180[3]	--	1B[5]
Average - North Retaining Wall					*5,180*	--	--
42	Deck - Roadway[4]	4.17	3.69	1.13	9,240	--	3
46	Deck - Roadway[4]	4.01	3.72	1.08	6,870	--	3
Average - Deck - Roadway					*8,050*		--
49	Deck - Sidewalk	7.30	3.69	1.98	8,870	--	3
50	Deck - Sidewalk	7.11	3.68	1.93	7,350	4,925	3
51	Deck - Sidewalk	7.26	3.72	1.95	7,460	5,375	3
53	Deck - Sidewalk	7.22	3.72	1.94	6,360	4,800	3
54	Deck - Sidewalk	6.62	3.71	1.78	6,920	--	3
Average - Deck - Sidewalk					*7,390*	*5,030*	--
61	Lower Spandrel Column and Walls	6.12	3.72	1.64	6,960	--	1B[5]
83	Lower Spandrel Column and Walls	4.56	3.72	1.23	4,810	--	1B[5]
84	Lower Spandrel Column and Walls	6.19	3.72	1.66	2,580[1]	--	1B[5]
Average - Lower Spandrel Column and Walls					*4,780*	--	--

[1] Voiding present around aggregates
[2] Different concrete than other pier cores based on aggregate type and size; not included in average
[3] Cracking in top surface layer of core removed prior to testing
[4] Wearing surface/overlay removed prior to testing
[5] Estimated to be Concrete Mixture 1B

6.1.2.3. Petrographic Analyses

The scope of the petrographic analysis is outlined in Table 6.3 below and consisted of various levels of examination, as outlined in Section 3.3.2.2 - Petrographic Analysis:

- Concrete Mixture Classification
  - Nearly all core samples were visually assessed and relative differences in aggregate and paste properties were used to characterize the various mixtures present in the structure
- Petrographic Examination
  - Limited and full petrographic studies were conducted on representative core samples from each concrete mixture type
  - Includes depth of freeze-thaw damage
- Depths of Carbonation and Freeze-thaw Damage
  - Depth of carbonation was performed on nearly all core samples
  - Depth of freeze-thaw damage was performed on selected additional core samples (i.e., in addition to those examined petrographically)

The complete results of these studies are provided in Appendix 10 - Petrographic Analysis. Results from these studies as they relate to specific element types will be discussed in Section 6.2.

Table 6.3. Scope of Petrographic Analysis

Scope	Cores
Concrete Mixture Classification	All cores from the project, nearly 80 cores
Petrographic Examination	10, 12, 30, 21, 33, 34, 37, 48, 79, 85, 98, 102
Depths of Paste Carbonation	All cores from the project, nearly 80 cores
Depths of Freeze-thaw Damage	2, 5, 7, 22, 27

Concrete Mixture Classification and General Descriptions

The results of the concrete mixture classification are provided in Table 6.4. Seven different concrete mixtures and various repair mortar-like cementitious mixtures (likely shotcrete) were identified based on visual and petrographic examinations of all cores from the project. Characteristics to differentiate these mixtures mainly include coarse aggregate type (crushed basalt, crushed granite, or gravel), top size (ranging from 2 inches to sand-size), paste color, estimated w/c, and air-entrainment.

The original concrete (Concrete Mixture 1) consists of crushed basalt coarse aggregate and natural siliceous sand fine aggregate dispersed in non-air-entrained (as expected for concrete at the age) portland cement paste. The observed maximum top size of basalt was 2.5 inches. The basalt was hard and dense, and appeared to have performed satisfactorily. The concrete is generally well consolidated. Gapped gradation, manifested mainly as frequently low volume of intermediate-sized particles, was noted in a few cores. Non-uniform distribution of coarse aggregate particles was observed in a few cores. Small separation gaps between coarse aggregate particles and paste was common. These features may be related to the poor workability in association with the angular and frequently non-equant texture of the basalt coarse aggregate. The basalt particles are mainly angular. Near-flat or near-elongate particles are not uncommon.

The concrete associated with Concrete Mixture 1 appeared to include two sub-groups: Concrete Mixture 1A and Concrete Mixture 1B. Concrete Mixture 1A and Concrete Mixture 1B were mainly different in volume of paste and estimated w/c. Historic documentation (Richter, Vol. 74, No.27, 1915) indicates that the mixture proportions used for the original concrete (1918) were different in the pier and arch ribs. The pier concrete was reportedly mixed at a ratio of 1:3:6 (cement: sand: coarse aggregate) by volume, and the

arch rib concrete was reportedly mixed at a 1:2:4 ratio by volume. These mixes appeared to be roughly correlated to Concrete Mixture 1A and Concrete Mixture 1B, respectively, as described in Table 6.1. Estimated w/c for Concrete Mixture 1A was 0.57 to 0.63; estimated w/c for Concrete Mixture 1B was 0.54 to 0.60. Evidence of minor alkali-silica reaction (ASR) was observed in few cores, typically associated with small amounts of shale (opaline shale) in the fine aggregate. However, no evidence of distress associated with the ASR was observed. Considering the overall small amounts of the shale and the age of the concrete, ASR is not likely to cause damage and is judged not to be a concern for this structure.

The other concrete mixtures represent either repair concrete materials or concrete used in new structural elements constructed during rehabilitation projects (e.g., prestressed concrete girders). Concrete Mixture 2 likely represents a repair concrete prior to 1940s and is not air-entrained. Concrete Mixture 3 through Concrete Mixture 6 (from 1980 construction) are generally air-entrained (with variations in estimated air contents and in air-void systems) and exhibited substantially improved paste characteristics (compared to the original concrete) that are consistent with comparatively lower w/c. The concretes are generally well consolidated and appear to be in overall good condition. No evidence of freeze-thaw deterioration was observed. No evidence of distress caused by ASR activity was observed, although evidence of minor ASR formation was observed in a few cores.

The repair mortars were observed in several cores (1, 7, 20, 23, 45, 58, 65, and 81), generally at the exterior end of the samples. The repair mortars frequently exhibited alternate layering texture, likely consistent with shotcrete. The repair shotcrete generally did not exhibit evidence of substantial freeze-thaw related distress, and the material appeared to be air entrained.

Petrographic Examination Results by Concrete Mixture

The results of the petrographic examination are summarized in Table 6.4. These studies indicate that, aside from chloride-exposure, the main mechanisms of deterioration are carbonation and freeze-thaw distress. There was no evidence of distress associated with alkali-silica reaction (ASR) or other deleterious material-related concerns.

Table 6.4. Concrete Mixtures Identified From Cores Samples

Mixture Designations	Cores Examined/ Structural Elements Represented	Mixture Descriptions	Notes
1A - 1918: 2-in. Basalt (Cement : FA : CA=1:3:6 by volume)	10, 85 Arch Pier Walls and Bases	CA: crushed basalt coarse aggregate (CA), 2-inch top size. Mainly angular particles. Near-flat and near-elongate particles not uncommon. Paste: non-air-entrained portland cement paste. Large residual cement particles. Estimated w/c: 0.57 to 0.63	• Poor workability expected in association with the angular and non-equant CA texture. • Gapped gradation of CA in a few cores; frequently low volume of intermediate-sized particles. • Non-uniform distribution of CA was frequent. • Separation gaps frequently observed between CA and paste. • Cyclic freeze-thaw caused damage (spalling, delamination, incipient delamination, and surface-parallel cracking) observed to a maximum depth of 8.0 inches in the core samples (up to 15.0 inches total including surface erosion measured prior to coring). • Core 1 contained few CA particles.
1B - 1918: 1- to 2-in. Basalt (Cement : FA : CA=1:2:4 by volume)	21, 30, 79, 102 Arch Ribs, Barrel Vaults, North Approach Retaining Wall, and Lower Spandrel Column/Walls	Generally similar to Mix 1A but higher volume of paste, lower volumes of coarse and fine aggregates, and lower estimated w/c. Estimated w/c: 0.54 to 0.60	• Poor workability expected in association with the angular and non-equant CA texture. • Gapped gradation of CA in a few cores; frequently low volume of intermediate-sized particles. • Non-uniform distribution of CA was frequent. • Separation gaps frequently observed between CA and paste. • Cyclic freeze-thaw caused damage (spalling, delamination, incipient delamination, and surface-parallel cracking) observed to a maximum depth of 8.5 inches in barrel arches (up to 9.5 inches total including surface erosion measured prior to coring). • Cores 65, 81, 85, 102 in general and the outer segment of Core 30 contained only a few CA particles.
2 - Pre 1980s: 3/4-in. Gravel	12 Arch Pier Walls (Pier 6 Only)	CA: siliceous and calcareous gravel, 3/4-inch top size. Rounded to angular and mainly equant particles were well graded and uniformly distributed. Paste: non-air-entrained portland cement paste. Estimated w/c: 0.47 to 0.53 for Core 13, and 0.57 to 0.63 for Core 12; possibly representing two different placements	• Core 12 exhibited paste characteristics similar to Mix 1B. Large residual cement particles, generally weak paste, non-air entrainment, and substantial carbonation depth suggest the concrete belongs to pre-1940s. • Core 13 exhibited paste characteristics consistent with lower w/cm, but contained generally similar aggregates to Core 12. • No evidence of materials-related distress or freeze-thaw damage was observed in Core 12 or Core 13. The near-surface cracks in Core 12 appeared to be related to corrosion of the reinforcing.
3 - 1980: Deck: 3/4-in. Gravel	48 Deck Roadway and Sidewalk	CA: siliceous and calcareous gravel, 3/4-inch top size. Paste: adequately air-entrained portland cement paste. Tight paste-aggregate bond. Estimated w/c: 0.38 to 0.43	• No evidence of distress caused by cyclic freeze-thaw was observed • No evidence of distress was observed in association with the minor ASR.
4 - 1980: 3/8-in. Crushed Granite	48 Deck Roadway and Deck Rail Elements	CA: crushed granite, 3/8 or 1/4-inch top size. Paste: marginally air-entrained portland cement paste. Tight paste-aggregate bond. Estimated w/c: 0.36 to 0.41	• No evidence of distress caused by cyclic freeze-thaw was observed. • No evidence of distress was observed in association with the minor ASR observed in a few air voids.
5 - 1980: 1/2-in. Gravel	34 Prestressed Girder (North Approach)	CA: mainly siliceous gravel, 1/2-inch top size. Tight to moderately tight paste-aggregate bond. Paste: Less-than-optimal air-entrained portland cement paste. Estimated w/c: 0.39 to 0.44	• The air-void system does not appear optimal for freeze-thaw damage protection; however, no evidence of freeze-thaw damage was observed, likely due to the comparatively low w/c. • The concrete appeared to be in good condition. • No evidence of materials-related distress such as ASR or freeze-thaw damage was observed, although the air-void system is considered in adequate.
6 -1980: 3/4-in. Gravel	33, 37, 98 Abutments, Bent Piers, and Upper Spandrel Columns	CA: siliceous and calcareous gravel, 3/4-inch top size (1/2-inch in Core 36). Paste: finely/adequately air-entrained portland cement paste. Tight paste-aggregate bond. Estimated w/c: 0.36 to 0.41	• Similar aggregates to Mix 3; estimated w/c was marginally lower. • Minor variations in estimated air contents between the three cores. • No evidence of materials-related distress or freeze-thaw damage was observed. • Core 62 exhibited lighter paste color than remaining cores in the group.

Definitions: CA = Coarse Aggregate; FA = Fine Aggregate; w/c = water to cementitious material ratio.

Freeze-Thaw Distress and Paste Carbonation Results for Cores Examined Petrographically

Freeze-thaw distress evaluation was performed on several samples that were examined petrographically. Freeze-thaw distress was found to be most severe in the arch pier bases, arch ribs, barrel arches and the north retaining wall.

Depth of carbonation was also evaluated for all cores extracted (see detailed results in Section 6.2) and is listed below for cores examined petrographically. The results indicate that carbonation was variable throughout the structure, but generally consistent within a given element category. Carbonation was most advanced in older elements including the arch piers, lower spandrel columns, and the north retaining wall.

Table 6.5. Depths of Paste Carbonation and Freeze-Thaw Distress in Laboratory Samples Where Petrographic Examination Was Performed

Core ID	Element Type	Mix Identification (see Table 6.1)	Depth of Carbonation, inches	Depth of Severe Freeze-Thaw Distress, inches	Maximum Depth of Freeze-Thaw Distress, inches
2	Arch Pier Base	1A	0.7	3.0 (4.8)	8.0 (9.8)
5	Arch Pier Base	1A	0.1	1.0 (8.0)	8.0 (15.0)
7	Arch Pier Base	1A	0.3	--	7.0
85	Arch Pier Base	1A	1.0	2.5 (8.0)	5.0 (10.5)
10	Arch Pier Wall	1A	2.0	--	None obs.
12	Arch Pier Wall	2	1.5	--	None obs.
102	Arch Rib	1B	0.5	--	None obs.
21	Barrel Arch	1B	0.2	--	None obs.
22	Barrel Arch	1B	0.4	3.5 (4.5)	8.5 (9.5)
27	North Retaining Wall	1B	2.0	--	1.5
30	North Retaining Wall	1B	1.5	2.0	4.0
33	North Bent Pier	6	0.4 (locally 0.8)	--	None obs.
34	Prestressed Girder - North Approach	5	0.5 (ext.); 0.3 (int.)	--	None obs.
37	South Bent Pier	6	0.01	--	None obs.
48	Deck Roadway	3 & 4	0.02	--	None obs.
79	Lower Spandrel Column	1A	2.2	--	None obs.
98	Upper Spandrel Column	6	0.13	--	None obs.

Notes:

- *This table only provides data for the cores where petrographic examination was performed. During the in-depth inspection, depth of visible concrete erosion from freeze-thaw damage was noted to be deeper elsewhere, as summarized in Table 4.3.*
- *Tabulated depths including surface erosion (loss of concrete from the original concrete surface) are listed parenthetically.*

6.1.3. Steel Strength and Composition

As detailed in Appendices 8 and 9, tensile properties (yield strength, ultimate strength, and percent elongation) and chemical composition were determined for four steel samples (#109 through #112) extracted from the arch rib Melan truss reinforcement and cut from six reinforcing bars (#113 through #118) exposed at the north abutment retaining wall, an arch pier, and lower columns/walls. The ten specimens

were tested by Engineering Systems, Inc. (ESI), of Aurora, IL. For comparison purposes, common grades of ASTM A15 steel and ASTM A36 steel are provided in Table 6.6 and Table 6.7, respectively.

Table 6.6. Tensile Properties and Chemical Composition Requirements for ASTM A15 (1914) Steel

Property	Structural Grade	Intermediate Grade	Hard Grade
Tensile strength, ksi	55 to 70	70 to 85	80 min.
Min. Yield strength, ksi	33	40	50
Elongation, min. % - Plain Bars	1,400/Tensile Strength (ksi)	1,300/Tensile Strength (ksi)	1,200/Tensile Strength (ksi)
Elongation, min. % - Deformed Bars	1,400/Tensile Strength (ksi)	1,300/Tensile Strength (ksi)	1,200/Tensile Strength (ksi)
Phosphorus, max. %	0.10 (Bessemer) 0.05 (Open-hearth)		

Table 6.7. Tensile Properties and Chemical Composition Requirements for ASTM A36 (2014) Steel

Property	A36 Requirement
Tensile strength, ksi	58-80
Yield strength, ksi	36, min.
Elongation, %	23, min.
Carbon, %	0.26, min.
Manganese, %	0.80-1.20
Sulfur, %	0.05, max.
Phosphorus, %	0.04, max.
Silicon, %	0.04, max.

Tensile and chemical composition properties of selected steel samples are summarized in Table 6.8. The tensile and chemical composition properties of the four Melan truss samples (#109 through #112) are generally consistent with the properties specified for A36 structural grade steel. The tensile and chemical properties of the reinforcing bars taken from the arch pier and lower columns/walls (#114 through #118) are generally consistent with the properties specified for A15 (1914) “structural grade” reinforcing steel.

The tensile properties and chemistry of the bar taken from the north retaining wall (#113) were different from the other five bars; this bar exhibited higher strength and lower elongation and greater concentrations of carbon, manganese, sulfur and phosphorus. The higher carbon would be expected to increase the tensile and yield strengths of the reinforcing bar, but would also be expected to decrease its weldability and ductility. Given its unique features compared to the other samples, this bar is judged to be an anomaly that is not representative of the bridge as a whole.

Table 6.8. Tensile Properties and Chemical Composition of Steel Samples

Sample	#109	#110	#111	#112	#113	#114	#115	#116	#117	#118
Location	Arch Rib (Span 3)	Arch Rib (Span 3)	Arch Rib (Span 2)	Arch Rib (Span 5)	North Retaining Wall	Arch Pier Walls	Arch Pier Walls	Lower Spandrel Columns and Walls	Lower Spandrel Columns and Walls	Lower Spandrel Columns and Walls
Sample Type	Truss Angle	Truss Angle	Truss Angle	Truss Angle	Round Bar	Round Bar	Square Bar	Square Bar	Square Bar	Square Bar
Dimensions (est. original)	3/8-in. thick	1/2-in. thick	1/2-in. thick	1/2-in. thick	5/8-in. diam.	5/8-in. diam.	1/2-in. square	1/2-in. square	3/4-in. square	1/2-in. square
Tensile Strength, ksi	64	58.5	57.5	58	120	62.5	71	59.5	61	65
Yield Strength, ksi	41.1	40.5	41.5	36.6	82	39.2	42	41.1	39.5	47.6
Elongation, %	36	42	38	41	18	37	35	41	47	37
Carbon, %	0.13	0.20	0.17	0.18	0.52	0.24	0.27	0.19	0.25	0.20
Manganese, %	0.32	0.35	0.32	0.34	1.02	0.48	0.67	0.46	0.39	0.35
Sulfur, %	0.03	0.047	0.037	0.044	0.08	0.04	0.02	0.045	0.029	0.02
Phosphorus, %	0.01	0.007	0.007	0.008	0.12	0.01	0.01	0.016	0.007	0.026
Silicon, %	0.065	0.046	0.04	0.043	0.053	0.015	0.008	0.048	0.051	0.089
Chromium, %	0.069	0.033	0.029	0.028	0.007	0.01	0.008	0.021	0.024	0.009
Molybdenum, %	0.012	0.012	0.011	0.012	0.011	0.01	0.01	0.011	0.011	0.012
Vanadium, %	0.002	0.002	0.002	0.002	0.01	0.002	0.002	0.002	0.002	0.002
Nickel, %	0.028	0.019	0.014	0.012	0.011	0.01	0.009	0.015	0.015	0.018
Niobium, %	0.005	0.005	0.004	0.004	0.003	0.004	0.004	0.005	0.004	0.004
Aluminum, %	0.017	0.012	0.009	0.014	0.002	0.028	0.007	0.076	0.012	0.012
Titanium, %	0.001	<0.001	0.001	0.001	<0.001	0.002	0.001	0.001	<0.001	<0.001
Carbon Equivalent, %	0.20	0.27	0.23	0.25	0.70	0.33	0.39	0.27	0.32	0.26

6.2. Test Results By Element Type

In this section, results of the follow-up testing are summarized by element category or sub-category in terms of physical condition and the results of the various field tests and laboratory analyses in each study area. These results are then interpreted and the deterioration mechanisms for each element type are identified.

The "distress quantity ratio" also referred to as "distress quantity," as defined in Section 4.5.1, was used to describe the physical conditions locally within each study area. For general comparative purposes, the distress quantity was characterized as one of the following:

- Less than 1 percent distress
- 1 to 10 percent distress
- 10 to 30 percent distress
- Greater than 30 percent distress

6.2.1. Deck Topside (Roadway, Sidewalk, and Underside) - Arch Spans

Follow-up test locations on the deck roadway and sidewalks were spaced across the bridge as shown in Appendix 13. In general, the survey approach for the deck topside included NDE testing in approximately 25 percent of the deck surface; study areas were staggered such that every fourth joint-to-joint section of the deck roadway and sidewalk were tested, and different sections were studied in the outer lanes and the middle lanes (i.e., "checker-board" pattern). Core locations within the topside study areas are provided in Table 6.9. A total of twelve cores were collected through the deck topside: three cores were collected through the sidewalk, and nine cores were collected through the roadway. Of the cores collected in the deck roadway, three were taken through the thickness of the deck, and five of the cores were taken at locations of cracks in the deck.

Table 6.9. Core Locations Within Deck Topside Study Areas - Arch Spans

Core Label	Element Type	Span	Side of Bridge	Located Between Columns	Notes
44A	Roadway	5	Middle	F-I	Through-Thickness
44B	Roadway	5	Middle	F-I	Through-Thickness
45	Roadway	6	Middle	G-J	Through Thickness
46	Roadway	5	Downstream	K-N	--
48	Roadway	4	Upstream	D-F	Topside Crack
200	Roadway	7	Middle	E-F	Topside Crack
201	Roadway	7	Middle	E-F	Topside Crack
202	Roadway	7	Middle	D-E	Topside Crack
203	Roadway	7	Middle	F-G	Topside Crack
47	Sidewalk	4	Upstream	D-F	--
52	Sidewalk	5	Downstream	I-K	--
53	Sidewalk	5	Downstream	K-N	--

Follow-up testing on the deck underside was conducted at the specific study areas shown in Table 6.10.

Table 6.10. Study Areas - Deck Underside (Arch Spans)

Location ID	Span	Side of Bridge	Proximity of Core to Joint	Proximity of Study Area to Joint	Located Between Columns	Test Type
44.1	5	Middle	12 inches north of joint	0 to 6 ft	F-I	NDE and Core
45.1	6	Middle	60 inches north of joint	0 to 5 ft	G-J	NDE and Core
86	2	Downstream	N/A	Midway between joints - along downstream edge	K-N	NDE only

6.2.1.1. Physical Condition

The conditions of the deck topside and underside are summarized in Chapter 4. In general, the conditions were consistent among the seven arch spans: the deck topside (including roadway and sidewalks), averaged around 1 percent distress; and the deck underside averaged 15 percent. Typical distress included concrete spalls and delaminations, and deteriorated repairs. Cracking was observed in both the roadway and sidewalk, and the type and density of cracking varied. In the roadway, a dense network of longitudinal and transverse cracks was observed (see Figure 4.20), and some random cracking (likely from structural behavior) around manholes was observed. Lesser quantities of longitudinal and transverse cracking were observed in the sidewalks, and in some instances localized "D-Cracking"-like crack patterns were observed; this cracking may be related to freeze-thaw distress, though the severity of the cracking was minor. Concrete delaminations were isolated; however, due to the deep cover depth over the reinforcement it is possible that early corrosion-related distress is present but not detectable through conventional sounding methods.

For each of the study areas on the deck underside, the local distress quantity is presented in Table 6.11. Typical distress included concrete delaminations and deteriorated repairs. Along the downstream edge (e.g., Study Area 86), significant distress was observed; concrete had delaminated and exposed reinforcement was present along nearly the entire edge of the deck.

Table 6.11. Condition and Sampling of Study Areas - Deck Underside (Arch Spans)

Location ID	Core Samples	Date Inspected	Distress Quantity (%)
44.1	44A, 44B	8/4/2017	> 30
45.1	45	8/4/2017	1 to 10
86	N/A	8/6/2017	10 to 30

6.2.1.2. Corrosion Survey

Across the deck surface, 31 NDE study areas were selected including both the roadway and sidewalk. In each area, a half-cell survey was performed (rolling half-cell electrode between expansion joints in study area, with one reading collected every 6 inches and with scans spaced at 2 feet apart across the survey lane), and three locations were selected for local corrosion testing (i.e., resistivity and corrosion rate); these

locations were selected at features such as cracks, construction joints, and delaminations as well as at typical, un-deteriorated areas of the deck.

The upper layer of reinforcement in the deck roadway and sidewalk (topside) is epoxy-coated, while the bottom layer of the deck is uncoated (black bar). Because of the epoxy coating, interpretation of the corrosion survey findings is more complex. The results of the corrosion surveys at any given location have been compared relative to other locations to identify areas of likely corrosion in the deck element. In addition, the greater connectivity of the bottom uncoated bar mat compared to the epoxy coated mat means that the corrosion potential and corrosion rate test results represent the top bar condition, where local corrosion on the top bars is present, but are influenced by the bottom layer condition in areas where the epoxy coating is largely intact.

Corrosion Potential

Results of half-cell potential survey data from among all 31 NDE topside deck study areas and 3 NDE underside deck study areas are summarized in Table 6.12 (topside) and Table 6.13 (underside). The results indicate that active corrosion is probable in both the deck and the sidewalk. In general, HCP results were more negative at locations of cracks, construction joints, and deteriorated repairs, indicating a higher likelihood of corrosion in these areas. The sidewalk has a higher probability of corrosion, as expected given the absence of a protective overlay. The deck underside has a moderate to high probability of corrosion at the locations tested. See graphical summaries in Figure 6.12 and Figure 6.13 for example contour plots of the HCP data.

Table 6.12. HCP Testing Results - Deck Topside (Arch Spans)

Location	Percent of Survey Points More Negative Than -500mV	Percent of Survey Points More Negative Than -350mV	Percent of Survey Points Between -200mV and -350mV	Percent of Survey Points More Positive Than -200mV	Half-Cell Potentials (mV vs. CSE)	
					Average	Minimum
Roadway	6%	27%	48%	25%	-287	-661
Sidewalk	18%	45%	46%	9%	-356	-715

** Thresholds (see 3.4.4.1): > -200mV low, -200 to -350mV moderate, < -350 mV high probability of corrosion*

Table 6.13. HCP Testing Results - Deck Underside (Arch Spans)

Location ID	HCP - Avg. (mV vs. CSE)	HCP - Min. (mV vs. CSE)	HCP - Std. Dev. (mV vs. CSE)	Distress Quantity (%)
44.1	41	-340	356	> 30
45.1	-53	-215	70	1 to 10
86	-243	-537	151	10 to 30

** Thresholds (see 3.4.4.1): > -200mV low, -200 to -350mV moderate, < -350 mV high probability of corrosion*

Resistivity

Results of resistivity testing are provided in Table 6.14 (topside) and Table 6.15 (underside). Resistivity values were approximately 50 percent lower in the cracked areas compared to uncracked areas. Resistivity values are also more than 50 percent lower in the sidewalk compared to the roadway. Assuming corrosion

has initiated, the results indicate a low to moderate rate of corrosion in the sidewalk, and a low rate of corrosion where corrosion is occurring in the roadway.

The resistivity measurements on the deck underside indicate a low rate of corrosion where corrosion is occurring.

Table 6.14. Resistivity Testing Results - Deck Topside (Arch Spans)

Location	Resipod - Resistivity Avg. (kOhm-cm)	Notes
Roadway	93	Near Crack, Joint, or Delam.
	169	Away From Crack, Joint, or Delam.
Sidewalk	27	Near Crack, Joint, or Delam.
	56	Away From Crack, Joint, or Delam.

** Thresholds (see 3.4.4.2): 50-100 low, 10-50 moderate, <10 kOhm-cm high corrosion rates possible in active areas*

Table 6.15. Resistivity Testing Results - Deck Underside (Arch Spans)

Location ID	Resipod - Resistivity Avg. (kOhm-cm)	iCOR - Resistivity Avg. (kOhm-cm)	Distress Quantity (%)
44A.1	594	423	> 30
45.1	247	--	1 to 10
86	62	--	10 to 30

** Thresholds (see 3.4.4.2): 50-100 low, 10-50 moderate, <10 kOhm-cm high corrosion rates possible in active areas*

Corrosion Rate

Corrosion rate testing results at the deck topside and underside are provided in Table 6.16 and Table 6.17, respectively. Corrosion rate was on average 50 percent higher at locations of cracks and joints compared to uncracked areas. Also, the corrosion rate was more than 50 percent higher in the sidewalk compared to the roadway. Corrosion rate in the sidewalks is moderate, and corrosion rate in the roadway is low to moderate.

Low corrosion rates were measured on the deck underside.

Table 6.16. Corrosion Rate Testing Results - Deck Topside (Arch Spans)

Location	BAC Meter - Corrosion Rate - Avg. (um/yr) †	Notes
Roadway	11.0	Near Crack, Joint, or Delam.
	5.1	Away From Crack, Joint, or Delam.
Sidewalk	24.8	Near Crack, Joint, or Delam.
	12.2	Away From Crack, Joint, or Delam.

† Thresholds (see 3.4.4.3): <10 low, 10-30 moderate, 30-100 high, >100 um/yr severe instantaneous corrosion rate.

Table 6.17. Corrosion Rate Testing Results - Deck Underside (Arch Spans)

Location ID	iCOR - Current Density Avg. (uA/cm^2) *	BAC Meter - Current Density Avg. (um/yr) †	Distress Quantity (%)
44.1	0.0	--	> 30
45.1	--	3.2	1 to 10
86	--	--	10 to 30

** Thresholds (see 3.4.4.3): <1 low, 1-3 moderate, 3-10 high, >10 severe uA/cm2 instantaneous corrosion rate*
† Thresholds (see 3.4.4.3): <10 low, 10-30 moderate, 30-100 high, >100 um/yr severe instantaneous corrosion rate.

6.2.1.3. Reinforcement Cover Survey

On the topside, GPR measurements were taken across the full lane width, with several lines of scans (i.e., 3 to 4) per study area; on the underside, GPR measurements were located in representative areas of the study area. In both the deck topside and underside, the longitudinal bars are closest to the surface. The results of the reinforcement cover surveys in the deck underside study areas are provided in Table 6.18. The statistical information results of the cover surveys are summarized in Table 6.19 (topside) and Table 6.20 (underside). The cover in the roadway and sidewalk are similar despite the presence of the overlay in the deck roadway.

Table 6.18. Cover Depth Measurements - Deck Underside (Arch Spans)

Location ID	Cover Transverse Bars - Avg. (in.)	Cover Transverse Bars - Rep. Minimum (in.)	Cover Longitudinal Bars - Avg. (in.)	Cover Longitudinal Bars - Rep. Minimum (in.)	Distress Quantity (%)
44.1	1.4	1.0	1.0	0.7	> 30
45.1	1.8	1.8	0.8	0.8	1 to 10
86	--	--	1.0	0.9	10 to 30

Table 6.19. Cover Depth Statistics - Deck Topside (Arch Spans)

Value	Roadway	Sidewalk
	Longitudinal Bar - Including Overlay	Longitudinal Bar
Average (in.)	3.9	3.7
Standard Deviation (in.)	0.4	0.5
Coefficient of Variation	10%	14%
Minimum (in.)	2.0	1.7
Maximum (in.)	5.6	5.3

Table 6.20. Cover Depth Statistics - Deck Underside (Arch Spans)

Value	Longitudinal Bar	Transverse Bar
Average (in.)	1.0	1.5
Standard Deviation (in.)	0.2	0.3
Coefficient of Variation	16%	24%
Minimum (in.)	0.7	0.7
Maximum (in.)	1.3	2.2

6.2.1.4. Field and Lab Carbonation Tests

Synthesis of field and lab carbonation measurement results are provided in Table 6.21 (topside) and Table 6.22 (underside). Carbonation was negligible compared to the depth of reinforcement.

Table 6.21. Carbonation Measurements - Deck Topside (Arch Spans)

Location ID	Carbonation - Rep. Maximum (in.)	Cover Longitudinal Bars - Minimum (in.)	Distress Quantity (%)
Roadway	Negligible	2.0	Varies
Sidewalk	Negligible	1.7	Varies

Table 6.22. Carbonation Measurements - Deck Underside (Arch Spans)

Location ID	Carbonation - Rep. Maximum (in.)	Cover Transverse Bars - Rep. Minimum (in.)	Cover Longitudinal Bars - Rep. Minimum (in.)	Distress Quantity (%)
44.1	0.1	1.0	0.7	> 30
45.1	0.2	1.8	0.8	1 to 10
86	0.0	--	0.9	10 to 30

6.2.1.5. Other Tests

No other tests were conducted in this element category.

6.2.1.6. Chloride Profile Analysis

Chloride profiles are shown in Figure 6.10 (Roadway, topside), Figure 6.11 (Roadway, underside), and Figure 6.12 (Sidewalk, topside). The results on the deck topside roadway represent typical profiles resulting from surface chloride exposure. Cores 44A and 45, both uncracked, show elevated chlorides through the overlay but below-threshold chlorides in the substrate. Cores 48, 200, and 202, all cracked through the overlay and substrate, indicate higher concentrations of chlorides in the substrate at or near the depth of reinforcement. In the sidewalk, where there is no overlay, the cores show similar diffusion behavior, though a lower surface chloride concentration was observed indicating a lower exposure than seen in the roadway. Recall that the reinforcement in the top mat of both the roadway and the sidewalk is epoxy-coated, so in general a higher range in chloride concentration would be required to initiate corrosion (see Section 3.2.1.2).

Profiles on the deck underside (Figure 6.11) indicate variable exposure. Recall that the underside reinforcement is not epoxy coated. Both Core 44B and 45 were taken near expansion joints (see Table 6.10). Core 44 was taken approximately 1 foot from the expansion joint and also near a repair on the underside; above-threshold chloride contamination is present. Core 45 was taken near an expansion joint but shows lower (at threshold) chloride contamination due to greater distance (approximately 5 feet) from the joint.

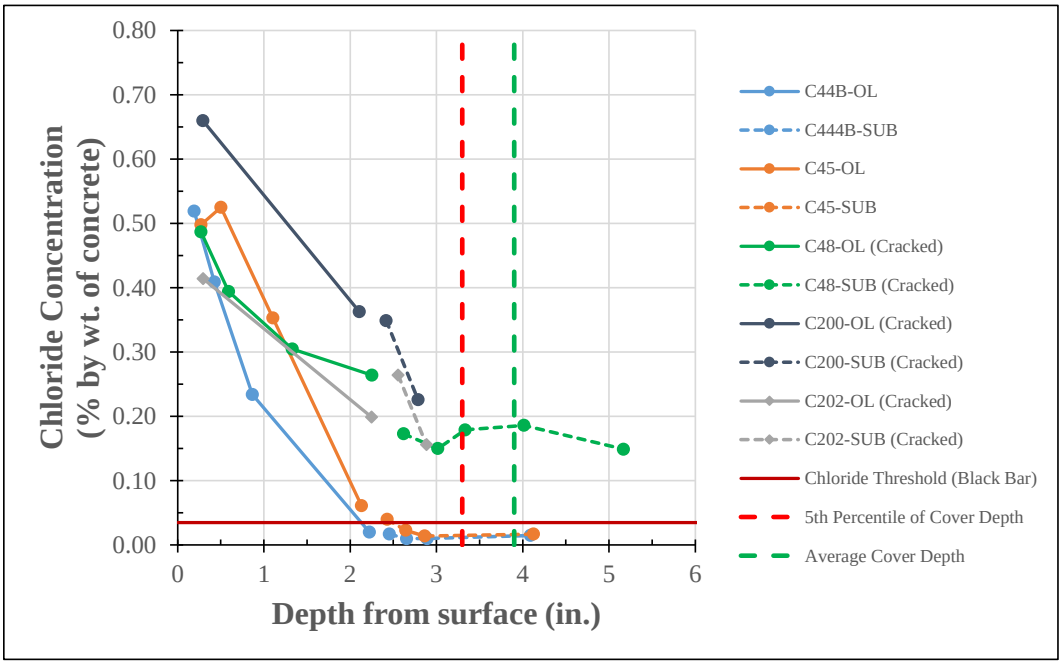

Figure 6.10. Chloride profiles for Deck Roadway - Arch Span (topside) cores compared to chloride threshold for corrosion initiation (for black bar as a reference) and reinforcement cover depth measurements. Note top bars are actually epoxy-coated, so threshold is higher - see Section 3.2.1.2.

(Overlay = OL; Substrate = SUB)

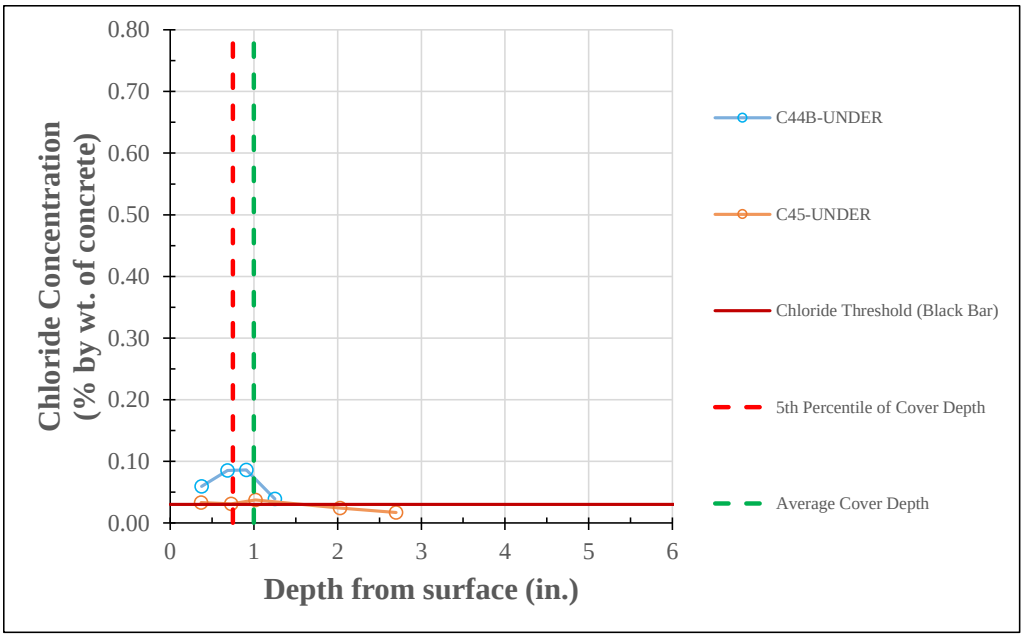

Figure 6.11. Chloride profiles for Deck Roadway - Arch Span (underside) cores compared to chloride threshold for corrosion initiation and reinforcement cover depth measurements.

(Underside = UNDER)

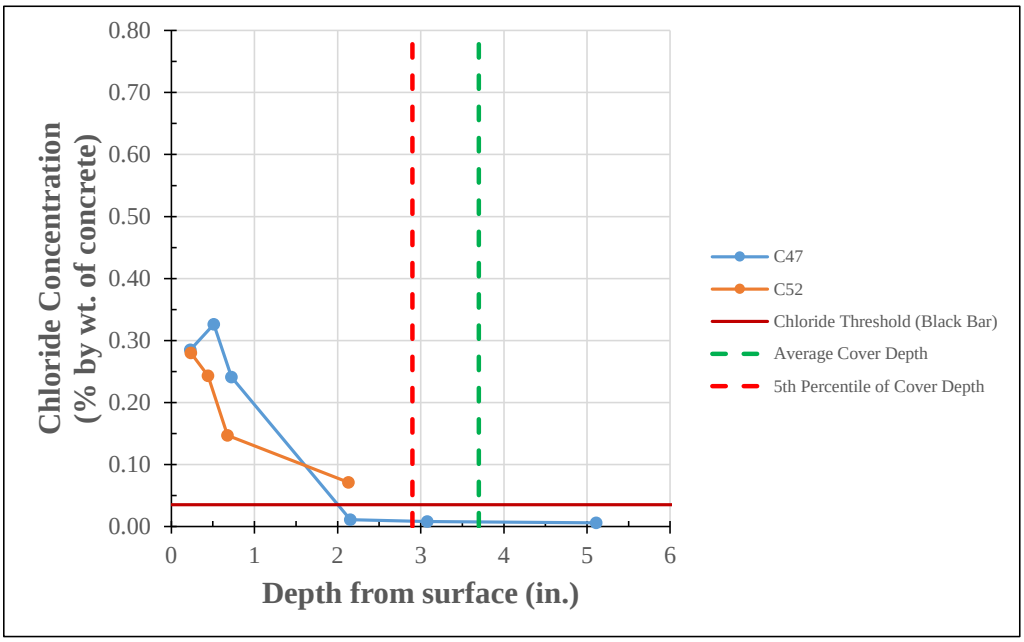

Figure 6.12. Chloride profiles for Deck Sidewalk - Arch Span (Topside) cores compared to chloride threshold for corrosion initiation (for black bar as a reference) and reinforcement cover depth measurements. Note top bars are actually epoxy-coated, so threshold is higher - see Section 3.2.1.2.

6.2.1.7. Petrographic Analysis

The deck substrate was identified as Concrete Mixture 3 - Deck 3/4 inch Gravel, while the overlay was identified as Concrete Mixture 4 - 3/8 inch Crushed Granite (overlay). Limited petrographic studies were performed on the overlay and substrate of Core 48, and the results are summarized below:

- The bond between the overlay and deck substrate was generally intact;
- The concrete in both overlay and the substrate was well-consolidated;
- Estimated w/c was 0.36 to 0.41 in the overlay concrete and 0.38 to 0.43 in the substrate concrete, and the concrete in both overlay and the substrate was air-entrained;
- No evidence of distress caused by cyclic freeze-thaw was observed; and
- While some evidence of alkali-silica reaction (ASR) gel in air voids was noted, this was infrequent and no distress due to ASR was observed.

Additionally, several of the cracked cores from the topside of the overlay were examined. Evidence of previous crack sealants and other debris were observed indicating the cracks have been present for some time. The cracks extended through some aggregate particles, and therefore the cracking observed is not likely plastic cracking or other cracking that occurred while the paste-aggregate bond was still developing. Cracking generally extended through the overlay and sometimes into the substrate, and widths were variable (ranging from less than 5 mils to 20 mils and very occasionally greater than 50 mils).

Depth of carbonation at the topside and underside surfaces was negligible in this element.

6.2.1.8. Interpretation

Based on the follow-up evaluation of the deck (roadway, sidewalk, and underside), chloride-induced corrosion is the primary deterioration mechanism. Many of the cracks in the overlay extend through the overlay and sometimes propagate into the deck down to the depth of the reinforcing steel. This has permitted direct chloride ingress to reinforcement, as evidenced by the beginning of delamination/spalling, elevated HCP's, and elevated corrosion rates measured in the deck. The cracking has likely resulted in active corrosion of reinforcement. The sidewalk is in a similar condition as the roadway despite lack of a protective overlay. The epoxy-coating on the deck reinforcement offers some level of protection against chloride exposure; however, at cracked locations the chlorides have accumulated to concentrations expected to result in corrosion of epoxy-coated rebar. In uncracked regions of the deck, chloride ingress has not progressed to levels expected to result in corrosion. Given the high density of cracking present in the roadway overlay (see Figure 4.20), uncracked regions of the deck topside are infrequent.

Carbonation was negligible compared to the depth of reinforcement at both the deck topside and underside surfaces. Evidence of deterioration due to ASR or freeze-thaw cycling was not observed in most areas of the deck; however, the cracking around joints in the sidewalk is similar in nature to "D-cracking", which is symptomatic of freeze-thaw cycling and the onset of freeze-thaw damage.

A graphical representation of the follow-up testing in the Arch Span Decks is provided in Figure 6.13 Appendix 14. In the areas surveyed, chloride-induced corrosion is the controlling deterioration mechanism. In the middle lanes, corrosion activity is apparent near the longitudinal construction joint and near the repairs near the expansion joints. Along the sidewalk, the corrosion activity is also widespread along the downstream edge.

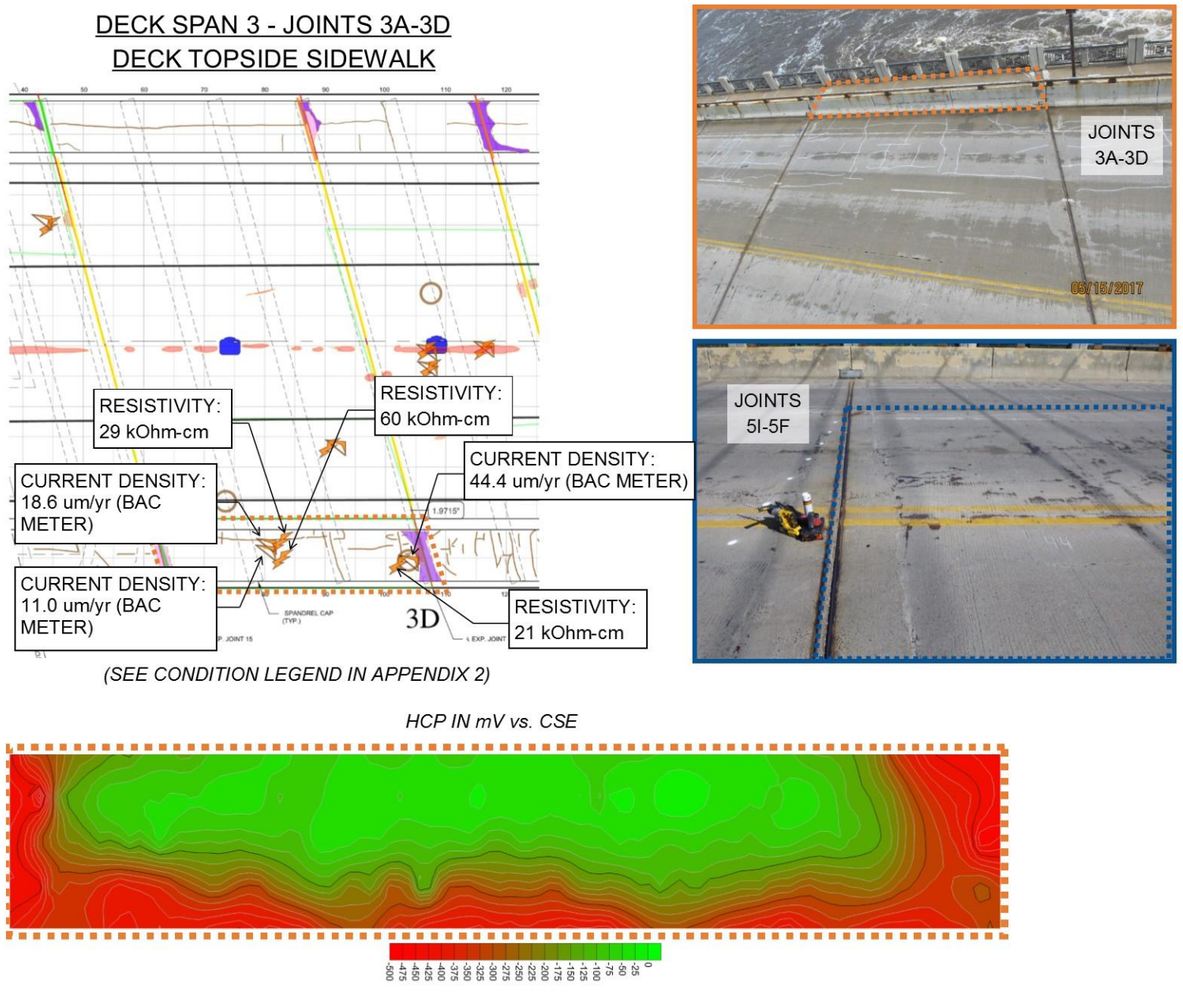

Study Area	Element	Inspection Date	Type	Distress Quantity (%)	Cores Sample(s)	HCP - Avg. (mV vs. CSE)	HCP - Min. (mV vs. CSE)	Resipod - Resistivity Avg. (kOhm-cm)	iCOR - Current Density Avg. (uA/cm^2)	iCOR - Resistivity Avg. (kOhm-cm)	BAC Meter - Current Density Avg. (um/yr)	Cover Vertical Bars - Rep. Minimum (in.)	Cover Horizontal Bars - Rep. Minimum (in.)	Carbonation Avg. (in.)	Deterioration Mechanism(s)
3A-3D	Deck Sidewalk	5/25/2017	NDE ONLY	1 to 10	--	-365	-734	37	N/A	N/A	24.7	3.5	3.1	N/A	Chloride Exposure
5F-5I	Deck Roadway	7/8/2017	NDE & CORE	1 to 10	44A & 44B	-217	-616	54	N/A	N/A	16.4	4.0	3.1	N/A	Chloride Exposure

Figure 6.13. Graphical Summary of Testing Data for Study Areas in Deck Topside - Arch Spans.

6.2.2. Upper Spandrel Columns and Walls (1980 Construction) - 1980 Expansion Joint

The location of the follow-up testing study areas in the Upper Spandrel Columns and Walls constructed in 1980, where an expansion joint has always been present, are shown in Table 6.23. These study areas included the cap beams.

Table 6.23. Study Areas - Upper Spandrel Columns and Walls - 1980 Expansion Joint

Location ID	Span	Side of Bridge	Column ID	Elevation of Study Area - Range Below Deck Underside (ft.)	At Expansion Joint - Y/N?	Face	Test Type
59	1	Downstream	N	0 to 6	Y	South	NDE only
62	2	Downstream	N	3 to 8	Y	South	NDE & core
69	6	Downstream	J	0 to 5	Y	South	NDE only
80	7	Upstream	A	0 to 6	Y	South	NDE & core
81	7	Upstream	J	4 to 7	Y	North	NDE Only
88	1	Downstream	A	7 to 11	Y	South	NDE & core
90	2	Upstream	D	0 to 3	Y	South	NDE & core
91	3	Downstream	N	3 to 10	Y	North	NDE only
93	5	Middle	N	0 to 5	Y	South	NDE & core
95	6	Upstream	G	0 to 7	Y	North	NDE only
96	6	Upstream	A	0 to 8	Y	South	NDE only
97	1	Downstream	N	0 to 3	Y	South	NDE only
98	2	Middle	N	3 to 7	Y	South	NDE & core

6.2.2.1. Physical Condition Survey

The condition of the upper spandrel columns and walls is summarized in Chapter 4. The conditions among the columns adjacent to joints were variable, and in general higher distress was observed on either the upstream or downstream columns compared to the middle column. On average, distress in these elements was 12 percent in Spans 1-5, and 7 percent in Spans 6 and 7.

For each of the study areas, the local distress quantity is presented in Table 6.24. The condition varied between study areas, but moderate to high levels of distress were generally observed. Typical distress observed included delaminated concrete, often around the perimeter of the 1980 repair concrete and in the cap beams. Based on the conditions associated with the distress (e.g., cracking and moisture staining) some of the distress in the cap beams is attributable to corrosion while some appears to be related to mechanical movements at the joints (see Chapter 5).

Table 6.24. Condition and Sampling of Study Areas - Upper Spandrel Columns and Walls - 1980 Expansion Joint

Location ID	Core Samples	Date Inspected	Distress Quantity (%)	Joint Condition
59	N/A	5/26/2017	> 30	1980 Expansion Joint
62	62	7/15/2017	10 to 30	1980 Expansion Joint
69	N/A	7/15/2017	< 1	1980 Expansion Joint
80	80	7/16/2017	10 to 30	1980 Expansion Joint
81	N/A	7/17/2017	1 to 10	1980 Expansion Joint
88	88	7/15/2017	10 to 30	1980 Expansion Joint
90	90	7/16/2017	10 to 30	1980 Expansion Joint
91	N/A	7/15/2017	> 30	1980 Expansion Joint
93	93	7/16/2017	> 30	1980 Expansion Joint
95	N/A	8/6/2017	1 to 10	1980 Expansion Joint
96	96	7/16/2017	10 to 30	1980 Expansion Joint
97	N/A	8/6/2017	10 to 30	1980 Expansion Joint
98	98	7/15/2017	1 to 10	1980 Expansion Joint

6.2.2.2. Corrosion Survey

Corrosion Potential

Results of half-cell potential surveys are summarized in Table 6.25. The results generally indicate moderate to high probability of corrosion.

Table 6.25. HCP Testing Results - Upper Spandrel Columns and Walls - 1980 Expansion Joint

Location ID	HCP - Avg. (mV vs. CSE)	HCP - Min. (mV vs. CSE)	HCP - Std. Dev. (mV vs. CSE)	Distress Quantity (%)
59	-373	-519	67	> 30
62	-296	-377	68	10 to 30
69	-292	-386	44	< 1
80	-300	-443	76	10 to 30
81	-304	-461	69	1 to 10
88	-286	-344	26	10 to 30
90	-387	-476	42	10 to 30
91	-368	-595	80	> 30
93	-231	-333	44	> 30
95	-263	-425	44	1 to 10
96	-163	-293	61	10 to 30

Location ID	HCP - Avg. (mV vs. CSE)	HCP - Min. (mV vs. CSE)	HCP - Std. Dev. (mV vs. CSE)	Distress Quantity (%)
97	-358	-442	51	10 to 30
98	-282	-411	58	1 to 10

** Thresholds (see 3.4.4.1): > -200mV low, -200 to -350mV moderate, < -350 mV high probability of corrosion*

Resistivity

Results of resistivity testing are summarized in Table 6.26. Resistivity was variable, but the results indicate a low to moderate corrosion rate would expected where corrosion is active. Resistivity typically decreased with proximity to the deck underside.

Table 6.26. Resistivity Testing Results - Upper Spandrel Columns and Walls - 1980 Expansion Joint

Location ID	Resipod - Resistivity Avg. (kOhm-cm)	iCOR - Resistivity Avg. (kOhm-cm)	Distress Quantity (%)
59	42	--	> 30
62	38	53	10 to 30
69	50	--	< 1
80	38	35	10 to 30
81	42	--	1 to 10
88	61	56	10 to 30
90	10	--	10 to 30
91	34	--	> 30
93	63	108	> 30
95	139	--	1 to 10
96	106	185	10 to 30
97	118	--	10 to 30
98	66	105	1 to 10

** Thresholds (see 3.4.4.2): 50-100 low, 10-50 moderate, <10 kOhm-cm high corrosion rates possible in active areas*

Corrosion Rate

Corrosion rate testing results are provided in Table 6.27. Corrosion rate testing was not performed in all areas due to difficulties in making favorable connections of the probe to the reinforcing steel. The measured corrosion rate was generally low to moderate, with some isolated exceptions.

Table 6.27. Corrosion Rate Testing Results - Upper Spandrel Columns and Walls - 1980 Expansion Joint

Location ID	iCOR - Current Density Avg. (uA/cm^2) *	BAC Meter - Current Density Avg. (um/yr) †	Distress Quantity (%)
59	--	--	> 30
62	0.3	--	10 to 30
69	--	9.7	< 1
80	0.4	--	10 to 30
81	--	--	1 to 10
88	0.2	--	10 to 30
90	53.6	--	10 to 30
91	--	9.2	> 30
93	0.8	--	> 30
95	--	11.0	1 to 10
96	0.1	--	10 to 30
97	--	11.3	10 to 30
98	0.1	--	1 to 10

** Thresholds (see 3.4.4.3): <1 low, 1-3 moderate, 3-10 high, >10 severe uA/cm2 instantaneous corrosion rate*
† Thresholds (see 3.4.4.3): <10 low, 10-30 moderate, 30-100 high, >100 um/yr severe instantaneous corrosion rate.

6.2.2.3. Reinforcement Cover Survey

The results of the reinforcement cover surveys are provided in Table 6.28. The statistical information for this element for all exposure conditions (i.e., all expansion joint histories) is summarized in Figure 6.29. Cover depth was highly variable between study areas.

Table 6.28. Cover Depth Measurements - Upper Spandrel Columns and Walls - 1980 Expansion Joint

Location ID	Cover Vertical Bars - Avg. (in.)	Cover Vertical Bars - Rep. Minimum (in.)	Cover Horizontal Bars - Avg. (in.)	Cover Horizontal Bars - Rep. Minimum (in.)	Distress Quantity (%)
59	2.5	2.4	3.0	2.6	> 30
62	2.6	2.6	2.1	1.9	10 to 30
69	6.0	5.4	6.6	6.4	< 1
80	2.2	1.7	2.1	1.7	10 to 30
81	5.6	5.6	3.9	3.9	1 to 10
88	2.9	2.8	2.4	2.2	10 to 30
90	2.6	2.6	3.0	3.0	10 to 30
91	3.7	2.4	2.6	2.1	> 30

Location ID	Cover Vertical Bars - Avg. (in.)	Cover Vertical Bars - Rep. Minimum (in.)	Cover Horizontal Bars - Avg. (in.)	Cover Horizontal Bars - Rep. Minimum (in.)	Distress Quantity (%)
93	2.3	1.5	2.3	2.2	> 30
95	2.3	1.6	2.8	2.5	1 to 10
96	1.6	1.6	2.4	2.2	10 to 30
97	2.2	2.1	3.2	2.9	10 to 30
98	3.1	2.9	2.4	2.1	1 to 10

Table 6.29. Cover Depth Statistics - Upper Spandrel Columns and Walls (All Study Areas)

Value	Upper Spandrel Columns & Walls	
	Cover Vertical Bar	Cover Horizontal Bar
Average (in.)	2.9	2.8
Standard Deviation (in.)	1.2	1.0
Coefficient of Variation	40%	37%
Minimum (in.)	1.5	1.6
Maximum (in.)	6.9	6.7

6.2.2.4. Field and Lab Carbonation Tests

Synthesis of field and lab carbonation measurement results are provided in Table 6.30. At present, carbonation is negligible compared to the depth of reinforcement.

Table 6.30. Carbonation Measurements - Upper Spandrel Columns and Walls -1980 Expansion Joint

Location ID	Carbonation - Rep. Maximum (in.)	Cover Vertical Bars - Rep. Minimum (in.)	Cover Horizontal Bars - Rep. Minimum (in.)	Distress Quantity (%)
59	0.1	2.4	2.6	> 30
62	0.2	2.6	1.9	10 to 30
69	0.2	5.4	6.4	< 1
80	0.3	1.7	1.7	10 to 30
81	0.1	5.9	3.9	1 to 10
88	0.3	2.8	2.2	10 to 30
90	0.3	2.6	3.0	10 to 30
91	0.1	2.4	2.1	> 30
93	0.4	1.5	2.2	> 30
95	0.1	1.6	2.5	1 to 10

Location ID	Carbonation - Rep. Maximum (in.)	Cover Vertical Bars - Rep. Minimum (in.)	Cover Horizontal Bars - Rep. Minimum (in.)	Distress Quantity (%)
96	N/A	1.6	2.2	10 to 30
97	0.1	2.1	2.9	10 to 30
98	0.1	2.9	2.1	1 to 10

6.2.2.5. Other Tests

No other tests were conducted in this element category.

6.2.2.6. Chloride Profile Analysis

Chloride profiles for the Upper Spandrel Columns and Walls with the 1980 Expansion joints are shown in Figure 6.14. The chloride profiles are indicative of surface chloride exposure in concrete with negligible background chloride concentration; all profiles decrease from near maximum concentrations near the surface, to above-threshold concentrations at rebar depth, to near zero concentrations at depth. The profiles indicate variable exposure conditions, likely associated with the conditions of, and proximity to, the deck expansion joints. In all cores, considering the measured cover depths, corrosion due to chlorides is expected.

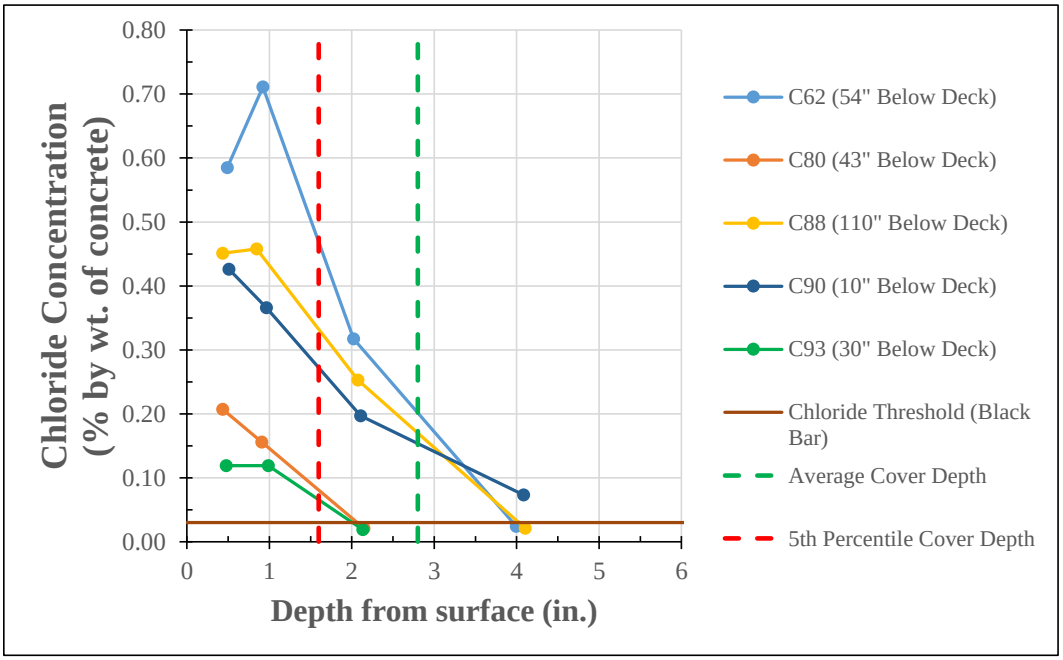

Figure 6.14. Chloride profiles for cores from Upper Spandrel Columns and Walls below 1980 expansion joints.

6.2.2.7. Petrographic Analysis

Cores extracted from the upper spandrel columns indicate a similar mix design as the approach abutments and bent piers (i.e., Mixture 6 - 3/4 inch Gravel). This concrete mixture is characterized by adequate air entrainment and w/c of 0.36 to 0.41.

Core 98, located approximately 6 inches below the cap beam, was examined petrographically and possible freeze-thaw distress was observed in the outer 2 inches; however, the cracking observed was limited to short microcracks and, given the adequate air entrainment, widespread distress due to freeze-thaw cycling is not expected. No other materials-related deterioration mechanisms were identified.

6.2.2.8. Interpretation

The results of the follow-up testing in the Upper Spandrel Columns and Walls that have been positioned below an expansion joint since the deck was reconstructed in 1980 indicate that, apart from the areas of joint-movement related distress discussed separately in Chapter 5, chloride-induced corrosion is the primary deterioration mechanism for these elements. Given that chlorides have diffused to high concentrations in all cores examined, it is likely that, even if future exposure is limited, widespread corrosion would be expected.

Carbonation was negligible compared to the depth of reinforcement, and there was no evidence of other materials related distress except in one location where minor freeze-thaw distress was noted; this condition appeared unique and is likely the result of locally abundant moisture exposure.

A graphical representation of the follow-up testing in the Upper Spandrel Columns and Walls is provided in Figure 6.15, Figure 6.16 and Figure 6.17 and Appendix 14. In the areas surveyed, conditions favorable for corrosion were observed and distress was indicative of chloride-induced corrosion and distress related to structural movements.

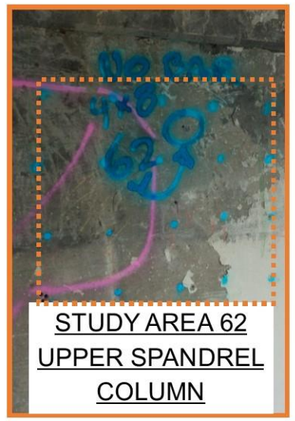

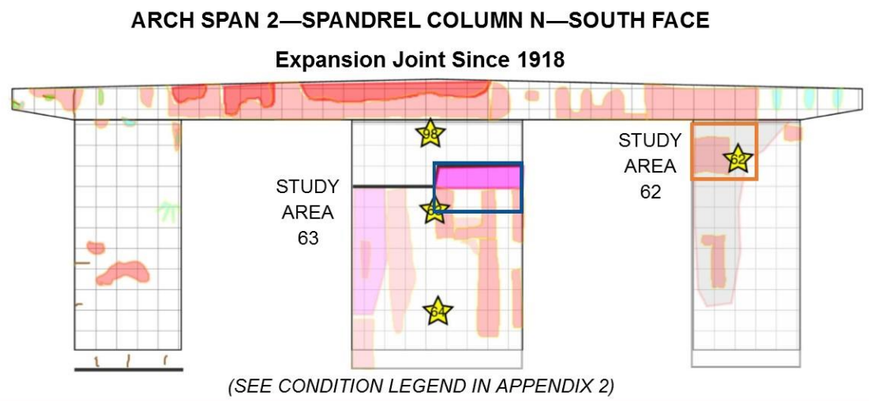

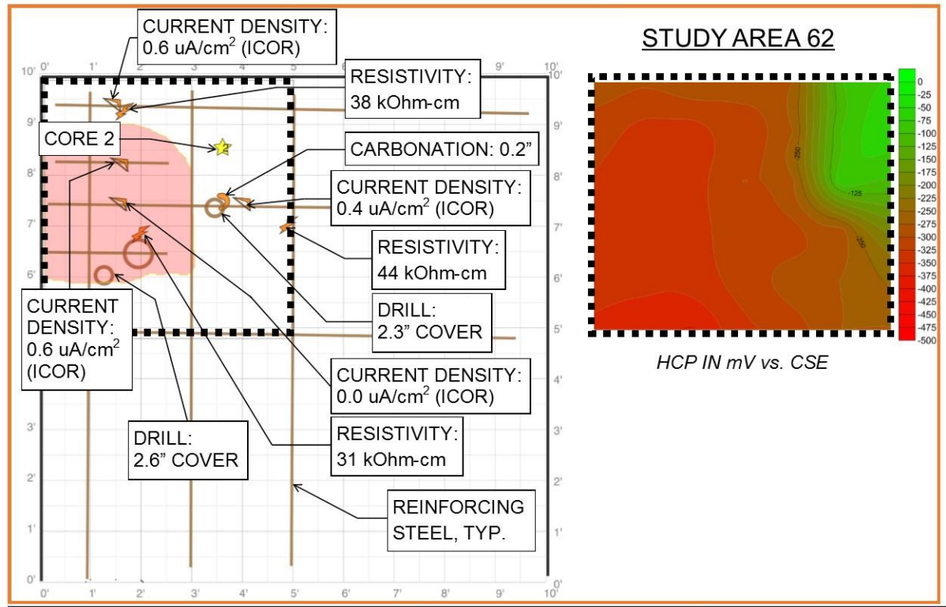

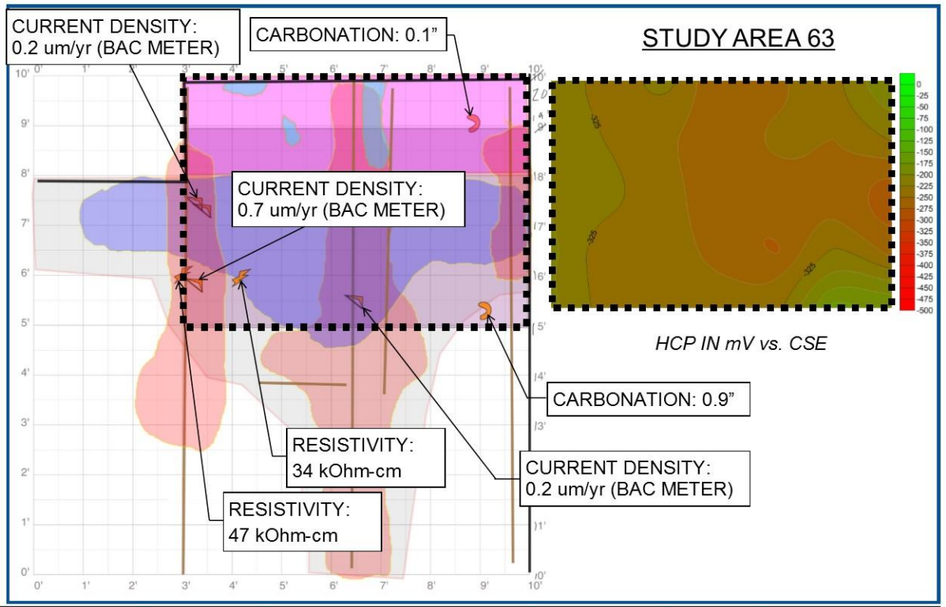

Study Area	Element	Inspection Date	Type	Distress Quantity (%)	Cores Sample(s)	HCP - Avg. (mV vs. CSE)	HCP - Min. (mV vs. CSE)	Resipod - Resistivity Avg. (kOhm-cm)	iCOR - Current Density Avg. (uA/cm^2)	iCOR - Resistivity Avg. (kOhm-cm)	BAC Meter - Current Density Avg. (um/yr)	Cover Vertical Bars - Rep. Minimum (in.)	Cover Horizontal Bars - Rep. Minimum (in.)	Carbonation Avg. (in.)	Deterioration Mechanism(s)
62	Upper Column	7/15/2017	NDE & CORE	10 to 30	62	-296	-377	38	0.3	53	N/A	2.6	1.9	0.2	Chloride Exposure
63	Lower Column	7/15/2017	NDE ONLY	10 to 30	--	-331	-396	41	0.4	46	N/A	1.3	2.3	0.5	Chloride Exposure; Carbonation

Figure 6.15. Graphical Summary of Testing Data for Study Areas 62 and 63 - Spandrel Column.

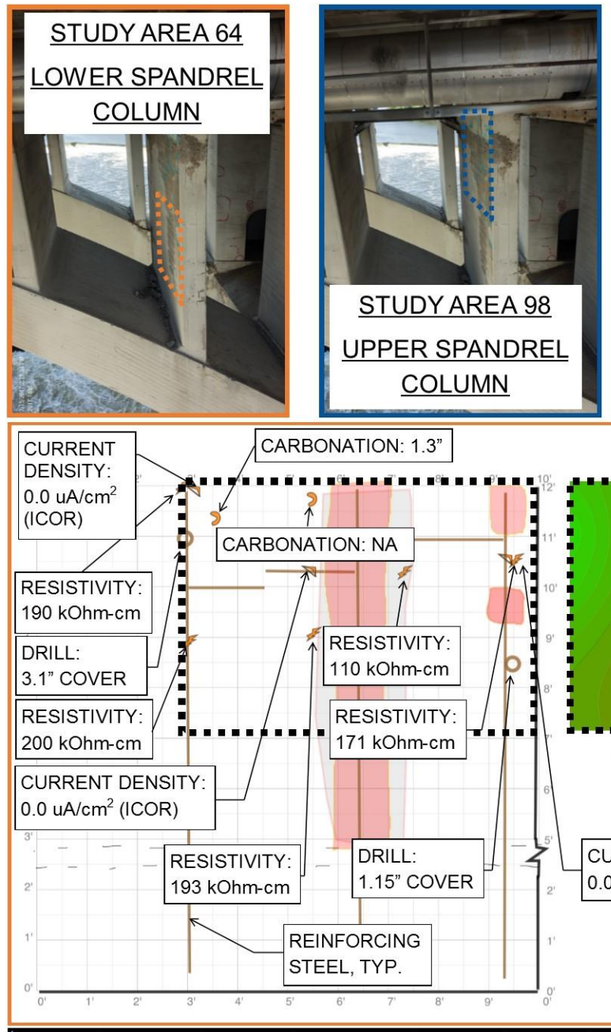

Study Area	Element	Inspection Date	Type	Distress Quantity (%)	Cores Sample(s)	HCP - Avg. (mV vs. CSE)	HCP - Min. (mV vs. CSE)	Resipod - Resistivity Avg. (kOhm-cm)	iCOR - Current Density Avg. (uA/cm²)	iCOR - Resistivity Avg. (kOhm-cm)	BAC Meter - Current Density Avg. (um/yr)	Cover Vertical Bars - Rep. Minimum (in.)	Cover Horizontal Bars - Rep. Minimum (in.)	Carbonation Avg. (in.)	Deterioration Mechanism(s)
64	Lower Column	7/15/2017	NDE ONLY	10 to 30	--	-213	-326	173	0.0	301	N/A	1.0	2.5	N/A	Chloride Exposure; Carbonation
98	Upper Column	7/15/2017	NDE & CORE	1 to 10	98	-282	-411	66	0.1	105	N/A	2.9	2.1	0.1	Chloride Exposure

Figure 6.16. Graphical Summary of Testing Data for Study Area 64 and 98 - Spandrel Column.

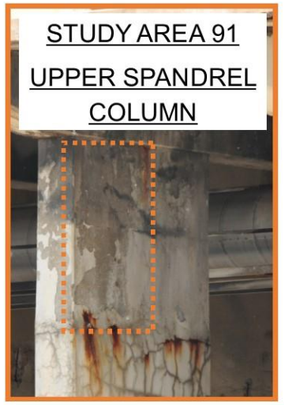

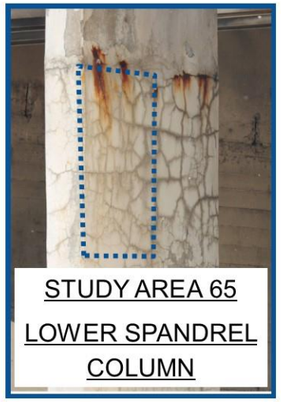

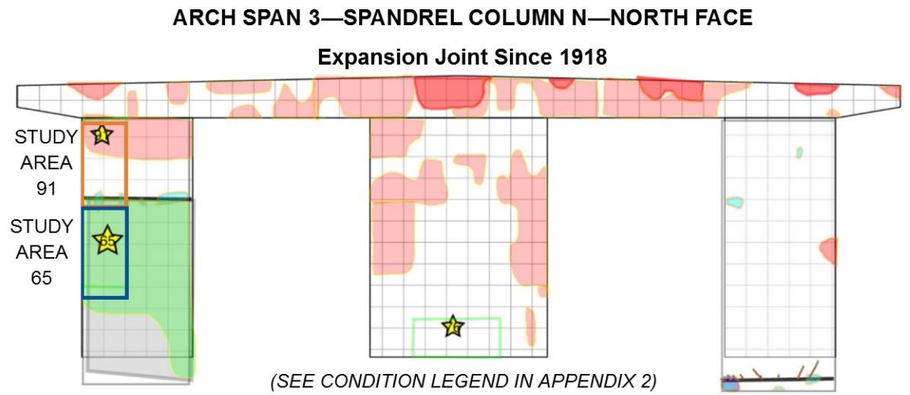

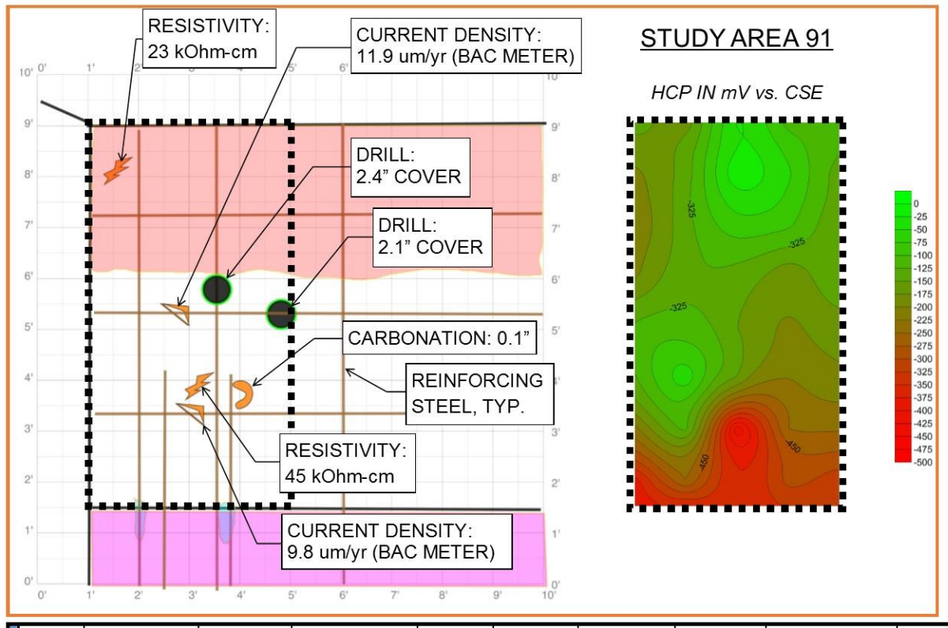

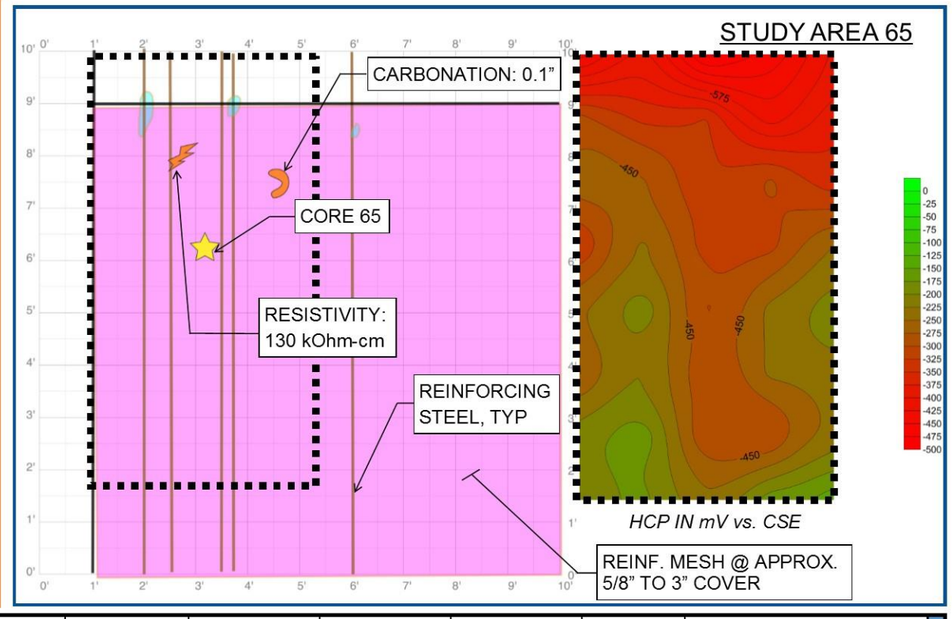

Study Area	Element	Inspection Date	Type	Distress Quantity (%)	Cores Sample(s)	HCP - Avg. (mV vs. CSE)	HCP - Min. (mV vs. CSE)	Resipod - Resistivity Avg. (kOhm-cm)	iCOR - Current Density Avg. (uA/cm²)	iCOR - Resistivity Avg. (kOhm-cm)	BAC Meter - Current Density Avg. (um/yr)	Cover Vertical Bars - Rep. Minimum (in.)	Cover Horizontal Bars - Rep. Minimum (in.)	Carbonation Avg. (in.)	Deterioration Mechanism(s)
91	Upper Column	7/15/2017	NDE ONLY	> 30	--	-368	-595	34	N/A	N/A	9.2	2.4	2.1	0.1	Chloride Exposure
65	Lower Column	7/15/2017	NDE & CORE	> 30	65	-466	-683	130	N/A	N/A	N/A	5/8" MESH	N/A	0.1	Chloride Exposure; Moisture Ingress and Cracking

Figure 6.17. Graphical Summary of Testing Data for Study Area 65 and 91 - Spandrel Column.

6.2.3. Upper Spandrel Columns and Walls (1980 Construction) - Never Expansion Joint

The location of the follow-up testing study areas in the Upper Spandrel Columns and Walls constructed in 1980, where an expansion joint has never been present, are shown in Table 6.31. These study areas included the cap beams.

Table 6.31. Location of Study Areas - Upper Spandrel Columns and Walls - Never Expansion Joint

Location ID	Span	Side of Bridge	Column ID	Elevation of Study Area - Range Below Deck Underside (ft.)	At Expansion Joint - Y/N?	Face	Test Type
60	2	Downstream	M	3 to 7	N	North	NDE Only
89	2	Upstream	C	0 to 3	N	North	NDE only
92	4	Downstream	M	3 to 8	N	South	NDE only
94	5	Upstream	M	3 to 11	N	North	NDE only

6.2.3.1. Physical Condition Survey

The condition of these Upper Spandrel Columns and Walls is summarized in Chapter 4. The conditions among the columns away from expansion joints were generally consistent, averaging 1 percent distress; however, at least two of the shorter spandrel columns (Span 1) were observed to have distress greater than 10 percent related to movement-related distress and were considered atypical.

For each of the study areas, the local distress quantity is presented in Table 6.32. Distress was negligible in these elements aside from an isolated concrete delamination in Study Areas 94, near the transition between the 1980 concrete (upper spandrel column) and the original concrete below (lower spandrel column).

Table 6.32. Condition and Sampling of Study Areas - Upper Spandrel Columns and Walls - Never Expansion Joint

Location ID	Core Samples	Date Inspected	Distress Quantity (%)	Joint Condition
60	N/A	7/15/2017	< 1	Never Expansion Joint
89	N/A	7/16/2017	< 1	Never Expansion Joint
92	N/A	7/15/2017	< 1	Never Expansion Joint
94	N/A	7/16/2017	1 to 10	Never Expansion Joint

6.2.3.2. Corrosion Survey

Corrosion Potential

Results of half-cell potential surveys are provided in Table 6.33. The results indicate a low probability for corrosion activity.

Table 6.33. HCP Testing Results - Upper Spandrel Columns and Walls - Never Expansion Joint

Location ID	HCP - Avg. (mV vs. CSE)	HCP - Min. (mV vs. CSE)	HCP - Std. Dev. (mV vs. CSE)	*Distress Quantity (%)*
60	-20	-100	40	*< 1*
89	-19	-64	16	*< 1*
92	-26	-82	26	*< 1*
94	-70	-92	57	*1 to 10*

** Thresholds (see 3.4.4.1): > -200mV low, -200 to -350mV moderate, < -350 mV high probability of corrosion*

Resistivity

Results of resistivity testing are provided in Table 6.34. The high resistivity values indicate a low corrosion rates would be expected for any corrosion activity.

Table 6.34. Resistivity Testing Results - Upper Spandrel Columns and Walls - Never Expansion Joint

Location ID	Resipod - Resistivity Avg. (kOhm-cm)	iCOR - Resistivity Avg. (kOhm-cm)	*Distress Quantity (%)*
60	--	--	*< 1*
89	481	--	*< 1*
92	502	--	*< 1*
94	235	381	*1 to 10*

** Thresholds (see 3.4.4.2): 50-100 low, 10-50 moderate, <10 kOhm-cm high corrosion rates possible in active areas*

Corrosion Rate

Corrosion rate testing results are provided in Table 6.35. Corrosion rate testing was not performed in all areas due to difficulties in making connections of the probe to the reinforcing steel. Measured corrosion rates were low.

Table 6.35. Corrosion Rate Testing Results - Upper Spandrel Columns and Walls - Never Expansion Joint

Location ID	iCOR - Current Density Avg. (uA/cm^2) *	BAC Meter - Current Density Avg. (um/yr) †	*Distress Quantity (%)*
60	--	--	*< 1*
89	--	3.8	*< 1*
92	--	0.3	*< 1*
94	0.0	--	*1 to 10*

** Thresholds (see 3.4.4.3): <1 low, 1-3 moderate, 3-10 high, >10 severe uA/cm2 instantaneous corrosion rate*
† Thresholds (see 3.4.4.3): <10 low, 10-30 moderate, 30-100 high, >100 um/yr severe instantaneous corrosion rate.

6.2.3.3. Reinforcement Cover Survey

The results of the reinforcement cover surveys are provided in Table 6.36. The statistical information for this element for all exposure conditions (i.e. all expansion joint histories) is summarized in Table 6.37.

Table 6.36. Cover Depth Measurements - Upper Spandrel Columns and Walls - Never Expansion Joint

Location ID	Cover Vertical Bars - Avg. (in.)	Cover Vertical Bars - Rep. Minimum (in.)	Cover Horizontal Bars - Avg. (in.)	Cover Horizontal Bars - Rep. Minimum (in.)	*Distress Quantity (%)*
60	3.0	2.2	2.3	1.8	*< 1*
89	3.0	3.0	3.3	3.0	*< 1*
92	3.1	3.0	2.5	2.3	*< 1*
94	3.0	2.2	2.3	1.9	*1 to 10*

Table 6.37. Cover Depth Statistics - Upper Spandrel Columns and Walls (All Study Areas)

Value	Upper Spandrel Columns & Walls	
	Cover Vertical Bar	Cover Horizontal Bar
Average (in.)	2.9	2.8
Standard Deviation (in.)	1.2	1.0
Coefficient of Variation	40%	37%
Minimum (in.)	1.5	1.6
Maximum (in.)	6.9	6.7

6.2.3.4. Field and Lab Carbonation Tests

Synthesis of field and lab carbonation measurement results are provided in Table 6.38. Depth of carbonation was negligible compared to the depth of reinforcement.

Table 6.38. Carbonation Measurements - Upper Spandrel Column

Location ID	Carbonation - Rep. Maximum (in.)	Cover Vertical Bars - Rep. Minimum (in.)	Cover Horizontal Bars - Rep. Minimum (in.)	Distress Quantity (%)
60	--	2.2	1.8	< 1
89	0.1	3.0	3.0	< 1
92	0.3	3.0	2.3	< 1
94	0.1	2.2	1.9	1 to 10

6.2.3.5. Other Tests

No other test were performed in this element category.

6.2.3.6. Chloride Profile Analysis

Chloride analysis was not warranted due to limited exposure (i.e., no adjacent expansion joints) and low levels of background chlorides observed in other similar cores.

6.2.3.7. Petrographic Analysis

See Section 6.2.2.7 for discussion of petrographic results.

6.2.3.8. Interpretation

The results of the follow-up testing in the Upper Spandrel Columns and Walls that have never had an expansion joint indicate a low probability of active corrosion or any other materials-related deterioration mechanism. Carbonation was low compared to the depth of reinforcement, and the petrographic studies indicate low probability for distress from ASR or freeze-thaw. Any damage observed in these elements may be attributable to atypically low cover depths, mechanical distress from global structural movements, or incipient-anode effects at the interface between the upper columns constructed in 1980 and previously constructed columns below.

6.2.4. Lower Spandrel Columns and Walls (1918 Construction) - Always Expansion Joint and 1980 Expansion Joint

The locations of the follow-up testing study areas in the Lower Spandrel Columns and Walls constructed in 1918 where an expansion joint has always been present or has been present since 1980 are shown in Table 6.39.

Table 6.39. Location of Study Areas - Lower Spandrel Columns and Walls - Always Expansion Joint and 1980 Expansion Joint

Location ID	Span	Side of Bridge	Column ID	Elevation of Study Area - Range Below Deck Underside (ft.)	At Expansion Joint - Y/N?	Face	Test Type
58	1	Downstream	N	8 to 12	Y	South	NDE & core
63	2	Middle	N	6 to 12	Y	South	NDE only
64	2	Middle	N	14 to 20	Y	South	NDE only
65	3	Downstream	N	14 to 22	Y	North	NDE & core
68	6	Downstream	J	8 to 15	Y	South	NDE & core
72	1	Middle	A	14 to 17	Y	South	NDE only
73	1	Upstream	A	15 to 22	Y	South	NDE only
75	2	Upstream	D	5 to 9	Y	South	NDE & core
76	3	Middle	N	25 to 30	Y	North	NDE only
78	5	Middle	N	16 to 23	Y	South	NDE only
81	7	Upstream	J	6 to 8	Y	North	NDE & core
82	7	Middle	J	11 to 17	Y	North	NDE & core
83	7	Middle	J	15	Y	North	Core Only
99	6	Upstream	A	19 to 25	Y	South	NDE only

6.2.4.1. Physical Condition Survey

The condition of these Lower Spandrel Columns and Walls is summarized in Chapter 4. The conditions among the columns at expansion joints were generally consistent. The distress quantity averaged 32 and 55 percent distress in the Middle and Downstream Columns respectively (Spans 1-5), at locations which were always expansion joints. The distress quantity averaged 6, 29, and 45 percent distress in the Middle, Upstream, and Downstream Columns (Spans 1-5), at locations of expansion joints constructed in 1980. The distress quantity averaged 40 percent in the Spandrel Walls (Spans 6 and 7). Differences in exposure are likely attributable to the differences in observed conditions, in that the middle columns have less exposure potential relative to either the upstream or downstream columns.

For each of the study areas, the local distress quantity is presented in Table 6.40. Moderate to high levels of distress were observed, typically concrete delaminations. Large areas of these elements are covered with surface repairs that appear to be largely shotcrete.

Table 6.40. Condition and Sampling of Study Areas - Lower Spandrel Columns and Walls - Always Expansion Joint and 1980 Expansion Joint

Location ID	Core Samples	Date Inspected	Distress Quantity (%)	Joint Condition
58	58	5/26/2017	> 30	Always Expansion Joint
63	N/A	7/15/2017	10 to 30	Always Expansion Joint
64	N/A	7/15/2017	10 to 30	Always Expansion Joint
65	65	7/15/2017	> 30	Always Expansion Joint
68	68	7/15/2017	> 30	Always Expansion Joint
72	N/A	7/15/2017	> 30	Always Expansion Joint
73	N/A	8/6/2017	1 to 10	Always Expansion Joint
75	75	7/16/2017	> 30	1980 Expansion Joint
76	N/A	8/6/2017	1 to 10	Always Expansion Joint
78	N/A	7/16/2017	1 to 10	Always Expansion Joint
81	81	7/16/2017	> 30	Always Expansion Joint
82	82	7/15/2017	> 30	Always Expansion Joint
99	N/A	8/6/2017	>30	Always Expansion Joint

6.2.4.2. Corrosion Survey

Corrosion Potential

Results of half-cell potential surveys are summarized in Table 6.41. The results indicate a moderate to high probability of corrosion in these elements.

Table 6.41. HCP Testing Results - Lower Spandrel Columns and Walls - Always Expansion Joint and 1980 Expansion Joint

Location ID	HCP - Avg. (mV vs. CSE)	HCP - Min. (mV vs. CSE)	HCP - Std. Dev. (mV vs. CSE)	Distress Quantity (%)
58	--	--	--	> 30
63	-331	-396	34	10 to 30
64	-213	-326	83	10 to 30
65	-466	-683	80	> 30
68	-352	-400	28	> 30
72	-312	-363	44	> 30
73	-220	-405	65	1 to 10
75	-310	-372	43	> 30
76	-86	-224	69	1 to 10
78	-273	-327	36	1 to 10
81	-318	-439	60	> 30
82	-219	-292	51	> 30

Location ID	HCP - Avg. (mV vs. CSE)	HCP - Min. (mV vs. CSE)	HCP - Std. Dev. (mV vs. CSE)	Distress Quantity (%)
99	-309	-397	81	>30

** Thresholds (see 3.4.4.1): > -200mV low, -200 to -350mV moderate, < -350 mV high probability of corrosion*

Resistivity

Results of resistivity testing are provided in Table 6.42. Resistivity was variable, and the results indicate a low to moderate rate corrosion, assuming corrosion has initiated, with one area (No. 68) exhibiting conditions likely to support a high rate of corrosion.

Table 6.42. Resistivity Testing Results - Lower Spandrel Columns and Walls - Always Expansion Joint and 1980 Expansion Joint

Location ID	Resipod - Resistivity Avg. (kOhm-cm)	iCOR - Resistivity Avg. (kOhm-cm)	Distress Quantity (%)
58	11	--	> 30
63	41	46	10 to 30
64	173	301	10 to 30
65	130	--	> 30
68	7	--	> 30
72	46	--	> 30
73	83	120	1 to 10
75	27	--	> 30
76	306	--	1 to 10
78	58	387	1 to 10
81	33	--	> 30
82	65	246	> 30
99	184	--	>30

** Thresholds (see 3.4.4.2): 50-100 low, 10-50 moderate, <10 kOhm-cm high corrosion rates possible in active areas*

Corrosion Rate

Corrosion rate testing results are provided in Table 6.43. Due to the variable reinforcement placement (described below), consistent corrosion rate measurements were not obtained in all elements. Where measured, the corrosion rate was low to moderate.

Table 6.43. Corrosion Rate Testing Results - Lower Spandrel Columns and Walls - Always Expansion Joint and 1980 Expansion Joint

Location ID	iCOR - Current Density Avg. (uA/cm^2) *	BAC Meter - Current Density Avg. (um/yr) †	Distress Quantity (%)
58	--	--	> 30
63	0.4	--	10 to 30
64	0.0	--	10 to 30
65	--	--	> 30
68	--	32.5	> 30
72	--	--	> 30
73	0.1	--	1 to 10
75	--	--	> 30
76	--	--	1 to 10
78	0.0	--	1 to 10
81	--	--	> 30
82	0.0	--	> 30
99	--	2.3	>30

** Thresholds (see 3.4.4.3): <1 low, 1-3 moderate, 3-10 high, >10 severe uA/cm2 instantaneous corrosion rate*
† Thresholds (see 3.4.4.3): <10 low, 10-30 moderate, 30-100 high, >100 um/yr severe instantaneous corrosion rate.

6.2.4.3. Reinforcement Cover Survey

The results of the reinforcement cover surveys are provided in Table 6.44. The statistical information for this element for all exposure conditions (i.e., all expansion joint histories) is summarized in Table 6.45. The general location and cover depth of reinforcement in the Lower Spandrel Columns was highly variable, resulting in localized areas of shallow cover. Typically, bars were found in the Lower Columns and Walls spaced at approximately 4 feet, and it was not uncommon for "vertical" bars to deviate significantly from vertical. Reinforcement in the lower spandrel column in Study Area 81 was too deep to obtain accurate measurements.

Table 6.44. Cover Depth Measurements - Lower Spandrel Columns and Walls - Always Expansion Joint and 1980 Expansion Joint

Location ID	Cover Vertical Bars - Avg. (in.)	Cover Vertical Bars - Rep. Minimum (in.)	Cover Horizontal Bars - Avg. (in.)	Cover Horizontal Bars - Rep. Minimum (in.)	Distress Quantity (%)
58	4.4	3.9	4.4	4.3	> 30
63	1.6	1.3	2.3	2.3	10 to 30
64	2.3	1.0	3.5	2.5	10 to 30
65	0.6	0.6	--	--	> 30
68	3.6	3.3	--	--	> 30
72	3.0	2.9	3.5	3.2	> 30
73	2.1	1.8	1.4	1.4	1 to 10
75	3.5	3.5	5.5	5.5	> 30
76	3.8	3.0	6.0	5.0	1 to 10
78	2.3	1.8	3.1	3.1	1 to 10
81	--	--	--	--	> 30
82	1.4	0.4	--	--	> 30
99	2.3	1.5	3.6	3.4	>30

Table 6.45. Cover Depth Statistics - Lower Spandrel Columns and Walls (All Study Areas)

Value	Lower Spandrel Columns and Walls	
	Cover Vertical Bar	Cover Horizontal Bar
Average (in.)	2.8	3.7
Standard Deviation (in.)	1.0	1.7
Coefficient of Variation	37%	46%
Minimum (in.)	0.4	1.4
Maximum (in.)	5.9	7.3

6.2.4.4. Field and Lab Carbonation Tests

Synthesis of field and lab carbonation measurement results in the Lower Spandrel Columns and Walls where an expansion joint is currently present are provided in Table 6.46. Carbonation was highly variable, but in four study areas has progressed to depths of approximately 2 inches or more; this is beyond the cover depth to the reinforcing in seven of the twelve study areas with measured cover. There was no clear correlation between the variation in carbonation and the location of the individual spandrel columns; however, carbonation was generally higher on the upstream and downstream columns, compared to the middle columns.

Table 6.46. Carbonation Measurements - Lower Spandrel Columns and Walls - Always Expansion Joint and 1980 Expansion Joint

Location ID	Carbonation - Rep. Maximum (in.)	Cover Vertical Bars - Rep. Minimum (in.)	Cover Horizontal Bars - Rep. Minimum (in.)	Distress Quantity (%)
58	1.8	3.9	4.3	> 30
63	0.5	1.3	2.3	10 to 30
64	--	1.0	2.5	10 to 30
65	0.1	0.6	--	> 30
68	1.5	3.3	--	> 30
72	--	2.9	3.2	> 30
73	0.0	1.8	1.4	1 to 10
75	1.5	3.5	5.5	> 30
76	3.0	3.0	5.0	1 to 10
78	1.9	1.8	3.1	1 to 10
81	0.1	--	--	> 30
82	0.9	0.4	--	> 30
99	2.4	1.5	3.4	>30

6.2.4.5. Other Tests

No other tests were conducted in this element category.

6.2.4.6. Chloride Profile Analysis

Chloride profiles for the Lower Spandrel Columns and Walls where an expansion joint is currently present are shown in Figure 6.18. In general, the chloride exposure in these Lower Spandrel Columns and Walls is variable, though all profiles in the original concrete exhibit a peak concentration at a depth of 2 inches. Chloride concentrations at bar depth are well in excess of the corrosion threshold and decrease to near zero with depth. In some cases, there is also another peak near the surface (i.e., within 1 inch of surface). This is atypical of chloride profiles that might be expected for simple exposure to a constant chloride source and suggests that the chloride exposure has varied over time. For the time period immediately after the 1980 deck replacement, and since the joint repairs performed in 2003, chloride exposure has likely been significantly reduced on the surface of the Lower Spandrel Columns. The diffusion profiles indicate possible inward diffusion of some original chloride exposure, possible "washing" of near-surface concrete with non-chloride-containing moisture (such as non-wintertime precipitation), as well as possible build-up on the surface from new exposure (after a repaired joint began to leak). The peak chloride concentrations near 2 inches are likely due to diffusion of chlorides form the surface after exposure had been reduced or stopped. Surface "washing" from run-off from the deck surface is possible at some locations; though, this would expected to be low given the position of the columns. At the cracked location (Core 68), chloride ingress is higher. For the repair concrete (Core 65), the chloride profile shows a moderate surface chloride exposure, with low chlorides through the depth of the core; this is consistent with only relatively recent chloride exposure.

Based on the profiles, chloride exposure is well beyond the corrosion threshold and has likely resulted in corrosion of the reinforcement for the typical cover conditions in the Lower Spandrel Columns and Walls where an expansion joint is currently present.

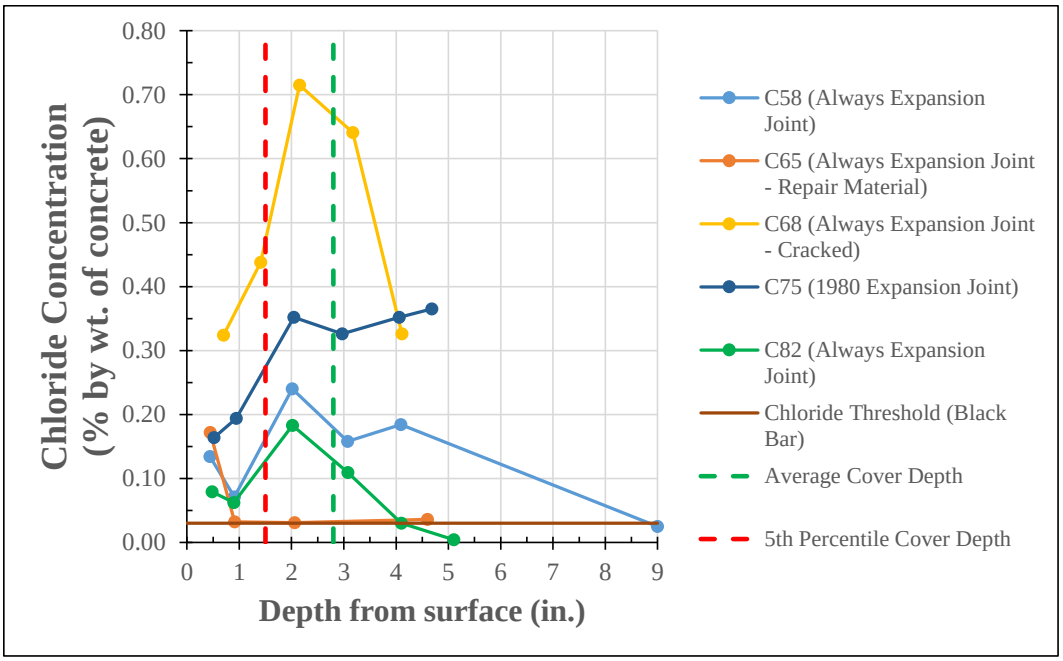

Figure 6.18. Chloride profiles for cores from Lower Spandrel Columns and Walls compared to chloride threshold.

6.2.4.7. Petrographic Analysis

The lower spandrel columns are comprised of a similar mix design as the arch ribs, barrel arches, and north approach wing walls (i.e., Concrete Mixture 1B - 1918: 1 to 2 inch Basalt). This mixture is not air entrained and has a w/c of 0.54 to 0.60.

Core 79 (which was taken from Lower Spandrel Columns and Walls constructed in 1918 where an expansion joint is not currently present; see Section 6.2.5) was selected for petrographic studies for these element categories. No evidence of deleterious chemical reactions that involved aggregates and paste were observed, and no distress due to freeze-thaw was observed. However, paste erosion from the surface of these elements was common and, based on similar conditions observed petrographically in the Arch Pier Walls, North Retaining Walls, and Barrel Arches, the paste erosion is attributed to freeze thaw cycling where moisture exposure is prevalent.

6.2.4.8. Interpretation

Based on the results of the follow-up testing, the primary deterioration mechanism in these Lower Spandrel Columns is chloride-induced corrosion. However, a contributing mechanism is carbonation-induced corrosion, especially in locations were cover is low and the depth of carbonation was high because of locally variable exposure conditions or characteristics of the concrete (e.g., locally high w/c).

Freeze-thaw distress or other materials related reactions were not observed in most core samples; however, given the lack of air entrainment, freeze-thaw distress may occur at areas of the Lower Spandrel Columns

exposed to moisture and freeze-thawing cycles (e.g., near drains). Freeze-thaw action has also caused paste erosion at surfaces.

The shotcrete repairs were largely sound and generally not subject to an on-going deterioration mechanisms. Where deterioration of the patches is occurring, the distress appears to be mainly characterized by map cracking and/or debonding of the interface with the original concrete at the perimeter of the repairs.

A graphical representation of the follow-up testing in the Lower Spandrel Columns and Walls is provided in Figure 6.19 through Figure 6.22 and in Appendix 14. In the areas surveyed, conditions favorable for corrosion were observed and distress was indicative of chloride- and carbonation-induced corrosion.

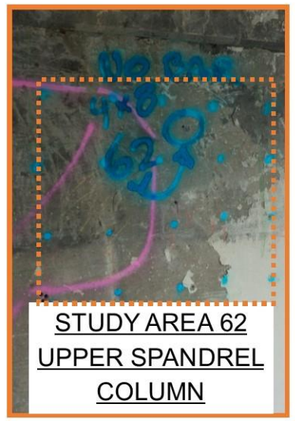

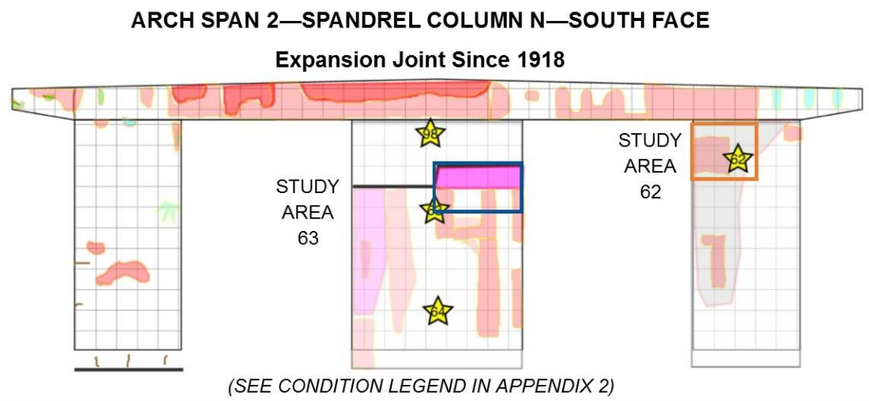

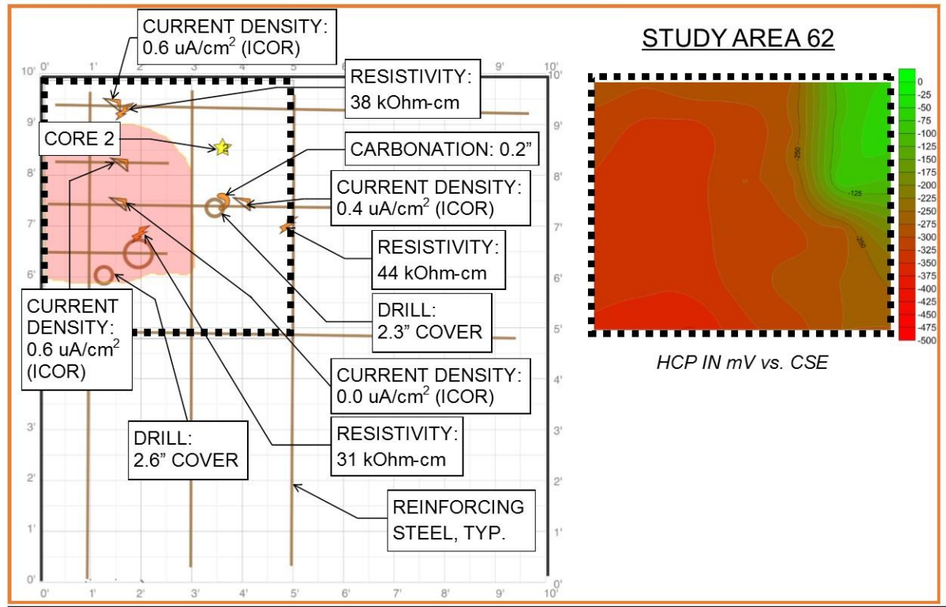

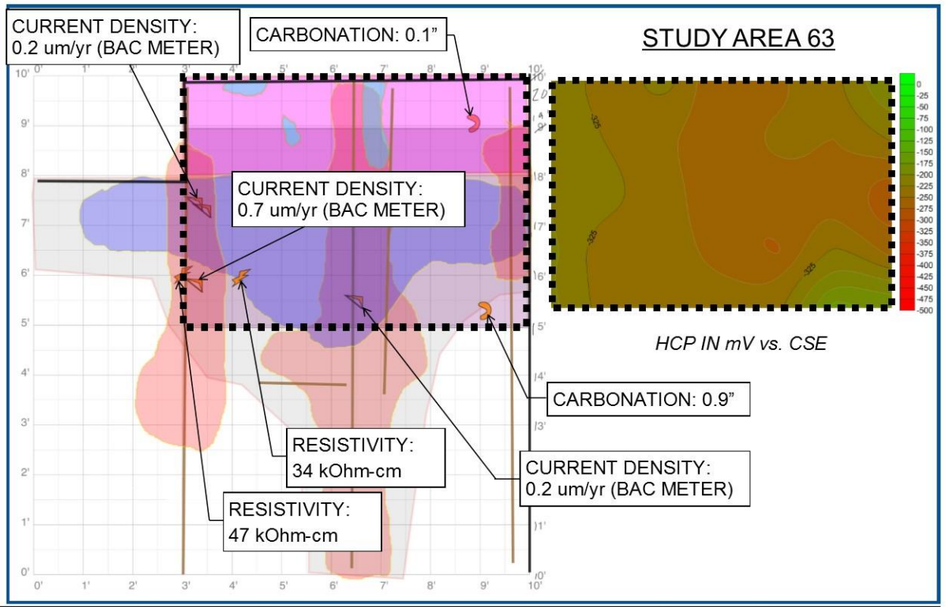

Study Area	Element	Inspection Date	Type	Distress Quantity (%)	Cores Sample(s)	HCP - Avg. (mV vs. CSE)	HCP - Min. (mV vs. CSE)	Resipod - Resistivity Avg. (kOhm-cm)	iCOR - Current Density Avg. (uA/cm^2)	iCOR - Resistivity Avg. (kOhm-cm)	BAC Meter - Current Density Avg. (um/yr)	Cover Vertical Bars - Rep. Minimum (in.)	Cover Horizontal Bars - Rep. Minimum (in.)	Carbonation Avg. (in.)	Deterioration Mechanism(s)
62	Upper Column	7/15/2017	NDE & CORE	10 to 30	62	-296	-377	38	0.3	53	N/A	2.6	1.9	0.2	Chloride Exposure
63	Lower Column	7/15/2017	NDE ONLY	10 to 30	--	-331	-396	41	0.4	46	N/A	1.3	2.3	0.5	Chloride Exposure; Carbonation

Figure 6.19. Graphical Summary of Testing Data for Study Areas 62 and 63 - Spandrel Column.

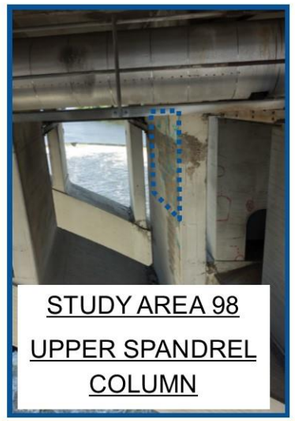

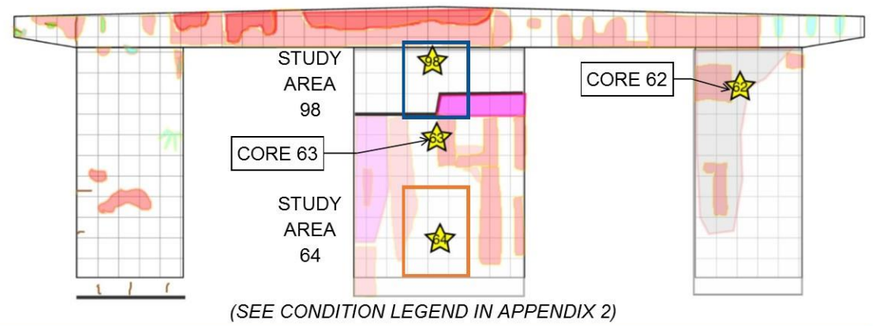

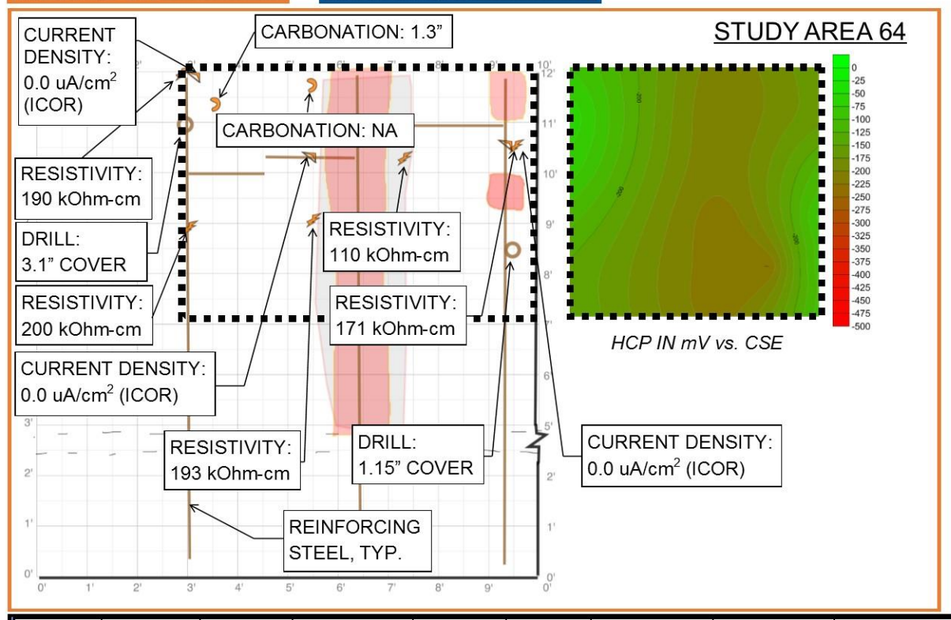

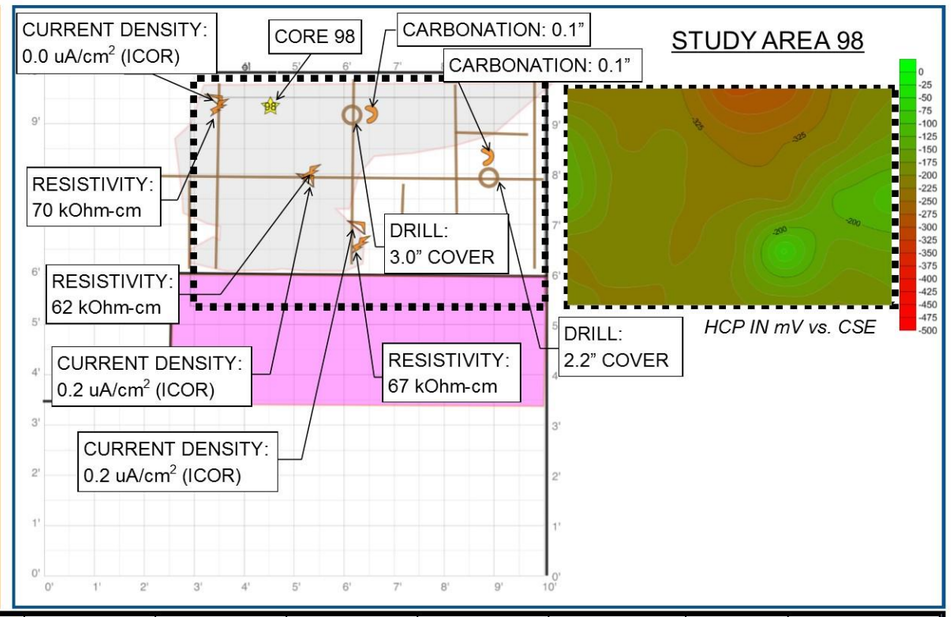

Study Area	Element	Inspection Date	Type	Distress Quantity (%)	Cores Sample(s)	HCP - Avg. (mV vs. CSE)	HCP - Min. (mV vs. CSE)	Resipod - Resistivity Avg. (kOhm-cm)	iCOR - Current Density Avg. (uA/cm²)	iCOR - Resistivity Avg. (kOhm-cm)	BAC Meter - Current Density Avg. (um/yr)	Cover Vertical Bars - Rep. Minimum (in.)	Cover Horizontal Bars - Rep. Minimum (in.)	Carbonation Avg. (in.)	Deterioration Mechanism(s)
64	Lower Column	7/15/2017	NDE ONLY	10 to 30	--	-213	-326	173	0.0	301	N/A	1.0	2.5	N/A	Chloride Exposure; Carbonation
98	Upper Column	7/15/2017	NDE & CORE	1 to 10	98	-282	-411	66	0.1	105	N/A	2.9	2.1	0.1	Chloride Exposure

Figure 6.20. Graphical Summary of Testing Data for Study Area 64 and 98 - Spandrel Column.

STUDY AREA 76

LOWER SPANDREL COLUMN

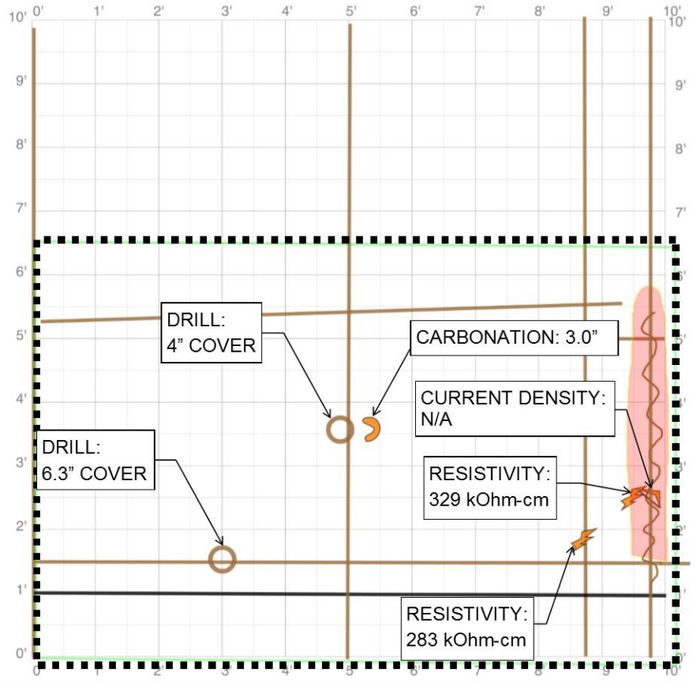

ARCH SPAN 3—SPANDREL COLUMN N—NORTH FACE

Expansion Joint Since 1918

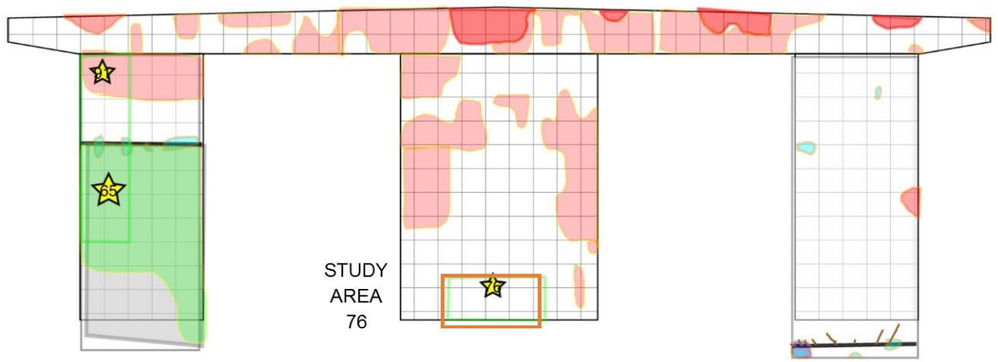

(SEE CONDITION LEGEND IN APPENDIX 2)

HCP IN mV vs. CSE

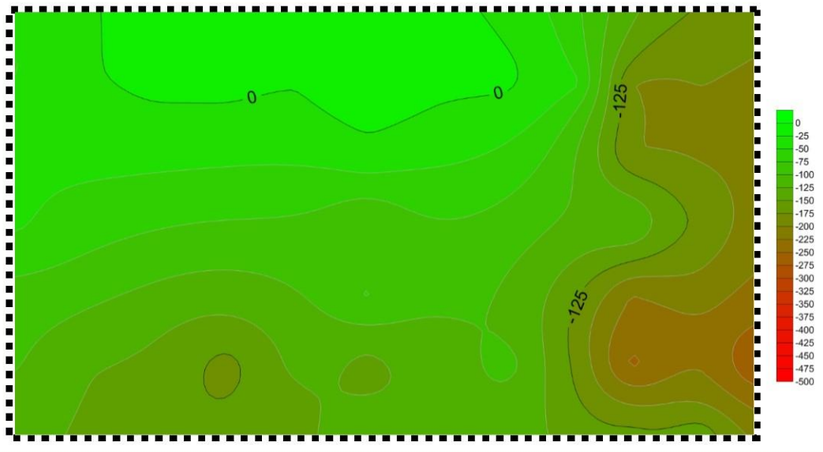

Study Area	Element	Inspection Date	Type	Distress Quantity (%)	Cores Sample(s)	HCP - Avg. (mV vs. CSE)	HCP - Min. (mV vs. CSE)	Resipod - Resistivity Avg. (kOhm-cm)	iCOR - Current Density Avg. (uA/cm^2)	iCOR - Resistivity Avg. (kOhm-cm)	BAC Meter - Current Density Avg. (um/yr)	Cover Vertical Bars - Rep. Minimum (in.)	Cover Horizontal Bars - Rep. Minimum (in.)	Carbonation Avg. (in.)	Deterioration Mechanism(s)
76	Lower Column	8/6/2017	NDE ONLY	1 to 10	--	-86	-224	306	N/A	N/A	N/A	3.0	5.0	3.0	Chloride Exposure; Carbonation

Figure 6.21. Graphical Summary of Testing Data for Study Area 76 - Spandrel Column.

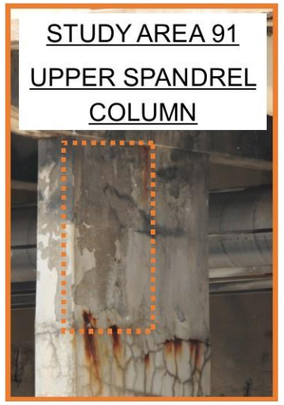

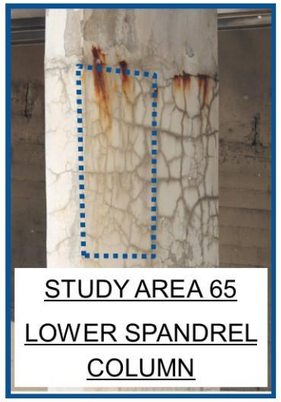

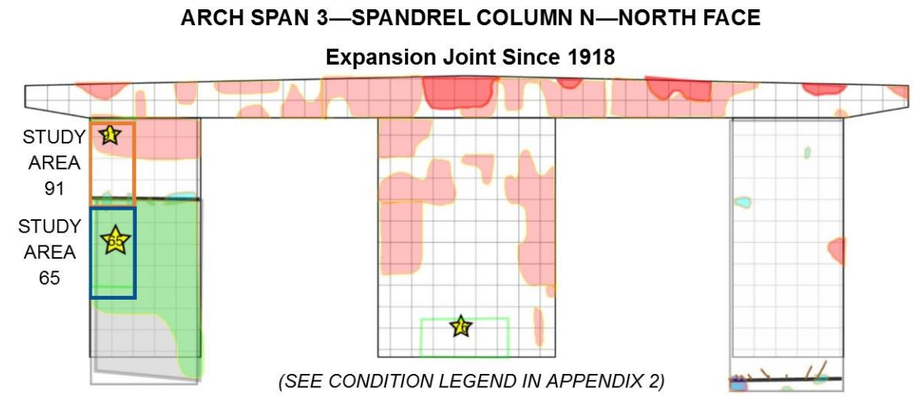

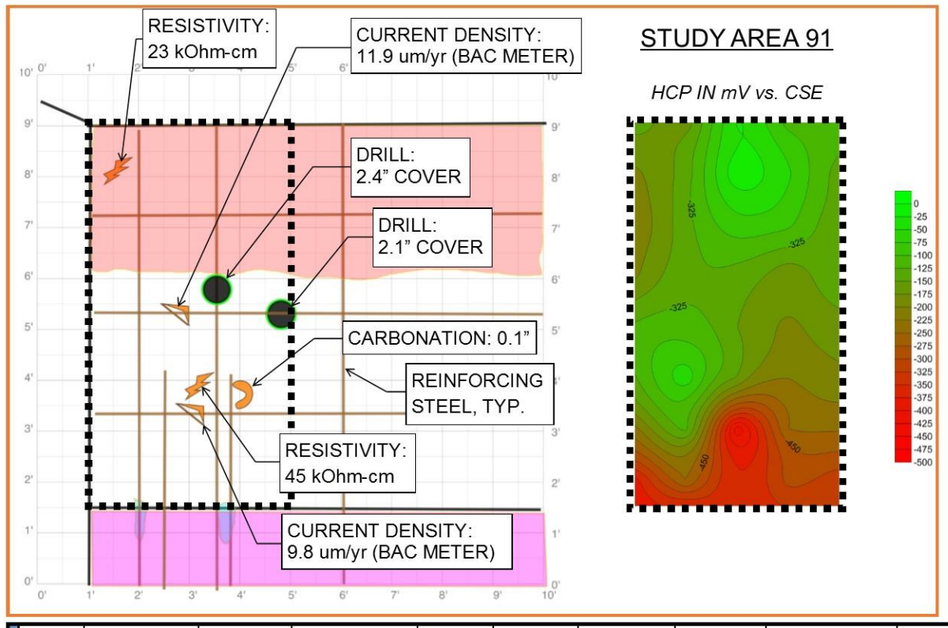

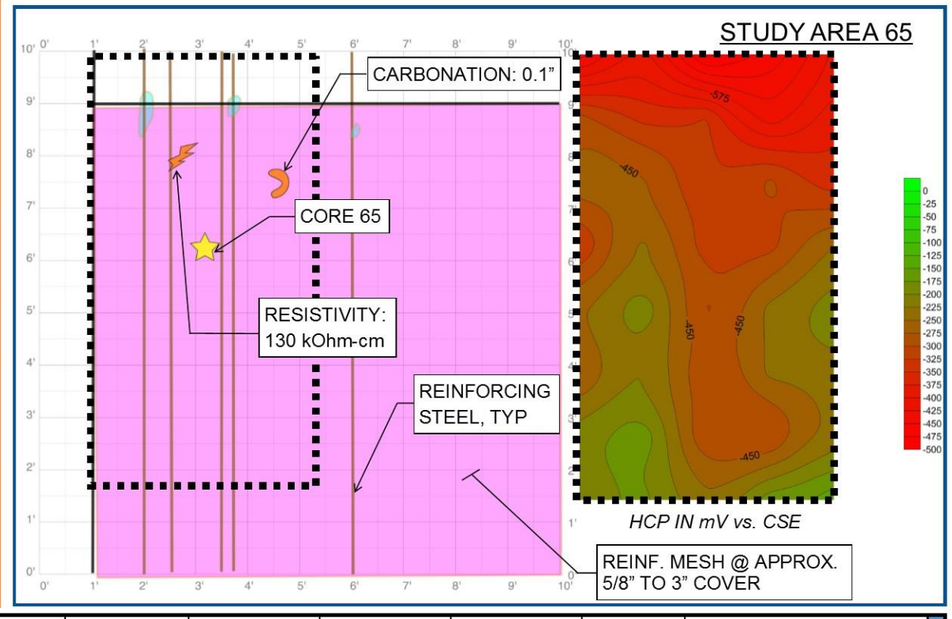

Study Area	Element	Inspection Date	Type	Distress Quantity (%)	Cores Sample(s)	HCP - Avg. (mV vs. CSE)	HCP - Min. (mV vs. CSE)	Resipod - Resistivity Avg. (kOhm-cm)	iCOR - Current Density Avg. (uA/cm²)	iCOR - Resistivity Avg. (kOhm-cm)	BAC Meter - Current Density Avg. (um/yr)	Cover Vertical Bars - Rep. Minimum (in.)	Cover Horizontal Bars - Rep. Minimum (in.)	Carbonation Avg. (in.)	Deterioration Mechanism(s)
91	Upper Column	7/15/2017	NDE ONLY	> 30	--	-368	-595	34	N/A	N/A	9.2	2.4	2.1	0.1	Chloride Exposure
65	Lower Column	7/15/2017	NDE & CORE	> 30	65	-466	-683	130	N/A	N/A	N/A	5/8" MESH	N/A	0.1	Chloride Exposure; Moisture Ingress and Cracking

Figure 6.22. Graphical Summary of Testing Data for Study Area 65 and 91 - Spandrel Column.

6.2.5. Lower Spandrel Columns and Walls (1918 Construction) – Never Expansion Joint and 1918 to 1980 Expansion Joint

The locations of the follow-up testing study areas in the Lower Spandrel Columns and Walls constructed in 1918 where an expansion joint has never been present or was only present from 1918 to 1980 are shown in Table 6.47.

Table 6.47. Location of Study Areas - Lower Spandrel Columns and Walls - Never Expansion Joint and 1918 to 1980 Expansion Joint

Location ID	Span	Side of Bridge	Column ID	Elevation of Study Area - Range Below Deck Underside (ft.)	At Expansion Joint - Y/N?	Face	Test Type
61	2	Downstream	M	9 to 13	N	North	NDE only
66	5	Middle	L	8 to 12	N	North	NDE & core
67	5	Downstream	M	10 to 20	N	South	NDE only
70	4	Downstream	L	9 to 13	N	North	NDE only
71	4	Downstream	M	10 to 18	N	South	NDE only
74	2	Middle	C	10 to 14	N	North	NDE only
79	6	Middle	B	9 to 15	N	North	NDE & core
84	6	Downstream	B	7	N	North	Core Only

6.2.5.1. Physical Condition Survey

The condition of the Lower Spandrel Columns is summarized in Chapter 4. The conditions among the columns away from joints were variable, and in general higher distress was observed on either the upstream or downstream columns compared to the middle column. Distress in these elements averaged 8 percent but varied widely from 0 to 57 percent among individual columns.

For each of the study areas, the local distress quantity is presented in Table 6.48. Observed distress was variable, and typical distress observed included deteriorated repairs and concrete delaminations over reinforcing bars. Corrosion-related distress was most pronounced at Study Area 66 and 67 near the transition between the 1980 concrete (upper spandrel column) and the original concrete below (lower spandrel column). Also, corrosion-related distress (likely due to carbonation) was observed over reinforcing steel with low cover in Study Area 67 (see below - Reinforcement Cover Survey).

Table 6.48. Condition and Sampling of Study Areas - Lower Spandrel Columns and Walls - Never Expansion Joint and 1918 to 1980 Expansion Joint

Location ID	Core Samples	Date Inspected	Distress Quantity (%)	Joint Condition
61	61	7/15/2017	< 1	Never Exp. Joint
66	66	7/15/2017	10 to 30	1918 to 1980 Expansion Joint
67	N/A	7/15/2017	> 30	Never Exp. Joint
70	N/A	8/5/2017	< 1	1918 to 1980 Expansion Joint
71	N/A	8/5/2017	1 to 10	Never Exp. Joint
74	N/A	7/16/2017	1 to 10	1918 to 1980 Expansion Joint
79	79	8/5/2017	1 to 10	Never Exp. Joint

6.2.5.2. Corrosion Survey

Corrosion Potential

Results of half-cell potential surveys are summarized in Table 6.49. The results indicate a low potential for corrosion, even in locations where distress was observed. Study Area 61 was not surveyed due to the presence of the mesh reinforcement within a large repair.

Table 6.49. HCP Testing Results - Lower Spandrel Columns and Walls - Never Expansion Joint and 1918 to 1980 Expansion Joint

Location ID	HCP - Avg. (mV vs. CSE)	HCP - Min. (mV vs. CSE)	HCP - Std. Dev. (mV vs. CSE)	Distress Quantity (%)
61	--	--	--	< 1
66	-92	-165	49	10 to 30
67	-13	-173	52	> 30
70	-88	-170	42	< 1
71	-61	-170	50	1 to 10
74	-32	-80	29	1 to 10
79	-28	-183	64	1 to 10

** Thresholds (see 3.4.4.1): > -200mV low, -200 to -350mV moderate, < -350 mV high probability of corrosion*

Resistivity

Results of resistivity testing are summarized in Table 6.50. The high measured resistivity values indicate a low rate of corrosion where corrosion is occurring.

Table 6.50. Resistivity Testing Results - Lower Spandrel Columns and Walls - Never Expansion Joint and 1918 to 1980 Expansion Joint

Location ID	Resipod - Resistivity Avg. (kOhm-cm)	iCOR - Resistivity Avg. (kOhm-cm)	Distress Quantity (%)
61	516	433	< 1
66	220	--	10 to 30
67	425	--	> 30
70	571	857	< 1
71	263	275	1 to 10
74	181	--	1 to 10
79	1317	--	1 to 10

** Thresholds (see 3.4.4.2): 50-100 low, 10-50 moderate, <10 kOhm-cm high corrosion rates possible in active areas*

Corrosion Rate

Corrosion rate testing results are provided in Table 6.51. Where measured, corrosion rates were low.

Table 6.51. Corrosion Rate Testing Results - Lower Spandrel Columns and Walls - Never Expansion Joint and 1918 to 1980 Expansion Joint

Location ID	iCOR - Current Density Avg. (uA/cm^2) *	BAC Meter - Current Density Avg. (um/yr) †	Distress Quantity (%)
61	0.0	--	< 1
66	--	1.5	10 to 30
67	--	--	> 30
70	0.8	--	< 1
71	0.0	--	1 to 10
74	--	0.8	1 to 10
79	--	--	1 to 10

** Thresholds (see 3.4.4.3): <1 low, 1-3 moderate, 3-10 high, >10 severe uA/cm2 instantaneous corrosion rate*

† Thresholds (see 3.4.4.3): <10 low, 10-30 moderate, 30-100 high, >100 um/yr severe instantaneous corrosion rate.

6.2.5.3. Reinforcement Cover Survey

The results of the reinforcement cover surveys are provided in Table 6.52. The statistical information for this element for all exposure conditions (i.e., all expansion joint histories) is summarized in Table 6.53. Variability in cover depth and bar spacing was similar to that described for the Lower Spandrel Columns under Section 6.2.4.3.

Table 6.52. Cover Depth Measurements - Lower Spandrel Columns and Walls - Never Expansion Joint and 1918 to 1980 Expansion Joint

Location ID	Cover Vertical Bars - Avg. (in.)	Cover Vertical Bars - Rep. Minimum (in.)	Cover Horizontal Bars - Avg. (in.)	Cover Horizontal Bars - Rep. Minimum (in.)	Distress Quantity (%)
61	2.7	2.5	--	--	< 1
66	3.4	3.4	4.1	4.1	10 to 30
67	1.6	1.4	2.5	2.5	> 30
70	2.3	2.0	2.0	2.0	< 1
71	2.5	1.5	--	--	1 to 10
74	2.0	1.5	3.6	3.4	1 to 10
79	3.3	2.5	4.3	4.3	1 to 10

Table 6.53. Cover Depth Statistics - Lower Spandrel Columns and Walls (All Study Areas)

Value	Lower Spandrel Columns/Walls	
	Cover Vertical Bar	Cover Horizontal Bar
Average (in.)	2.8	3.7
Standard Deviation (in.)	1.0	1.7
Coefficient of Variation	37%	46%
Minimum (in.)	0.4	1.4
Maximum (in.)	5.9	7.3

6.2.5.4. Field and Lab Carbonation Tests

Synthesis of field and lab carbonation measurement results in the Lower Spandrel Columns and Walls where an expansion joint is not currently present are provided in Table 6.54. Carbonation was variable, but in at least two study areas has progressed to depths of about 2.5 inches or more; this is beyond the cover depth to the reinforcing in six of the seven study areas with measured cover. There was no clear correlation between the variation in carbonation and the location of the spandrel columns.

Table 6.54. Carbonation Measurements - Lower Spandrel Columns and Walls - Never Expansion Joint and 1918 to 1980 Expansion Joint

Location ID	Carbonation - Avg. (in.)	Cover Vertical Bars - Rep. Minimum (in.)	Cover Horizontal Bars - Rep. Minimum (in.)	Distress Quantity (%)
61	1.2	2.5	--	< 1
66	1.5	3.4	4.1	10 to 30
67	2.5	1.4	2.5	> 30
70	0.0	2.0	2.0	< 1
71	0.8	1.5	--	1 to 10
74	0.9	1.5	3.4	1 to 10
79	2.8	2.5	4.3	1 to 10

6.2.5.5. Other Tests

No other tests were conducted in this element category.

6.2.5.6. Chloride Profile Analysis

The chloride profiles are shown in Figure 6.23 and indicate negligible chloride exposure at the condition where no joint has ever been present (C79). Near or slightly above-threshold chlorides are observed in the core from the spandrel column below a joint from 1918 to 1980 (C66, approximately 10 feet below joint); however, since the joint was removed in 1980, additional chloride exposure has likely been negligible.

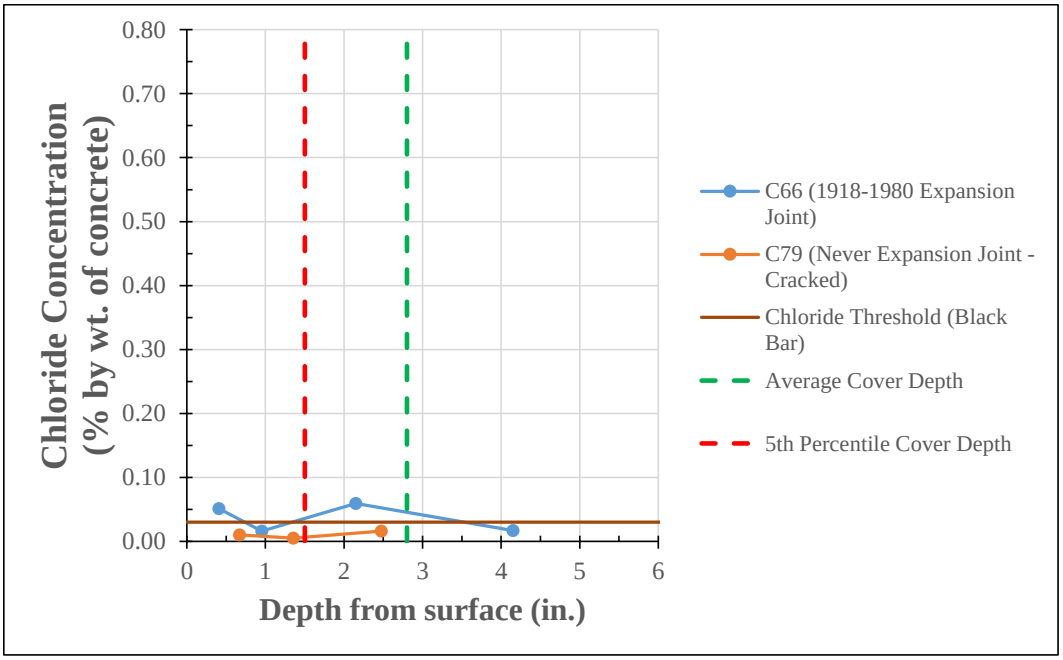

Figure 6.23. Chloride profiles for cores from Lower Spandrel Columns and Walls compared to chloride threshold.

6.2.5.7. Petrographic Analysis

See Section 6.2.4.7 for a discussion of the petrographic analysis for the Lower Spandrel Columns and Walls.

6.2.5.8. Interpretation

Based on the results of the follow-up testing, the primary deterioration mechanism in the Lower Spandrel Columns and Walls is carbonation-related corrosion. Depending on the condition of the joint between 1918 and 1980, some chloride exposure may have occurred that may contribute to corrosion, but this is unlikely to be widespread. The lower chloride data from elements below the 1918-1980 joints, as compared to those below the 1980-present joints, is expected because application of deicing salts to roadways in the United States generally began in the 1950s and has increased since then (see Figure 6.24). As such, the 1918-1980 joints received approximately 30 years of relatively moderate salt exposure, whereas the 1980-present joints have received almost 40 years of more severe salt exposure.

Freeze-thaw distress or other materials related reactions were not observed in most core samples; however, given the lack of air entrainment, freeze-thaw distress may occur at areas of the Lower Spandrel Columns and Walls exposed to moisture and freeze-thawing cycles (e.g., near drains). Also, surface paste erosion due to freeze-thaw action is occurring.

The shotcrete repairs were largely sound and generally not subject to any on-going deterioration mechanisms. Where deterioration of the patches is occurring, the distress appears to be mainly characterized by map cracking and/or debonding of the interface with the original concrete at the perimeter of the repairs.

A graphical representation of the follow-up testing in the Lower Spandrel Columns and Walls is provided in Figure 6.25 and Figure 6.26 and in Appendix 14. In the areas surveyed, observed distress was indicative of and carbonation related corrosion.

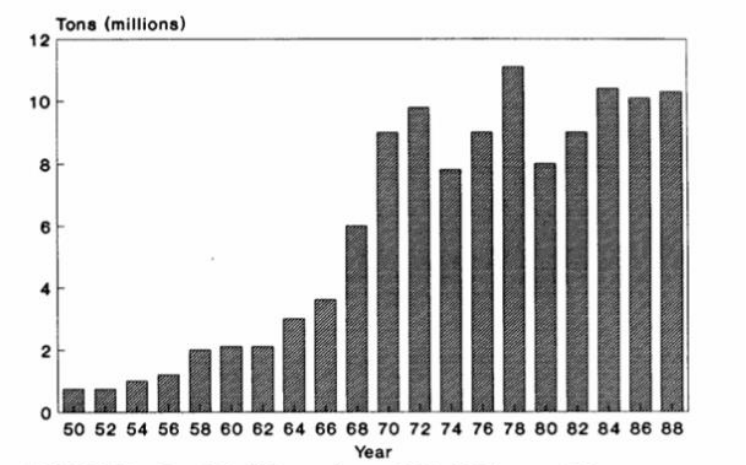

FIGURE 2-1 Trends in highway salt use, 1950–1988 (source: Salt Institute).

Figure 6.24. "Historic Use of Deicing Salts" from the Transportation Research Board Special Report 235.

STUDY AREA 66

LOWER SPANDREL COLUMN

ARCH SPAN 5—SPANDREL COLUMN L—NORTH FACE

Expansion Joint 1918 to 1980 Only

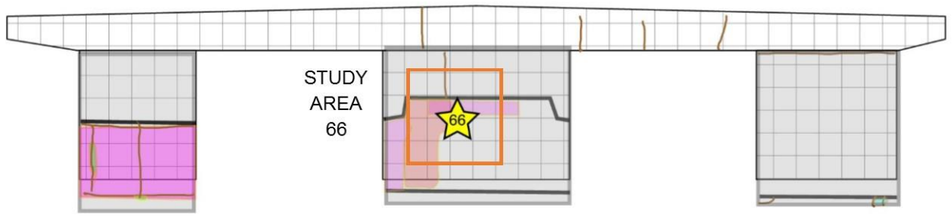

(SEE CONDITION LEGEND IN APPENDIX 2)

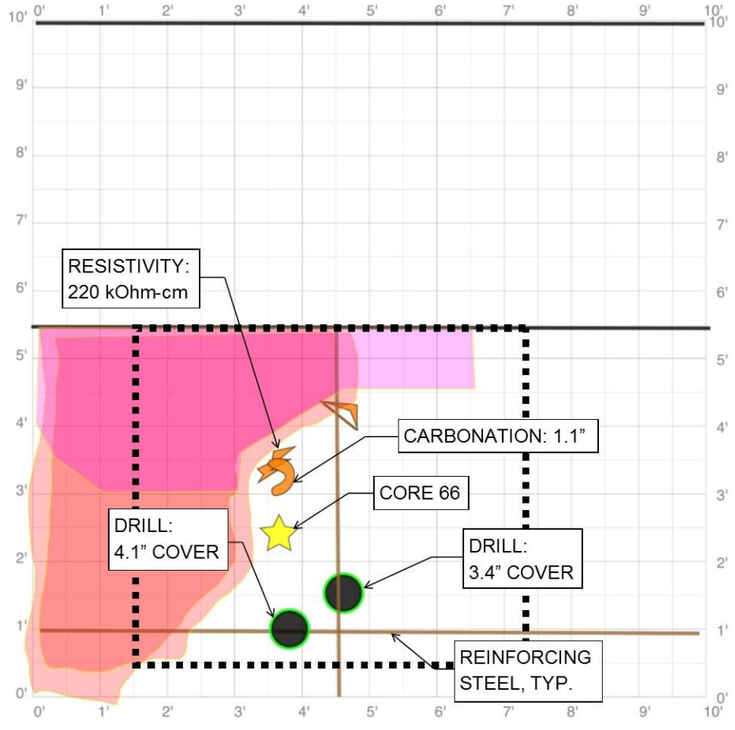

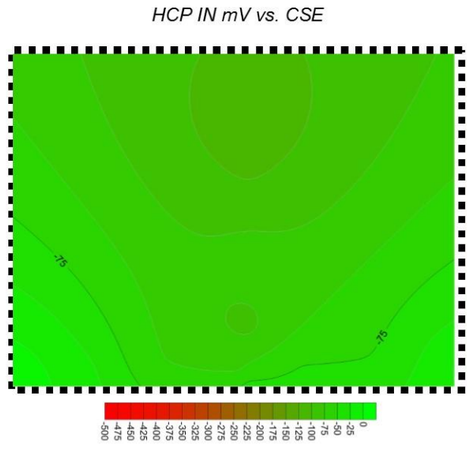

Study Area	Element	Inspection Date	Type	Distress Quantity (%)	Cores Sample(s)	HCP - Avg. (mV vs. CSE)	HCP - Min. (mV vs. CSE)	Resipod - Resistivity Avg. (kOhm-cm)	iCOR - Current Density Avg. (uA/cm^2)	iCOR - Resistivity Avg. (kOhm-cm)	BAC Meter - Current Density Avg. (um/yr)	Cover Vertical Bars - Rep. Minimum (in.)	Cover Horizontal Bars - Rep. Minimum (in.)	Carbonation Avg. (in.)	Deterioration Mechanism(s)
66	Lower Column	7/15/2017	NDE & CORE	10 to 30	66	-92	-165	220	N/A	N/A	1.5	3.4	4.1	1.1	Chloride Exposure; Carbonation

Figure 6.25. Graphical Summary of Testing Data for Study Area 66 - Spandrel Column.

STUDY AREA 79

LOWER SPANDREL WALL

ARCH SPAN 6—SPANDREL COLUMN B—NORTH FACE

Never Expansion Joint

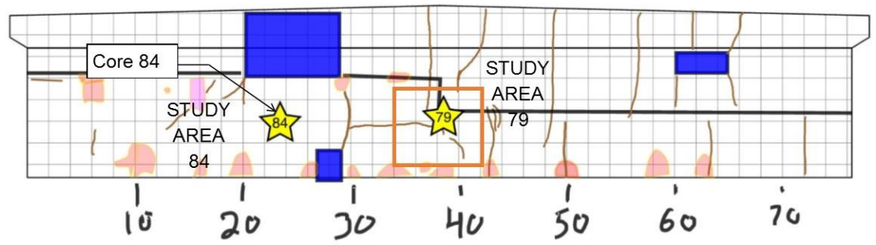

(SEE CONDITION LEGEND IN APPENDIX 2)

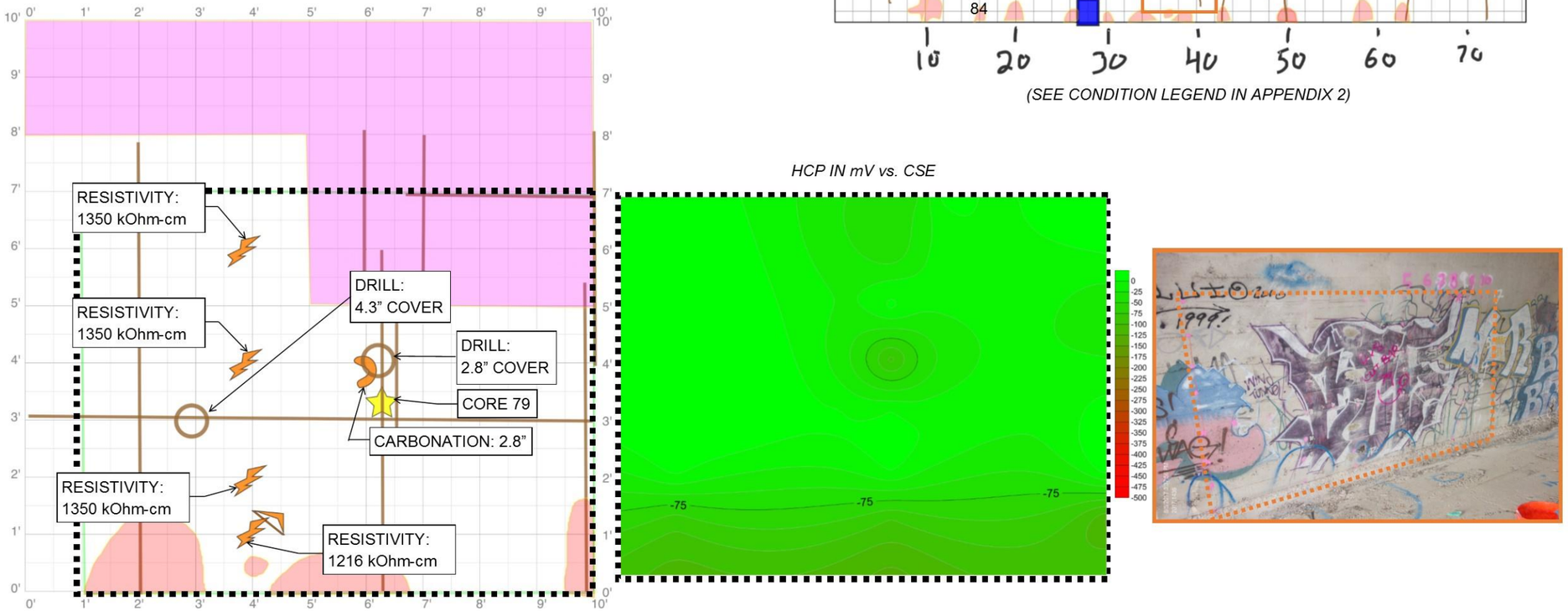

Study Area	Element	Inspection Date	Type	Distress Quantity (%)	Cores Sample(s)	HCP - Avg. (mV vs. CSE)	HCP - Min. (mV vs. CSE)	Resipod - Resistivity Avg. (kOhm-cm)	iCOR - Current Density Avg. (uA/cm^2)	iCOR - Resistivity Avg. (kOhm-cm)	BAC Meter - Current Density Avg. (um/yr)	Cover Vertical Bars - Rep. Minimum (in.)	Cover Horizontal Bars - Rep. Minimum (in.)	Carbonation - Avg. (in.)	Deterioration Mechanism(s)
79	Lower Column	8/5/2017	NDE & CORE	1 to 10	79	-28	-183	1317	N/A	N/A	N/A	2.5	4.3	2.8	Carbonation

Figure 6.26. Graphical Summary of Testing Data for Study Area 79 - Spandrel Wall.

6.2.6. Arch Ribs

The locations of the follow-up testing study areas in the Arch Ribs are shown in Table 6.55.

Table 6.55. Location of Study Areas - Arch Ribs

Location ID	Span	Side of Bridge	Between Columns or Below Column	Below Expansion Joint - Y/N?	Face	Test Type
23	2	Downstream	A	N	Underside	NDE & core
24	2	Downstream	A	N	Downstream Face	Core Only
25	4	Upstream	M	N	Upstream Face	Core Only
26	3	Upstream	E	N	Upstream Face	Core Only
100	2	Upstream	C-D	Y	Topside	NDE & core
100.1	2	Upstream	C-D	Y	Underside	Core Only
101	5	Middle	L-M	N	Topside	NDE & core
102	5	Middle (Upstream)	K-L	Y	Upstream Topside Corner	NDE & core
103	4	Downstream	L-M	N	Downstream Underside Corner	NDE & core
104	1	Upstream	A	Y	Upstream Topside Corner	NDE only
105	3	Upstream	J-K	N	Upstream Underside Corner	NDE only
106	4	Upstream	I-J	Y	Upstream	NDE only
107	5	Downstream	B-C	NA	Underside	NDE only
108	3	Upstream	M-N	NA	Underside	NDE only
119	5	Middle (Upstream)	K-L	Y	Upstream Topside Corner	Ultrasonic Thickness
120	4	Downstream	L-M	N	Downstream Underside Corner	Ultrasonic Thickness
122	3	Downstream	P3-A	Y	Upstream	Ultrasonic Thickness
123	2	Upstream	P2-A	Y	Upstream	Ultrasonic Thickness
124	5	Downstream	N-P6	Y	Downstream	Ultrasonic Thickness
125	5	Upstream	J-K	Y	Upstream Topside Corner	Ultrasonic Thickness
130	5	Upstream	J-K	Y	Upstream Topside Corner	Strain Relief

6.2.6.1. Physical Condition Survey

The condition of the Arch Ribs is summarized in Chapter 4. The conditions were relatively consistent among the fifteen arch ribs, averaging 13 percent distress. The middle rib was typically in better condition, exhibiting 10 percent distress or less; this is likely related to differences in exposure, similar to that discussed for the Lower Spandrel Columns and Walls.

For each of the study areas, the general condition and associated distress are presented in Table 6.56. The distress included spalled concrete and deteriorated repairs at the arch rib corners, cracking on the topside and underside of the ribs along the lines of the Melan truss angles, concrete delaminations, and freeze-thaw distress at the groin and other isolated locations of the arches.

Table 6.56. Condition and Sampling of Study Areas - Arch Ribs

Location ID	Core Samples	Date Inspected	Distress Quantity (%)
23	23	5/24/2017	10 to 30
100	100	8/6/2017	10 to 30
101	101	7/16/2017	< 1
102	102	7/16/2017	> 30
103	103	8/5/2017	10 to 30
104	N/A	7/16/2017	1 to 10
105	N/A	8/6/2017	< 1
106	N/A	8/6/2017	1 to 10
107	N/A	8/5/2017	1 to 10
108	N/A	8/6/2017	< 1

6.2.6.2. Corrosion Survey

Corrosion Potential

Results of half-cell potential surveys are summarized in Table 6.57. The results indicate moderate probability of corrosion, and the corrosion potentials were generally more negative at locations of cracks indicating higher probability of corrosion compared to the surrounding, uncracked concrete.

Table 6.57. HCP Testing Results - Arch Ribs

Location ID	HCP - Avg. (mV vs. CSE)	HCP - Min. (mV vs. CSE)	HCP - Std. Dev. (mV vs. CSE)	Distress Quantity (%)
23	-152	-315	94	10 to 30
100	-258	-354	47	10 to 30
101	-85	-164	32	< 1
102	-140	-210	39	> 30
103	-219	-324	58	10 to 30
104	-300	-448	87	1 to 10
105	-144	-249	45	< 1
106	-278	-371	58	1 to 10
107	-251	-289	33	1 to 10
108	-175	-245	51	< 1

** Thresholds (see 3.4.4.1): > -200mV low, -200 to -350mV moderate, < -350 mV high probability of corrosion*

Resistivity

Results of resistivity testing are provided in Table 6.58. In general, the measured resistivity was high indicating a low rate of corrosion where corrosion has initiated.

Table 6.58. Resistivity Testing Results - Arch Ribs

Location ID	Resipod - Resistivity Avg. (kOhm-cm)	Distress Quantity (%)
23	87	10 to 30
100	31	10 to 30
101	316	< 1
102	506	> 30
103	298	10 to 30
104	162	1 to 10
105	61	< 1
106	50	1 to 10
107	134	1 to 10
108	88	< 1

** Thresholds (see 3.4.4.2): 50-100 low, 10-50 moderate, <10 kOhm-cm high corrosion rates possible in active areas*

Corrosion Rate

Corrosion rate testing was not successful at the arch ribs study areas due to the high cover and atypical configuration of the truss angles.

6.2.6.3. Reinforcement Cover Survey

The results of the reinforcement cover surveys are provided in Table 6.59. The statistical information for this element is summarized in Table 6.60. Concrete cover over the Melan truss angles was variable, and less than 2 inches at one location on the underside of the arch ribs.

Table 6.59. Cover Depth Measurements - Arch Ribs

Location ID	Cover Truss Topside - Avg. (in.)	Cover Truss Topside - Rep. Minimum (in.)	Cover Truss Vertical Face - Avg. (in.)	Cover Truss Vertical Face - Rep. Minimum (in.)	Cover Truss Underside - Avg. (in.)	Cover Truss Underside - Rep. Minimum (in.)	Distress Quantity (%)
23	--	--	--	--	2.5	1.8	10 to 30
100	3.4	2.9	--	--	--	--	10 to 30
101	4.3	3.8	--	--	--	--	< 1
102	3.4	2.8	--	--	--	--	> 30
103	4.8	4.8	5.1	4.1	2.5	2.4	10 to 30
104	4.0	4.0	--	--	--	--	1 to 10
105	--	--	--	--	3.2	2.6	< 1
106	3.9	3.9	--	--	--	--	1 to 10
107	--	--	--	--	3.0	2.6	1 to 10
108	--	--	--	--	3.6	3.3	< 1

Table 6.60. Cover Depth Statistics - Arch Ribs

Value	Cover to Truss Angles Topside of Rib	Cover to Truss Angles Vertical Face of Rib	Cover to Truss Angles Underside of Rib
Average (in.)	3.9	5.1	3.1
Standard Deviation (in.)	0.6	0.5	0.5
Coefficient of Variation	15%	10%	16%
Minimum (in.)	2.8	4.1	1.8
Maximum (in.)	4.9	5.5	4.3

6.2.6.4. Field and Lab Carbonation Tests

Synthesis of field and lab carbonation measurement results are provided in Table 6.61. Carbonation was negligible compared to the depth of the Melan truss angles.

Table 6.61. Carbonation Measurements - Arch Ribs

Location ID	Carbonation - Avg. (in.)	Cover Truss Topside - Rep. Minimum (in.)	Cover Vertical Face - Rep. Minimum (in.)	Cover Truss Underside - Rep. Minimum (in.)	Distress Quantity (%)
23	0.1	--	--	1.8	10 to 30
100	0.3	2.9	--	--	10 to 30
101	0.6	3.8	--	--	< 1
102	0.4	2.8	--	--	> 30
103	0.0	4.8	4.1	2.4	10 to 30
104	0.1	--	4.0	--	1 to 10
105	0.3	--	--	2.6	< 1
106	0.0	3.9	--	--	1 to 10
107	0.0	--	--	2.6	1 to 10
108	0.0	--	--	3.3	< 1

6.2.6.5. Other Tests

Ultrasonic thickness (UT) testing and a strain relief test were completed in the arch ribs.

Ultrasonic Thickness measurements

The results of UT testing are summarized in Table 6.62 and in Appendix 9. Measured section loss in the outermost Melan truss angle legs ranged from negligible to approximately 50 percent. The most severe section loss occurred at the arch spring line below drain outlets at the base of the piers. However, in at least one location near midspan in Span 5, where wide cracks and delaminated concrete was observed, section loss of up to 20 percent was noted.

Table 6.62. Ultrasonic Thickness Test Results at Outermost Melan Truss Angle Legs in Arch Ribs

Study Area ID	Span	Rib*	Location	Comments	Element	Min. Measured Thickness (inches)	Approx. Section Loss (%)
119	5	M	Topside/upstream corner btwn K and L	Wide cracks in concrete leading to steel; exposed steel surfaces have heavy surface corrosion, some rust scale, and localized deep pits.	Horiz. leg	0.463	7.4%
					Vert. leg	0.398	20.4%
120	4	DS	Underside/downstream corner btwn L and M	At delamination.	Horiz. leg	0.455	9.0%
					Vert. leg	0.437	12.6%
122	3	DS	Upstream face at P3	Three truss members exposed underneath drain spout; bottom chord and vert. strut corroded to "knife edge" (i.e., extreme section loss at tip of leg and little section loss near fillet region)	Horiz. leg	0.25**	50.0%**
					Vert. leg	0.35**	30.9%**
123	2	US	Underside/downstream corner btwn P2 and A	Truss fully exposed. Heavy pack rust.	Horiz. leg	0.41	18.0%
					Vert. leg	0.368	26.4%
124	5	DS	Underside/downstream corner btwn N and P6	Underside crack with minor rust staining and patch of poorly consolidated concrete existed at test location	Horiz. leg	0.466	6.8%
					Vert. leg	0.471	5.8%
125	5	M	Topside/upstream corner btwn J and K	At strain relief test location.	Horiz. leg	0.503	~0%
					Vert. leg	0.507	~0%

**DS = downstream, M=middle, and US = Upstream*

***Legs of angles tapered to "knife edge" (i.e., extreme section loss at outer edge and minor section loss near fillet region of angle). Numbers shown indicate approximate average thickness and section loss values across width of leg.*

Strain Relief Testing

The results of the stress relief testing are provided in Appendix 9 and are summarized in Table 6.63. The location of the field testing was selected in coordination with HNTB at the upstream, topside corner of the Span 5 middle arch rib, between spandrel columns J and K. Testing indicated that the stress relieved after cutting, including any effects of residual stresses, was 16.5 ksi of compression. Similar testing was performed in WJE's laboratory (mock-up test) and the results indicated 2.9 ksi of tension was relieved after cutting, which is a measure of the residual stress in the angle leg used in the mock-up test.

Table 6.63. Results of Strain Relief Testing in Laboratory Mock-up and Field Tests

	Measured Strain Change			Calculated Longitudinal Stress Before Cutting (ksi)
	45 Degree (με)	Transverse (με)	Longitudinal (με)	
Mock-Up Test	9	67	-101	-2.9 (disc in tension before cutting)
Field Test	281	-121	568	16.5 (disc in compression before cutting)

6.2.6.6. Chloride Profile Analysis

Chloride profiles for several core samples extracted from the arch ribs are shown in Figure 6.27. The results indicate that chloride diffusion is occurring on both the topside and underside of the arch ribs. Chloride ingress is being facilitated by cracks, which ranged in width from less than 5 mils (i.e., Core 101) to 50 mils (Core 100.1). In all cases, chlorides have diffused to levels expected to cause corrosion within the upper 2 to 3 inches of the arch ribs, which is more than the minimum cover depths but less than the average cover depths. Note that the cited cover depths are in reference to the Melan truss angles.

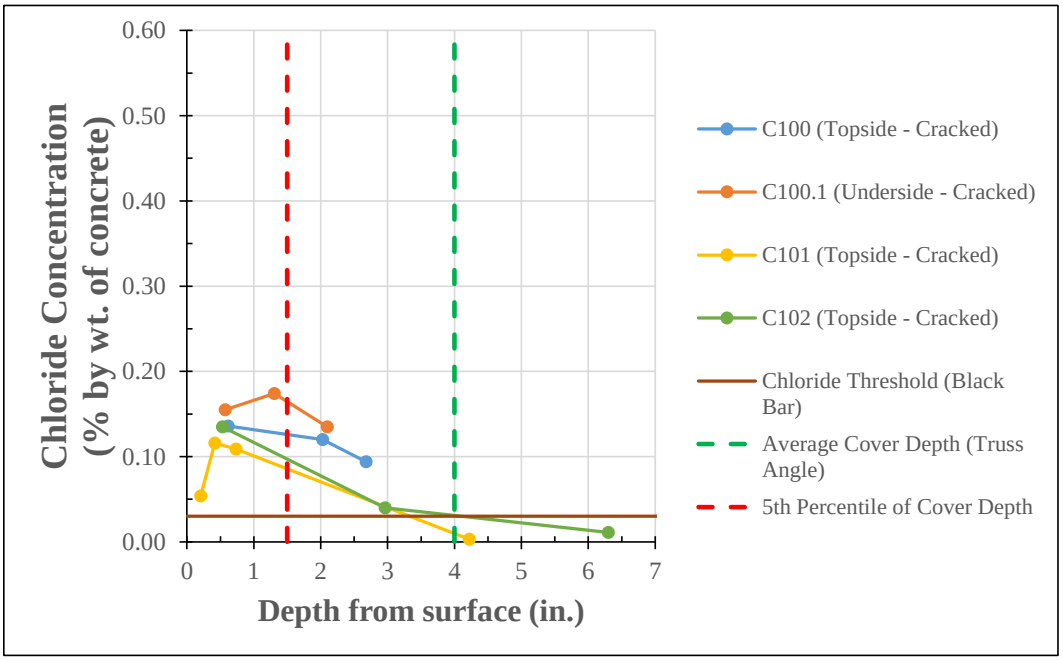

Figure 6.27. Chloride profiles for Arch Rib cores compared to chloride threshold for corrosion initiation and reinforcement cover depth measurements.

6.2.6.7. Petrographic Analysis

The arch rib concrete is characterized by Mixture 1B - 1918: 1 to 2 inch Basalt. Sample 102 was selected for limited petrographic analysis. There was no evidence of freeze-thaw distress or ASR in the core sample, and carbonation was approximately 0.5 inches.

6.2.6.8. Interpretation

The primary deterioration mechanism in the arch ribs is chloride-induced corrosion, especially at locations of cracks over the Melan truss angles. Based on the visual inspection, freeze-thaw damage is a contributing factor in areas subject to water saturation, such as at the arch rib groins and near drain outfalls. No freeze-thaw damage was identified in the core selected for petrographic analysis from the arch ribs, although a

core from the spring line of a barrel arch showed significant depth of freeze-thaw damage. Deep erosion was also measured below drain outfalls (see Table 4.3).

UT measurements indicate section loss is generally minor, but in isolated areas of delamination and spalling is as high as 20 to 50 percent of the outstanding angle leg.

Measured carbonation depths were negligible and there was no evidence of distress from freeze-thaw or ASR in the core examined; however, numerous areas of freeze-thaw damage were observed during the visual inspection, and given the lack of air entrainment, freeze-thaw distress should be expected to occur at areas of the arch ribs exposed to moisture and freeze-thawing cycles (e.g., near drains).

The shotcrete repairs were largely sound and generally not subject to an on-going deterioration mechanisms. Where deterioration of the patches is occurring, the distress appears to be mainly characterized by map cracking and/or debonding of the interface with the original concrete at the perimeter of the repairs.

A graphical representation of the follow-up testing in the arch ribs is provided in Figure 6.28 and Figure 6.29 as well as Appendix 14. In the areas surveyed (i.e., Study Area 102 - Topside/Corner and Study Area 105 - Underside), chloride-induced corrosion appears to be the controlling deterioration mechanism; while other areas of the arch rib exhibited freeze-thaw deterioration.

STUDY AREA 102

ARCH RIB

ARCH SPAN 5—TOPSIDE CORNER

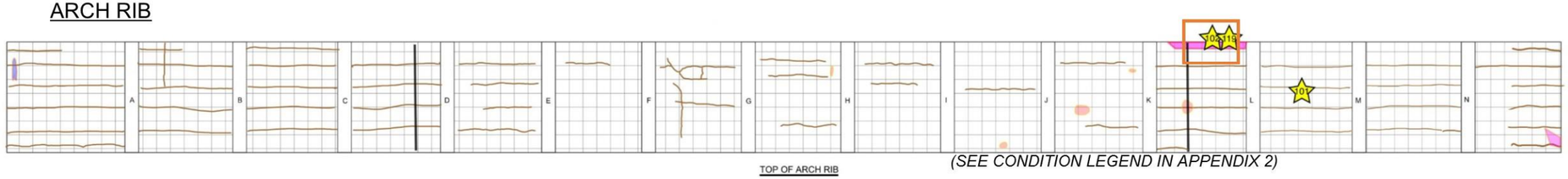

(SEE CONDITION LEGEND IN APPENDIX 2)

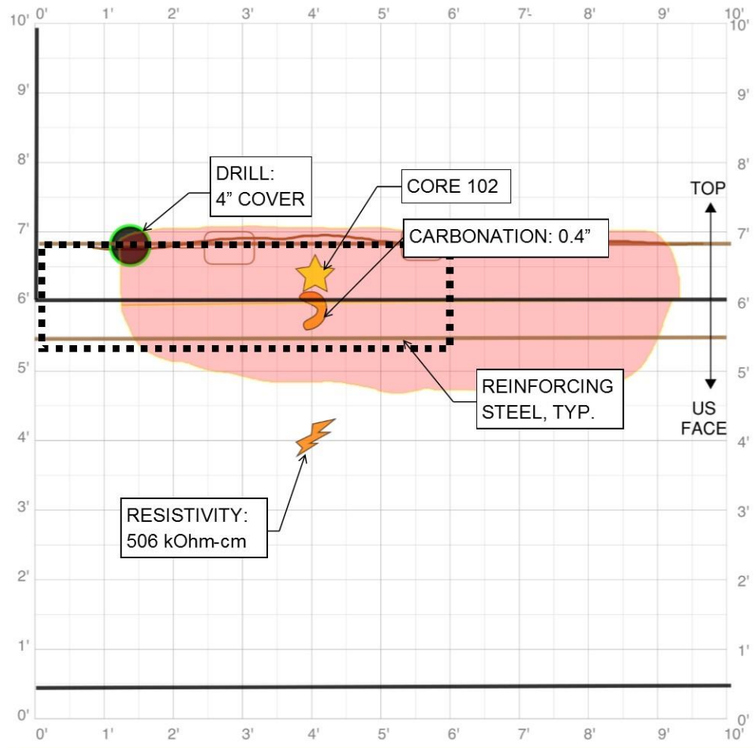

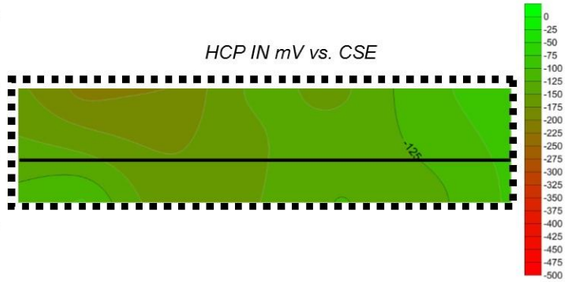

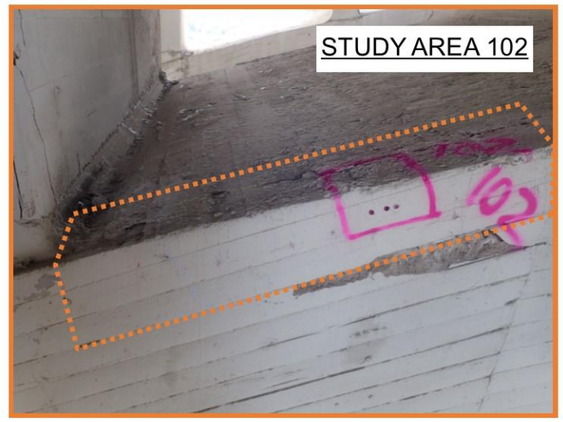

Study Area	Element	Inspection Date	Type	Distress Quantity (%)	Cores Sample(s)	HCP - Avg. (mV vs. CSE)	HCP - Min. (mV vs. CSE)	Resipod - Resistivity Avg. (kOhm-cm)	iCOR - Current Density Avg. (uA/cm^2)	iCOR - Resistivity Avg. (kOhm-cm)	BAC Meter - Current Density Avg. (um/yr)	Cover Truss Topside - Rep. Minimum (in.)	Cover Vertical Face - Rep. Minimum (in.)	Cover Truss Underside - Rep. Minimum (in.)	Carbonation Avg. (in.)	Deterioration Mechanism(s)
102	Arch Rib	7/16/2017	NDE & CORE	> 30	102	-140	-210	506	N/A	N/A	N/A	2.8	N/A	N/A	0.4	Chloride Exposure

Figure 6.28. Graphical Summary of Testing Data for Study Area 102 - Arch Rib.

STUDY AREA 105

ARCH RIB

ARCH SPAN 3—UNDERSIDE

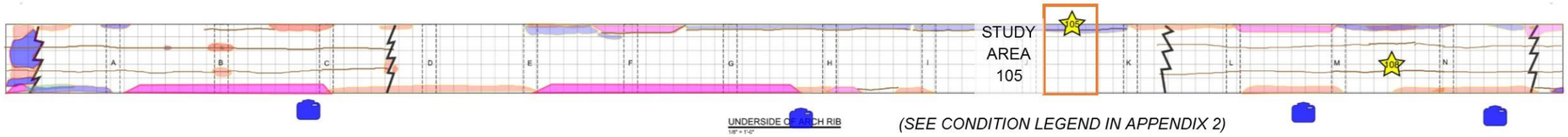

(SEE CONDITION LEGEND IN APPENDIX 2)

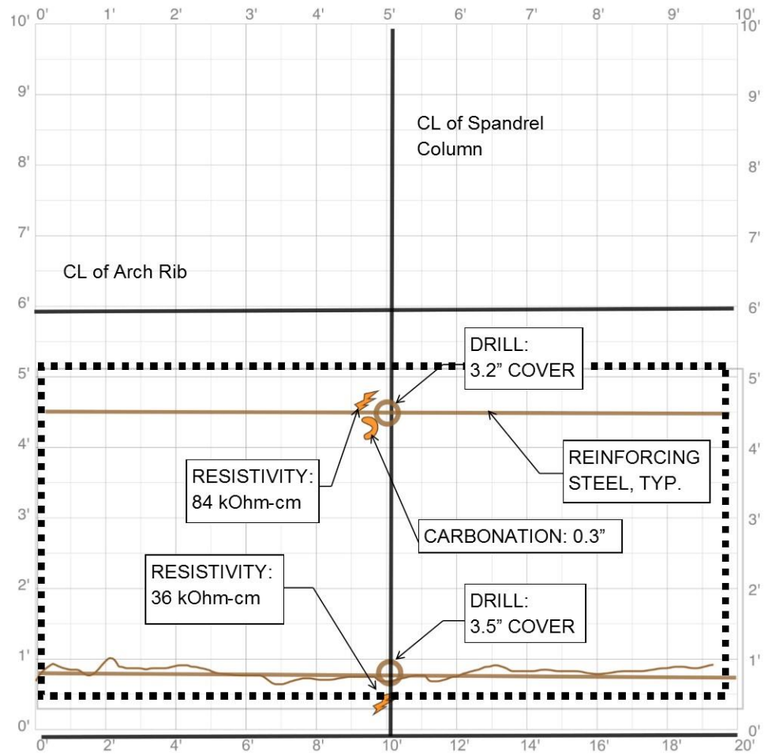

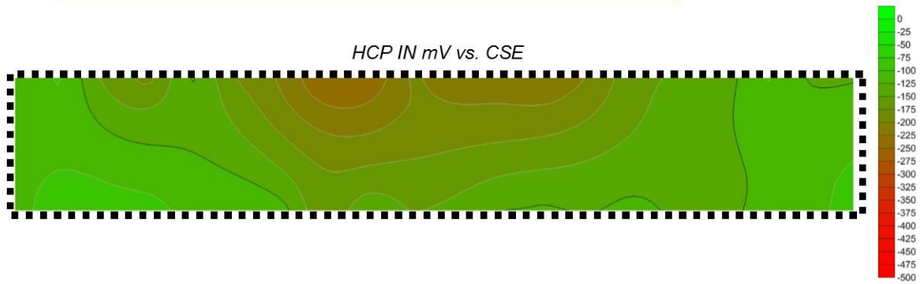

Study Area	Element	Inspection Date	Type	Distress Quantity (%)	Cores Sample(s)	HCP - Avg. (mV vs. CSE)	HCP - Min. (mV vs. CSE)	Resipod - Resistivity Avg. (kOhm-cm)	iCOR - Current Density Avg. (uA/cm^2)	iCOR - Resistivity Avg. (kOhm-cm)	BAC Meter - Current Density Avg. (um/yr)	Cover Truss Topside - Rep. Minimum (in.)	Cover Vertical Face - Rep. Minimum (in.)	Cover Truss Underside - Rep. Minimum (in.)	Carbonation Avg. (in.)	Deterioration Mechanism(s)
105	Arch Rib	8/6/2017	NDE ONLY	< 1	--	-144	-249	61	N/A	N/A	N/A	N/A	N/A	2.6	0.3	Chloride Exposure

Figure 6.29. Graphical Summary of Testing Data for Study Area 105 - Arch Rib.

6.2.7. Barrel Arches

The location of the follow-up testing study areas in the Barrel Arches are shown in Table 6.64.

Table 6.64. Location of Study Areas - Barrel Arches

Location ID	Span	Side of Bridge	Between Columns or Below Column	Below Expansion Joint - Y/N?	Face	Test Type
19	7	Downstream	J	N	Underside	NDE & core
20	7	Middle	J-P8	Y	Topside	NDE & core
21	7	Middle	J-P8	Y	Topside	Core Only
22	6	Downstream	A	Y	Downstream	NDE & core
57	6	Middle	A-B	N	Topside	NDE & core
121	6	Downstream	J-P7	Y	Downstream	UT

6.2.7.1. Physical Condition Survey

The condition of the Barrel Arches is summarized in Chapter 4. In general the conditions were consistent among the two Barrel Arches, averaging 13 percent distress.

For each of the study areas, the local distress quantity is presented in Table 6.65. The distress included cracking on the topside and underside of the ribs, concrete delaminations, freeze-thaw distress at the groin of the arches, and spalled concrete and deteriorated repairs at the corners.

Table 6.65. Condition and Sampling of Study Areas - Barrel Arches

Location ID	Core Samples	Date Inspected	Distress Quantity (%)
19	19	5/25/2017	1 to 10
20	20/21	5/23/2017	1 to 10
22	22	5/25/2017	< 1
57	57	5/23/2017	1 to 10

6.2.7.2. Corrosion Survey

Corrosion Potential

Results of half-cell potential surveys are summarized in Table 6.66. The results indicate moderate probability of corrosion, and the corrosion potentials were generally more negative at locations of cracks indicating higher probability of corrosion compared to the surrounding, uncracked concrete.

Table 6.66. HCP Testing Results - Barrel Arches

Location ID	HCP - Avg. (mV vs. CSE)	HCP - Min. (mV vs. CSE)	HCP - Std. Dev. (mV vs. CSE)	Distress Quantity (%)
19	-161	-234	36	1 to 10
20	-179	-397	58	1 to 10
22	--	--	--	< 1
57	-212	-316	68	1 to 10

** Thresholds (see 3.4.4.1): > -200mV low, -200 to -350mV moderate, < -350 mV high probability of corrosion*

Resistivity

Results of resistivity testing are provided in Table 6.67. The high resistivity would suggest that corrosion rate would be low where corrosion has initiated.

Table 6.67. Resistivity Testing Results - Barrel Arches

Location ID	Resipod - Resistivity Avg. (kOhm-cm)	Distress Quantity (%)
19	155	1 to 10
20	--	1 to 10
22	--	< 1
57	--	1 to 10

** Thresholds (see 3.4.4.2): 50-100 low, 10-50 moderate, <10 kOhm-cm high corrosion rates possible in active areas*

Corrosion Rate

Corrosion rate testing was not successful at the Barrel Arch study areas due to the high cover and atypical configuration of the truss angles.

6.2.7.3. Reinforcement Cover Survey

The results of the reinforcement cover surveys are provided in Table 6.68. The statistical information for this element is summarized in Table 6.69. Concrete cover over the Melan truss angles was generally variable and as low as 1.4 inch on the topside of the Barrel Arches. Cover was highest near the arch spring line, as represented by Location 22.

Table 6.68. Cover Depth Measurements - Barrel Arches

Location ID	Cover Truss Topside - Avg. (in.)	Cover Truss Topside - Rep. Minimum (in.)	Cover Truss Vertical Face - Avg. (in.)	Cover Vertical Face - Rep. Minimum (in.)	Cover Truss Underside - Avg. (in.)	Cover Truss Underside - Rep. Minimum (in.)	Distress Quantity (%)
19	--	--	--	--	8.6	7.7	1 to 10
20	3.1	1.4	--	--	--	--	1 to 10
22	--	--	9.0	8.6	--	--	< 1
57	5.0	3.7	--	--	--	--	1 to 10

Table 6.69. Cover Depth Statistics - Barrel Arches

Value	Cover to Truss Angles Topside of Rib	Cover to Truss Angles Vertical Face of Rib	Cover to Truss Angles Underside of Rib
Average (in.)	4.0	9.0	8.6
Standard Deviation (in.)	1.6	0.3	0.6
Coefficient of Variation	39%	4%	7%
Minimum (in.)	1.4	8.6	7.7
Maximum (in.)	8.0	9.4	9.3

** Values influenced by deep measurements at arch spring line region.*

6.2.7.4. Field and Lab Carbonation Tests

Synthesis of field and lab carbonation measurement results are provided in Table 6.70. Carbonation was negligible compared to the depth of the Melan truss angles.

Table 6.70. Carbonation Measurements - Barrel Arches

Location ID	Carbonation - Rep. Maximum (in.)	*Cover Truss Topside - Rep. Minimum (in.)*	*Cover Vertical Face - Rep. Minimum (in.)*	*Cover Truss Underside - Rep. Minimum (in.)*	*Distress Quantity (%)*
19	0.2	--	--	*7.7*	1 to 10
20	0.2	*1.4*	--	--	1 to 10
22	0.4	--	*8.6*	--	< 1
57	0.5	*3.7*	--	--	1 to 10

6.2.7.5. Other Tests

Ultrasonic thickness (UT) testing was completed in the Barrel Arches.

Ultrasonic Thickness measurements

The results of UT testing are summarized in Table 6.71. Between 14 and 23 percent section loss to the outermost Melan truss angle leg was observed at the study area in Span 6, where the truss had been exposed through freeze-thaw deterioration.

Table 6.71. Ultrasonic Thickness Test Results at Outermost Melan Truss Angle Legs - Barrel Arches

Study Area ID	Span	Rib	Location	Comments	Element	Min. Measured Thickness (in.)	Approx. Section Loss (%)
121	6	BA	Topside/downstream corner btwn J and P7	Truss fully exposed. Heavy pack rust.	Horiz. leg	0.322	14.1%
					Vert. leg	0.29	22.7%

6.2.7.6. Chloride Profile Analysis

Chloride profiles for core extracted from the Barrel Arches are shown in Figure 6.30. These results are similar to those observed in the arch ribs (see Section 6.2.6), indicating chlorides are penetrating to the truss members at cracks. Chloride ingress is being facilitated by cracks, ranging from 5 mils to 50 mils (15 mils in Core 57). Note that the cited cover depths are in reference to the Melan truss angles.

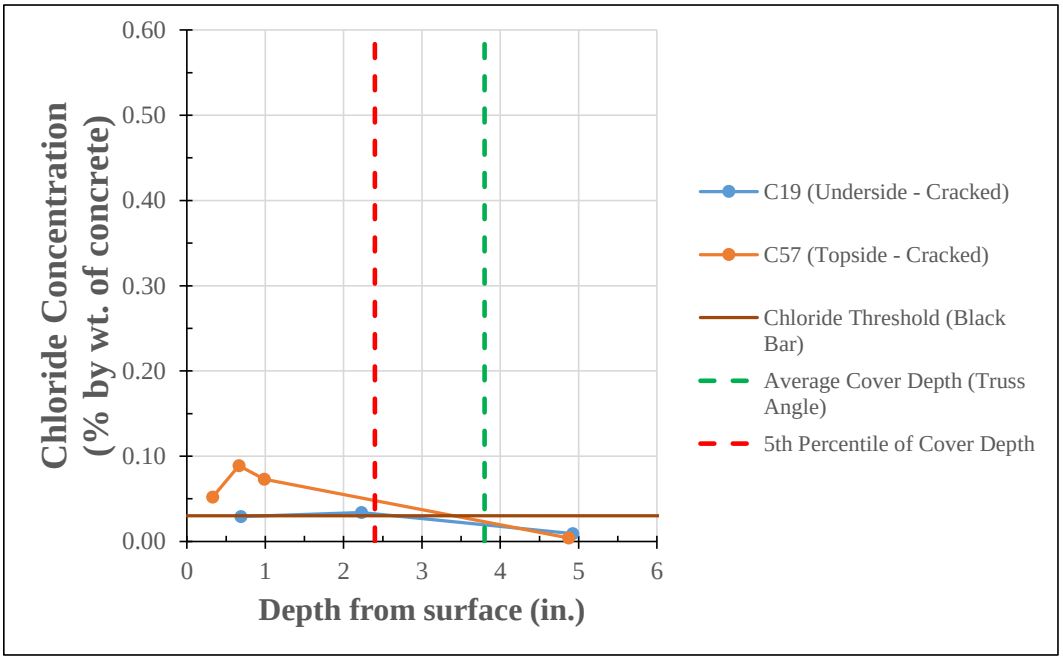

Figure 6.30. Chloride profiles for Barrel Arches cores compared to chloride threshold.

6.2.7.7. Petrographic Analysis

The Barrel Arch concrete is characterized by Mixture 1B - 1918: 1 to 2 inch Basalt. Core 21 was selected for limited petrographic analysis, and Core 22 was evaluated for freeze-distress. The results are summarized in Table 6.72. Freeze-thaw distress was observed in Core 22, and the distress was severe in the upper 4 inches and less severe (but present) through approximately 9 inches. There was no evidence of other deleterious distress (e.g., ASR).

Table 6.72. Measured Depth of Freeze-Thaw Distress - Barrel Arches

Core ID	Depth of Severe Freeze-Thaw Distress, inches	Maximum Depth of Freeze-Thaw Distress, inches
21	--	None obs.
22	4.5	9.5

Note: Depth values reported here include measured surface erosion at core location

6.2.7.8. Interpretation

The primary deterioration mechanism in the Barrel Arches is chloride-induced corrosion, especially at locations of cracks above the Melan truss angles. Freeze-thaw is also a contributing factor and was observed in one core sample; given the lack of air entrainment, freeze-thaw distress may occur at areas of the Barrel Arches exposed to moisture and freeze-thawing cycles (e.g., near drains). UT measurements indicate section loss in the outermost Melan truss angle leg at isolated exposed spall locations as high as 23 percent. Carbonation was negligible and there was no evidence of distress from ASR.

The shotcrete repairs were largely sound and generally not subject to any on-going deterioration mechanisms. Where deterioration of the patches is occurring, the distress appears to be mainly characterized by map cracking and/or debonding of the interface with the original concrete of the perimeter at the repairs.

A graphical representation of the follow-up testing in the Barrel Arches is provided in Figure 6.31 and in Appendix 14. In the area surveyed (i.e., Study Area 57 - Topside), chloride-induced corrosion appears to be the controlling deterioration mechanism, and areas of identified distress correlate with corrosion activity as measured with HCP testing.

STUDY AREA 57

BARREL ARCH

ARCH SPAN 6—TOPSIDE

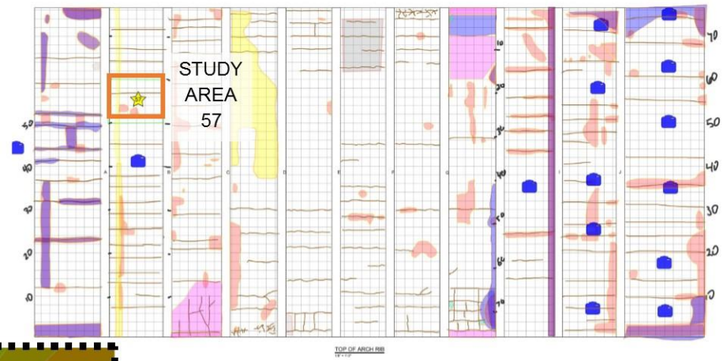

(SEE CONDITION LEGEND IN APPENDIX 2)

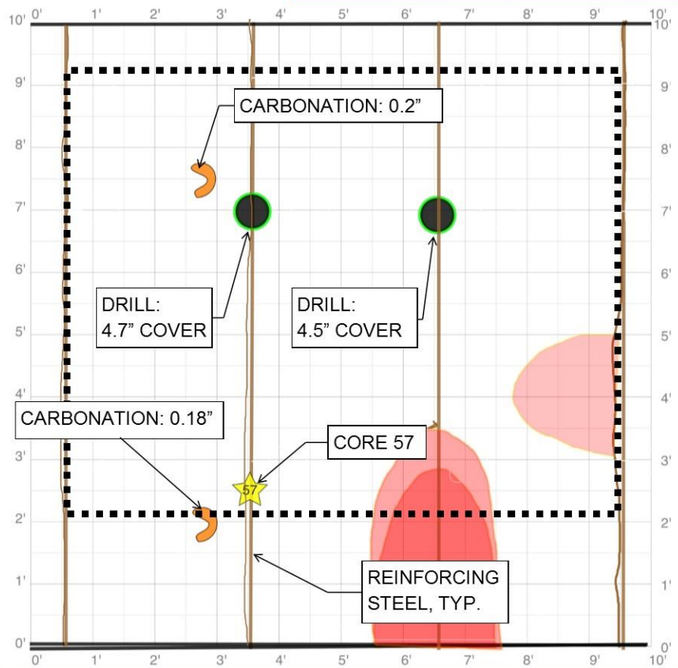

HCP IN mV vs. CSE

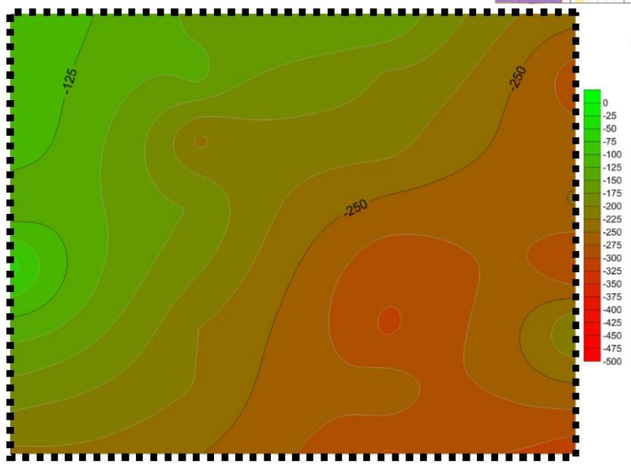

Study Area	Element	Inspection Date	Type	Distress Quantity (%)	Cores Sample(s)	HCP - Avg. (mV vs. CSE)	HCP - Min. (mV vs. CSE)	Resipod - Resistivity Avg. (kOhm-cm)	iCOR - Current Density Avg. (uA/cm^2)	iCOR - Resistivity Avg. (kOhm-cm)	BAC Meter - Current Density Avg. (um/yr)	Cover Truss Topside - Rep. Minimum (in.)	Cover Vertical Face - Rep. Minimum (in.)	Cover Truss Underside - Rep. Minimum (in.)	Carbonation Avg. (in.)	Deterioration Mechanism(s)
57	Barrel Arch	5/23/2017	NDE & CORE	1 to 10	57	-212	-316	N/A	N/A	N/A	N/A	3.7	N/A	N/A	0.2	Chloride Exposure

Figure 6.31. Graphical Summary of Testing Data for Study Area 57 - Barrel Arch.

6.2.8. Arch Pier Walls

The locations of the follow-up testing study areas and material sampling locations in the Arch Pier Walls are shown in Table 6.73. Note that the cap beams at the top of the Arch Pier Walls were constructed in 1980 and can be expected to perform similarly to the Upper Spandrel Columns and Walls (1980 Construction) of similar joint condition; see relevant discussion above.

Table 6.73. Location of Study Areas - Arch Pier Walls

Location ID	Pier No.	Side of Bridge	Pier Face (Interior/Exterior)	Face	Test Type
1	1	Upstream	Exterior	South	NDE & core
2	1	Upstream	Exterior	South	Core only
3	1	Upstream	Exterior	South	Core only
6	3	Downstream	Exterior	North	NDE & core
7	4	Downstream	Exterior	North	Core only
8	4	Downstream	Exterior	North	NDE & core
9	4	Downstream	Exterior	North	Core only
10	5	Upstream	Exterior	North	NDE & core
11	5	Upstream	Exterior	North	Core only
12	6	Middle	Interior	Upstream	NDE & core
13	6	Middle	Interior	Upstream	Core only
14	7	Upstream	Exterior	South	NDE & core
15	7	Upstream	Exterior	South	Core only
16	8	Middle	Interior	Upstream	NDE & core
17	8	Middle	Interior	Upstream	Core only
18	2	Downstream	Exterior	South	Core only
87	1	Upstream	Exterior	North	NDE only
114	8	Upstream	Interior	-	Bar Sample
115	8	Upstream	Interior	-	Bar Sample

6.2.8.1. Physical Condition Survey

The condition of the Arch Pier Walls is summarized in Chapter 4. In general the conditions were consistent among the eight Arch Pier Walls, averaging 3 percent distress on the interior and 4 percent distress on the exterior surfaces. However, Arch Piers 1 and 8 exhibited higher quantities of distress (10 percent average), particularly at the approach-side faces due to exposure from the deck joints above.

For each of the study areas, the local distress quantity is presented in Table 6.74. Typical distress included cracking and delaminations, and some locations of freeze-thaw distress.

Table 6.74. Condition and Sampling of Study Areas - Arch Pier Walls

Location ID	Core Samples	Date Inspected	Distress Quantity (%)
1	1 & 3	5/22/2017	1 to 10
6	6	5/24/2017	> 30
8	8 & 9	5/24/2017	>30
10	10 & 11	5/22/2017	1 to 10
12	12 & 13	5/23/2017	1 to 10
14	14 & 15	5/22/2017	< 1
16	16 & 17	5/25/2017	> 30
87	--	7/16/2017	1 to 10

6.2.8.2. Corrosion Survey

Corrosion Potential

Results of half-cell potential surveys are summarized in Table 6.75. The risk for corrosion varies by study area and appears to correlate with the observed physical condition. Study Area 16 has a high probability of corrosion through most of the area surveyed, and Study Areas 6, 8, and 12 have high probability of corrosion over portions of the area surveyed. Study Areas 1, 10, 14, and 87 have moderate to low probabilities for corrosion.

Table 6.75. HCP Testing Results - Arch Pier Walls

Location ID	HCP - Avg. (mV vs. CSE)	HCP - Min. (mV vs. CSE)	HCP - Std. Dev. (mV vs. CSE)	Distress Quantity (%)
1	-41	-136	43	1 to 10
6	-151	-347	57	> 30
8	-215	-329	93	>30
10	0	-49	28	1 to 10
12	-265	-367	59	1 to 10
14	-24	-60	26	< 1
16	-436	-500	40	> 30
87	-168	-251	41	1 to 10

** Thresholds (see 3.4.4.1): > -200mV low, -200 to -350mV moderate, < -350 mV high probability of corrosion*

Resistivity

Results of resistivity testing are provided in Table 6.76. Study Areas 6 and 16 had the lowest measured resistivity values (56 and 11 kOhm-cm, respectively), indicating a low and moderate corrosion rate, respectively, where corrosion has initiated. Areas 1 and 87 had a higher resistivity values (92 and 228

kOhm-cm, respectively), indicating corrosion rate is low to negligible where corrosion has initiated in these areas.

Table 6.76. Resistivity Testing Results - Arch Pier Walls

Location ID	Resipod - Resistivity Avg. (kOhm-cm)	iCOR - Resistivity Avg. (kOhm-cm)	Distress Quantity (%)
1	--	92	1 to 10
6	51	--	> 30
8	--	--	>30
10	--	--	1 to 10
12	--	--	1 to 10
14	--	--	< 1
16	11	--	> 30
87	228	--	1 to 10

** Thresholds (see 3.4.4.2): 50-100 low, 10-50 moderate, <10 kOhm-cm high corrosion rates possible in active areas*

Corrosion Rate

Corrosion rate testing results are provided in Table 6.77. Testing was attempted in most study areas; however, meaningful results were only obtained in Study Areas 1 and 87. The results indicate low rates of corrosion in the areas where tests were successful; however tests were not successful in some areas where corrosion-related distress was prevalent.

Table 6.77. Corrosion Rate Testing Results - Arch Pier Walls

Location ID	iCOR - Current Density Avg. (uA/cm^2) *	BAC Meter - Current Density Avg. (um/yr) †	Distress Quantity (%)
1	1.0	--	1 to 10
6	--	--	> 30
8	--	--	>30
10	--	--	1 to 10
12	--	--	1 to 10
14	--	--	< 1
16	--	--	> 30
87	--	1.1	1 to 10

** Thresholds (see 3.4.4.3): <1 low, 1-3 moderate, 3-10 high, >10 severe uA/cm2 instantaneous corrosion rate*
† Thresholds (see 3.4.4.3): <10 low, 10-30 moderate, 30-100 high, >100 um/yr severe instantaneous corrosion rate.

6.2.8.3. Reinforcement Cover Survey

The results of the reinforcement cover surveys are provided in Table 6.78, and the statistical information for this element type is summarized in Table 6.79. The cover depth to the reinforcement was highly variable for a given study area, and for the arch pier elements as a whole. The measured cover was less 1.5 inches at some locations. Typically bars were found in the Arch Pier Walls spaced at approximately 4 feet, and it was not uncommon for high variation in cover depth of both the horizontal and vertical bars; these observations are similar to the reinforcement patterns identified in the Lower Spandrel Columns.

Table 6.78. Cover Depth Measurements - Arch Pier Walls

Location ID	Cover Vertical Bars - Avg. (in.)	Cover Vertical Bars - Rep. Minimum (in.)	Cover Horizontal Bars - Avg. (in.)	Cover Horizontal Bars - Rep. Minimum (in.)	Distress Quantity (%)
1	1.5	1.2	2.5	2.2	1 to 10
6	3.5	2.8	3.6	2.1	> 30
8	4.4	2.9	5.4	4.0	>30
10	2.3	1.7	3.9	3.7	1 to 10
12	2.5	1.3	3.4	2.0	1 to 10
14	3.7	3.0	4.3	4.1	< 1
16	2.5	1.7	3.6	2.9	> 30
87	3.5	3.5	3.0	3.0	1 to 10

Table 6.79. Cover Depth Statistics - Arch Pier Walls

Value	Cover Vertical Bar	Cover Horizontal Bar
Average (in.)	3.0	3.9
Standard Deviation (in.)	1.4	1.3
Coefficient of Variation	45%	35%
Minimum (in.)	1.1	1.8
Maximum (in.)	6.6	7.3

6.2.8.4. Field and Lab Carbonation Tests

Synthesis of field and lab carbonation measurement results are provided in Table 6.80, including the representative minimum cover depths to the reinforcing steel in each of the study areas. Average carbonation depth varied widely from 0.1 to 2.3 inches with an average of 1.0 inch. In two areas, the carbonation depth was 2 inches or more, which is greater than the cover depth in four of the eight study areas.

Table 6.80. Carbonation Measurements - Arch Pier Walls

Location ID	Carbonation - Rep. Maximum (in.)	Cover Vertical Bars - Rep. Minimum (in.)	Cover Horizontal Bars - Rep. Minimum (in.)	Distress Quantity (%)
1	0.6	1.2	2.2	1 to 10
6	1.4	2.8	2.1	> 30
8	2.5	2.9	4.0	>30
10	2.0	1.7	3.7	1 to 10
12	1.5	1.3	2.0	1 to 10
14	1.6	3.0	4.1	< 1
16	0.9	1.7	2.9	> 30
87	0.1	3.5	3.0	1 to 10

6.2.8.5. Other Tests

No other tests were conducted in this element category.

6.2.8.6. Chloride Profile Analysis

The results of the chloride analyses of cores extracted from the Arch Pier Walls are shown in Figure 6.32. Chloride diffusion due to surface driven chloride exposure is occurring in the arch piers; however, other factors that are unclear may be contributing to the observed chloride profiles. Cores C1 and C14 exhibited typical surface driven chloride exposure with elevated chloride concentrations in the outer portions of the core, and decreasing with depth. Cores 6, 8, 10, and 12 exhibited peak chloride concentrations at depth of about 2 inches or more, which is not typical of a consistent surface exposure. At approximately half of the studied locations (where cover is less than average), there is potential for chloride concentrations nears the depth of reinforcement to have accumulated to concentrations necessary for initiation of corrosion.

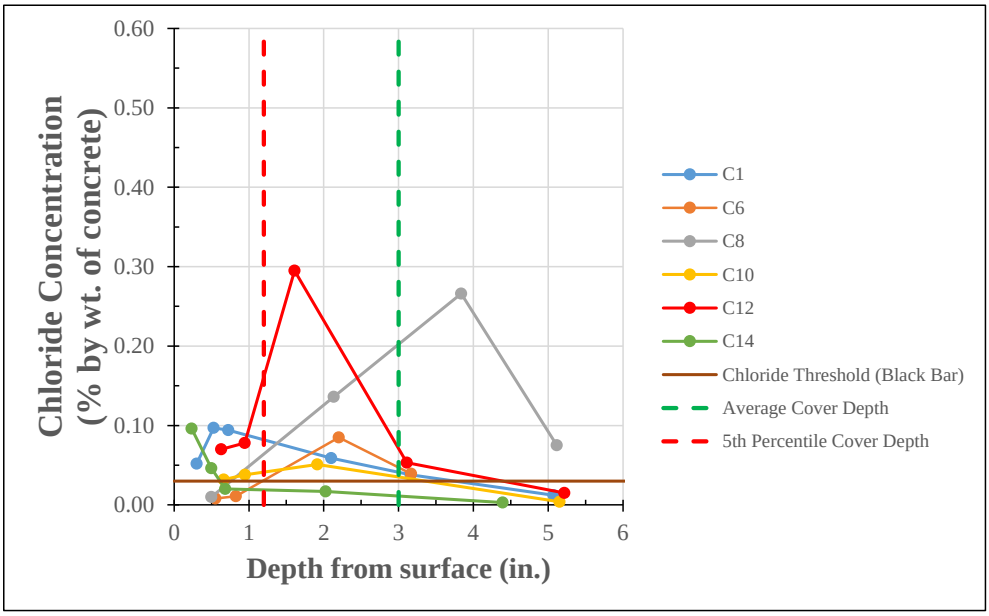

Figure 6.32. Chloride profiles for arch pier cores compared to chloride threshold.

6.2.8.7. Petrographic Analysis

Cores 10 and 12 were selected for in-depth petrographic studies. Core 10 was comprised of Concrete Mixture 1A - 1918: 2 inch Basalt. There was no evidence of deleterious chemical reactions related to aggregates or paste, nor was distress caused by cyclic freeze-thaw observed. Core 12 was comprised of Concrete Mixture 2 - Pre-1980s: 3/4 inch Gravel, and similarly no evidence of materials-related distress or freeze-thaw damage was observed.

6.2.8.8. Interpretation

Based on the field testing and laboratory analysis performed for areas of the Arch Pier Walls, the primary deterioration mechanisms appear to be carbonation- and chloride-induced corrosion. Freeze-thaw distress in local areas near drains or other areas of high moisture exposure or saturation is a contributing cause. At areas of low concrete cover, the carbonation front may have reached the depth of reinforcing causing depassivation and promoting corrosion activity or corrosion-related damage. Chloride exposure may also be affecting portions of the structure; while typical surface driven exposure was not identified in some of the cores from the Arch Pier Walls, most cores showed elevated chloride concentration in the outer 2 to 3 inches. There was no evidence of other distress mechanisms (e.g., ASR) which may affect future performance of the Arch Piers Walls.

A graphical representation of the follow-up testing in the Arch Pier Walls is provided in Figure 6.33 and in Appendix 14. In the area surveyed (i.e., Study Area 1), chloride-induced corrosion appears to be the controlling deterioration mechanism; while other areas of the Arch Pier Walls exhibited carbonation-induced corrosion and freeze-thaw deterioration.

STUDY AREA 1

ARCH PIER WALL

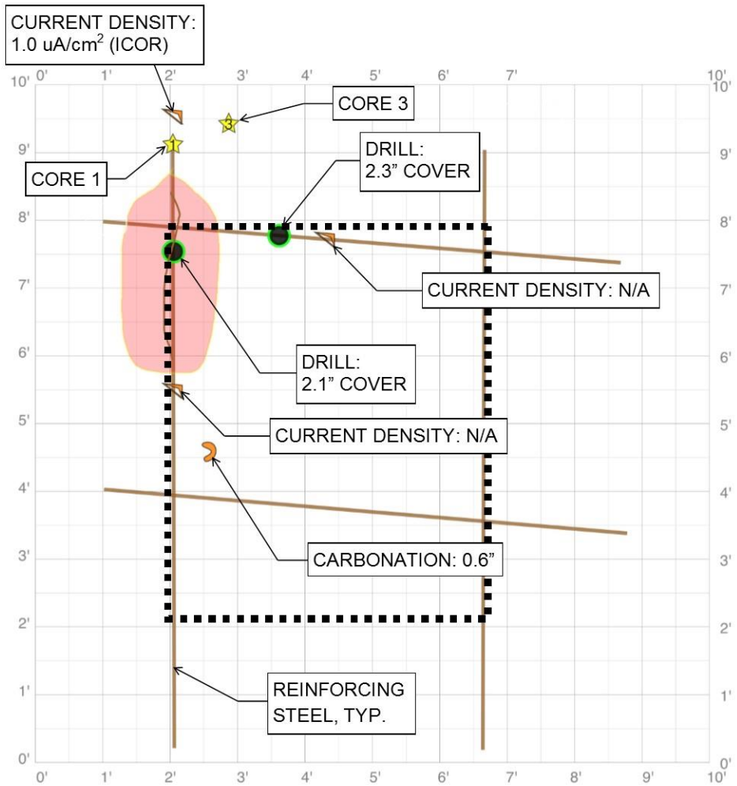

HCP IN mV vs. CSE

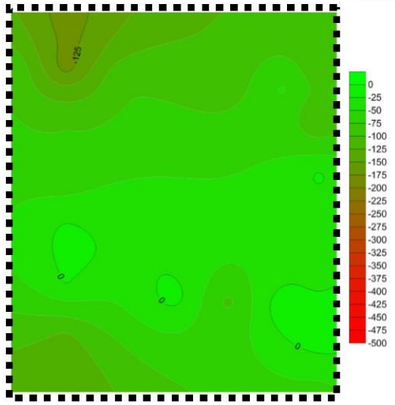

PIER 1—SOUTH WALL—EXTERIOR FACE

(SEE CONDITION LEGEND IN APPENDIX 2)

Study Area	Element	Inspection Date	Type	Distress Quantity (%)	Cores Sample (s)	HCP - Avg. (mV vs. CSE)	HCP - Min. (mV vs. CSE)	Resipod - Resistivity Avg. (kOhm-cm)	iCOR - Current Density Avg. (uA/cm^2)	iCOR - Resistivity Avg. (kOhm-cm)	BAC Meter - Current Density Avg. (um/yr)	Cover Vertical Bars - Rep. Minimum (in.)	Cover Horizontal Bars - Rep. Minimum (in.)	Carbonation Avg. (in.)	Deterioration Mechanism(s)
1	Arch Pier - Wall	5/22/2017	NDE & CORE	1 to 10	1 & 3	-41	-136	N/A	1.0	92	N/A	1.2	2.2	0.6	Chloride Exposure; Carbonation

Figure 6.33. Graphical Summary of Testing Data for Study Area 1 - Arch Pier Wall.

6.2.9. Arch Pier Bases

The locations of the follow-up testing study areas in the Arch Pier Bases are shown in Table 6.81. The primary focus of the field testing was material sampling to assess freeze-thaw depth, which appeared severe based on the visual inspection. The steel embedded in the arch pier bases is very sparse, so corrosion of reinforcement is not a prominent concern.

Table 6.81. Location of Study Areas - Arch Pier Bases

Location ID	Span/ Pier No./ Approach	Side of Bridge	Pier Face (Interior/Exterior)	Face	Test Type
2	1	Upstream	Exterior	South	Core Only
5	3	Downstream	Exterior	North	Core Only
7	4	Downstream	Exterior	North	Core Only
85	6	Downstream	Exterior	South	Core only

6.2.9.1. Physical Condition Survey

The condition of the Arch Pier Bases is summarized in Chapter 4. In general the conditions were consistent among the eight Arch Pier Bases, averaging more than 20 percent and usually much more than 50 percent distress. Erosion of the concrete surface due to river flow was also noted, especially below drain outfalls.

For each of the study areas, the local distress quantity is presented in Table 6.82. In general, a high level of distress (typically freeze-thaw and deteriorated repairs) was observed in the pier bases.

Table 6.82. Condition and Sampling of Study Areas - Arch Pier Bases

Location ID	Core Samples	Date Inspected/ Core	Distress Quantity (%)
2	2	5/24/2017	10 to 30
5	5	5/26/2017	> 30
7	7	5/26/2017	10 to 30
85	85	7/15/2017	>30

6.2.9.2. Corrosion Survey

Corrosion surveys were not performed in the Arch Pier Bases.

6.2.9.3. Reinforcement Cover Survey

Reinforcement cover surveys were not performed in the Arch Pier Bases.

6.2.9.4. Field and Lab Carbonation Tests

Field carbonation testing was not performed in the Arch Pier Bases. Results of the laboratory evaluations are presented below (see Petrographic Analysis).

6.2.9.5. Other Tests

No other tests were conducted in this element category.

6.2.9.6. Chloride Profile Analysis

The results of the chloride analyses of one core (Core 85) extracted from the Arch Pier Bases are shown in Figure 6.34. Severe, surface driven chloride exposure is present, and likely related to the close proximity to a drain.

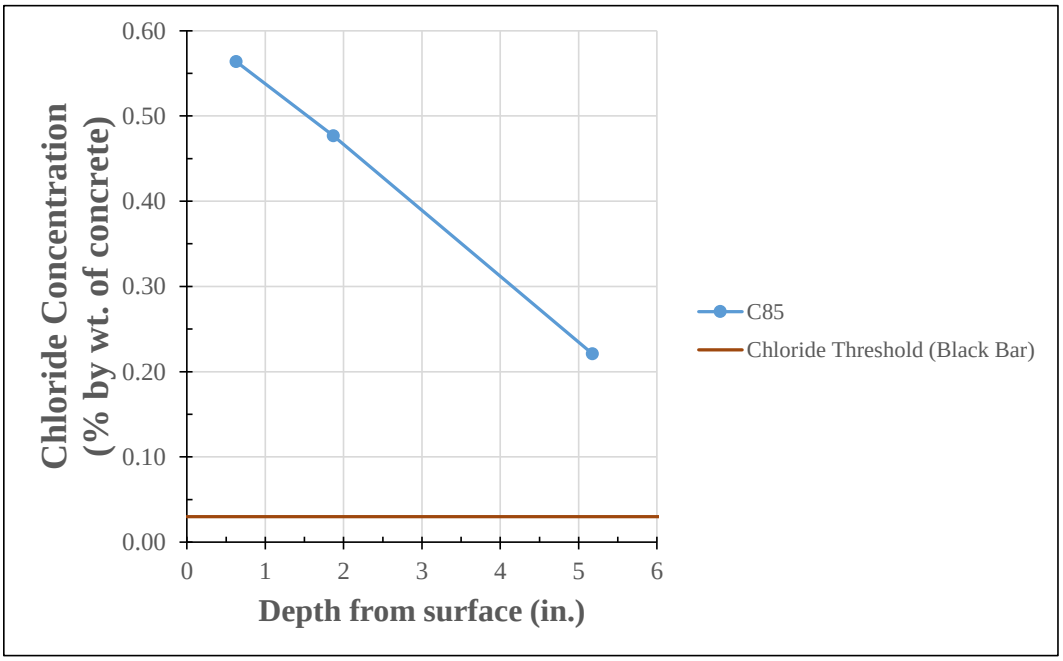

Figure 6.34. Chloride profile for Core 85 extracted from the Arch Pier Base near a drain location.

6.2.9.7. Petrographic Analysis

Cores extracted from the Arch Pier Bases are comprised of Concrete Mixture 1A - 1918: 2 inch Basalt. Cores 2, 5, 7, and 85 from the Arch Pier - Bases were evaluated for depth of carbonation and freeze thaw distress, and these results are summarized in Table 6.83. Freeze-thaw distress extended between 7 to 15 inches into the concrete.

Table 6.83. Measured Depth of Carbonation and Freeze-Thaw Distress - Arch Pier Bases

Core ID	Depth of Carbonation, inches	Depth of Severe Freeze-Thaw Distress, inches	Maximum Depth of Freeze-Thaw Distress, inches
2	0.7	4.8	9.8
5	0.1	8.0	15.0
7	0.3	--	7.0
85	1.0	8.0	10.5

Note: Depth values reported here include measured surface erosion at core location

6.2.9.8. Interpretation

Based on the field testing and laboratory analysis performed for areas of the Arch Pier Bases, freeze thaw distress is the primary deterioration mechanism. Chloride exposure and associated corrosion is a potential secondary cause of distress at locations of drains; however, there is limited embedded steel present, and global deterioration is not attributable to chloride-induced corrosion. With the exception of erosion at drain outfalls and due to river water movement, there was no evidence of other distress mechanisms (e.g., ASR) which may affect the future performance of the Arch Pier Bases.

It should also be noted that large areas of previous patching repairs are present on the pier bases, and many of these previous repairs have failed. The condition of the underlying original pier concrete is obscured and currently not known.

6.2.10. Deck Topside (Roadway, Sidewalk, & Underside) - Approach Spans

Follow-up test locations on the deck roadway and sidewalks were spaced across the approach spans as shown in Appendix 13. In general, the survey approach for the deck topside in the approach was similar to the arch spans and included NDE testing in approximately 25 percent of the deck surface; study areas were staggered such that each a portion of each joint-to-joint section of the deck roadway and sidewalk were tested, and different sections were studied in the outer lanes and the middle lanes (i.e., "checker-board" pattern). Core locations are listed in Table 6.84. A total of eight cores were collected through the deck topside: four cores were collected through the sidewalk, and four cores were collected through the roadway. Of the cores collected in the deck roadway, one was taken through the thickness of the deck.

Follow-up testing on the deck underside was conducted in the specific study area shown in Table 6.85.

Table 6.84. Core Locations Within Deck Topside Study Areas (Approach Spans)

Core Label	Element Type	Span	Side of Bridge	Notes
39	Roadway	S. Approach	Upstream	--
41	Roadway	N. Approach	Upstream	Through-Thickness
42	Roadway	S. Approach	Upstream	--
43	Roadway	N. Approach	Downstream	--
49	Sidewalk	S. Approach	Upstream	--
50	Sidewalk	N. Approach	Upstream	--
51	Sidewalk	S. Approach	Downstream	--
54	Sidewalk	N. Approach	Downstream	--

Table 6.85. Location of Study Areas - Deck Underside (Approach Spans)

Location ID	Element Type	Span/ Pier No./ Approach	Side of Bridge	Proximity of Study Area Relative to Joint	Test Type
41.1	Deck Underside	N. Approach	Upstream	35 ft. South of Joint	NDE and Core

6.2.10.1. Physical Condition Survey

The condition of the Approach Span deck and sidewalk is summarized in Chapter 4. In general, the conditions were consistent among the North and South Approach spans, with the deck topside (including roadway and sidewalks) and underside averaging 1 percent distress or less. The distress observed in the deck of the approach spans was similar to that of the arch spans; however, less cracking and delamination was observed overall. For the underside study area, the local distress quantity is presented in Table 6.86. Negligible distress was observed in this study area, and in general the underside was in good condition.

Table 6.86. Condition and Sampling of Study Areas - Deck Underside (Approach Spans)

Location ID	Core Samples	Date Inspected	Distress Quantity (%)
41.1	41	8/5/2017	< 1

6.2.10.2. Corrosion Survey

Across the deck surface, six NDE test locations were selected including both the roadway and sidewalk. In each area, a half-cell survey was performed on a network of grid points like in the arch spans, and three locations were selected for local corrosion testing (i.e., resistivity and corrosion rate); these locations were selected at features such as cracks, construction joints, and delaminations as well as at typical, un-deteriorated areas of the deck. Note that due to difficulty in making grounds, half-cell and corrosion rate testing was not successfully completed in each study area.

The upper layer of reinforcement in the Deck Roadway and Sidewalk (topside) is epoxy-coated, while the bottom layer of the deck is uncoated (black bar). Because of the epoxy coating, interpretation of the corrosion survey findings is more complex, as described in Section 6.2.1.2.

Corrosion Potential

The HCP results for the deck topside are summarized in Table 6.87. The results of this testing indicate that potential for corrosion is generally low in the deck roadway and sidewalk. However, there were a few isolated areas where the potential for corrosion is higher, likely due to local damage from cracking or the presence of construction joints.

The results of HCP testing on the deck underside are presented in Table 6.88, and the results indicate that the corrosion potential is low throughout the area surveyed.

Table 6.87. HCP Testing Results Summary - Deck Topside (Approach Spans)

Location	Percent of Survey Points More Negative Than -350mV	Percent of Survey Points Between -200mV and -350mV	Percent of Survey Points More Positive Than -200mV	Half-Cell Potentials (mV vs. CSE)	
				Average	Minimum
Roadway	6%	40%	54%	-185	-680
Sidewalk	7%	39%	54%	-185	-622

** Thresholds (see 3.4.4.1): > -200mV low, -200 to -350mV moderate, < -350 mV high probability of corrosion*

Table 6.88. HCP Testing Results - Deck Underside (Approach Spans)

Location ID	HCP - Avg. (mV vs. CSE)	HCP - Min. (mV vs. CSE)	HCP - Std. Dev. (mV vs. CSE)
41.1	51	-20	23

** Thresholds (see 3.4.4.1): > -200mV low, -200 to -350mV moderate, < -350 mV high probability of corrosion*

Resistivity

Resistivity testing was performed at and away from locations of cracks and construction joints, and these results are summarized in Table 6.89. Resistivity was typically lower near cracks and construction joints; however, the results indicate a low rate of corrosion where corrosion has initiated. Resistivity was lower in the sidewalk compared to the roadway, which may reflect lower deicing salt exposure.

Resistivity testing performed on the underside of the deck study area is presented in Table 6.90, and the results indicate a low rate of corrosion.

Table 6.89. Resistivity Testing Results - Deck Topside (Approach Spans)

Location	Resipod - Resistivity Avg. (kOhm-cm)	Notes
Roadway	96	Near Crack or Joint
	175	Away From Crack or Joint
Sidewalk	221	Away From Crack or Joint

** Thresholds (see 3.4.4.2): 50-100 low, 10-50 moderate, <10 kOhm-cm high corrosion rates possible in active areas*

Table 6.90. Resistivity Testing Results - Deck Underside (Approach Spans)

Location ID	Resipod - Resistivity Avg. (kOhm-cm)	iCOR - Resistivity Avg. (kOhm-cm)
41.1	642	309

** Thresholds (see 3.4.4.2): 50-100 low, 10-50 moderate, <10 kOhm-cm high corrosion rates possible in active areas*

Corrosion Rate

Corrosion rate testing on the deck topside was performed at the same locations as resistivity. The results are summarized in Table 6.91. Corrosion rates were higher near locations of cracks and construction joints; however, the results indicate a low rate of corrosion. Corrosion rate was slightly higher in the sidewalk compared to the roadway.

Corrosion rate testing on the deck underside (Table 6.92) indicated a low corrosion rate.

Table 6.91. Corrosion Rate Testing Results - Deck Topside (Approach Spans)

Location	BAC Meter - Current Density Avg. (um/yr) †	Notes
Roadway	6.1	Near Crack or Joint
	2.4	Away From Crack or Joint
Sidewalk	3.4	Away From Crack or Joint

† Thresholds (see 3.4.4.3): <10 low, 10-30 moderate, 30-100 high, >100 um/yr severe instantaneous corrosion rate.

Table 6.92. Corrosion Rate Testing Results - Deck Underside (Approach Spans)

Location ID	iCOR - Current Density Avg. (uA/cm^2) *
41.1	0.1

** Thresholds (see 3.4.4.3): <1 low, 1-3 moderate, 3-10 high, >10 severe uA/cm2 instantaneous corrosion rate*

6.2.10.3. Reinforcement Cover Survey

The results of the reinforcement cover surveys based on a network of GPR grid points like described for the arch spans are provided in Table 6.93 (topside) and Table 6.94 (underside). The cover in the sidewalk is variable and is slightly higher, on average, than in the roadway despite the presence of the overlay in the deck roadway.

Table 6.93. Cover Depth Statistics - Deck Topside (Approach Spans)

Value	Roadway	Sidewalk
	Cover Transverse Bar - Including Overlay	Cover Transverse Bar
Average (in.)	3.9	4.6
Standard Deviation (in.)	0.4	1.5
Coefficient of Variation	11%	33%
Minimum (in.)	3.0	1.4
Maximum (in.)	5.6	8.0

Table 6.94. Cover Depth Statistics - Deck Underside (North Approach Study Area 41)

Value	Cover Longitudinal Bar (in.)	Cover Transverse Bar (in.)
Average (in.)	1.1	0.9
Standard Deviation (in.)	0.2	0.1
Coefficient of Variation	20%	6%
Minimum (in.)	0.6	0.8
Maximum (in.)	1.2	1.0

6.2.10.4. Field and Lab Carbonation Tests

Field carbonation measurements were not performed. Core samples evaluated exhibited negligible carbonation on either the topside or underside.

6.2.10.5. Other Tests

No other tests were conducted in this element category.

6.2.10.6. Chloride Profile Analysis

Chloride profiles from cores extracted through the deck roadway are shown in Figure 6.35 (topside) and Figure 6.36 (underside). There were no cores from the approach span sidewalks tested for chloride concentration. Cores 39 and 41 indicate typical chloride diffusion resulting from an elevated surface exposure; chloride concentrations are elevated near the surface, and decrease with depth though the overlay to negligible levels in the substrate. Core 43 exhibited voiding in the overlay and the elevated chloride level in this core is likely due to these voids. Recall that the reinforcement in the top mat of both the roadway and the sidewalk is epoxy-coated, so a higher range in chloride concentration would be required to initiate corrosion (see Section 3.2.1.2).

Core 41 was taken through the full thickness of the deck, and chloride testing was performed for the underside of the deck. Negligible chlorides were found indicating that exposure of chlorides on the deck underside is low away from expansion joints and other locations of possible leaking and surface run-off.

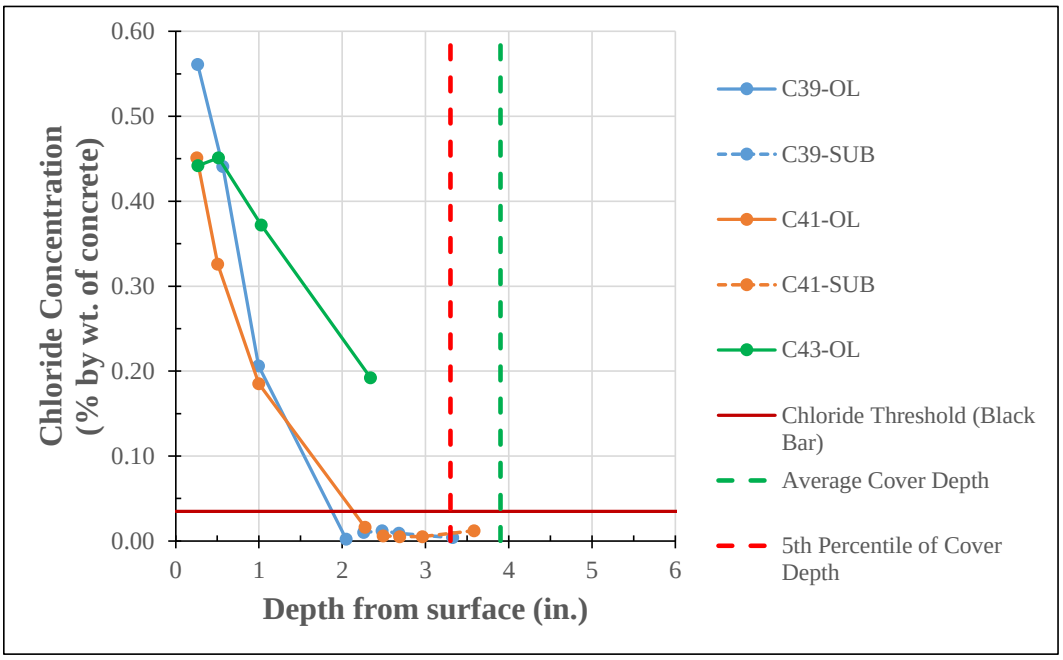

Figure 6.35. Chloride profiles for Deck Roadway - Approach (topside) cores compared to chloride threshold for corrosion initiation for black bar as a reference and reinforcement cover depth measurements. Note top bars are actually epoxy-coated, so threshold is higher - see Section 3.2.1.2.
(Overlay = OL; Substrate = SUB)

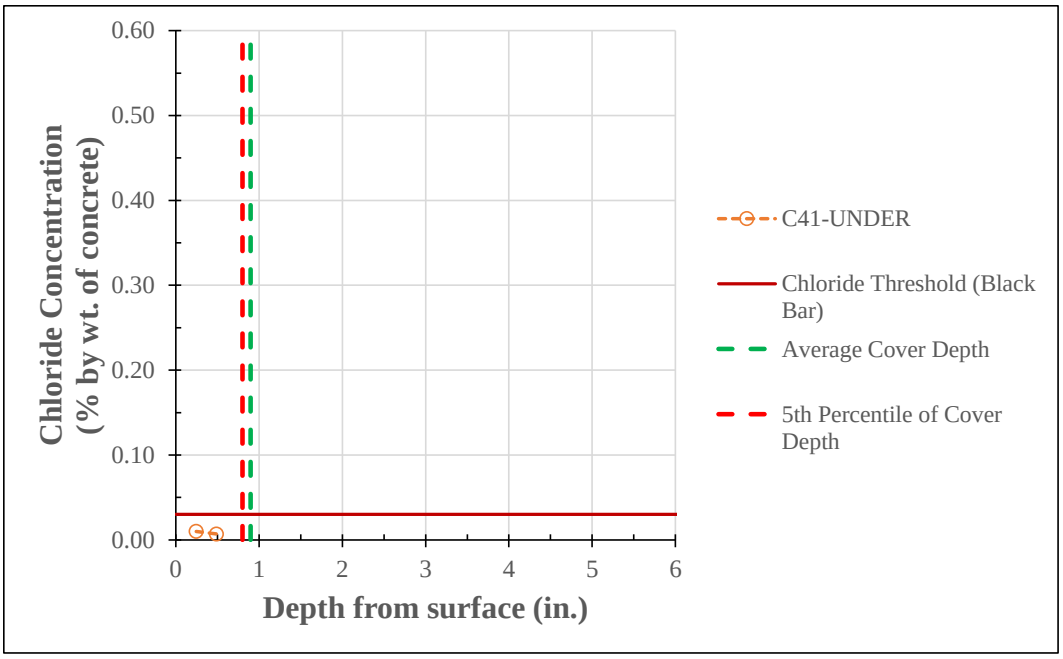

Figure 6.36. Chloride profiles for Deck Roadway - Approach (underside) cores compared to chloride threshold for corrosion initiation and reinforcement cover depth measurements.
(Underside = UNDER)

6.2.10.7. Petrographic Analysis

The concrete for the Approach Span Deck is similar to that of the other areas of the deck: Concrete Mixture 3 - Deck 3/4 inch Gravel (see Section 6.2.1.7). There was no indication of freeze-thaw distress or ASR related distress in the core sample examined.

Carbonation was negligible in the core samples evaluated, including the overlay (deck topside) and deck underside.

6.2.10.8. Interpretation

The deck roadway, sidewalk, and underside in the approach spans are in good condition. Chloride-induced corrosion due to exposure from de-icing salts is the primary deterioration mechanism. At cracks and near joints and previous repairs, chloride levels are likely higher, and corrosion surveys at these locations indicate a higher risk of corrosion activity at these locations. The overlay appears well bonded and is generally effectively protecting the deck from chloride exposure.

A graphical representation of the follow-up testing in the Approach Span Decks is provided in Figure 6.37 and Figure 6.38 and in Appendix 14. In the areas surveyed, chloride-induced corrosion appears to be the controlling deterioration mechanism; however, minimal distress and corrosion activity were occurring at present.

NORTH APPROACH

AREA 41.1

DECK UNDERSIDE

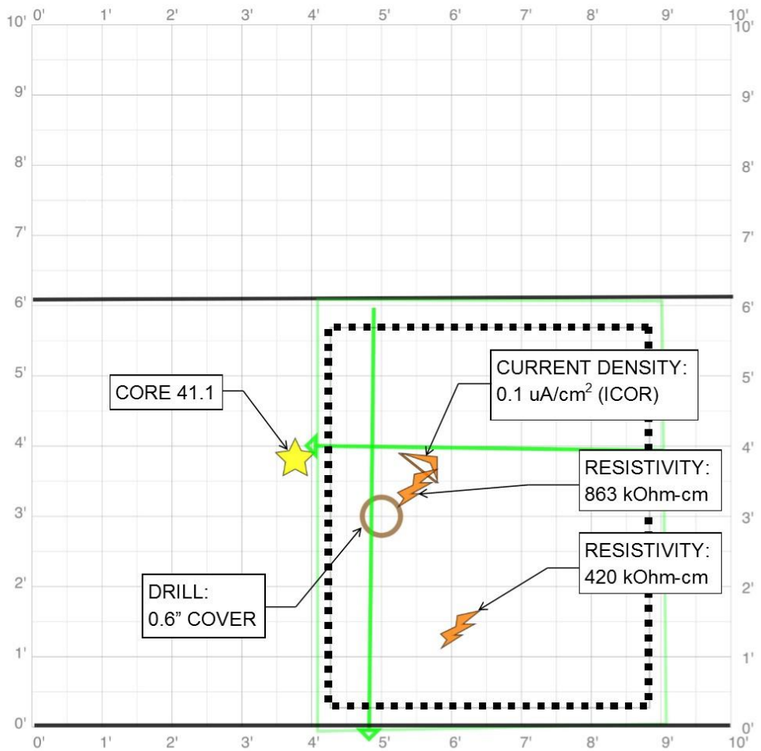

HCP IN mV vs. CSE

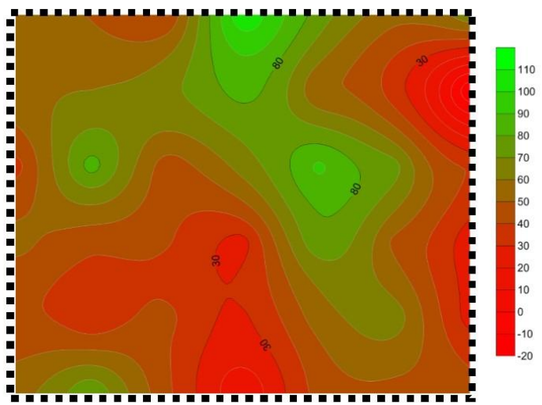

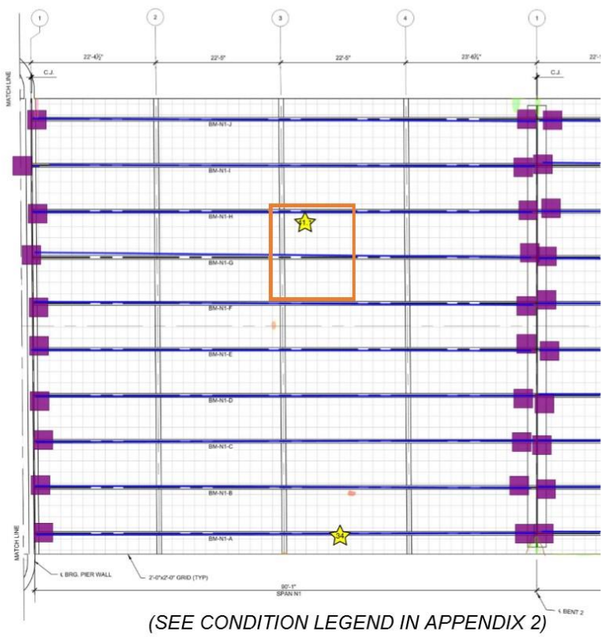

(SEE CONDITION LEGEND IN APPENDIX 2)

Study Area	Element	Inspection Date	Type	Distress Quantity (%)	Cores Sample(s)	HCP - Avg. (mV vs. CSE)	HCP - Min. (mV vs. CSE)	Resipod - Resistivity Avg. (kOhm-cm)	iCOR - Current Density Avg. (uA/cm^2)	iCOR - Resistivity Avg. (kOhm-cm)	BAC Meter - Current Density Avg. (um/yr)	Cover Vertical Bars - Rep. Minimum (in.)	Cover Horizontal Bars - Rep. Minimum (in.)	Carbonation Avg. (in.)	Deterioration Mechanism(s)
41.1	Deck Underside	8/5/2017	NDE & CORE	< 1	41	51	-20	642	0.1	309	N/A	1.0	0.6	N/A	Chloride Exposure

Figure 6.37. Graphical Summary of Testing Data for Study Area 41 - Deck Underside (Approach Span).

NORTH APPROACH - RIGHT LANE

DECK TOPSIDE ROADWAY

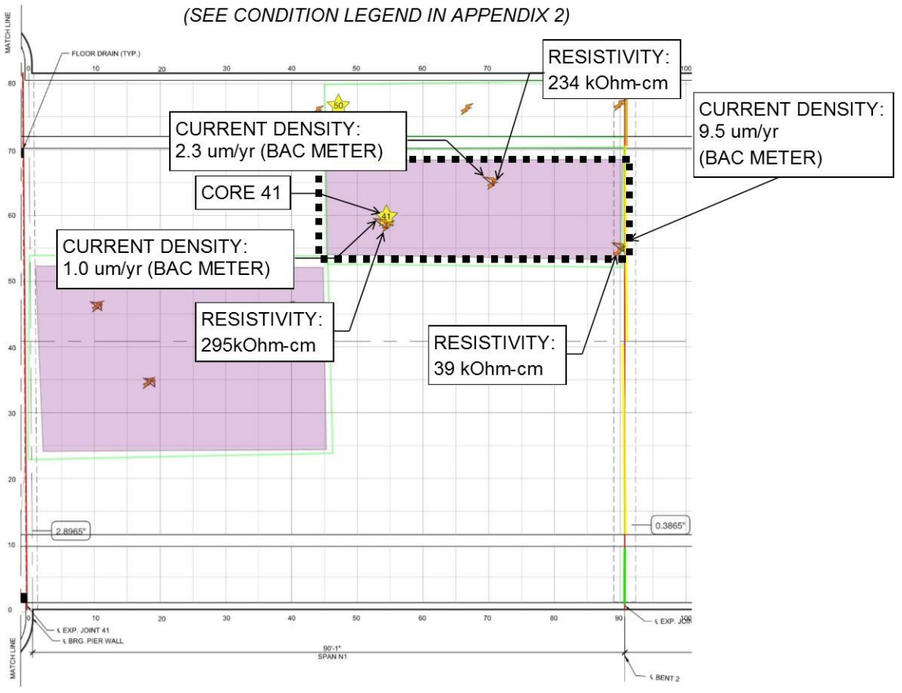

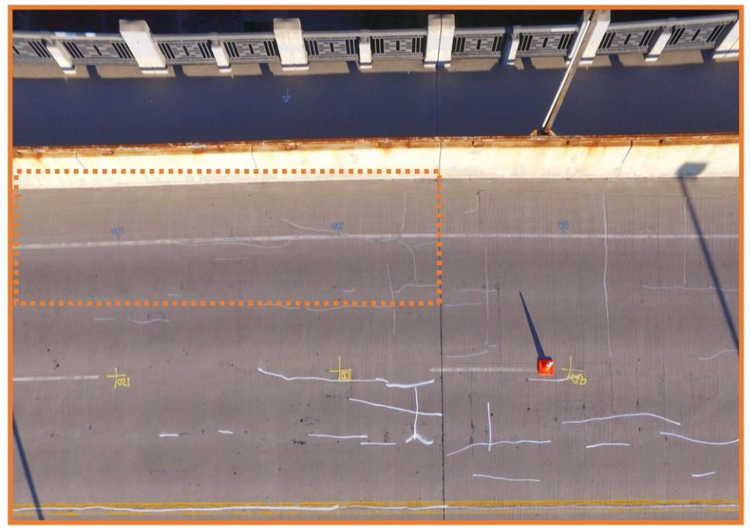

HCP IN mV vs. CSE

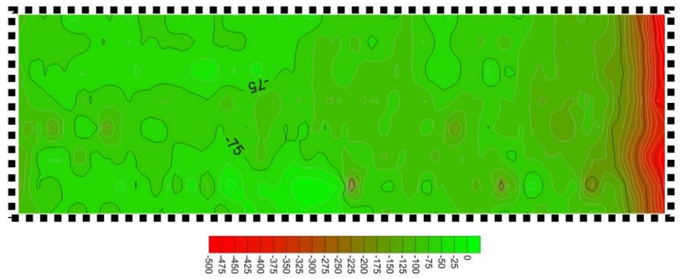

Study Area	Element	Inspection Date	Type	Distress Quantity (%)	Cores Sample(s)	HCP - Avg. (mV vs. CSE)	HCP - Min. (mV vs. CSE)	Resipod - Resistivity Avg. (kOhm-cm)	iCOR - Current Density Avg. (uA/cm^2)	iCOR - Resistivity Avg. (kOhm-cm)	BAC Meter - Current Density Avg. (um/yr)	Cover Vertical Bars - Rep. Minimum (in.)	Cover Horizontal Bars - Rep. Minimum (in.)	Carbonation Avg. (in.)	Deterioration Mechanism(s)
N. App.	Deck Roadway	5/23/2017	NDE & CORE	< 1	41	-109	-553	189	N/A	N/A	4.3	4.3	3.8	N/A	Chloride Exposure

Figure 6.38. Graphical Summary of Testing Data for Study Area in Deck Topside - North Approach Spans.

6.2.11. Weathering Steel Girders (South Approach)

The locations of the follow-up testing study areas in the weathering steel girders in the south approach are shown in Table 6.95. Ultrasonic thickness testing was the only follow-up testing performed on these elements. The results are as shown in Table 6.96.

Table 6.95. Location of Study Areas - South Approach Girders

Location ID	Span	Girder	Location	Face	Test Type
126	S2	Girder S2-H	Near Pier 1	Upstream	Ultrasonic Thickness
127	S1	Girder S1-I	Near South Abutment	Upstream	Ultrasonic Thickness

Table 6.96. Ultrasonic Thickness Test Results at South Approach Girders

Study Area ID	Span	Girder	Location	Comments	Element	Min. Measured Thickness (in.)	Approx. Section Loss (%)
126	South Approach	Girder S2-H	Near Pier 1	Some surface corrosion	Bottom flange	0.831	5.0%
					Web	0.37	1.3%
127	South Approach	Girder S1-I	Near South abutment	Some surface corrosion	Bottom Flange	0.455	9.0%
					Web	0.383	~0%

6.2.11.1. Interpretation

The primary deterioration mechanism on the south approach girders is corrosion exacerbated by deicer runoff through the expansion joints and over the deck edges. Ultrasonic thickness testing was conducted at the locations of most severe section loss identified during visual assessment. Up to 9% section loss was identified at some spots of the bottom flange.

6.2.12. South Abutment

The locations of the follow-up testing study areas for the South Abutment are shown in Table 6.97.

Table 6.97. Location of Study Areas - South Abutment

Location ID	Approach	Side of Bridge	Face	Test Type
35	South Approach	Downstream	North	NDE & core
36	South Approach	Upstream	North	NDE & core

6.2.12.1. Physical Condition Survey

The condition of the South Abutment is summarized in Chapter 4. In general, less than one percent distress was identified in these elements.

For each of the study areas, the local distress quantity is presented in Table 6.98. Minimal distress was observed.

Table 6.98. Condition and Sampling of Study Areas - South Abutment

Location ID	Core Samples	Date Inspected	Distress Quantity (%)
35	35	5/26/2017	< 1
36	36	8/5/2017	< 1

6.2.12.2. Corrosion Survey

Corrosion Potential

Results of half-cell potential surveys are provided in Table 6.99. The results fall into ranges that would ordinarily be interpreted to indicate moderate to high probability of corrosion activity; however, measured potentials are highly negative for this element because the trapped moisture in the soil on the backside of the abutment limits the availability of oxygen. This will tend to shift measured potentials in a negative direction. In these conditions, the risk of corrosion is best assessed by examination of the potential gradients. At these locations, no indication of active corrosion was identified.

Table 6.99. HCP Testing Results - South Abutment

Location ID	HCP - Avg. (mV vs. CSE)	HCP - Min. (mV vs. CSE)	HCP - Std. Dev. (mV vs. CSE)	Distress Quantity (%)
35	-333	-520	74	< 1
36	-310	-392	30	< 1

** Thresholds (see 3.4.4.1): > -200mV low, -200 to -350mV moderate, < -350 mV high probability of corrosion*

Resistivity

Results of resistivity testing are provided in Table 6.100. The results indicate a low to moderate corrosion rate where active corrosion has initiated.

Table 6.100. Resistivity Testing Results - South Abutment

Location ID	Resipod - Resistivity Avg. (kOhm-cm)	iCOR - Resistivity Avg. (kOhm-cm)	Distress Quantity (%)
35	91	--	< 1
36	42	44.3	< 1

** Thresholds (see 3.4.4.2): 50-100 low, 10-50 moderate, <10 kOhm-cm high corrosion rates possible in active areas*

Corrosion Rate

Corrosion rate testing results are provided in Table 6.101. Corrosion rate testing was not completed successfully in all areas due to the high cover. The measured corrosion rate was low.

Table 6.101. Corrosion Rate Testing Results - South Abutment

Location ID	iCOR - Current Density Avg. (uA/cm^2) *	Distress Quantity (%)
35	--	< 1
36	0.5	< 1

** Thresholds (see 3.4.4.3): <1 low, 1-3 moderate, 3-10 high, >10 severe uA/cm2 instantaneous corrosion rate*

6.2.12.3. Reinforcement Cover Survey

The results of the reinforcement cover surveys are provided in Table 6.102. The statistical information for this element is summarized in Table 6.103. Cover depths were greater than 2 inches and generally consistent in the areas surveyed.

Table 6.102. Cover Depth Measurements - South Abutment

Location ID	Cover Vertical Bars - Avg. (in.)	Cover Vertical Bars - Rep. Minimum (in.)	Cover Horizontal Bars - Avg. (in.)	Cover Horizontal Bars - Rep. Minimum (in.)	*Distress Quantity (%)*
35	3.4	3.0	4.6	4.4	*< 1*
36	2.9	2.5	2.3	2.1	*< 1*

Table 6.103. Cover Depth Statistics - South Abutment

Value	Cover Vertical Bar	Cover Horizontal Bar
Average (in.)	3.2	3.5
Standard Deviation (in.)	0.4	1.2
Coefficient of Variation	11%	35%
Minimum (in.)	2.3	2.1
Maximum (in.)	3.9	4.8

6.2.12.4. Field and Lab Carbonation Tests

Synthesis of field and lab carbonation measurement results are provided in Table 6.104. Negligible carbonation depth, relative to the depth of reinforcement, was measured.

Table 6.104. Carbonation Measurements - South Abutment

Location ID	Carbonation - Rep. Maximum (in.)	*Cover Vertical Bars - Rep. Minimum (in.)*	*Cover Horizontal Bars - Rep. Minimum (in.)*	*Distress Quantity (%)*
35	0.2	3.0	4.4	*< 1*
36	0.1	2.5	2.1	*< 1*

6.2.12.5. Other Tests

No other tests were conducted in this element category.

6.2.12.6. Chloride Profile Analysis

The chloride profile for Core 36 is shown in Figure 6.39. The results indicate low surface-chloride exposure and negligible diffusion into the concrete.

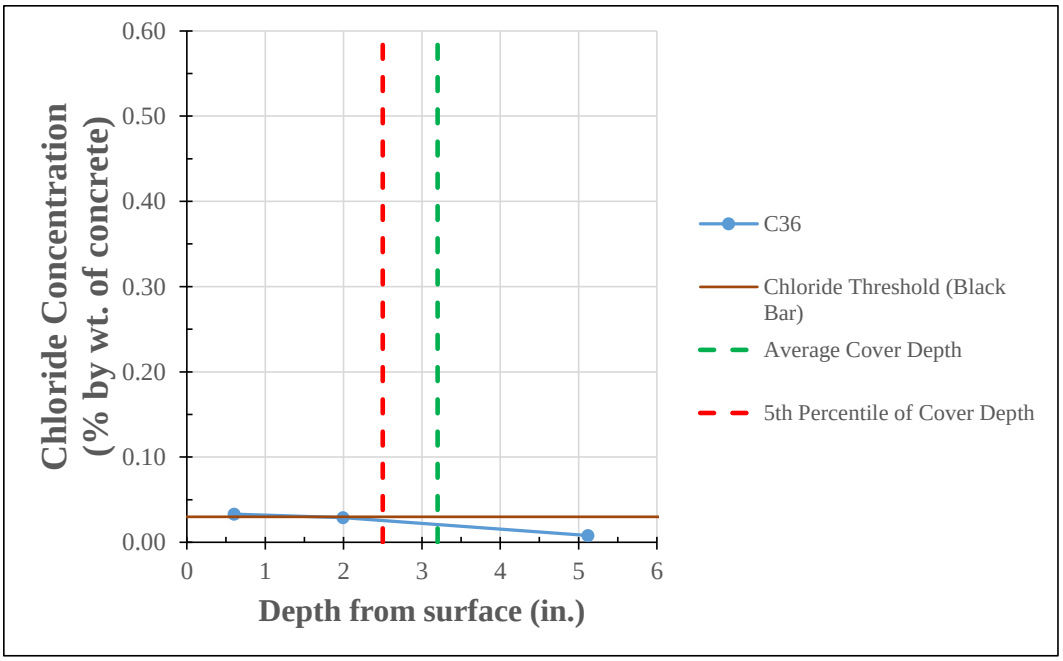

Figure 6.39. Chloride profiles for South Abutment core compared to chloride threshold.

6.2.12.7. Petrographic Analysis

The concrete in the South Abutment is identified as Concrete Mixture 6 - 3/4 inch Gravel. There was no observed distress due to ASR or freeze-thaw in similar cores examined.

6.2.12.8. Interpretation

At present, limited chloride exposure and carbonation have occurred and little distress was observed in this element. Long-term durability will likely be controlled by chloride exposure where drains or deck joints permit deicer runoff to reach the abutment. Long-term carbonation may also be a critical mechanism; however, the low water to cement ratio of the concrete mixture will likely mitigate carbonation for many years. Other mechanisms of distress such as ASR or freeze-thaw were not observed in core samples examined.

6.2.13. South Bent Pier

The locations of the follow-up testing study areas are shown in Table 6.105.

Table 6.105. Location of Study Areas - South Bent Pier

Location ID	Approach	Side of Bridge	Face	Test Type
37	South Approach	Downstream	North	NDE & core
38	South Approach	Downstream	North	NDE only

6.2.13.1. Physical Condition Survey

The condition of the South Bent Pier is summarized in Chapter 4. In general, less than one percent distress was identified in these elements.

For each of the study areas, the local distress quantity is presented in Table 6.106. Minimal distress was observed.

Table 6.106. Condition and Sampling of Study Areas - South Bent Pier

Location ID	Core Samples	Date Inspected	Distress Quantity (%)
37	37	5/26/2017	< 1
38	N/A	5/26/2017	< 1

6.2.13.2. Corrosion Survey

Corrosion Potential

Results of half-cell potential surveys are provided in Table 6.107. The results indicate a low to moderate probability of corrosion at Study Area 37, which is located close to grade adjacent to traffic on West River Parkway.

Table 6.107. HCP Testing Results - South Bent Pier

Location ID	HCP - Avg. (mV vs. CSE)	HCP - Min. (mV vs. CSE)	HCP - Std. Dev. (mV vs. CSE)	Distress Quantity (%)
37	-125	-350	94	< 1
38	66	6	25	< 1

** Thresholds (see 3.4.4.1): > -200mV low, -200 to -350mV moderate, < -350 mV high probability of corrosion*

Resistivity

Results of resistivity testing are provided in Table 6.108. The results indicate a negligible corrosion rate.

Table 6.108. Resistivity Testing Results - South Bent Pier

Location ID	Resipod - Resistivity Avg. (kOhm-cm)	*Distress Quantity (%)*
37	580	*< 1*
38	430	*< 1*

** Thresholds (see 3.4.4.2): 50-100 low, 10-50 moderate, <10 kOhm-cm high corrosion rates possible in active areas*

Corrosion Rate

Corrosion rate testing was not performed due to the high cover in this element.

6.2.13.3. Reinforcement Cover Survey

The results of the reinforcement cover surveys are provided in Table 6.109. The statistical information for this element is summarized in Table 6.110. Cover depths were greater than 2.5 inches and consistent within the areas surveyed.

Table 6.109. Cover Depth Measurements - South Bent Pier

Location ID	Cover Vertical Bars - Avg. (in.)	Cover Vertical Bars - Rep. Minimum (in.)	Cover Horizontal Bars - Avg. (in.)	Cover Horizontal Bars - Rep. Minimum (in.)	*Distress Quantity (%)*
37	5.3	4.0	4.2	2.5	*< 1*
38	2.6	2.6	3.6	3.4	*< 1*

Table 6.110. Cover Depth Statistics - South Bent Pier

Value	Cover Vertical Bar	Cover Horizontal Bar
Average (in.)	5.1	4.0
Standard Deviation (in.)	1.4	1.1
Coefficient of Variation	28%	28%
Minimum (in.)	2.5	2.3
Maximum (in.)	7.2	6.3

6.2.13.4. Field and Lab Carbonation Tests

Synthesis of field and lab carbonation measurement results are provided in Table 6.111. Negligible carbonation depth, relative to the depth of reinforcement, was measured.

Table 6.111. Carbonation Measurements - South Bent Pier

Location ID	Carbonation - Rep. Maximum (in.)	*Cover Vertical Bars - Rep. Minimum (in.)*	*Cover Horizontal Bars - Rep. Minimum (in.)*	*Distress Quantity (%)*
37	0.0	4.0	2.5	*< 1*
38	0.1	2.6	3.4	*< 1*

6.2.13.5. Other Tests
No other tests were conducted in this element category.

6.2.13.6. Chloride Profile Analysis
The chloride profile for Core 37 is shown in Figure 6.40. The results indicate low surface-chloride exposure and negligible diffusion into the concrete.

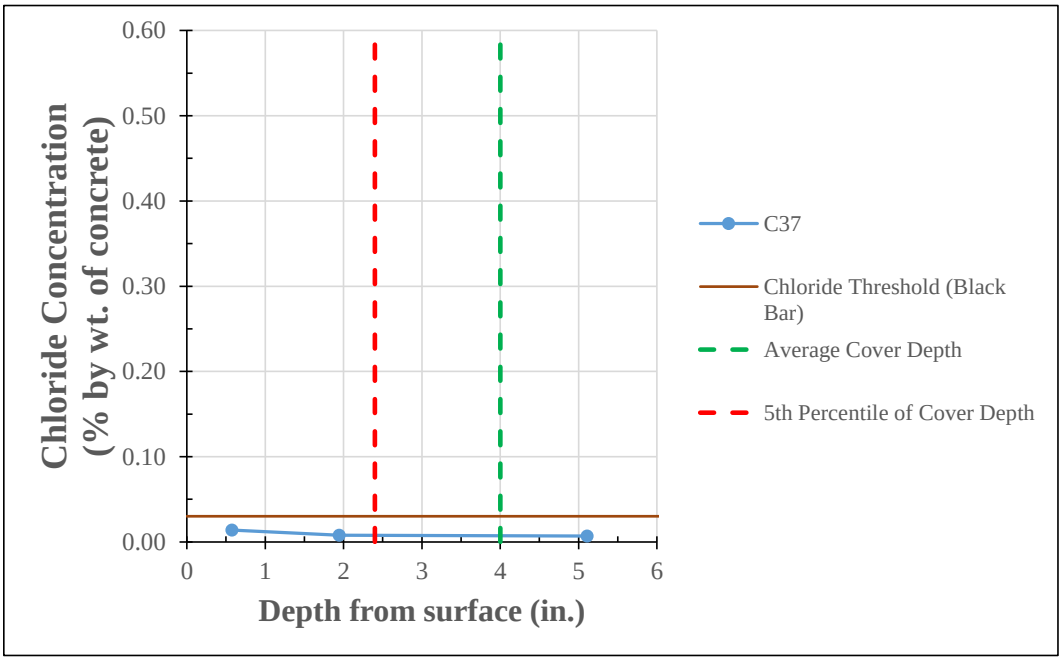

Figure 6.40. Chloride profiles for South Bent Pier core compared to chloride threshold.

6.2.13.7. Petrographic Analysis
Limited petrographic studies were conducted on Cores 37 from the South Bent Pier, and the concrete was identified as Concrete Mixture 6-3/4 inch Gravel. The concrete appeared to be in good condition, with negligible carbonation and no evidence of freeze-thaw damage or damage due to ASR.

6.2.13.8. Interpretation
At present, limited chloride ingress and carbonation have occurred and little distress was observed in this element. Long-term durability will likely be controlled by chloride exposure and associated corrosion near the roadway at the base of the pier. Other mechanisms of distress such as ASR or freeze-thaw were not observed.

6.2.14. Prestressed Girders (North Approach)

The location of the follow-up testing study area in the prestressed girders in the north approach is shown in Table 6.112. This was an exterior girder on the downstream side of the bridge.

Table 6.112. Location of Study Areas - Prestressed Girders (North Approach)

Location ID	Span	Girder	Face	Test Type
34	N1	A	Downstream	NDE & core

6.2.14.1. Physical Condition Survey

The condition of the Prestressed Girders is summarized in Chapter 4. In general, less than one percent distress was identified in these elements.

For the study area, the local distress quantity is presented in Table 6.113. Observed distress was limited to isolated delaminations near leaks at the expansion joint at the north abutment. The core was taken through the web of the beam.

Table 6.113. Condition and Sampling of Study Areas - Prestressed Girders (North Approach)

Location ID	Core Samples	Date Inspected	Distress Quantity (%)
34	34	5/24/2017	< 1

6.2.14.2. Corrosion Survey

Corrosion Potential

Results of half-cell potential surveys are provided in Table 6.114. The results indicate a low probability of corrosion.

Table 6.114. HCP Testing Results - Prestressed Girders (North Approach)

Location ID	HCP - Avg. (mV vs. CSE)	HCP - Min. (mV vs. CSE)	HCP - Std. Dev. (mV vs. CSE)	Distress Quantity (%)
34	-3	-91	38	< 1

** Thresholds (see 3.4.4.1): > -200mV low, -200 to -350mV moderate, < -350 mV high probability of corrosion*

Resistivity
Resistivity testing was not performed.

Corrosion Rate
Corrosion rate testing results are provided in Table 6.115. The results indicate a low rate of corrosion.

Table 6.115. Corrosion Rate Testing Results - Prestressed Girders (North Approach)

Location ID	BAC Meter - Current Density Avg. (um/yr) †	*Distress Quantity (%)*
34	1.6	*< 1*

† Thresholds (see 3.4.4.3): <10 low, 10-30 moderate, 30-100 high, >100 um/yr severe instantaneous corrosion rate.

6.2.14.3. Reinforcement Cover Survey
The results of the reinforcement cover surveys are provided in Table 6.116. The statistical information for this element is summarized in Table 6.117. The cover depths measured to the stirrups were consistent (as would be expected for precast concrete elements).

Table 6.116. Cover Depth Measurements - Prestressed Girders (North Approach)

Location ID	Cover Vertical Bars - Avg. (in.)	Cover Vertical Bars - Rep. Minimum (in.)	*Distress Quantity (%)*
34	2.2	1.8	*< 1*

Table 6.117. Cover Depth Statistics - Prestressed Girder (North Approach)

Value	Cover Vertical Bar - Stirrups
Average (in.)	2.2
Standard Deviation (in.)	0.2
Coefficient of Variation	11%
Minimum (in.)	1.8
Maximum (in.)	2.4

6.2.14.4. Field and Lab Carbonation Tests
The core sample extracted was evaluated for carbonation and the results are provided in Table 6.118. Negligible carbonation depth, relative to the depth of reinforcement, was measured.

Table 6.118. Carbonation Measurements - Prestressed Girders (North Approach)

Location ID	Carbonation - Rep. Maximum (in.)	*Cover Vertical Bars - Rep. Minimum (in.)*	Distress Quantity (%)
34	0.5	2.2	< 1

6.2.14.5. Other Tests

No other tests were conducted in this element category.

6.2.14.6. Chloride Profile Analysis

The chloride profile for Core 34 is shown in Figure 6.41. The exterior face is potentially exposed to water and deicer run-off from the deck surface and this appears to have resulted in some chloride ingress; however, chloride concentration at the depth of the stirrups is well below threshold levels required to initiate corrosion. Based on these results, the interior face has limited exposure; chloride ingress was negligible at this location.

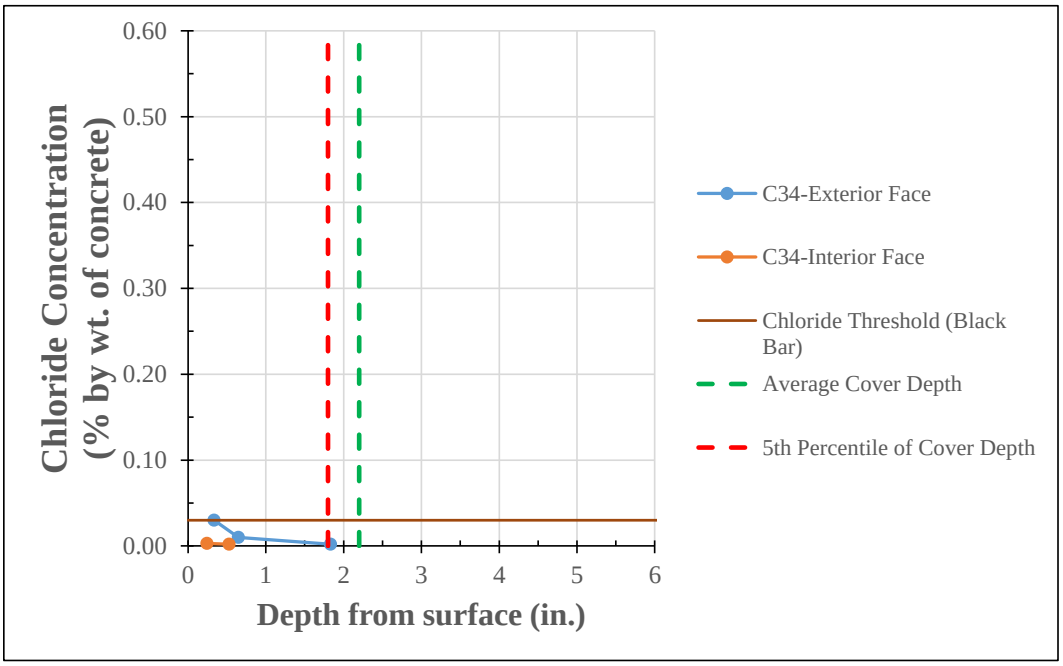

Figure 6.41. Chloride profiles for Prestressed Girder core compared to chloride threshold.

6.2.14.7. Petrographic Analysis

Limited petrographic studies were conducted on Core 34 (Concrete Mixture 5 - 1/2 inch Gravel). Depth of carbonation was 0.5 inches and 0.3 on the interior and exterior surfaces, respectively. The sampled concrete was in good condition. No evidence of materials-related distress such as ASR or freeze-thaw damage was observed.

6.2.14.8. Interpretation

At present, very limited chloride exposure and carbonation have occurred even on the exterior face of the exterior girder that was tested; interior girders are typically more sheltered. Long-term durability will likely be controlled by chloride exposure where drains or deck joints permit deicer runoff to reach the girders. Long-term carbonation may also be a critical mechanism; however, the low water to cement ratio of the concrete mixture will likely mitigate carbonation for many years. For this concrete mixture, other mechanisms of distress such as ASR or freeze-thaw were not observed in core samples examined.

6.2.15. North Abutment

The locations of the follow-up testing study areas in the North Abutment are shown in Table 6.119.

Table 6.119. Location of Study Areas - North Abutment

Location ID	Approach	Side of Bridge	Face	Test Type
28	North Approach	Downstream	South	NDE & core
29	North Approach	Middle	South	NDE only

6.2.15.1. Physical Condition Survey

The condition of the North Abutment is summarized in Chapter 4. Approximately 2 percent distress on average was identified in this element.

For each of the study areas, the local distress quantity is presented in Table 6.120. Little distress was observed, with some isolated locations of concrete delaminations. Study Area 28 was performed in an area of moisture staining.

Table 6.120. Condition and Sampling of Study Areas - North Abutment

Location ID	Core Samples	Date Inspected	Distress Quantity (%)
28	28	5/23/2017	1 to 10
29	N/A	5/24/2017	< 1

6.2.15.2. Corrosion Survey

Corrosion Potential

Results of half-cell potential surveys are provided in Table 6.121. The results fall into ranges that would ordinarily be interpreted to indicate moderate to high probability of corrosion activity; however, like the South Abutment, the risk of corrosion in concrete against soil is best assessed by examination of the potential gradients. At these locations, no indication of active corrosion was identified.

Table 6.121. HCP Testing Results - North Abutment

Location ID	HCP - Avg. (mV vs. CSE)	HCP - Min. (mV vs. CSE)	HCP - Std. Dev. (mV vs. CSE)	Distress Quantity (%)
28	-223	-273	32	1 to 10
29	-185	-416	65	< 1

** Thresholds (see 3.4.4.1): > -200mV low, -200 to -350mV moderate, < -350 mV high probability of corrosion*

Resistivity

Results of resistivity testing are provided in Table 6.122. The results indicate a low rate of corrosion.

Table 6.122. Resistivity Testing Results - North Abutment

Location ID	Resipod - Resistivity Avg. (kOhm-cm)	Distress Quantity (%)
28	119	1 to 10
29	--	< 1

** Thresholds (see 3.4.4.2): 50-100 low, 10-50 moderate, <10 kOhm-cm high corrosion rates possible in active areas*

Corrosion Rate

Corrosion rate testing results are provided in Table 6.123. The results indicate a low rate of corrosion.

Table 6.123. Corrosion Rate Testing Results - North Abutment

Location ID	BAC Meter - Current Density Avg. (um/yr) †	Distress Quantity (%)
28	4.0	1 to 10
29	3.5	< 1

† Thresholds (see 3.4.4.3): <10 low, 10-30 moderate, 30-100 high, >100 um/yr severe instantaneous corrosion rate.

6.2.15.3. Reinforcement Cover Survey

The results of the reinforcement cover surveys are provided in Table 6.124. The statistical information for this element is summarized in Table 6.125. The results indicate consistent cover depths, typically about 2 inches or greater.

Table 6.124. Cover Depth Measurements - North Abutment

Location ID	Cover Vertical Bars - Avg. (in.)	Cover Vertical Bars - Rep. Minimum (in.)	Cover Horizontal Bars - Avg. (in.)	Cover Horizontal Bars - Rep. Minimum (in.)	Distress Quantity (%)
28	2.6	2.6	1.9	1.9	1 to 10
29	2.7	2.6	2.1	1.8	< 1

Table 6.125. Cover Depth Statistics - North Abutment

Value	Cover Vertical Bar	Cover Horizontal Bar
Average (in.)	2.7	2.1
Standard Deviation (in.)	0.1	0.2
Coefficient of Variation	4%	11%
Minimum (in.)	2.6	1.8
Maximum (in.)	2.9	2.5

6.2.15.4. Field and Lab Carbonation Tests

The core sample extracted was evaluated for carbonation and the results are provided in Table 6.126. Negligible carbonation depth, relative to the depth of reinforcement, was measured.

Table 6.126. Carbonation Measurements - North Abutment

Location ID	Carbonation - Rep. Maximum (in.)	Cover Vertical Bars - Rep. Minimum (in.)	Distress Quantity (%)
28	0.3	1.9	1 to 10

6.2.15.5. Other Tests

No other tests were conducted in this element category.

6.2.15.6. Chloride Profile Analysis

The results of the chloride analyses of Core 28, extracted from the North Abutment, are shown in Figure 6.42. The chloride profile indicates typical surface driven chloride exposure, likely due to run-off from the deck surface leaking through the expansion joint. Chloride concentrations near the depth of the reinforcement are just below thresholds for chloride-induced corrosion; however, even if the chloride exposure is stopped, the chloride will continue to diffuse into the concrete and additional corrosion initiation can be expected. Based on the observed conditions, this appears to be limited only to the area on the north abutment where the leakage through the joint has occurred.

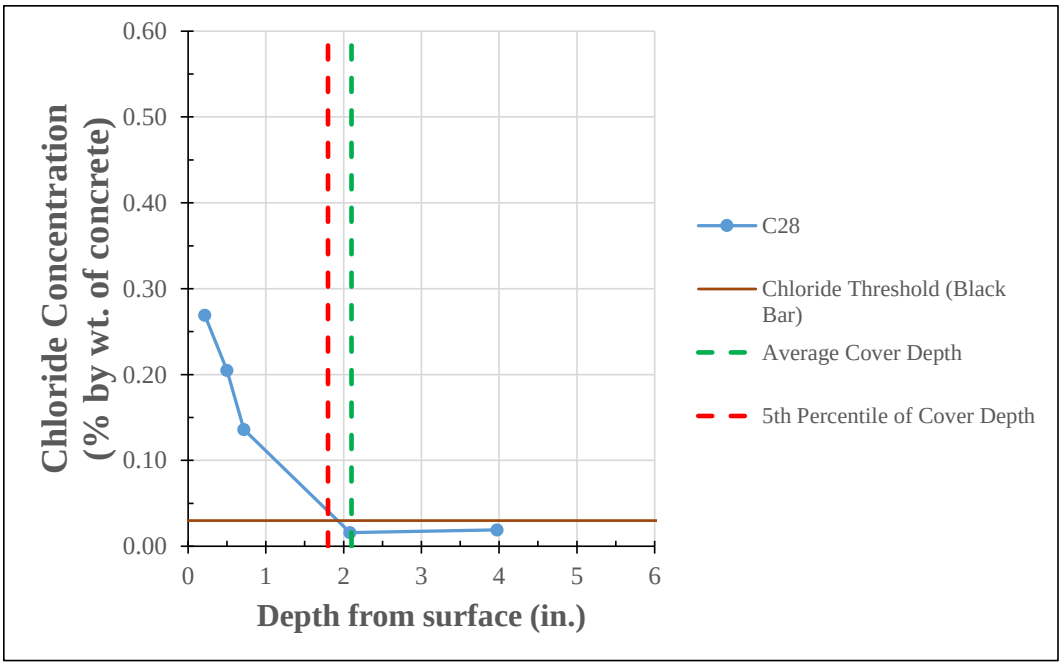

Figure 6.42. Chloride profile for North Abutment core compared to chloride threshold.

6.2.15.7. Petrographic Analysis

The concrete was identified as Concrete Mixture 6 - 3/4 inch Gravel. There was no evidence of ASR or freeze-thaw distress in similar cores of this mixture.

6.2.15.8. Interpretation

The primary deterioration mechanism is chloride-induced corrosion. Deicer run-off from the deck has likely resulted in chloride exposure and associated corrosion. With time, chloride ingress and associated damage will increase where deicer leakage has occurred. Carbonation, freeze-thaw, and ASR are not expected to cause widespread deterioration.

6.2.16. North Bent Pier

The locations of the follow-up testing study areas in the North Bent Pier are shown in Table 6.127.

Table 6.127. Location of Study Areas - North Bent Pier

Location ID	Approach	Side of Bridge	Face	Test Type
32	North Approach	Downstream	South	NDE & core
33	North Approach	Upstream	South	NDE & core

6.2.16.1. Physical Condition Survey

The condition of the North Bent Pier is summarized in Chapter 4. In general, less than one percent distress was identified in these elements.

For each of the study areas, the local distress quantity is presented in Table 6.128. Minimal distress was observed in the areas surveyed.

Table 6.128. Condition and Sampling of Study Areas - North Bent Pier

Location ID	Core Samples	Date Inspected	Distress Quantity (%)
32	32	5/24/2017	< 1
33	33	5/24/2017	< 1

6.2.16.2. Corrosion Survey

Corrosion Potential

Results of half-cell potential surveys are summarized in Table 6.129. The results indicate a low probability of corrosion activity.

Table 6.129. HCP Testing Results - North Bent Pier

Location ID	HCP - Avg. (mV vs. CSE)	HCP - Min. (mV vs. CSE)	HCP - Std. Dev. (mV vs. CSE)	Distress Quantity (%)
32	35	-54	36	< 1
33	-46	-143	46	< 1

** Thresholds (see 3.4.4.1): > -200mV low, -200 to -350mV moderate, < -350 mV high probability of corrosion*

Resistivity

Resistivity testing was not performed on this element.

Corrosion Rate

Corrosion rate testing results are provided in Table 6.130. Corrosion rate testing was not performed in all areas. The measured corrosion rate was low.

Table 6.130. Corrosion Rate Testing Results - North Bent Pier

Location ID	BAC Meter - Current Density Avg. (um/yr) †	Distress Quantity (%)
32	2.0	< 1
33	--	< 1

† Thresholds (see 3.4.4.3): <10 low, 10-30 moderate, 30-100 high, >100 um/yr severe instantaneous corrosion rate.

6.2.16.3. Reinforcement Cover Survey

The results of the reinforcement cover surveys are provided in Table 6.131. The statistical information for this element is summarized in Table 6.132. Cover depths were greater than 2 inches.

Table 6.131. Cover Depth Measurements - North Bent Pier

Location ID	Cover Vertical Bars - Avg. (in.)	Cover Vertical Bars - Rep. Minimum (in.)	Cover Horizontal Bars - Avg. (in.)	Cover Horizontal Bars - Rep. Minimum (in.)	Distress Quantity (%)
32	2.8	2.0	2.9	--	< 1
33	4.1	3.8	2.7	2.3	< 1

Table 6.132. Cover Depth Statistics - North Bent Pier

Value	Cover Vertical Bar (in.)	Cover Horizontal Bar (in.)
Average (in.)	3.3	2.7
Standard Deviation (in.)	0.9	0.2
Coefficient of Variation	27%	9%
Minimum (in.)	1.9	2.3
Maximum (in.)	4.5	3.1

6.2.16.4. Field and Lab Carbonation Tests

Carbonation measured in the core samples from this element was 0.4 inches, with local areas as deep as 0.8 inches, which is much less than the minimum cover depths.

6.2.16.5. Other Tests

No other tests were conducted in this element category.

6.2.16.6. Chloride Profile Analysis

The results of the chloride analyses of Core 32, extracted from the North Bent Pier in the pier cap at the upper downstream corner of the element, are shown in Figure 6.43. The results indicate typical surface driven chloride exposure, with a low surface concentration driving the chloride ingress.

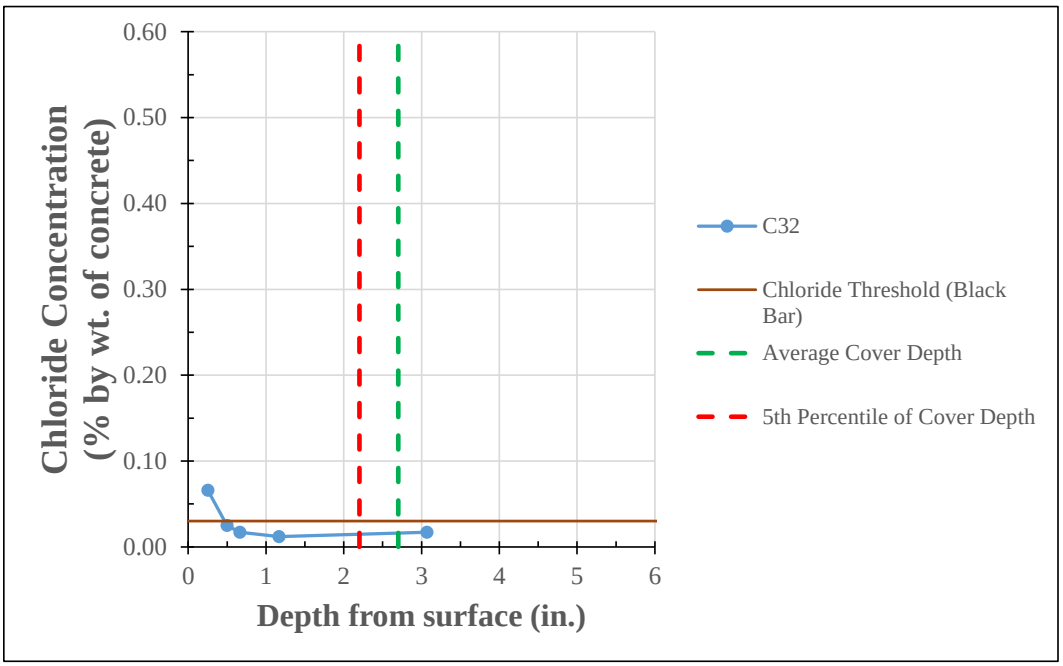

Figure 6.43. Chloride profile for North Bent Pier core compared to chloride threshold.

6.2.16.7. Petrographic Analysis

Limited petrographic studies were conducted on Core 33. The concrete was identified as Concrete Mixture ID 6 - 3/4 inch Gravel. The concrete represented by this sample appeared to be in good condition, and no freeze-thaw distress was observed. No evidence of damage due to ASR was observed.

6.2.16.8. Interpretation

At present, limited chloride exposure and carbonation have occurred. Long-term durability is expected to be good and will likely be controlled by chloride exposure where deicer runoff or associated spray is permitted to reach the pier. Long-term carbonation may also be a critical mechanism; however, the low water to cement ratio of the concrete mixture will likely mitigate against carbonation. Other mechanisms of distress such as ASR or freeze-thaw were not observed.

6.2.17. North Retaining Walls

The locations of the follow-up testing study areas in the North Retaining Walls are shown in Table 6.133. All study areas were in the original (1918) concrete.

Table 6.133. Location of Study Areas - North Retaining Walls

Location ID	Approach	Side of Bridge	Face	Approximate Distance Below Construction Joint With 1980 Repair (ft)	Test Type
27	North Approach	Upstream	Upstream	5	NDE & core
30	North Approach	Downstream	Downstream	2	NDE & core
31	North Approach	Downstream	Downstream	20	Core Only

6.2.17.1. Physical Condition Survey

The condition of the North Retaining Walls is summarized in Chapter 4. Approximately 8 percent distress on average was identified in this element, and significant freeze-thaw damage was present along the top edge.

For each of the study areas, the local distress quantity is presented in Table 6.134. The distress to the original concrete in the North Retaining Walls included freeze-thaw deterioration and concrete delaminations, as well as associated cracking and moisture staining.

Table 6.134. Condition and Sampling of Study Areas - North Retaining Walls

Location ID	Core Samples	Date Inspected	Distress Quantity (%)
27	27	5/25/2017	> 30
30	30	5/25/2017	1 to 10

6.2.17.2. Corrosion Survey

Corrosion Potential

Results of half-cell potential surveys are provided in Table 6.135. The results fall into ranges that would ordinarily be interpreted to indicate high probability of corrosion activity; however, like the Abutments, the risk of corrosion in concrete against soil is best assessed by examination of the potential gradients. At both tested locations, high gradients suggest that there is a risk of active corrosion.

Table 6.135. HCP Testing Results - North Retaining Walls

Location ID	HCP - Avg. (mV vs. CSE)	HCP - Min. (mV vs. CSE)	HCP - Std. Dev. (mV vs. CSE)	Distress Quantity (%)
27	-514	-589	50	> 30
30	-467	-550	56	1 to 10

** Thresholds (see 3.4.4.1): > -200mV low, -200 to -350mV moderate, < -350 mV high probability of corrosion*

Resistivity

Results of resistivity testing are provided in Table 6.136. The results indicate a moderate to high risk of corrosion.

Table 6.136. Resistivity Testing Results - North Retaining Walls

Location ID	Resipod - Resistivity Avg. (kOhm-cm)	Distress Quantity (%)
27	6	> 30
30	17	1 to 10

** Thresholds (see 3.4.4.2): 50-100 low, 10-50 moderate, <10 kOhm-cm high corrosion rates possible in active areas*

Corrosion Rate

Corrosion rate testing was not performed on this element.

6.2.17.3. Reinforcement Cover Survey

The results of the reinforcement cover surveys are provided in Table 6.137. The statistical information for this element is summarized in Table 6.138. Cover depths were typically approximately 2 inches or more.

Table 6.137. Cover Depth Measurements - North Retaining Walls

Location ID	Cover Vertical Bars - Avg. (in.)	Cover Vertical Bars - Rep. Minimum (in.)	Cover Horizontal Bars - Avg. (in.)	Cover Horizontal Bars - Rep. Minimum (in.)	Distress Quantity (%)
27	2.2	1.9	2.5	2.0	> 30
30	3.0	2.2	4.3	4.0	1 to 10

Table 6.138. Cover Depth Statistics - North Retaining Walls

Value	Cover Vertical Bar	Cover Horizontal Bar
Average (in.)	2.6	3.1
Standard Deviation (in.)	0.7	1.0
Coefficient of Variation	26%	31%
Minimum (in.)	1.9	2.0
Maximum (in.)	4.1	4.6

6.2.17.4. Field and Lab Carbonation Tests

Synthesis of field and lab carbonation measurement results are provided in Table 6.139. The depth of carbonation was approximately 1 inch; this is roughly half the measured cover depth in the areas surveyed.

Table 6.139. Carbonation Measurements - North Retaining Walls

Location ID	Carbonation - Rep. Maximum (in.)	Cover Vertical Bars - Rep. Minimum (in.)	Cover Horizontal Bars - Rep. Minimum (in.)	Distress Quantity (%)
27	1.1	1.9	2.0	> 30
30	0.9	2.2	4.0	1 to 10

6.2.17.5. Other Tests

No other tests were conducted in this element category.

6.2.17.6. Chloride Profile Analysis

The results of the chloride analyses of Cores 27 and 30, extracted from the North Retaining Walls, are shown in Figure 6.44. In both cores, some exposure had occurred. In Core 30 concentrations at the depth of reinforcement are above the threshold for initiation of corrosion.

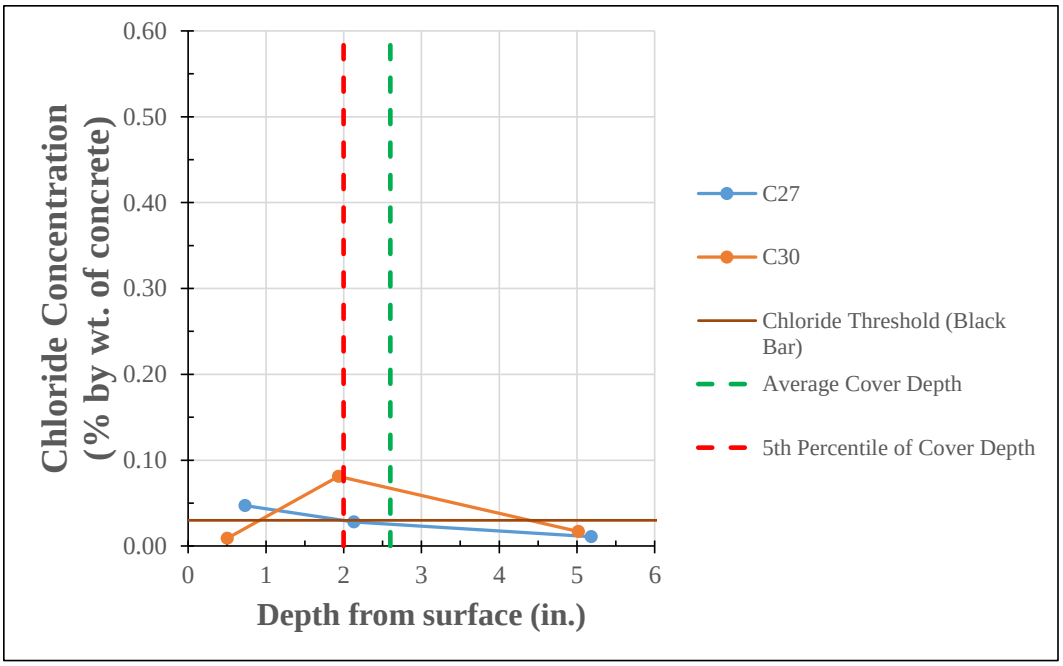

Figure 6.44. Chloride profiles for North Retaining Walls cores compared to chloride threshold.

6.2.17.7. Petrographic Analysis

Cores extracted from the North Retaining Walls indicate a similar mix design as the Arch Ribs, Barrel Arches, and Lower Spandrel Columns and Walls (i.e., Concrete Mixture 1B - 1918: 1- to 2-in. Basalt). Cores 27 and 30 were evaluated for carbonation and freeze-thaw distress, and Core 30 was selected for limited petrographic examinations. The depths of freeze-thaw distress are summarized in Table 6.83. Freeze-thaw distress was moderate relative to other areas of the bridge, and extends approximately 4 inch beyond the vertical surface at Core 30. Carbonation depth is not near the depth of reinforcement.

No other mechanism of distress (e.g., ASR) were identified in core samples of this mixture designation.

Table 6.140. Measured Depth of Freeze-Thaw Distress - North Retaining Walls

Core ID	Depth of Severe Freeze-Thaw Distress, inches	Maximum Depth of Freeze-Thaw Distress, inches
27	--	1.5
30	2.0	4.0

Note: Depth values reported here include measured surface erosion at core location

6.2.17.8. Interpretation

The primary deterioration mechanisms are freeze-thaw and chloride-related corrosion, depending on the exposure to moisture. The concrete is not air-entrained and is therefore susceptible to freeze-thaw distress. Outward displacement of the top portions of the retaining wall at the downstream side is occurring; this may be exacerbated by the deep freeze-thaw distress occurring at the top of the original section of wall.

6.2.18. Deck Rail Elements

Follow up testing in the bridge rail elements included two cores extracted for laboratory evaluations: Core 55 was collected from the Traffic Barrier, and Core 56 was collected from a concrete post of the Pedestrian Railing. UT and X-ray Florescence (XRF) testing were also performed on the aluminum railing segments for the Pedestrian Railing. Locations of the core samples are listed in Table 6.141.

Table 6.141. Location of Study Areas - Deck Rail Elements

Location ID	Element Type	Span/ Pier No./ Approach	Side of Bridge	Face	Test Type
55	Traffic Barrier	4	Upstream	Downstream	Core Only
56	Pedestrian Railing Post	4	Upstream	Downstream	Core Only

6.2.18.1. Physical Condition Survey

The condition of these elements is discussed in Chapter 4. In general, the Pedestrian Railing posts are in good condition and the Traffic Barrier J-rail is in fair condition, with frequent spalling adjacent to expansion joints.

6.2.18.2. Corrosion Survey

Corrosion surveys were not performed on the deck rail elements.

6.2.18.3. Reinforcement Cover Survey

Reinforcement cover surveys were not performed on the deck rail elements. The following information is based on the core samples collected:

- Traffic Barrier - epoxy-coated No. 5 rebar, with 2-3/8 inches of clear cover
- Pedestrian Railing Post - uncoated No. 4 rebar, with 1-1/4 inches of clear cover

6.2.18.4. Field and Lab Carbonation Tests

Carbonation measured on the core samples extracted from these elements were negligible.

6.2.18.5. Other Tests

The other tests conducted on the Pedestrian Railings, including ultrasonic thickness testing and X-ray florescence testing on the metal components, are described in Appendix 11.

XRF testing positively identified the following components as aluminum: top rail, bottom rail, mullions, and castings. XRF alloy analysis suggested that the aluminum alloys specified on the 1939 drawings for the members (Alloy 53S and 43) were in fact utilized. The bolt assemblies that attach the aluminum railing segments to the concrete posts consist of a galvanized steel bolt and nut, and a plain carbon steel cap. The caps are typically heavily corroded in the field, and the protective zinc on the nuts is largely consumed such that the nuts are also showing red corrosion products.

Although the aluminum members have a light oxide coating, no oxidation (corrosion) that would result in section loss to the metal was observed during the inspection. UT testing reported in Appendix 11 established the base thickness of the primary members for future reference.

6.2.18.6. Chloride Profile Analysis

The results of chloride testing are shown in Figure 6.45. Chloride exposure appears to be higher in the traffic barrier, as expected given the proximity of exposure to de-icing salts applied to the deck roadway. The chloride threshold for black bar reinforcement is shown for reference; however, the reinforcement in the traffic barrier is epoxy-coated, and a higher threshold would be applicable assuming the coating is intact (see Section 3.2.1.2).

Exposure is comparatively lower on the Pedestrian Rail post and chloride ingress to date has not yet resulted in chloride concentrations greater than the threshold to initiate corrosion at the bar depth. However, the chloride that is present can be expected to continue to diffuse into the concrete resulting in concentrations exceeding the chloride threshold at the depth of the steel in the near future.

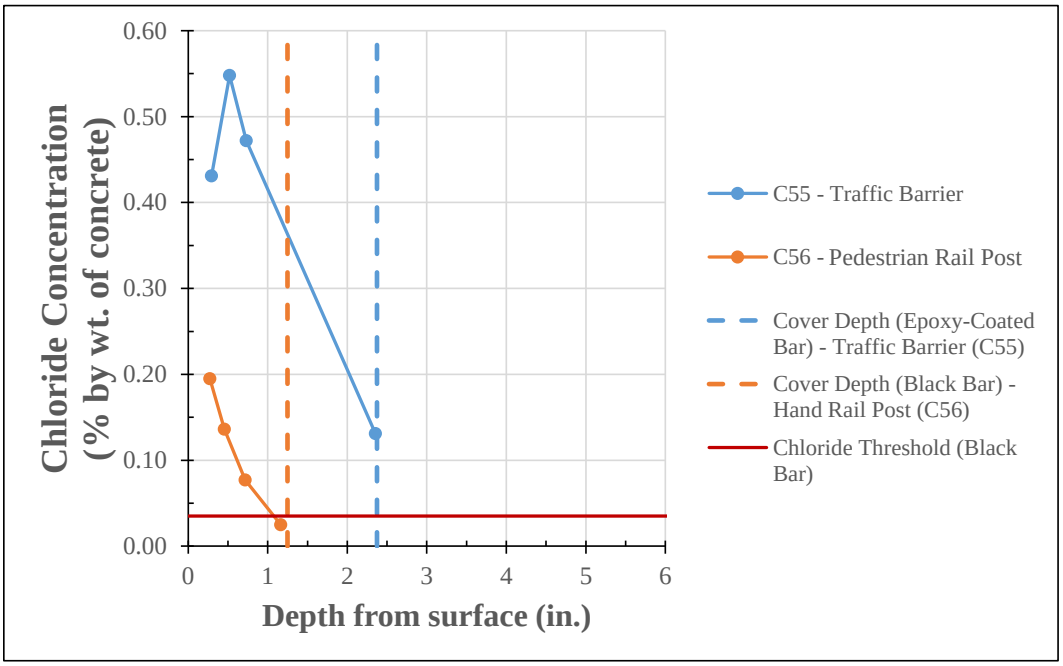

Figure 6.45. Chloride profiles for Deck Rail Elements compared to chloride threshold for black bar as a reference. Note that the bars in the Traffic Barrier are epoxy-coated reinforcing, which has a higher corrosion threshold - see Section 3.2.1.2.

6.2.18.7. Petrographic Analysis

Cores 55 and 56 were of similar concrete mixtures which was identified as Concrete Mixture 4 - 3/8 inch Crushed Gravel. No evidence of materials related distress were observed in similar cores.

6.2.18.8. Interpretation

Chloride-induced corrosion will likely be the primary deterioration mechanism in the concrete deck rail elements. Chloride exposure was high and is expected to continue in the Traffic Barrier; however, the epoxy-coated reinforcement offers some level of protection against chloride-induced corrosion. The Pedestrian Railing post contains uncoated reinforcement and exhibited lower chloride exposure compared to the Traffic Barrier; however, chloride-induced corrosion can be expected to develop soon.

Carbonation was negligible in the core samples extracted, and other materials related distress (e.g., freeze-thaw damage and ASR) were not observed in cores samples of the similar mix design.

For the Pedestrian Railing, impact and abrasion are the primary deterioration mechanisms, along with corrosion of the carbon steel connection hardware.

7. FINDINGS

7.1. Results That Could Impact As-Inspected Structural Model

The structural analysis and load rating of the bridge was carried out by HNTB in parallel with WJE's bridge inspection. As such, it was necessary for WJE to provide HNTB with inspection findings that could affect the structural behavior and performance. This was accomplished by means of WJE memoranda that were shared with HNTB during the course of the inspection.

Final versions of two memoranda are included in Appendices 4 and 9 for reference: "Inspection Results That Could Affect As-Inspected Structural Model" and "Follow-up Testing Results That Could Affect As-Inspected Structural Model." Items addressed in the memoranda are listed below. The information that is pertinent to this report is repeated and summarized under Chapters 4, 5, and 6.

Inspection Results That Could Affect As-Inspected Structural Model:
- Structural distress in Piers 1 and 8
- Structural distress at bases of spandrel columns and walls
- Shear or torsional cracking in cap beams
- Spalling of cap beams below deck joints
- Flexural cracking in arch ribs at spring lines
- Loss of cross-sectional area of arch ribs due to concrete deterioration
- Section loss due to corrosion of reinforcing bars
  - Arch piers
  - Spandrel columns
  - Cap beams
  - Deck underside
- Exposure of Melan truss reinforcing angles due to spalling

Follow-up Testing Results That Could Affect As-Inspected Structural Model:
- Reinforcing steel cover depth measurements by element
- Section loss measurements by ultrasonic thickness testing (Melan truss reinforcing)
- Reinforcing steel tensile properties and chemical composition
  - 1918 rebar
  - 1918 Melan truss reinforcing steel angles
- Melan truss reinforcement strain relief testing
- Concrete compressive strength and modulus of elasticity testing

Information was provided by means of narrative descriptions, tabular listings of conditions, graphical diagrams illustrating the conditions, and links to the Plannotate inspection annotations for individual conditions. Plannotate links were provided in cases where engineering judgment was needed regarding how to incorporate the conditions into the structural model. For example, distress conditions at the bases of spandrel columns were provided as Plannotate links so that HNTB could, if necessary, review the exact condition at each column and decide if it warranted a hinge in the structural model. Refer to HNTB's load rating report for the manner in which the various conditions were considered.

7.2. Interpretation of Distress Quantity Ratios

The distress quantity ratios and condition state quantities presented in Chapter 4 provide a quantitative view of the current condition of the structure. In this sub-section, these quantities are compared to state and

federal guidelines for interpretation of severity. Comparison is also made to the conditions encountered at the Franklin Avenue Bridge before its recent rehabilitation since it is a very similar structure and since HNTB and WJE were the designers and have access to the distress quantity data.

7.2.1. MnDOT Guideline Thresholds for Corrective Actions

MnDOT establishes general guidelines for corrective actions in the document titled "Fiscal Year 2016 through 2020 – Bridge Preservation and Improvement Guidelines" (MnDOT Preservation Guidelines). The two main categories of actions in this document are "Preservation" and "Improvement." Preservation can take the form of either maintenance or major preservation, whereas improvement includes both bridge rehabilitation and bridge replacement. For the 3rd Avenue Bridge, replacement of the entire structure is not considered given its historic nature.

As defined in the MnDOT Preservation Guidelines, major preservation activities include, but are not limited to, actions such as joint repair or replacement; deck overlays; partial deck replacement; concrete element patching repairs; or installation of cathodic protection. Bridge rehabilitation activities are more extensive types of work, such as full-scale replacement of components (deck, superstructure, substructure), bridge widening, or major structural repairs that increase capacity.

The guideline thresholds for each of these actions are presented in Table 7.1. For interpretation of the thresholds presented for bridge decks, the bridge is categorized as an Urban Minor Arterial, with an ADT of 15,500 (last counted in 2004).

The criteria in the table are based on a percent of the structure that is in condition state CS3 or CS4. For concrete elements, in general, this refers to "unsound" concrete, or concrete that has spalled, exhibits exposed reinforcement, or contains wide cracks, but also can include more minor aspects such as build-up of efflorescence or surface scaling. Notably, however, this criteria does not always include delaminated areas of concrete. WJE defined the "distress quantity ratio" (see Section 4.5.1) to include CS3 and CS4 conditions and to also include delaminations and freeze-thaw damage because these conditions will also require concrete repair. As such, the "distress quantity ratios" calculated by WJE based on the inspection findings are directly comparable to the thresholds in the MnDOT guide.

Table 7.1. MnDOT Preservation and Improvement Guidelines
Summary of Action Thresholds based on Unsound Area as Related to the 3rd Avenue Bridge

Component	Element Category	Preventive Maintenance	Major Preservation[1]	Rehabilitation[2]
Deck	Wearing Surface	≤ 2% Do Nothing or Spot Repairs	2 to 10% Mill and Patch or Re-Overlay	10 to 25%: Deck Repairs and Re-Overlay >25%: Replace Deck
	Deck and Slab Underside			
	Sidewalk			
	Joints	≤ 10%	> 10%	-
Superstructure	Upper Spandrel Columns and Cap Beams (1980 Construction)	≤ 10%	10 to 20%	>20%
	Lower Spandrel Columns (1918 Construction)			
	Arch Ribs (Spans 1-5)			
	Barrel Arches (Spans 6-7)			
	Prestressed Concrete Girders			
	Weathering Steel Girders	≤ 10%	15 to 20%	
Substructure	Arch Pier Walls (Arch Spans)	≤ 10%	10 to 40%	>40%
	Arch Pier Bases (Arch Spans)			
Other Elements	Pedestrian Railing	≤ 15%	> 15%	--
	Deck Rail Elements	≤ 10%	10%	>10%

[1] *Major preservation activities include but are not limited to actions such as joint repair or replacement; deck overlays; partial deck replacement; concrete element patching repairs; or installation of cathodic protection.*
[2] *Rehabilitation activities include more extensive types of work, such as full-scale replacement of components (deck, superstructure, substructure), bridge widening, or major structural repairs that increase capacity.*

7.2.2. Federal Guidelines

The MnDOT Preservation Guidelines reference the FHWA "Bridge Preservation Guide." The FHWA document is intended to provide a framework for a systematic approach to a preservation maintenance program. This document is intended to mesh with the National Bridge Inventory (NBI) inspection programs and associated bridge ratings that are performed. The document defines a few key terms:

- **Bridge Preservation** – Actions or strategies that prevent, delay, or reduce deterioration of bridges of bridge elements, restore the function of existing bridges, keep bridges in good condition and extend their life. Preservation actions may be preventive or condition-drive.
- **Preventive Maintenance** – A planned strategy of cost-effective treatments to an existing roadway system and its appurtenances that preserves the system, retards future deterioration, and maintains or improves the functional condition of the system (without substantially increasing structural capacity).
- **Rehabilitation** – Major work required to restore the structural integrity of a bridge as well as work necessary to correct major safety defects.
- **Replacement** – Total replacement of a structurally deficient or functionally obsolete bridge…

The document provides general guidance for commonly employed actions for components based on the general condition ratings. These ratings range from 0 (failed) to 9 (excellent). This guidance is summarized in Table 7.2.

The element level bridge inspection report generated by WJE as part of this inspection (Appendix 3), recommended NBI ratings for the deck of 5 (fair condition) and for the superstructure and substructure of 4 (poor condition). Based on the general guidance in the FHWA document, this indicates major repairs, rehabilitation or replacement of select elements in these categories would be a commonly employed and feasible action.

Table 7.2. FHWA Bridge Preservation Guide
General Condition Rating Guidance

Condition Rating	Description	Commonly Employed Feasible Actions
9	Excellent	Preventive Maintenance
8	Very Good Condition	
7	Good Condition	
6	Satisfactory Condition	Preventive Maintenance; and/or Repairs
5	Fair Condition	
4	Poor Condition	Rehabilitation or Replacement
3	Serious Condition	
2	Critical Condition	
1	Imminent Failure Condition	
0	Failed Condition	

7.2.3. Distress Quantity Summaries by Element Category

For each element category (and sub-category) surveyed during the in-depth inspections, the distress quantity was calculated and compared to the corrective action guideline thresholds. As described in Section 4.4, distressed areas include areas of delaminated or spalled concrete; areas of freeze thaw deterioration; and areas of deteriorated or failed patches. The results are summarized in Table 7.3 through Table 7.6. For reference, the primary deterioration mechanisms identified in Chapter 6 for each element category are also listed in the tables.

Table 7.3. Distress Quantity Summary for Deck Elements (Relative to MnDOT Guideline Threshold Ranges*)

Region of Bridge	Element Category	No. of Elements	No. of Elements with Distressed Surface Area				Distress Quantity for all Elements in Category	Deterioration Mechanism(s) (See Section 6)
			0 to 2%	2 to 10%	10 to 25%	25% or more		
Arch Spans	Deck Underside	7	0	0	7	0	15%	Chloride
	Deck Roadway	7	7	0	0	0	< 1%	Chloride
	Deck Sidewalk	7	7	0	0	0	< 1%	Chloride
Approach Spans	Deck Underside	4	4	0	0	0	1%	Chloride
	Deck Roadway	4	4	0	0	0	< 1%	Chloride
	Deck Sidewalk	4	4	0	0	0	< 1%	Chloride

** Guideline thresholds: Major preservation 2-10%; Rehabilitation 10-25%*

Table 7.4. Distress Quantity Summary for Superstructure Elements (Relative to MnDOT Guideline Threshold Ranges*)

Region of Bridge	Element Category	Sub-Categories	No. of Elements	No. of Elements with Distressed Surface Area			Distress Quantity for all Elements in Category	Deterioration Mechanism(s) (See Section 6)
				0 to 10%	10 to 20%	20% or more		
Arch Spans	Cap Beams (1980 Construction)	Never Expansion Joint	47	47	0	0	1%	Chloride
		Expansion Joint 1980-Present	38	5	9	24	34%	Chloride; Structural Movement
	Upper Spandrel Columns and Walls (1980 Construction)	Never Expansion Joint	130	128	2	0	< 1%	Carbonation
		Expansion Joint 1980-Present	98	76	17	5	7%	Chloride; Structural Movement
	Lower Spandrel Columns and Walls (1918 Construction)	Never Expansion Joint	33	25	6	2	7%	Carbonation; Freeze-Thaw
		Expansion Joint 1918-1980	16	8	7	1	10%	Chloride; Carbonation; Freeze-Thaw
		Expansion Joint 1980-Present	20	10	3	7	17%	Chloride; Carbonation; Freeze-Thaw; Structural Movement
		Always Expansion Joint	17	0	5	12	36%	Chloride; Carbonation; Freeze-Thaw; Structural Movement
	Arch Ribs (Spans 1-5)	--	15	6	4	5	12%	Chloride; Carbonation; Freeze-Thaw
	Barrel Arches (Spans 6-7)	--	2	0	2	0	14%	Chloride; Carbonation; Freeze-Thaw
Approach Spans	Prestressed Girders	--	20	20	0	0	< 1%	Chloride; Carbonation
	Weathering Steel Girders	--	19	19	1	0	2%	Chloride; Poor Drainage

** Guideline thresholds: Major preservation 10-20%; Rehabilitation >20%.*

Table 7.5. Distress Summary for Substructure Elements (Relative to MnDOT Guideline Threshold Ranges*)

Region of Bridge	Element Category	Sub-Categories	No. of Elements	No. of Elements with Distressed Surface Area			Distressed Area for all Elements in Category	Deterioration Mechanism(s) (See Section 6)
				0 to 10%	10 to 20%	20% or more		
Arch Spans	Arch Pier Walls	Exterior Walls	8†	6	2	0	4%	Chloride; Carbonation; Freeze-Thaw; Structural Movement
		Interior Walls	8†	6	2	0	3%	Chloride; Carbonation; Freeze-Thaw; Structural Movement
	Arch Pier Bases	--	8†	0	2	6	72%	Freeze-Thaw; Erosion
Approach Spans	Bent Piers	--	2†	2	0	0	< 1%	Chloride
	Abutments	--	2	2	0	0	1%	Chloride
	Retaining Walls	--	4	4	0	0	8%	Chloride; Carbonation; Freeze-Thaw; Structural Movement

** Guideline thresholds: Major preservation 10-40%; Rehabilitation >40%.*
† Each pier counted as a single element.

Table 7.6. Distress Summary for Other Elements (Relative to MnDOT Guideline Threshold Ranges)

Region of Bridge	Element Category	Sub-Categories	Quantity	Units	Quantity with CS Rating				Distressed Percentage* for all Elements in Category	Deterioration Mechanism(s) (See Section 6)
					CS1 Good	CS2 Fair	CS3 Poor	CS4 Severe		
All Spans	Deck Rail Elements	Pedestrian Railing - Aluminum Segments	607	EA	530	57	16	4	3%	Impact & Abrasion; Corrosion of Fasteners
		Pedestrian Railing - Concrete Posts	606	EA	485	115	6	0	1%	Chloride
		Traffic Barrier - Metal Rails	4091	LF	0	3927	109	55	4%	Chloride; Impact
		Traffic Barrier - Concrete J-Rail	4091	LF	3499	302	198	92	15%	Chloride

**For aluminum pedestrian railing and metal rails, includes sum of CS3 and CS4 conditions. For concrete J-rail, includes sum of CS2 (delaminations only), SC3 and CS4 conditions). The value reported in this table for the Concrete J-Rail is greater than the value reported in Table 4.23; this is because Table 4.23 calculates the ratio in terms of square feet, but Table 7.6 calculates the ratio in terms of linear feet.*

7.2.4. Comparison with Franklin Avenue Bridge

To provide a frame of reference, the general condition of the 3rd Avenue Bridge was compared to previous assessment performed recently by HNTB and WJE for the Franklin Avenue Bridge. The Franklin Avenue Bridge is located downstream a few miles and was built using a concrete arch design, construction techniques, and materials that are similar to those used at the 3rd Avenue Bridge. The team of HNTB and WJE performed a condition investigation, in-depth evaluation, and repair design and construction observations for restoration of the Franklin Avenue Bridge between 2007 and 2017.

The general findings for each component of the two bridges is compared and contrasted in Table 7.7 and discussed in the paragraphs below. In the table, areas of significant quantity differences are marked by bold red text. WJE performed two inspections of the Franklin Avenue Bridge: an initial condition assessment in 2007-2008 and an updated condition assessment and repair estimate in 2013. Information from the two inspections are consolidated in the table below, with the more recent 2013 data cited when available.

Table 7.7. Comparison of Distress Quantities in Franklin Avenue Bridge and 3rd Avenue Bridge

Bridge Element Category	Sub-category	Percentage of Surface Area Exhibiting Distress	
		Franklin Avenue (2008 or 2013)	3rd Avenue (2017)
Deck	Topside	**0.2 to 9.0**	0 to 2
	Underside	3	**13 to 16**
Cap Beams	Non-Expansion Joints	2	1
	Expansion Joints	10	**34**
Spandrel Columns	Non-Expansion Joints	2	2
	Expansion Joints	2	**10 (1918 joint)** **17 (1980 joint)** **36 (always joint)**
Abutments	--	**10 to 20**	1
Arch Ribs	--	14 (north arch) 20 (south arch)	9 to 24 (outside ribs) 1 to 10 (middle ribs) 11 to 14 (barrel arches)
Pier Walls	Piers without Joints	3 to 6 (Piers 2 and 3)	1 to 4 (Piers 2-5, 7)
	Piers with Joints / Manholes	**33 to 36 (Piers 1 and 4)**	7 to 17 (Piers 1, 6, 8)
Pier Bases	--	Not quantified separately	**20 to 100**

7.2.4.1. General Construction and History

Franklin Avenue Bridge was completed in 1923, soon after the 3rd Avenue Bridge. The original Franklin Avenue bridge deck and superstructure were reconstructed in 1970, 10 years before the 3rd Avenue deck was replaced. However, the 1970 reconstruction at Franklin was much more extensive, removing and replacing all of the spandrel columns and cap beams on the structure. A concrete overlay was applied to the 3rd Avenue deck as part of the deck replacement in 1980, whereas a concrete overlay was not added to the Franklin Avenue deck until 1984. At the time of the 2007-2008 assessment, the original Franklin Avenue bridge was 85 years old and its reconstructed deck and superstructure were 38 years old (24 years with overlay); in comparison, at the time of the 2017 inspection, the original 3rd Avenue structure was 99 years old and its reconstructed deck and superstructure were 37 years old (37 years with overlay).

For further information regarding the Franklin Avenue Bridge rehabilitation, refer to recent technical articles by HNTB and WJE.[17]

7.2.4.2. Deck

The deck topside at Franklin Avenue varied widely in the amount of distress that was identified. Although a full sounding survey was not completed, at the smaller study areas, topside distress ranged from 1 to 9 percent. In comparison, the deck topside distress at 3rd Avenue generally ranged from 0 to 2 percent.

In both structures, half-cell potential surveys indicated that corrosion had initiated over large areas of the deck, particularly at construction joints and cracks in the overlay. One key difference between the two decks is that the top mat of reinforcement is epoxy-coated at 3rd Avenue, but was not at Franklin Avenue. Bottom mats in both decks were uncoated (black) bars.

The deck underside at Franklin Avenue exhibited delaminations, spalls, and exposed reinforcement at many of the expansion joints (see Figure 7.1). Unlike 3rd Avenue, this distress was mostly concentrated at the joints, with fewer longitudinal cracks and spalls in the spans between the cap beams. The concrete distress at 3rd Avenue is more advanced on the sidewalk edges than was at Franklin (see Figure 7.2). Overall, the deck underside is in worse condition at 3rd Avenue, with approximately 15 percent of the underside deteriorated, as compared to 3 percent at Franklin Avenue.

a) Franklin Avenue Bridge (2008) *b) 3rd Avenue Bridge (2017)*

Figure 7.1. Deck underside - concrete deterioration at expansion joints

[17] "Franklin Avenue Bridge, Part 1: History, Investigation and Rehabilitation," Arne Johnson, John Lawler, Dan Enser, Travis Konda, and Paul Backer, *Concrete International*, June 2017.

a) Franklin Avenue Bridge (2008)

b) 3rd Avenue Bridge (2017)

Figure 7.2. Deck underside - concrete deterioration at edge

7.2.4.3. Cap Beams

Deterioration of the cap beams under expansion joints was widespread at both bridges. A higher percentage of the cap beams at expansion joints was found to be distressed at 3rd Avenue than at Franklin Avenue. Away from expansion joints, the amount of concrete distress was comparably low in both bridges.

7.2.4.4. Spandrel Columns

The spandrel columns at the Franklin Avenue Bridge had all been reconstructed as part of the 1970 deck replacement. Overall, the reconstructed columns had little distress, at just 2 percent overall. At the 3rd Avenue Bridge, the non-expansion joint, 1980 rebuilt spandrel columns were in similar condition. However, the remaining lower portions of the spandrel columns (from original construction in 1918) were in much worse condition.

7.2.4.5. Arch Ribs

Both bridges were constructed with embedded steel angles as part of the Melan truss construction technique. Overall, the nature and frequency of cracking, spalls, and delaminations along the corners of the elements and on the topside and underside were similar between the two structures (Figure 7.3).

Portions of the arch ribs on both bridges exhibited freeze thaw deterioration (Figure 7.4). At 3rd Avenue, however, much more freeze thaw deterioration was present at the base of the arches. This is likely partially due to the positioning of this intersection, which places the arch spring lines lower on the piers and below drain outfalls at some of the piers.

At Franklin Avenue, deterioration on the topside of the arch ribs included both longitudinal cracks over Melan angles and areas of deterioration where previous partial-depth repairs had failed. At 3rd Avenue, longitudinal cracking was present, but much less of the previous repair at the arch topside had been performed.

a) Franklin Avenue Bridge (2008).

b) 3rd Avenue Bridge (2017).

Figure 7.3. Arch rib corner distress and longitudinal cracking along Melan truss angles.

a) Franklin Avenue Bridge (2008) - View of freeze thaw deterioration near base of arch ribs (circled).

b) 3rd Avenue Bridge (2017) - View of freeze thaw deterioration near base of arch rib.

Figure 7.4. Arch rib freeze thaw deterioration at piers.

7.2.4.6. Pier Bases

The pier bases are in generally worse condition at 3rd Avenue than they were at the Franklin Avenue Bridge, and the height of freeze thaw distress on the pier bases is greater. The two environmental causes for this effect are likely the turbulent water at the horseshoe dam (leading to spray) and greater water elevation changes (Figure 7.5). The river elevation at Franklin Avenue is comparatively more constant because it is upstream of a dam.

Also, a large portion of the pier bases at 3rd Avenue has been previously repaired at an unknown date with partial-depth concrete repairs, and a concrete jacket had been installed around the bases of Piers 1 and 2 within the past 3 years (Figure 7.6). At Franklin Avenue, major repairs at the pier bases had not been performed. At 3rd Avenue, the jackets at Piers 1 and 2 are performing well, but the partial-depth repairs have largely failed.

At both structures, freeze thaw distress was present on almost all surfaces of the pier bases. Similarly, the depth of concrete material loss was greater where the bases had been exposed to run-off from drain outfalls. Chloride from roadway run-off is known to intensify freeze thaw distress.

a) Franklin Avenue Bridge (2008) - Overall view of river piers - note calm water conditions.

b) 3rd Avenue Bridge (2017) - Pier 3 - Note turbulent water conditions.

Figure 7.5. River pier comparison

a) Franklin Avenue Bridge (2008) - View at base of Pier 3. Note limited amount of freeze thaw distress above water pool elevation.

b) 3rd Avenue Bridge (2017) - Freeze thaw distress extending many feet above water level, and a concrete repair jacket was previously installed at this pier.

Figure 7.6. River pier comparison.

7.2.4.7. Abutments

The abutments at Franklin Avenue were in overall worse condition than 3rd Avenue. However, much of the Franklin Avenue abutments were original concrete from 1923, whereas the 3rd Avenue abutments were replaced as part of the 1980 rehabilitation.

7.3. Deterioration Mechanisms and Anticipated Remaining Service Life by Element

The following sections summarize the deterioration mechanisms and expected performance for each of the element categories investigated. Based on WJE's interpretation of the in-depth element level inspections and the follow-up testing results, the anticipated remaining service life of each element category (i.e., the element's "durability potential") was assessed. Predictions of future performance presented here are relative and qualitative. Numerical service life modeling has not been performed.

The anticipated remaining service life is used here to describe, in relative terms, the time until the quantity of distress in a given element, without corrective action or intervention,[18] is likely to reach or exceed the guideline thresholds for a "rehabilitation" action (as outlined in Section 7.2.1).[19] For the purpose of this report, the anticipated remaining service life was categorized as follows:

- Short - Rehabilitation action threshold already reached or likely to be reached within 5 years;
- Moderate - Rehabilitation action threshold likely to be reached in 5 to 15 years; and
- Long - Rehabilitation action threshold likely not to be reached for more than 15 years

For example, the observed conditions of upper and lower spandrel columns and walls near expansion joints are already beyond rehabilitation thresholds, and the anticipated remaining service life of these elements before rehabilitation is short. In contrast, the bent piers in the approach spans have a long anticipated remaining service life considering the generally good condition and low risk for widespread deterioration due to the distress mechanisms acting.

Based on the current distress quantity, the identified deterioration mechanisms, and severity of deterioration, the anticipated remaining service life of each element category and sub-category was assessed and is discussed in the following sections. Considerations for rehabilitation in light of these findings are discussed in Chapter 8.

For ease of reference, the primary deterioration mechanisms and anticipated remaining service life for the primary element categories are summarized below in Table 7.8. The subsequent sections discuss these findings by element.

[18] What constitutes the "end of life" of a member (onset of corrosion, collapse, etc.) must always be defined in a service life analysis. Using percent of damage to define end of life is one rational method, which is used herein. The most relevant percentage of damage values to use in this context are the MnDOT guideline thresholds for corrective action.

[19] As defined for the purpose of this current condition evaluation report, the "anticipate remaining service life" is the future life of an element assuming that corrective action or other interventions are not taken at this time. Service life estimates for bridge elements after they have been treated with various rehabilitation alternatives will be studied in the Rehabilitation Alternatives portion of this project to follow.

Table 7.8. Summary of Deterioration Mechanisms and Anticipated Remaining Service Life by Element

Element	Primary Deterioration Mechanism(s)	Secondary Deterioration Mechanism(s)	Anticipated Remaining Service Life
Deck Topside - Arch Spans	Chloride	--	Moderate
Deck Underside - Arch Spans	Chloride	--	Short
Upper Spandrel Columns and Walls (Always Expansion Joint), Including Cap Beams	Chloride, Structural Movement	--	Short to Moderate
Upper Spandrel Columns and Walls (Never Expansion Joint), Including Cap Beams	Chloride, Structural Movement	--	Long
Lower Spandrel Columns and Walls (Always Expansion Joint and 1980-Present Expansion Joint)	Chloride	Carbonation; Freeze-Thaw	Short
Lower Spandrel Columns and Walls (Never Expansion Joint and 1918-1980 Expansion Joint)	Carbonation	Chloride; Freeze-Thaw	Moderate
Arch Ribs	Chloride	Carbonation; Freeze-Thaw	Short to Moderate
Barrel Arches	Chloride	Carbonation; Freeze-Thaw	Moderate
Arch Pier Walls	Chloride; Carbonation; Structural Movement	Freeze-Thaw	Moderate to Long (Piers 2-7); Short to Moderate (Piers 1 and 8)
Arch Pier Bases	Freeze-thaw; Erosion	--	Short
Deck Topside - Approach Spans	Chloride	--	Moderate to Long
Deck Underside - Approach Spans	Chloride	--	Moderate to Long
South Approach Weathering Steel Girders	Chloride; Poor-Drainage	--	Long
South Abutment and Bent Pier	Chloride	Carbonation	Long
North Approach Prestressed Girders	Chloride	Carbonation	Long
North Abutment and Bent Pier	Chloride	Carbonation	Long
North Approach Retaining Walls	Freeze-Thaw; Structural Movement	Chloride; Carbonation	Moderate
Pedestrian Railing (Concrete)	Chloride	--	Long

7.3.1. Deck - Approach and Arch Spans

7.3.1.1. Overall Conditions and Deterioration Mechanisms

The deterioration of the deck topside will likely be controlled by chloride exposure and associated corrosion. The presence of epoxy-coated reinforcement in the top mat and the protective overlay in the roadway have provided protection against chloride-induced corrosion. In the sidewalk, despite the lack of an overlay, generally high cover to the epoxy-coated reinforcement has provided protection against chloride diffusion. These protective features have limited the distress quantities that have developed to date on the

deck topside through the nearly 40-year life of the deck. At present, distress quantities for the deck topside, in both the arch spans and approach decks, are below the guide threshold for a "Rehabilitation" action.

However, the density of cracking in the overlay surface in the arch spans is high (see Figure 4.20), and numerous cracks were observed in the sidewalks, especially near joints. Many of these cracks extend to the reinforcing bars, which provides a direct path for chloride ingress into the deck. Chloride concentrations observed in cores taken from the deck at cracks are at levels sufficient to initiate corrosion on epoxy coated bars at the depth of the reinforcing. While current distress is limited, the follow-up testing has indicated that active corrosion is occurring, particularly in regions of through-thickness cracking; the limited distress observed may be partially explained by the fact that propagation of damage due to corrosion after initiation may take 7 to 15 years longer in decks reinforced with epoxy coated bars compared to uncoated bars.[20] Given the conditions observed, it should be expected that delamination and spalling of the deck topside will occur at a gradually increasing rate in future years.

On the underside of the deck, the cover to the bottom mat of uncoated (i.e., black) reinforcing bars was as low as 3/4 inch. Exposure to chlorides from chloride-laden deicer runoff leaking through expansion joints, manhole openings, and through-thickness cracks has resulted in corrosion-related distress. In addition, along the downstream edge of the deck, advanced deterioration was observed due to chloride-laden run-off at the fascia, and at some locations the support of the pedestrian railings has been compromised. Many of the repairs on the deck underside adjacent to the joints installed as part of the 2003 joint replacement have failed. The current distress quantities on the deck underside in the arch spans are consistent with "Rehabilitation" as defined in Table 7.1. Given the comparatively better conditions in the decks of the approach spans (likely due to the lesser extent of through-thickness cracking), "Rehabilitation" is not indicated for the deck underside in those spans at this time.

7.3.1.2. Anticipated Remaining Service Life

Continued deterioration of the deck underside, which is already in poor condition, is expected. Deterioration on the deck topside in cracked-affected areas is expected to accelerate in the near future. Based on the corrosion surveys, favorable conditions for active corrosion were observed, especially at locations of cracking.

In the arch spans, the anticipated remaining service life is moderate for the deck topside (controlled by chloride-induced corrosion at cracks); however, anticipated remaining service life for the deck underside is short due to the widespread distress. In the approach spans, anticipated remaining service life in the topside and underside will be controlled by chloride-induced corrosion at cracks and is moderate-to-long.

7.3.2. Upper Spandrel Columns and Walls (Including Cap Beams)

7.3.2.1. Overall Conditions and Deterioration Mechanisms

Distress in the upper spandrel columns and walls and cap beams, constructed in 1980, is concentrated at elements below expansion joints. The cap beams have been damaged by structural movement and chloride-induced corrosion associated with leaking through the expansion joints. While the joint seals were repaired/replaced in 2003, chloride ingress prior to this repair program had apparently already progressed to the point of reaching critical concentrations for corrosion at the depths of the reinforcing steel. Based on the MnDOT guidelines summarized in Table 7.1, 5 of the 98 upper spandrel columns and walls and 24 of

[20] John Lawler, James Donnelly, and Paul Krauss, "Performance Evaluation of Iowa Bridge Decks Constructed with Epoxy-Coated Reinforcing Bars" For Iowa Department of Transportation, August 19, 2011.

the 38 cap beams at expansion joints exhibited current distress quantities consistent with a "Rehabilitation" action. Note that an additional 17 of the 98 upper spandrel columns and walls, and 9 of the 38 cap beams, exhibited distress quantities of at least 10 percent.

The upper spandrel columns and walls and cap beams that had not been associated with expansion joints are in generally good condition. None of the cap beams exhibited more than 10 percent distress, and only two upper spandrel columns and walls exhibited more than 10 percent distress.

7.3.2.2. Anticipated Remaining Service Life

The anticipated remaining service life is short for nearly all of the cap beams and about one-quarter of the upper spandrel columns and walls that are located near expansion joints. This estimate considers the mechanical damage and chloride exposure that has already occurred in these elements. In contrast, the anticipated remaining service life of almost all of the upper spandrel columns and walls and cap beams located away from expansion joints is long and will likely be controlled by the onset of corrosion if exposure conditions worsen in the future.

The shorter life of the 1918 lower spandrel columns (see next section) upon which the 1980 upper spandrel columns are supported could also limit the life of the upper columns. Where the 1980 spandrel columns extend to the arch ribs, movement-related distress in the cap beams and at the bases of the columns will continue until the deck joints are repaired/replaced, which will negatively impact anticipated remaining service life of the columns.

7.3.3. Lower Spandrel Columns and Walls

7.3.3.1. Overall Conditions and Deterioration Mechanisms

Similar to the upper spandrel columns and walls, at locations adjacent to current expansion joints, the primary deterioration mechanism in the lower spandrel columns and walls is chloride-induced corrosion; chloride contents several times the corrosion threshold were measured at the reinforcing depth. Some level of chloride-induced corrosion is also occurring in the lower spandrel columns and walls that had a joint between 1918 and 1980. Also, given the relative age of these elements (i.e., 1918 construction) and the identified concrete material properties (i.e., comparatively higher water-cement ratio and lack of air entrainment), carbonation-induced corrosion and some surficial freeze-thaw distress are contributing to the observed distress for all lower spandrel columns and walls (both adjacent to and away from expansion joints).

Based on the MnDOT guidelines summarized in Table 7.1, 19 of the 37 lower spandrel columns and walls with current expansion joints (always expansion joint and expansion joint 1980-present) currently exhibit distress quantities consistent with a "Rehabilitation" action. An additional 8 of the 37 lower spandrel columns and walls at expansion joints exhibit more than 10 percent distress.

In contrast, only 3 of the 49 lower spandrel columns and walls located away from current expansion joints (never expansion joint, or 1918-1980 expansion joint) exhibit distress quantities consistent with a "Rehabilitation" action, with an additional 13 of the 49 lower spandrel columns and walls away from expansion joints showing more than 10 percent distress. Typically, lower quantities of distress were observed in the middle columns, and the upstream spandrel columns were typically in better condition than the downstream spandrel columns.

7.3.3.2. Anticipated Remaining Service Life

The lower spandrel columns and walls near current expansion joints (always expansion joint and expansion joint 1980-present) have a short anticipated remaining service life due to the levels of chloride exposure and depth of carbonation. Distress quantities are already well above the "Rehabilitation" threshold, and, given the deterioration mechanisms that are acting, will worsen significantly in future years. At locations away from expansion joints, or where joints were removed in 1980, the anticipated remaining service life is moderate (controlled mostly by carbonation, and possibly due to distress from corrosion caused by chloride exposure prior to 1980).

Note that much of the surface of these lower spandrel columns and walls has been previously repaired. Many of these past repairs have failed. Repairs that are still sound were not included in the distress quantities; however, the long-term performance of these repairs may differ from other sound surfaces on the lower columns and walls. It is estimated that the majority of the currently sound repairs will perform well for another 15 years, but some will fail.

7.3.4. Arch Ribs and Barrel Arches

7.3.4.1. Overall Conditions and Deterioration Mechanisms

The primary deterioration mechanism in the arch ribs and barrel arches is chloride exposure and associated corrosion at locations of cracks over the Melan truss angles. The resultant concrete distress is most pronounced at the corners of the arch ribs and barrel arches, where exposure is most severe, but some delamination and spalling is present away from the corners on the top and underside surfaces. Local areas of freeze-thaw distress were observed, and should be considered a contributing factor of deterioration at areas exposed to moisture (e.g., near drains or where water collects at the bottoms of columns). Some section loss in the truss angles was observed at locations where the concrete deterioration was severe. Overall, the middle ribs exhibited less deterioration than the exterior ribs.

Based on the MnDOT guidelines summarized in Table 7.1, five of the 15 arch ribs currently exhibit distress quantities consistent with a "Rehabilitation" action, while four additional arch ribs and both barrel arches exhibited distress quantities greater than 10 percent. Distress observed was generally uniformly distributed along the length of the arch ribs and across the surfaces of the barrel arches, though some of the most pronounced free-thaw damage in the arch ribs and barrel arches was noted at the top of the arches at the intersection with the arch pier where water collects.

7.3.4.2. Anticipated Remaining Service Life

In general, the anticipated remaining service life of the arch ribs is moderate for the middle ribs, and short to moderate in the downstream and upstream ribs. The anticipated remaining service life is moderate in the barrel arches. The anticipated remaining service life of these elements could be extended by reducing moisture penetration into the concrete, as both reinforcing steel corrosion and freeze-thaw damage require moisture to occur.

Note that, like the lower spandrel columns and walls, much of the surface of the arch ribs and barrel arches has been previously repaired. Many previous repairs have failed. The repairs were not included in the distress quantities where the existing repairs are sound; however, the long-term performance of these repairs may differ from other sound surfaces on the arches. It is estimated that the majority of these remaining repairs will continue to perform well for another 15 years, but some will fail.

7.3.5. Arch Pier Walls

7.3.5.1. Overall Conditions and Deterioration Mechanisms

Carbonation and chloride-induced corrosion are the primary deterioration mechanism present in the arch pier walls, especially at locations where reinforcement cover, which was highly variable, was low. Freeze-thaw distress localized near regions of high moisture exposure is also a secondary cause of deterioration. Current distress quantities in these elements are relatively low. In Piers 1 and 8, structural movement has also resulted in significant concrete distress at the tops of the walls, and the approach-facing walls are in worse condition due to leakage from the expansion joints above them.

Based on the MnDOT guidelines summarized in Table 7.1, none of the arch pier walls currently exhibit distress quantities consistent with a "Rehabilitation" action. Considering existing distress, only two of the eight arch pier walls (Piers 1 and 8) exhibit distress quantities greater than 10 percent.

7.3.5.2. Anticipated Remaining Service Life

The anticipated remaining service life of the arch pier walls at Piers 2 through 7 is moderate to long and is controlled locally by some combination of carbonation- and/or chloride-induced corrosion and freeze-thaw distress where cover is low or where exposure to moisture and chlorides is high. Anticipated remaining service life at Piers 1 and 8 is short to moderate due to the structural distress that is present and the worse-than-typical concrete deterioration on the approach-span-facing walls.

7.3.6. Arch Pier Bases

7.3.6.1. Overall Conditions and Deterioration Mechanisms

Freeze-thaw distress and failure of previous patching repairs are the primary deterioration mechanisms for the arch pier bases. Based on laboratory analyses, the freeze-thaw distress extends up to 15 inches into the concrete from the original surfaces that were cored. Surface erosion was deeper elsewhere based on the visual inspection notes (17 inches maximum compared to 7 inches maximum at the cored locations). Accordingly, a conservative maximum for the freeze-thaw damage that is present on the pier bases is approximately 25 inches. This deterioration will continue as long as moisture saturation occurs. Considering the limited reinforcement in the footings, carbonation and chloride-induced corrosion are not expected to cause widespread distress.

Based on the observed distress quantities, six of the eight arch pier bases (Piers 1-4, 6, and 8) currently exhibit distress quantities consistent with a "Rehabilitation" action, while the other two (Piers 5 and 7) exhibit distress quantities of more than 20 percent.

7.3.6.2. Anticipated Remaining Service Life

In general, the anticipated remaining life of the arch pier bases is short due to the advanced levels of freeze-thaw deterioration currently present and the propensity of this deterioration to worsen with continued exposure to water saturation and freeze-thaw cycles. Based on past performance, a very rough estimate for further propagation of freeze-thaw damage into the pier base concrete is 1/2 to 1 inch of depth per year of continued exposure.

7.3.7. Approach Span Elements

7.3.7.1. Overall Conditions and Deterioration Mechanisms

Only limited distress is present in the abutments, bent piers, weathering steel girders, and prestressed girders in the north and south approach spans. Chloride exposure is localized (e.g., at leaking joints) and has

resulted in a small amount of localized chloride-induced corrosion; additional distress may develop if this exposure is prolonged. Carbonation and freeze-thaw exposure are not expected to cause widespread distress.

7.3.7.2. Anticipated Remaining Service Life

Assuming adequate future protection against chloride exposure (i.e., maintained joints and drains, and regular maintenance of protective coatings), the anticipated remaining service life of these elements is long.

7.3.8. North Retaining Walls

7.3.8.1. Overall Conditions and Deterioration Mechanisms

The primary deterioration mechanism present in the lower original portions of the retaining walls north of the north abutment is freeze-thaw damage, with carbonation- and chloride-induced corrosion as contributing factors. Taken as a whole, the north retaining walls do not exhibit deterioration consistent with either "Preservation" or "Rehabilitation" actions as defined in the MnDOT guidelines summarized in Table 7.1 based on the observed distress quantities (less than 10 percent). The original 1918 portions of the wall are marginally stable according to geotechnical evaluation, but the 1980 concrete caps are rotating outward, especially at the downstream wall. Local distress attributed to carbonation and chloride-induced corrosion at low cover, as well as freeze-thaw distress should be addressed. In addition, outward displacement of the 1980 cap should be rectified, which may require partial removal of the top of the original wall where freeze-thaw damage is advanced.

7.3.8.2. Anticipated Remaining Service Life

Assuming adequate protection against chloride exposure (i.e., maintained joints and drains, and regular maintenance of protective coatings), the anticipated remaining service life of these elements is moderate. This also assumes that the deep freeze-thaw damage at the top of the original wall is removed when the rotated cap is replaced.

7.3.9. Deck Railing Elements

7.3.9.1. Overall Conditions and Deterioration Mechanisms

While widespread deterioration was not observed at present, chloride-induced corrosion is expected to be the primary deterioration mechanism in the concrete deck rail elements. The traffic barrier has experienced a higher exposure to chlorides than the pedestrian railing; however, the traffic barrier was constructed with epoxy-coated reinforcement, which offers some protection against chloride exposure. Out of the over 4,000 linear feet of concrete traffic barrier, 92 linear feet has a CS4 rating and 198 linear feet has a CS3 rating.

The concrete posts in the pedestrian railing have seen a comparatively lower chloride exposure, but also have lower cover to the reinforcement and were constructed with uncoated (black bar) reinforcement. Of the 606 elements, none have a CS4 rating and only 6 have a CS3 rating.

The aluminum railing segments in the pedestrian railing are in generally good condition. Out of a total of 607 elements, only 4 have a CS4 rating, and only 16 have a CS3 rating. General distress included impact damage or abrasion, and corrosion of fasteners.

7.3.9.2. Anticipated Remaining Service Life

Assuming adequate maintenance and protection against chloride exposure (e.g., miscellaneous metal repairs and regular maintenance of protective coatings), the anticipated remaining service life of the traffic barriers and pedestrian railings is moderate and long, respectively.

8. SUMMARY AND CONSIDERATIONS FOR REHABILIATION ALTERNATIVES

As part of MnDOT Contract No. 1000045, WJE as subconsultant to HNTB performed an inspection and testing program for the 3rd Avenue Bridge (Bridge 2440) from May through October 2017. WJE's work was performed in two parts: an initial in-depth element level inspection of all components of the bridge, followed by testing and material sampling in representative study areas. The scope of the work was defined in the Final Bridge Inspection Work Plan. The results of the inspection and testing were provided incrementally in several interim presentations and memoranda, and a comprehensive summary is presented herein.

The next task in the 3rd Avenue Bridge project is the rehabilitation alternatives study, in which specific alternatives will be developed as a collaborative effort between MnDOT, the Project Historian, and the HNTB design team. Presented below are aspects regarding the different elements of the bridge, based on this inspection and condition evaluation effort, which should be considered in the development of rehabilitation alternatives.

8.1. Deck

The deck topside currently has a relatively small amount of distress (2 percent or less), but the overlay exhibits a high density of cracking, and elevated chloride concentrations are present at the level of the reinforcing steel where cracking is present in the deck. Accordingly, deck topside distress will continue and likely accelerate in the coming years. The deck underside in the arch spans currently exhibits a relatively high percentage of distress (approximately 15 percent), and full-depth deck replacement will be needed in several areas (e.g., at southbound lane manholes, along nearly the full length of the downstream fascia, and along the deck centerline). Given these factors, anticipated remaining service life of the deck (i.e., time until rehabilitation thresholds are reached, without intervention) is judged to be short (less than 5 years) for the underside and moderate (5 to 15 years) for the topside. The deck underside is in better condition in the approach spans, but scheduling rehabilitation actions separately for the arch and approach spans seems inefficient.

Given the condition of the deck and its supporting elements (cap beams and spandrel columns/walls), the deck will need to be either completely or partially replaced (i.e., in sections along the joints) in the not-too-distant future. If partial or complete replacement are delayed, two general options could be implemented in the interim: 1) remove and replace the existing overlay to protect the substrate deck and to keep options open for possible partial deck replacement in a larger future rehabilitation project; or 2) seal the cracks and repair the topside distress as it develops in the deck, and plan for complete deck replacement as part of a larger future rehabilitation project. In either option, full-depth deck repairs in localized areas will need to be performed.

8.2. Upper Spandrel Columns/Walls and Cap Beams at Expansion Joints

The 1980 upper spandrel columns and walls, including the cap beams, located at deck joints exhibit a high distress quantity (7 and 34 percentage on average for columns and cap beams, respectively) due to high chloride content at the level of the reinforcing steel as well as extensive mechanical spalling at the top corners of the cap beams. Distress quantities for some elements are already near or above rehabilitation thresholds. Movement-related structural distress is evident in cap beams and columns that are full-height. The viability of these elements is also limited by the even worse condition of the 1918 lower spandrel columns and walls upon which some are supported.

Given these factors, anticipated remaining service life for the cap beams and many of the upper spandrel columns and walls located at expansion joints is judged to be short (less than 5 years). Replacement seems prudent as a component of any partial or complete deck replacement project.

8.3. Upper Spandrel Columns/Walls and Cap Beams Away From Expansion Joints

Away from deck expansion joints, the 1980 cap beams and upper spandrel columns and walls are in generally good condition, with relatively low distress quantities, low chlorides, and little carbonation. These elements have the potential for reuse in a rehabilitation project, as long as the 1918 lower spandrel columns and walls upon which some are supported can be retained and properly repaired.

8.4. Lower Spandrel Columns and Walls at Current Expansion Joints

Approximately 142 of the original 228 spandrel columns and walls were replaced full-height in the 1980 rehabilitation project. Of the 86 lower spandrel columns and walls that remain, 37 are located at current expansion joints. These elements are in poor condition and have a short anticipated remaining service life (less than 5 years) without intervention. The elements exhibit a very high distress quantity (28 and 40 percent on average for columns and walls, respectively), have very high chloride levels at the depth of the reinforcing steel, and have deep carbonation in some areas. Movement-related structural distress exists at the bottom of some of these elements. Paste erosion has rendered the surfaces of these elements generally rough, making application of a protective surface treatment difficult.

Retaining the lower spandrel columns for the long term will require substantial rehabilitation and protection measures that will be costly and likely alter the appearance of the elements. Replacement of these elements in any long-term rehabilitation scheme seems likely once all factors are considered.

8.5. Lower Spandrel Columns and Walls Away From Current Expansion Joints

Of the 86 lower spandrel columns and walls that remain, 49 are located away from current expansion joints (i.e., never at a joint or at a joint only from 1918-1980). These columns and walls are in better condition than those at current joints. The distress quantity is 8 percent on average but varies widely (up to over 50 percent) among the columns and walls in this category. Chloride contents at the depth of the reinforcing steel are below or near the corrosion threshold, but carbonation has penetrated to the reinforcing steel in some areas. In addition, paste erosion has rendered the surface of these elements generally rough.

Given these factors, anticipated remaining service life for these elements is judged to be moderate (5 to 15 years) without intervention. Retaining these elements in a rehabilitation scheme is possible if protection measures are implemented, though such measures will be challenging, costly, and could alter the historic appearance. Surface treatments, sealers, or cathodic protection may all be options, but effectiveness, service life extension, and costs require further study. Surface roughness will create challenges for initial application and potentially future performance of surface treatments.

8.6. Arch Ribs and Barrel Arches

Current distress quantities for the outer arch ribs and barrel arches are 18 and 13 percent on average, respectively, which are similar quantities to those observed at the Franklin Avenue Bridge before its rehabilitation. The middle rib at the 3rd Avenue Bridge is in somewhat better condition due to sheltering from the deck. Deterioration mechanisms include corrosion due to elevated chlorides and freeze thaw damage in zones of water saturation. Section loss due to corrosion of the embedded Melan truss reinforcing

angles is limited to isolated locations where the corners have spalled and the angles have been exposed to chloride-laden run-off.

Long-term service life of the arch ribs and barrel arches is achievable if corrective actions are taken, such as well-designed localized concrete repairs and protection of the elements from water penetration (such as by application of an appropriate water-resistant coating). Since above-threshold chlorides are present at the depth of some Melan truss angles, targeted cathodic protection should be considered to enhance durability of these elements, particularly at the corners where exposure is worst. Drain outfalls should be redirected away from the arches. Longitudinal cracks, which are allowing chloride ingress, should be sealed against water penetration.

8.7. Arch Pier Walls and Bases

Distress quantities in the arch pier walls are low (3 to 4 percent on average at present), although testing showed chloride levels near the corrosion threshold in some areas and carbonation depths deeper than the cover depth in some areas. Approach-facing sides of Piers 1 and 8 have more distress due to past leakage from deck joints located above them. The pier walls have a long anticipated remaining service life, and service life could be enhanced by implementing protection measures to mitigate corrosion, such as applying a water-resistant coating.

The pier bases are suffering from widespread distress (typically well more than 40 percent at present) primarily due to deep freeze thaw damage and failed previous concrete repairs. The maximum depth of freeze thaw damage at the locations cored was 15 inches (i.e., surface erosion plus damage within remaining concrete); however, areas of even deeper surface erosion were visually observed and measured during the in-depth inspection. Considering the deepest surface erosion observed and the deepest freeze-thaw damage detected in the cores, a very conservative maximum damage depth of 25 inches could be considered for preliminary structural analysis. Freeze thaw damage will continue to penetrate into the pier base concrete as long as water saturation continues.

As a first priority, in any maintenance, preservation or rehabilitation scheme, the drain outfalls should be redirected away from the pier bases to forestall additional erosion and freeze thaw damage.

In any major rehabilitation project, the pier bases should be repaired. Such work will require considerations for the challenging access conditions that exist, including the turbulent river flow and underlying rock conditions. Given the widespread, deep deterioration that is present, a reinforced concrete jacket around the base of each pier seems to be the practical solution. At least a portion of the depth of the freeze thaw damaged concrete should be removed and a reinforced concrete layer applied around the full perimeter to restore the original profile lines of the piers. Pier jackets are not needed at the bases of Piers 1 and 2, which were repaired in this fashion in 2014.

To determine the available time window before pier jacketing is needed, a very conservative approach would be for HNTB to assess the structural performance of the piers discounting the outer 25 inches of concrete at the present time (around the full perimeter of the pier, when in actuality the deepest loss is concentrated under the drains) and considering an additional loss of material at a rate of approximately 1/2 to 1 inch per year in the future. The extent of damage and analysis could be refined, if needed.

8.8. Approach Spans

Condition of the 1980 abutments, bent piers, weathering steel girders spans, and precast girders spans is generally good at present. Anticipated remaining service life, assuming proper ongoing maintenance, is long.

The reinforced concrete caps constructed on top of the original 1918 north retaining walls are rotating outward, particularly at the downstream side. This condition should be repaired in any rehabilitation scheme. Geotechnical review by others determined that the 1918 concrete retaining walls below the 1980 caps are marginally stable but repairable. Rehabilitation of the 1918 wall sections should include surface repairs and removal of freeze-thaw damage along the tops of the walls.

8.9. Pedestrian Railings

The aluminum railing segments are in very good condition considering their age. Distress is limited primarily to impact damage and corrosion of anchor bolt hardware at the concrete posts. The concrete posts have a moderate anticipated remaining service life, although some have been undermined by deep deck spalling at the downstream fascia.

8.10. Structural Distress Conditions

In addition to the deterioration conditions described above, the inspection identified several conditions of significant structural distress caused by unintended volume change movement of the deck and superstructure when subjected to thermal changes. These conditions included the following:

- Pier 8 - Very wide diagonal shear cracking, sliding along horizontal construction joint, fractured and bent reinforcing steel across joint
- Pier 1 - Wide vertical and diagonal shear cracking
- Spandrel columns and walls, particularly below expansion joints - Structural distress at bases, including wide cracking, diagonal shear cracking, and delamination and spalling, sometimes severe
- Cap beams below expansion joints - Deep spalling along top corners and shear or torsional cracking
- South abutment - Missing and fractured anchor bolts at fixed bearings

The timing and nature of the repairs to address these structural distress conditions should be determined based on structural review of the individual conditions by HNTB in consultation with MnDOT. Some of the conditions appear relatively urgent, such as the very wide diagonal cracking in Pier 8, while others could be delayed until a major rehabilitation project is undertaken. Future structural distress can be avoided by rearticulating the bridge deck joints in a targeted program or as part of a major rehabilitation project.